Functional Morphology of the Vertebral Column in *Remingtonocetus* (Mammalia, Cetacea) and the Evolution of Aquatic Locomotion in Early Archaeocetes

by

Ryan Matthew Bebej

A dissertation submitted in partial fulfillment
of the requirements for the degree of
Doctor of Philosophy
(Ecology and Evolutionary Biology)
in The University of Michigan
2011

Doctoral Committee:

Professor Philip D. Gingerich, Co-Chair
Professor Philip Myers, Co-Chair
Professor Daniel C. Fisher
Professor Paul W. Webb

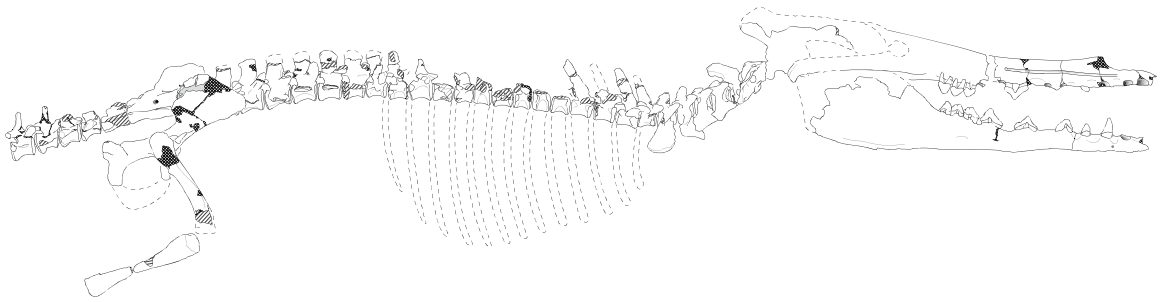

2011

To my wonderful wife Melissa, for her infinite love and support

Acknowledgments

First, I would like to thank each of my committee members. I will be forever grateful to my primary mentor, Philip D. Gingerich, for providing me the opportunity of a lifetime, studying the very organisms that sparked my interest in evolution and paleontology in the first place. His encouragement, patience, instruction, and advice have been instrumental in my development as a scholar, and his dedication to his craft has instilled in me the importance of doing careful and solid research. I am extremely grateful to Philip Myers, who graciously consented to be my co-advisor and co-chair early in my career and guided me through some of the most stressful aspects of life as a Ph.D. student (e.g., preliminary examinations). I also thank Paul W. Webb, for his novel thoughts about living in and moving through water, and Daniel C. Fisher, for his insights into functional morphology, 3D modeling, and mammalian paleobiology.

My research was almost entirely predicated on cetacean fossils collected through a collaboration of the University of Michigan and the Geological Survey of Pakistan before my arrival in Ann Arbor. Iyad S. Zalmout collected the new specimen of *Remingtonocetus domandaensis* described in Chapter 3 (as well as many others), and he generously permitted me to study this remarkable specimen for my dissertation work. Others who collected the fossils utilized in my work include Mohammad Anwar, Muhammad Arif, M. Akram Bhatti, William C. Clyde, Philip D. Gingerich, Munir ul-Haq,

Intizar Hussain Khan, William J. Sanders, and Neil A. Wells. I especially thank William J. Sanders for skillfully preparing these fossils; patiently training me in the art of preparing, molding, and casting fossils; and for all of our stimulating and insightful discussions about vertebral biomechanics, the evolution of cetaceans in general, and, on occasion, the St. Louis Cardinals vs. the New York Mets.

My research would also not have been possible without access to specimens of both modern and fossil mammals for comparison. I thank the following people for access to specimens in their care: Steve Hinshaw, Philip Myers, and Priscilla Tucker in the Mammal Division at the University of Michigan Museum of Zoology (Ann Arbor, MI); Judy Galkin and Eileen Westwig at the American Museum of Natural History (New York, NY); and David Bohaska, Linda Gordon, Jeremy Jacobs, and Charlie Potter at the National Museum of Natural History (Washington, DC). My dear friends Kyle and Michele Peterson graciously provided me with food, lodging, and wonderful tours of the District of Columbia during multiple research visits to the National Museum.

Many faculty, staff members, post-docs, and fellow students contributed to making the University of Michigan Museum of Paleontology a wonderful and vibrant place to work, including Catherine Badgley, Tom Baumiller, Robyn Burnham, Devapriya Chattopadhyay, Mike Cherney, Mike D'Emic, Tom Eiting, Julia Fahlke, John Finarelli, Brady Foreman, John Graf, Gregg Gunnell, Amber Heard, Takehito Ikejiri, Alex Janevski, Cait Lamborne, Carly Manz, Amy McKeighan, Dan Miller, Chrissy Minor, Vlad Miskevich, Pieter Missiaen, Emile Moacdieh, Meegan Novara, Shanan Peters, Gerald Smith, Cindy Stauch, John Whitlock, Jeff Wilson, Miriam Zelditch, and the myriad of students working

in the prep lab. Bonnie Miljour provided the beautiful reconstruction of *R. domandaensis* (see the frontispiece and Chapter 3), along with invaluable help in navigating Adobe Photoshop and Illustrator. Adam Rountrey was an invaluable resource on many topics, especially 3D scanning and modeling, and Katy Smith offered innumerable discussions about mammalian evolution, multivariate statistics, the latest episode of *Lost*, and Major League Baseball. I will forever be indebted to Aaron Wood for his depth of insight, his listening ear, his unwavering advice, and, most of all, his friendship.

I am also grateful for many faculty, staff members, and students in the Department of Ecology and Evolutionary Biology (EEB), including Prosanta Chakrabarty, Clay Cressler, Deborah Goldberg, Aaron Iverson, Mandy Izzo, George Kling, Gail Kuhnlein, Jessica Middlemis Maher, the late Beverly Rathcke, Nancy Smith, and Rachel Vannette. Julia Eussen and Jane Sullivan were fabulous graduate coordinators, and I am thankful for their willingness to deal with and answer any question, no matter how inane. My experiences teaching with Marc Ammerlaan, Bill Fink, Phil Myers, and Ron Nussbaum were fantastic. But most of my favorite memories teaching are from my three semesters as co-graduate student instructor with Lucia Luna; she taught me so much, and her enthusiasm and humor always made my day.

I also thank Chris Van Ee at Design Research Engineering (Novi, MI), whose time and expertise made it possible for me to develop the multibody dynamic models in Chapter 5; Brett Lyons and Eric Maslowski of the University of Michigan 3D Lab; my undergraduate mentors Ralph Stearley, Randy Van Dragt, and Dave Warners of Calvin

College (Grand Rapids, MI) for their continued encouragement and support; Rolf Bouma and all of the Au Sable Graduate Fellows who have come and gone in the past six years; and Matt Remy and Paul Steen for their camaraderie, graduate life commiseration, and board game acumen.

Lastly, I must express my sincere gratitude to my family, especially my parents and my in-laws, for all of their love and support over the years. Most of all, I am extremely thankful to my wife Melissa, who has given and sacrificed so much for me as I pursued my dream. Her love, encouragement, smile, and culinary skills are appreciated far more than she could ever know. And last, but not least, I am grateful for my wonderful little dog Duncan, who has never failed to greet me with a wagging tail, a belly to scratch, and/or a lick on the face after coming home from a long day at work—and who also never seemed to mind that I tried to gain insight into vertebral function by staring at his lumbar region while he gallivanted around our apartment.

This research was supported by EEB Block Grants, the Peter Olaus Okkelberg Award, and the University of Michigan Museum of Paleontology.

Table of Contents

List of Figures

List of Tables

List of Abbreviations

Anatomical Abbreviations

C	Cervical vertebra
Ca	Caudal vertebra
L	Lumbar vertebra
S	Sacral vertebra
T	Thoracic vertebra

Specimen Abbreviations

ChM	Charleston Museum collection
GSM	Georgia Southern Museum collection
GSP-UM	Geological Survey of Pakistan-University of Michigan collection
H-GSP	Howard University-Geological Survey of Pakistan collection
IITR-SB	Indian Institute of Technology, Roorkee, collection curated by Sunil Bajpai; this institution formerly used the abbreviation RUSB
K	Palaeontology Laboratory collection, Geological Survey of India, Kolkata
LUVP	Lucknow University vertebrate paleontology collection
MMNS	Mississippi Museum of Natural Science collection
NHML	Natural History Museum of London collection
SCSM	South Carolina State Museum collection

SMNS	Staatliches Museum für Naturkunde, Stuttgart, collection
UMMP	University of Michigan Museum of Paleontology collection
UMMZ	University of Michigan Museum of Zoology collection
USNM	United States National Museum of Natural History collection
VPL	Vertebrate Paleontology Laboratory collection, Panjab University
WH	Wadi Al-Hitan collection

Abstract

Knowledge of early cetacean evolution has grown greatly in recent decades due to the discovery of dozens of species of archaeocetes that bridge the gap between aquatic cetaceans and their terrestrial ancestors. However, many of the details of how this transition occurred have yet to be elucidated. Assessment of vertebral function in archaeocetes is crucial for understanding the ecologies of these taxa and reconstructing the evolution of aquatic locomotion in the earliest whales. This dissertation documents the vertebral morphology of an early archaeocete (*Remingtonocetus domandaensis*) and develops quantitative methods for assessing vertebral function in fossil forms.

Remingtonocetus domandaensis is known from the middle Eocene Domanda Formation of Pakistan and is one of six species in the archaeocete family Remingtonocetidae. A newly described, well-preserved specimen (GSP-UM 3552) demonstrates that this taxon had a long neck that was stabilized by robust cervical musculature and imbricating transverse processes. Its lumbar vertebrae suggest that this animal swam by powerful movements of the hind limbs rather than dorsoventral undulation of the vertebral column.

This interpretation is supported by two independent quantitative assessments of lumbar mobility in early cetaceans. Multivariate analyses of lumbar measurements in modern mammals demonstrate that the lumbar vertebrae of *Remingtonocetus*

domandaensis are more similar to those from stable lumbar regions, while vertebrae of protocetid and basilosaurid archaeocetes compare closely with those from mobile lumbar regions. Virtual rigid-body modeling simulations of the L4-L5 joints of *R. domandaensis* and the protocetid *Maiacetus inuus* demonstrate that *M. inuus* possessed a greater range of motion in flexion and extension than *R. domandaensis*, regardless of soft tissue parameters. These findings indicate that early protocetids had more mobile lumbar spines than their remingtonocetid contemporaries and suggest that the evolution of tail-powered swimming in early cetaceans was preceded by an increase in lumbar mobility.

By assessing the locomotor capabilities of an early cetacean in detail and providing two quantitative methods for elucidating vertebral function in fossil taxa, these studies can serve as a robust starting point for confidently assessing the evolution of swimming mode in later cetaceans and other aquatic mammals.

Chapter 1

Introduction

BACKGROUND

Vertebrates first invaded the terrestrial realm during the Devonian, more than 360 million years ago (Clack, 2009; Friedman and Brazeau, 2010). Several subsequent groups of reptiles, birds, and mammals have returned to the seas from whence their ancestors came and become readapted, to various degrees, to an aquatic lifestyle (Mazin and de Buffrénil, 2001; Uhen, 2007). Transitions between such disparate adaptive zones offer striking examples of macroevolution because they necessitate profound changes in the morphology, physiology, and behavior of the taxa involved. Yet, because the phylogenetic, ecological, environmental, and climatic contexts of each of these events were different, each transition offers a unique opportunity to study pattern and constraint in evolution, providing insight into the diversification of life on earth and the long-term structure and dynamics of terrestrial and aquatic communities.

Cetaceans are the most diverse group of secondarily aquatic mammals living today and are considered to be the most fully adapted to aquatic life, exhibiting a wide range of behaviors and occupying many different ecological niches in marine and even some freshwater communities (Berta et al., 2006). The origin of the mammalian order

Cetacea, which includes whales, dolphins, and porpoises, was long considered a mystery (e.g., Simpson, 1945), despite the fact that fossil cetaceans had been known since the early to middle 19th century (e.g., Harlan, 1834; Gibbes, 1845; Carus, 1847; Reichenbach, 1847). Until the 1970s, nearly all of the known species of fossil whales were clearly fully committed to life in the sea (Kellogg, 1928, 1936), leaving a relatively large gap in the fossil record between fully aquatic cetaceans and their purportedly terrestrial ancestors.

In the past several decades, the fossil record of early cetaceans has exploded (Table 1.1), with dozens of species of transitional whales discovered in India, Pakistan, Egypt, North America, and elsewhere (Fordyce and de Muizon, 2001; Gingerich, 2005; Uhen, 2010). Collectively, these taxa are called archaeocetes, a term used for cetaceans that lie basal to crown-group Cetacea (Odontoceti + Mysticeti; also called Neoceti). They are currently classified into five families (Pakicetidae, Ambulocetidae, Remingtonocetidae, Protocetidae, and Basilosauridae; Fig. 1.1) that are all restricted to the Eocene epoch (Fig. 1.2). These families represent different experiments in aquatic adaptation and illustrate different stages in the evolution of cetaceans from terrestrial ancestors. While much has been discovered about the origin and evolution of whales in recent years, there is still much left to learn. Study of the physiological and behavioral implications of transitional archaeocete fossils can allow us to elucidate the details of how this remarkable evolutionary event occurred.

EVOLUTION OF AQUATIC LOCOMOTION

One of the keys to understanding any land-to-sea transition involves reconstructing the evolution of aquatic locomotion. An animal's relative locomotor ability impacts many aspects of its ecology, including its ability to forage, evade predators, disperse, and migrate (Fish, 1992). Because the structural and functional requirements for efficient movement in terrestrial and aquatic environments are vastly different from one another, terrestrial mammals are typically poorly adapted for aquatic locomotion. Most terrestrial mammals have the ability to swim (Dagg and Windsor, 1972; Fish, 1992), doing so by paddling all four limbs in a modified terrestrial gait that is the most inefficient swimming mode performed by modern mammals (Williams, 1983; Fish, 1993a). Taxa well-adapted for aquatic locomotion possess adaptations that facilitate more efficient propulsion in the water, the most derived of which include limbs modified into flippers (Tarasoff et al., 1972; English, 1976; Feldkamp, 1987a) and the development of a tail fluke as a hydrofoil (Fish, 1993b, 1998a; Domning, 2000; Buchholtz, 2001; Kojeszewski and Fish, 2007).

In any evolutionary transition between land and water, early members of secondarily aquatic lineages must have possessed amphibious lifestyles, bridging the gap between their terrestrial ancestors and their aquatic descendants. Such lifestyles would have required them to maintain competence in both terrestrial and aquatic realms. But as taxa began to spend more and more time in the water, they would have begun to accumulate characteristics to facilitate that lifestyle. Assessing how and when these specialized traits evolved provides insight into the locomotor behavior of early

members of secondarily aquatic lineages, which is crucial for understanding the tempo and mode of their evolution.

Helpful insights into land-to-sea transitions can be gleaned from studying the swimming kinematics of extant mammals. Detailed studies of swimming behavior have been carried out for terrestrial and semiaquatic monotremes (Fish et al., 1997), marsupials (Fish, 1993a), artiodactyls (Coughlin and Fish, 2009), rodents (Fish, 1982a, 1982b, 1984; Fish and Baudinette, 1999), soricomorphs (Hickman, 1984), mustelid carnivores (Tarasoff et al., 1972; Williams, 1983, 1989; Fish, 1994; Fish and Baudinette, 2008), and pinnipeds (Tarasoff et al., 1972; Gordon, 1981; Feldkamp, 1987a, 1987b; Fish et al., 1988, 2003a), as well as for fully aquatic sirenians (Kojeszewski and Fish, 2007) and cetaceans (Slijper, 1961; Blake, 1983; Fish and Hui, 1991; Fish, 1993c, 1998b, 2002; Curren et al., 1994; Fish and Rohr, 1999; Skrovan et al., 1999; Yazdi et al., 1999; Rohr et al., 2002; Fish et al., 2003b; Weber et al., 2009). Based on such studies, Fish (1996, 2000, 2001) developed a model of locomotor evolution that proposes a sequence of swimming modes to bridge the gap between the quadrupedal paddling of terrestrial ancestors and the lift-based swimming modes performed by the most derived marine mammals (Fig. 1.3). Such models are certainly useful for envisioning the nature of such transitions, but, ultimately, their accuracy must be tested using the fossil record.

Relatively few studies have assessed locomotor evolution in aquatic mammals using fossil remains. Berta and Adam (2001) and Bebej (2009) studied the locomotor capabilities of fossil pinnipeds and assessed them in a phylogenetic context. Though the pictures of locomotor evolution offered by these studies were different, both

demonstrated problems with Fish's model since there appear to have been several switches between fore- and hind limb swimming modes in the history of pinnipeds. Studies of locomotor evolution across archaeocete cetaceans have generally been consistent with Fish's model (Fig. 1.4; Berta et al., 2006), but they are highly inadequate. Most treatments (Thewissen and Bajpai, 2001; Thewissen and Williams, 2002) have consisted of little more than brief reviews that inexplicably exclude taxa that are well-known skeletally, resulting in an oversimplified and potentially inaccurate picture of how swimming evolved in early whales.

One exception is a study performed by Buchholtz (1998), in which the locomotor capabilities of archaeocetes were assessed based on vertebral morphology. This study continues to provide important insights into the locomotor evolution of cetaceans, but it is already outdated. When it was published, it was essentially comprehensive in its scope, taking into account every relevant archaeocete taxon that was available. However, since then, many other more informative specimens have been discovered and described that need to be taken into account.

It must be emphasized that any assessment of locomotor evolution, no matter how wide or narrow the scope, is contingent on the functional interpretations of each individual taxon (Bebej, 2009). This presents a problem for understanding the evolution of swimming in early cetaceans because the locomotor capabilities attributed to some taxa are contentious. For example, *Pakicetus attocki* and *Ambulocetus natans* each possess features typically indicative of an immobile lumbar region (e.g., revolute zygapophyses in the former and anteroposteriorly expanded neural spines in the latter),

yet both have been interpreted as utilizing dorsoventral movements of the spine during swimming (Thewissen et al., 1994, 1996, 2001; Thewissen and Fish, 1997; Madar et al., 2002; Madar, 2007). These equivocal interpretations have taken hold in the literature, despite the fact that they are implausible and have never been quantitatively tested. In order for locomotor evolution in early cetaceans to be properly characterized, it is important to understand the constraints imposed by vertebral morphology.

CHANGES IN THE FUNCTION OF THE VERTEBRAL COLUMN

The function of the vertebral column plays a dominant role in cetacean behavior because aquatic locomotion is almost entirely dependent on it. Modern cetaceans swim via caudal oscillation (Fish, 1996), a locomotor mode in which a rigid, posteriorly-positioned appendage (the horizontally-oriented tail fluke) is oscillated in the sagittal plane to serve as the primary propulsor. Most taxa restrict these dorsoventral movements to the posterior third of the body (Fish and Hui, 1991; Fish, 1993c; Pabst, 1993, 2000; Fish et al., 2003b), with motion limited to the synclinal point anterior to the tail stock and the caudal peduncle anterior to the tail fluke (Buchholtz and Schur, 2004; Buchholtz et al., 2005). However, some taxa, including mysticetes and physeterid odontocetes, retain a more flexible spine anterior to the tail stock, which they undulate to a moderate degree during swimming (Buchholtz, 2001). In all modern cetaceans, regardless of their swimming mechanics, their vertebral columns have been greatly modified relative to the spines of terrestrial mammals.

The vertebral column of mammals typically has five subdivisions: the cervical, thoracic, lumbar, sacral, and caudal regions (Flower, 1885). The spines of modern cetaceans are so derived that is difficult to define these subdivisions, prompting some workers to use new terminology, dividing the vertebral column into neck, chest, torso, tail stock, and fluke regions (Buchholtz and Schur, 2004). Many adaptations in the spines of cetaceans involve simply modifications of vertebral morphology, such as shortening and fusion of cervical vertebrae, loss of fusion in sacral vertebrae, modification of terminal caudal vertebrae to accommodate a tail fluke, and elongation of various vertebral processes (Buchholtz et al., 2005). But, in addition, the cetacean column has undergone drastic changes in developmental modularity due to meristic, homeotic, and associational changes (Buchholtz, 2007).

The lumbar, sacral, and anterior caudal regions, in particular, have been "dramatically reconfigured" during cetacean evolution (Buchholtz and Schur, 2004, p. 392). These regions are discrete in both terrestrial mammals and the earliest cetaceans, but in fully aquatic whales, they achieve a continuity of form and function, which enables the entire post-thoracic spine to be incorporated into a single undulatory unit for swimming. The radical transformation undergone by this region of the spine is crucial to understanding the transition from foot-powered to tail-powered swimming, but the details of how it occurred have yet to be thoroughly elucidated.

The evolution of the lumbar region is especially intriguing. Models of locomotor evolution propose that early cetaceans passed through an undulatory stage of swimming, utilizing flexion and extension of a mobile vertebral column for propulsion

(Fish, 1996, 2000, 2001). However, most artiodactyls, the group from which cetaceans evolved (e.g., Gingerich et al., 2001b; Geisler et al., 2007; Spaulding et al., 2009), possess very immobile lumbar regions incapable of dorsoventral undulation (Howell, 1944; Slijper, 1946, 1947; Hildebrand, 1959; Getty, 1975; Alexander et al., 1985; Zhou et al., 1992; Gál, 1993; Grand, 1997; Boszczyk et al., 2001). Such a transition necessitates a drastic change in lumbar function early in cetacean history. An assessment of the lumbar region across multiple early archaeocetes is necessary in order to understand the functional changes in the lumbar region that preceded the eventual loss of the sacrum and the transition to a swimming mode no longer reliant on paddling of the hind limbs.

THE ARCHAEOCETE FAMILY REMINGTONOCETIDAE

Remingtonocetidae is an enigmatic family of archaeocetes known from the middle Eocene (Lutetian) of India and Pakistan. They are recognized primarily on the basis of their unusual cranial and mandibular morphology (Sahni and Mishra, 1972, 1975; Kumar and Sahni, 1986; Gingerich et al., 1995, 2001a; Bajpai and Thewissen, 1998; Thewissen and Hussain, 2000; Thewissen and Bajpai, 2009). Their crania are six times longer than they are wide across the frontals, their rostra encompass more than 60% of total skull length, and their mandibular symphyses extend back to at least P_3 (Gingerich et al., 1998).

The most widely studied member of this family is *Remingtonocetus*. This taxon possesses small orbits (Thewissen and Nummela, 2008; Bajpai et al., 2009, Fig. 5, p. 678)

and is the most basal cetacean to exhibit a hearing apparatus capable of transmitting underwater sound to the inner ear via the lower jaw and a mandibular fat pad (Nummela et al., 2004, 2007), indicating that sound played a more vital role than vision in its environmental perception (Thewissen and Nummela, 2008). In addition, *Remingtonocetus* possessed semicircular canals that were reduced in diameter, which is a characteristic of fully aquatic cetaceans (Spoor et al., 2002; Spoor and Thewissen, 2008). These cranial adaptations all suggest that *Remingtonocetus* was fairly well adapted for aquatic life, an interpretation that is corroborated by sedimentological (Gingerich et al., 1995; Bajpai et al., 2006) and isotopic (Roe et al., 1998; Clementz et al., 2006) evidence that they lived and foraged primarily in estuarine and/or near-shore marine ecosystems.

But in order to fully understand the lifestyle of remingtonocetids, their locomotor capabilities must be taken into account. Relatively little attention has been given to the postcranial skeleton, which retains many hallmarks of terrestrial ancestry. Vertebral, pelvic, and proximal hind limb elements have been recovered for several species of remingtonocetids. These indicate that they possessed relatively long necks (Gingerich et al., 1995; Bebej et al., 2007), robust limbs with evidence of some weight-bearing (Gingerich et al., 1995; Madar, 1998), and sacra composed of four fused vertebrae (Gingerich et al., 1995). But most postcranial material described to date has come from partial, disarticulated, and/or poorly preserved specimens. Nearly all assertions about locomotor mode in remingtonocetids are based on a single partial specimen of *Kutchicetus minimus*, which is very incomplete and poorly preserved (Bajpai

and Thewissen, 2000; Thewissen and Bajpai, 2009). Little can be confidently said about locomotion in remingtonocetids based on these specimens.

The best preserved remingtonocetid postcranial skeleton known to date was recovered in 2004 from the upper Domanda Formation of Pakistan. The specimen (GSP-UM 3552) belongs to the species *Remingtonocetus domandaensis* and includes a partial cranium, dentary, left innominate, and much of an articulated precaudal vertebral column. The vertebral column includes seven complete cervical vertebrae, ten partial to complete thoracic vertebrae, six complete lumbar vertebrae, and a mostly complete sacrum, which allow the vertebral function of a remingtonocetid to be studied in depth for the first time. The new specimen offers more insight into the locomotor capability of remingtonocetids than was possible before, while also providing a reliable starting point for assessing the relative functional capabilities of other early semiaquatic archaeocetes, especially protocetids, along the main line of cetacean evolution.

OVERVIEW

Reconstructing the evolution of aquatic locomotion in early cetaceans is crucial to understanding their transition from land to sea. Analysis of vertebral biomechanics offers important information about the locomotor capabilities of early whales, but little is known about vertebral function in early cetaceans. In addition, locomotor inferences based on gross morphology can be equivocal in the absence of other evidence. Filling in gaps in our knowledge of certain taxa and developing quantitative means to assess the

functional capabilities of fossil taxa are necessary to paint a clearer picture of locomotor evolution in cetaceans.

The overall aim of this dissertation is two-fold. One objective is to document and study the morphology and function of the vertebral column of *Remingtonocetus domandaensis*. This offers important insights into the functional capabilities of remingtonocetid cetaceans, filling in a critical gap in our knowledge of locomotor evolution in early whales. The other objective is to develop quantitative methods to assess vertebral function in modern and fossil mammals. These methods allow hypotheses of function based on gross morphology to be tested quantitatively, providing some degree of confidence about the validity of a given functional interpretation. Both objectives work together to constrain and clarify the evolution of aquatic locomotion in cetaceans by offering insight into early archaeocetes that have been poorly studied and developing methodologies that can more rigorously assess the functional capabilities of extinct taxa.

In Chapter 2, I begin with a systematic review of remingtonocetid archaeocetes. This synthesis summarizes the confusing taxonomic history of Remingtonocetidae, reviews the stratigraphic and geographic distributions of each taxon, highlights their diagnostic features, and compiles a list of all known specimens, including all remingtonocetid specimens collected thus far through the GSP-UM collaboration. Particular attention is paid to the remingtonocetids *Remingtonocetus domandaensis* and *Dalanistes ahmedi* in order to evaluate whether these two species are distinctly different taxa or potentially sexually-dimorphic females and males of a single species as

has been suggested (Gingerich et al., 2001a). This review clarifies the taxonomic affinity of the specimens analyzed in later chapters.

Chapter 3 includes an in-depth analysis of known vertebral morphology in *Remingtonocetus domandaensis* based primarily on GSP-UM 3552. Vertebral formulae in early archaeocetes are reviewed at length. Most of the chapter is devoted to detailed descriptions of morphology for individual vertebrae, providing diagnostic characteristics for many specific vertebral positions. The chapter concludes with functional interpretation of the spine based on probable anatomy of soft tissues derived from vertebral morphology. Interpretation of the lumbar region provides the basis for alternative hypotheses of lumbar function in the following two chapters.

Chapter 4 describes multivariate analyses of lumbar proportions in a range of modern mammals to assess the relative mobility of the lumbar spine in archaeocete cetaceans. These analyses, which follow the methodology of Gingerich (2003a), show which morphological characteristics are most indicative of a "dorsostable" or "dorsomobile" lumbar region in modern mammals, providing a quantitative means for comparing the lumbar vertebrae of archaeocetes with those of taxa whose locomotor capabilities are well-understood. These analyses focus on individual lumbar vertebrae, which means that taxa with incomplete skeletons can be included, increasing the number of fossil taxa that can be studied. The analyses here provide insight into the different functional capabilities of select Remingtonocetidae, Protocetidae, Basilosauridae, and modern cetaceans, elucidating some of the changes undergone by the vertebral column during the evolution of aquatic locomotion in archaeocetes.

Chapter 5 introduces multibody dynamic modeling as an additional method that can be used to test functional interpretations of the vertebral column. Three-dimensional virtual models of bone surfaces and reconstructed soft tissues are used to compare passive resistance to flexion and extension in the L4-L5 joints of *Remingtonocetus domandaensis* and the protocetid *Maiacetus inuus*. The range of motion possible at each of these joints is measured for a variety of soft tissue parameters to assess how sensitive the results are to soft tissue properties. Models utilizing different configurations of ligaments allow the relative contribution of each ligament in resisting movement to be assessed. The simulations highlight functional differences in the lumbar spines of *R. domandaensis* and *M. inuus*, providing additional justification for locomotor interpretations of these taxa.

Finally, in Chapter 6, I summarize the conclusions of the preceding chapters and assess their implications for the evolution of aquatic locomotion in archaeocete cetaceans.

Figure 1.1. Schematic of cetacean phylogeny focusing on proposed relationships for the five families of archaeocetes. Multiple pakicetid taxa have rarely been included in a single phylogenetic analysis. Those that have suggest that Pakicetidae may be a paraphyletic group (O'Leary, 1998; O'Leary and Uhen, 1999); however, the family has also been depicted as a monophyletic group (Uhen, 2010). Remingtonocetidae is almost certainly a monophyletic group (Uhen, 1999, 2004; Thewissen and Hussain, 2000; Uhen and Gingerich, 2001; Geisler et al., 2005), while Protocetidae has been repeatedly shown to be a paraphyletic group (O'Leary, 1999, 2001; O'Leary and Geisler, 1999; O'Leary and Uhen, 1999; Uhen, 1999, 2004; Gatesy and O'Leary, 2001; Geisler, 2001; Uhen and Gingerich, 2001; Geisler and Uhen, 2003, 2005; O'Leary et al., 2003; Geisler et al., 2005, 2007; O'Leary and Gatesy, 2008; Spaulding et al., 2009). Basilosauridae is most often found to be a paraphyletic group, with one taxon (typically *Basilosaurus*, *Zygorhiza*, or *Chrysocetus*) sister to Neoceti (O'Leary, 1999, 2001; O'Leary and Geisler, 1999; Uhen, 1999, 2004; Gatesy and O'Leary, 2001; Uhen and Gingerich, 2001; O'Leary et al., 2003; Geisler et al., 2007; O'Leary and Gatesy, 2008; Spaulding et al., 2009), though it is occasionally portrayed as the monophyletic sister group to Neoceti (O'Leary, 2001; Fitzgerald, 2010; Uhen, 2010).

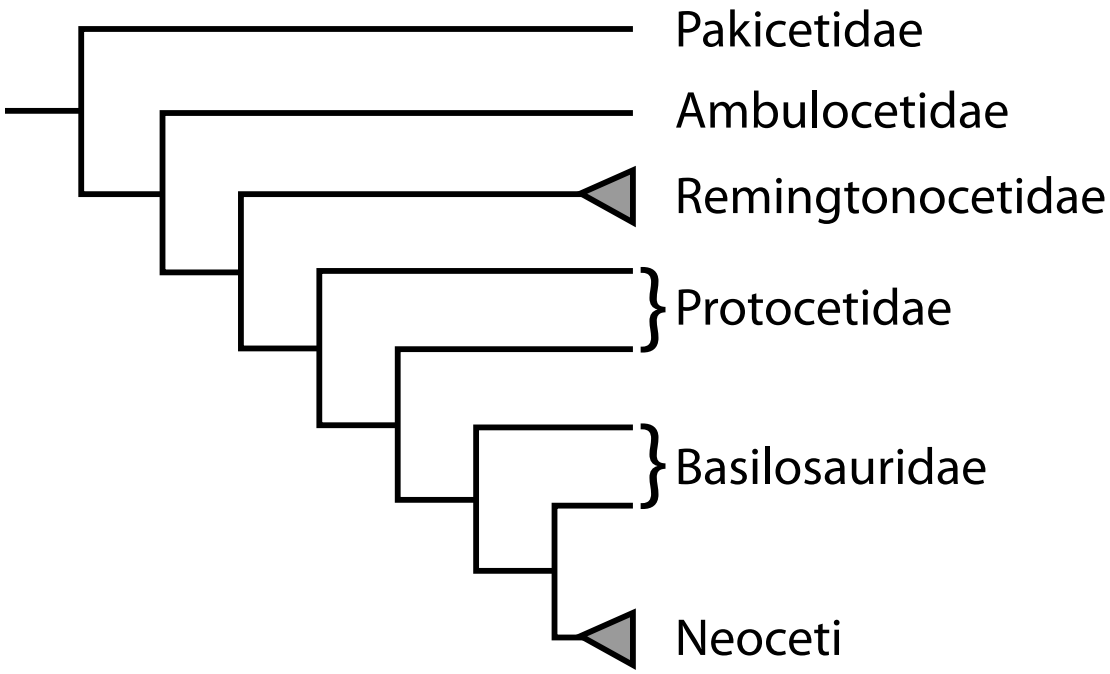

Figure 1.2. Stratigraphic ranges of select archaeocete cetaceans with proposed phylogenetic relationships. Polytomies reflect uncertainty of interrelationships. Ranges of archaeocete genera and modern cetacean suborders are denoted by gray and white bars respectively and are modified from Fordyce and de Muizon (2001) and Gingerich (2010), with additional data from other sources (Gingerich et al., 1994, 2001a, 2001b, 2009; Hulbert et al., 1998; Gingerich, 2003b; Peters et al., 2009; Bebej, this volume). The range of Odontoceti likely extends to the earliest Oligocene, but specimens documenting this have yet to be described (Uhen, 2010). Geologic time scale follows Walker and Geissman (2009). Abbreviations: *E.*, Early; *L.*, Late; *Plio.*, Pliocene; *Q.*, Quaternary.

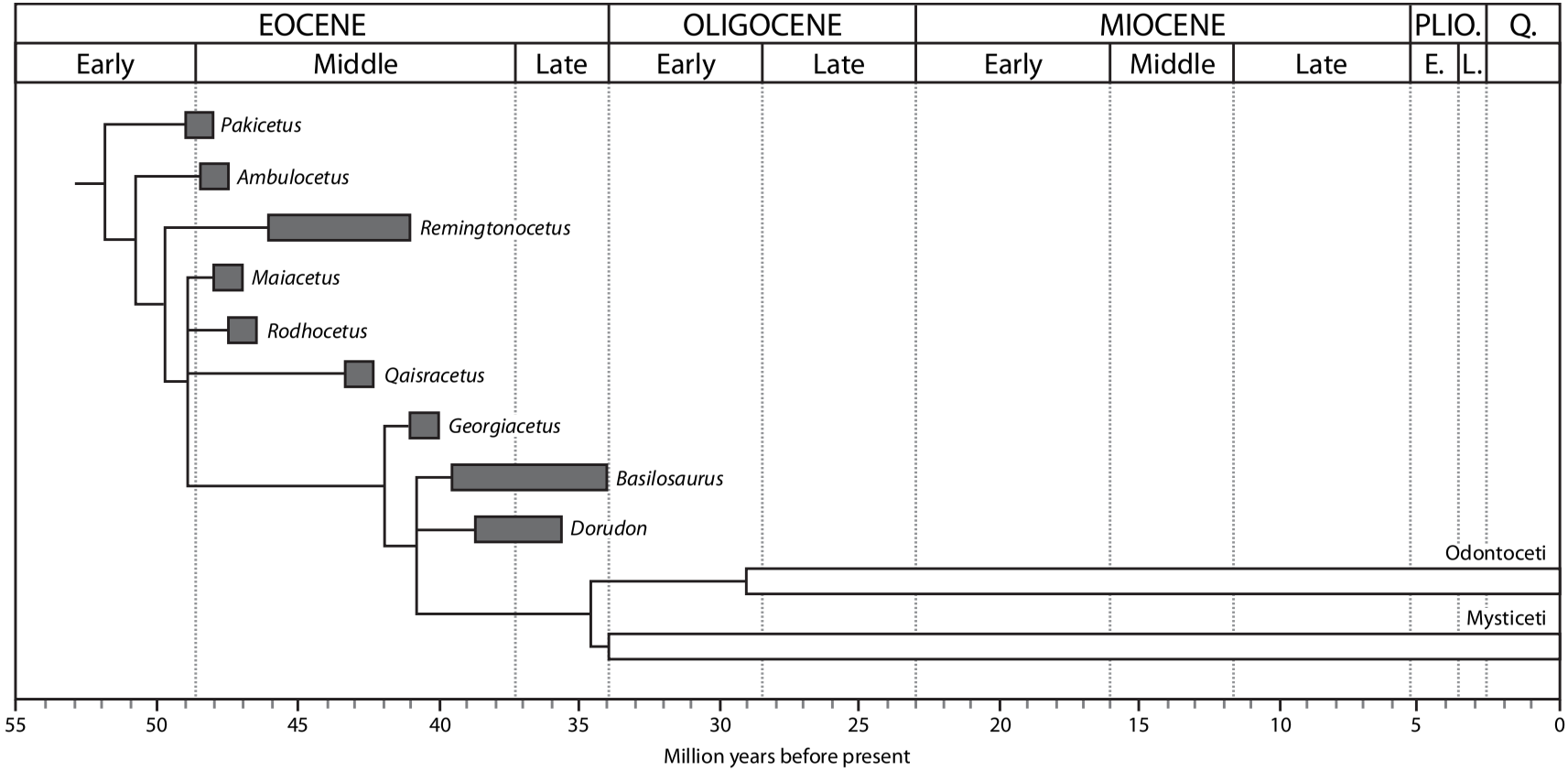

Figure 1.3. Hypothetical model for the evolution of aquatic locomotion in secondarily aquatic mammals. The schematic is modified from Fish (1996, 2000, 2001). Taxa in boxes represent examples of modern mammals that swim using the indicated swimming mode. The terrestrial ancestor of cetaceans likely swam using quadrupedal paddling. Subsequent semiaquatic cetaceans are proposed to have passed through stages utilizing alternate pelvic paddling, simultaneous pelvic paddling, and dorsoventral undulation, before evolving to use caudal oscillation in the most derived forms.

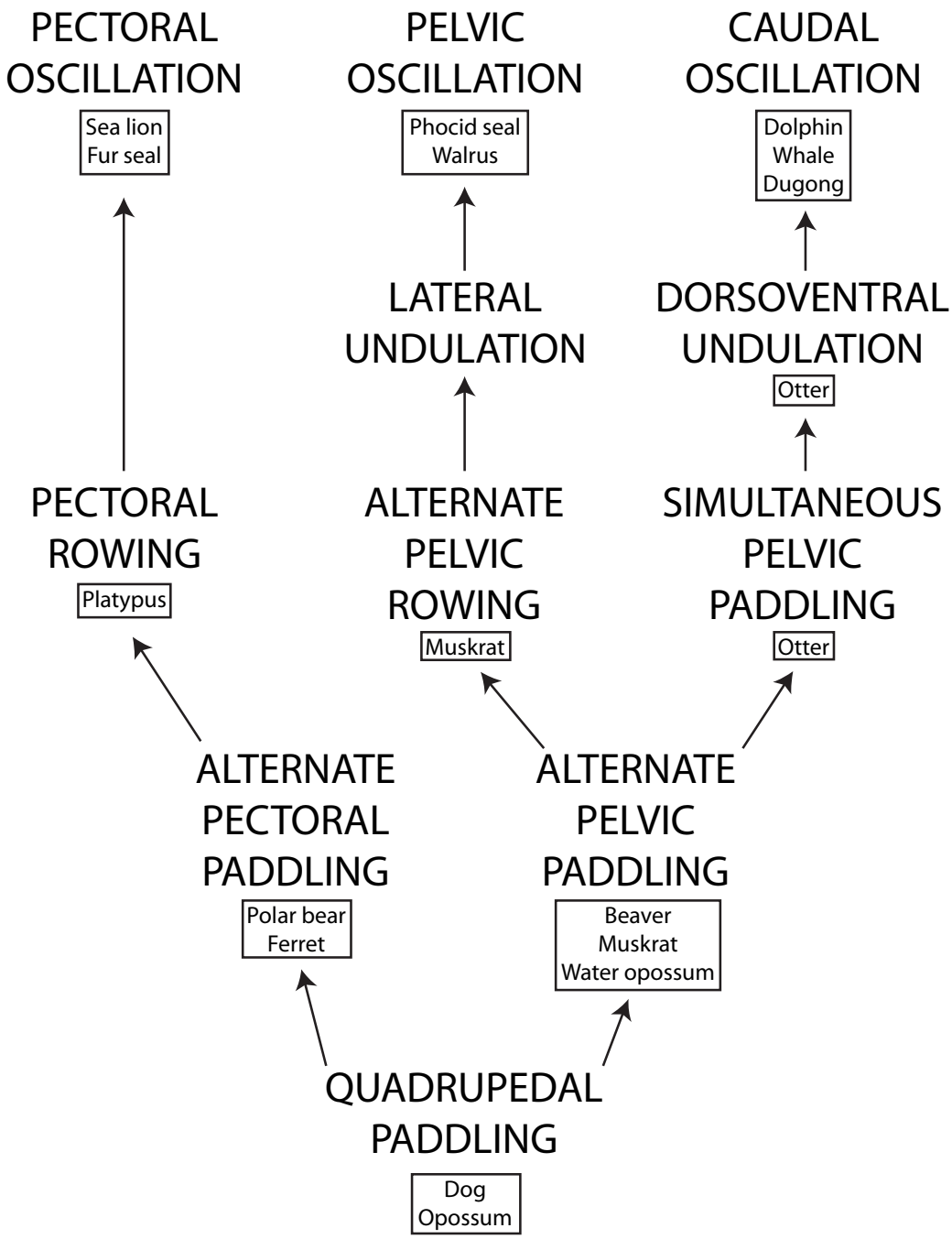

Figure 1.4. A representative portrayal of locomotor evolution in early cetaceans. This depiction, which is modified from Berta et al. (2006) and based on studies by Thewissen and Bajpai (2001) and Thewissen and Williams (2002), is an oversimplification that paints an inaccurate picture of locomotor evolution. Several protocetid and basilosaurid taxa with good skeletal remains are not included in these depictions, while locomotor interpretations are presented for taxa (e.g., *Kutchicetus*) based on very scant remains (Bajpai and Thewissen, 2000).

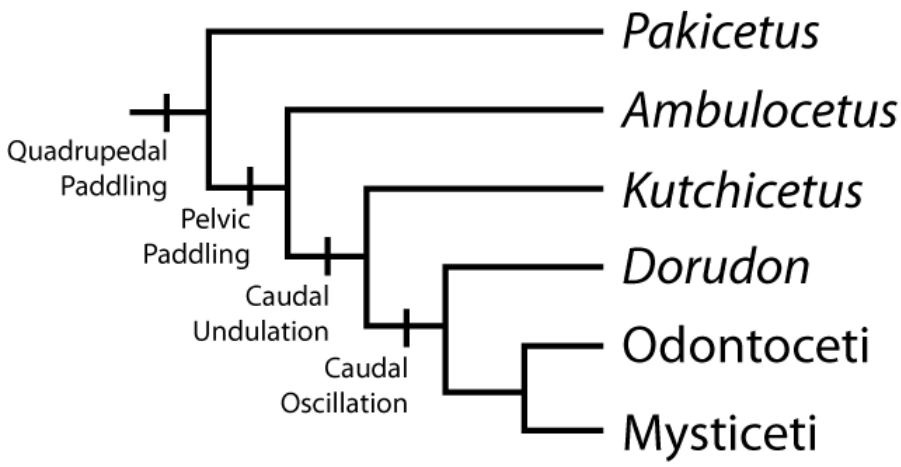

Table 1.1. Consensus classification of archaeocete families and species described to date. This taxonomy generally follows Uhen (2010). Of the 48 known species of archaeocetes, 37 have been described since 1972. The enigmatic genus *Kekenodon* has been considered an archaeocete by some (Mitchell, 1989; Uhen, 2010), but its phylogenetic position as an archaeocete or a stem neocete (Fordyce and de Muizon, 2001; Fitzgerald, 2010) is currently unknown. It is here provisionally viewed as a stem neocete, pending the recovery of additional remains that demonstrate otherwise.

Pakicetidae (6)

- *Ichthyolestes pinfoldi* (Dehm and Oettingen-Spielberg, 1958)[a]
- *Nalacetus ratimitus* (Thewissen and Hussain, 1998)
- *Pakicetus attocki* (West, 1980)
- *Pakicetus calcis* (Cooper et al., 2009)
- *Pakicetus chittas* (Cooper et al., 2009)
- *Pakicetus inachus* (Gingerich and Russell, 1981)

Ambulocetidae (3)

- *Ambulocetus natans* (Thewissen et al., 1994)
- *Gandakasia potens* (Dehm and Oettingen-Spielberg, 1958)[a]
- *Himalayacetus subathuensis* (Bajpai and Gingerich, 1998)[b]

Remingtonocetidae (6)

- *Andrewsiphius sloani* (Sahni and Mishra, 1972)
- *Attockicetus praecursor* (Thewissen and Hussain, 2000)
- *Dalanistes ahmedi* (Gingerich et al., 1995)
- *Kutchicetus minimus* (Bajpai and Thewissen, 2000)
- *Remingtonocetus domandaensis* (Gingerich et al., 2001a)
- *Remingtonocetus harudiensis* (Sahni and Mishra, 1975)

Notes:

[a] Originally described as Mesonychia

[b] Assigned to Pakicetidae by Bajpai and Gingerich (1998)

[c] Assigned to Basilosauridae by Bajpai and Thewissen (1998)

Protocetidae (20)

- *Artiocetus clavis* (Gingerich et al., 2001b)
- *Babiacetus indicus* (Trivedy and Satsangi, 1984)
- *Babiacetus mishrai* (Bajpai and Thewissen, 1998)
- *Carolinacetus gingerichi* (Geisler et al., 2005)
- *Crenatocetus rayi* (McLeod and Barnes, 2008)
- *Eocetus schweinfurthi* (Fraas, 1904)
- *Eocetus wardii* (Uhen, 1999)
- *Gaviacetus razai* (Gingerich et al., 1995)[c]
- *Gaviacetus sahnii* (Bajpai and Thewissen, 1998)[c]
- *Georgiacetus vogtlensis* (Hulbert et al., 1998)
- *Indocetus ramani* (Sahni and Mishra, 1975)
- *Maiacetus inuus* (Gingerich et al., 2009)
- *Makaracetus bidens* (Gingerich et al., 2005)
- *Natchitochia jonesi* (Uhen, 1998)
- *Pappocetus lugardi* (Andrews, 1920)
- *Protocetus atavus* (Fraas, 1904)
- *Qaisracetus arifi* (Gingerich et al., 2001a)
- *Rodhocetus balochistanensis* (Gingerich et al., 2001b)
- *Rodhocetus kasranii* (Gingerich et al., 1994)
- *Takracetus simus* (Gingerich et al., 1995)

Basilosauridae (13)

- *Ancalecetus simonsi* (Gingerich and Uhen, 1996)
- *Basilosaurus cetoides* (Harlan, 1834)
- *Basilosaurus drazindai* (Gingerich et al., 1997)
- *Basilosaurus isis* (Andrews, 1904)
- *Basiloterus hussaini* (Gingerich et al., 1997)
- *Chrysocetus healyorum* (Uhen and Gingerich, 2001)
- *Cynthiacetus maxwelli* (Uhen, 2005)
- *Dorudon atrox* (Andrews, 1906)
- *Dorudon serratus* (Gibbes, 1845)
- *Masracetus markgrafi* (Gingerich, 2007)
- *Saghacetus osiris* (Dames, 1894)
- *Stromerius nidensis* (Gingerich, 2007)
- *Zygorhiza kochii* (Reichenbach, 1847)

REFERENCES

Alexander, R. M., N. J. Dimery, and R. F. Ker. 1985. Elastic structures in the back and their role in galloping in some mammals. Journal of Zoology (London) 207: 467-482.

Andrews, C. W. 1904. Further notes on the mammals of the Eocene of Egypt, part III. Geological Magazine Series V 1: 211-215.

Andrews, C. W. 1906. A descriptive catalogue of the Tertiary Vertebrata of the Fayum, Egypt. British Museum of Natural History, London, 324 pp.

Andrews, C. W. 1920. A description of new species of zeuglodont and of leathery turtle from the Eocene of southern Nigeria. Proceedings of the Zoological Society of London for 1919 (no volume number): 309-319.

Bajpai, S., and P. D. Gingerich. 1998. A new Eocene archaeocete (Mammalia, Cetacea) from India and the time of origin of whales. Proceedings of the National Academy of Sciences of the United States of America 95: 15464-15468.

Bajpai, S., and J. G. M. Thewissen. 1998. Middle Eocene cetaceans from the Harudi and Subathu Formations of India. Pp. 213-233 in J. G. M. Thewissen (ed.), The Emergence of Whales: Evolutionary Patterns in the Origin of Cetacea. Plenum Press, New York.

Bajpai, S., and J. G. M. Thewissen. 2000. A new, diminutive Eocene whale from Kachchh (Gujarat, India) and its implications for locomotor evolution of cetaceans. Current Science 79: 1478-1482.

Bajpai, S., J. G. M. Thewissen, V. V. Kapur, B. N. Tiwari, and A. Sahni. 2006. Eocene and Oligocene sirenians (Mammalia) from Kachchh, India. Journal of Vertebrate Paleontology 26: 400-410.

Bajpai, S., J. G. M. Thewissen, and A. Sahni. 2009. The origin and early evolution of whales: macroevolution documented on the Indian subcontinent. Journal of Biosciences 34: 673-686.

Bebej, R. M. 2009. Swimming mode inferred from skeletal proportions in the fossil pinnipeds *Enaliarctos* and *Allodesmus* (Mammalia, Carnivora). Journal of Mammalian Evolution 16: 77-97.

Bebej, R. M., M. ul-Haq, I. S. Zalmout, and P. D. Gingerich. 2007. Functional interpretation of the neck in Eocene *Remingtonocetus* from Pakistan (Mammalia, Cetacea, Archaeoceti). Journal of Vertebrate Paleontology 27: 45A.

Berta, A., and P. J. Adam. 2001. Evolutionary biology of pinnipeds. Pp. 235-260 in J.-M. Mazin and V. de Buffrénil (eds.), Secondary Adaptation of Tetrapods to Life in Water. Verlag Dr. Friedrich Pfeil, München.

Berta, A., J. L. Sumich, and K. M. Kovacs. 2006. Marine Mammals: Evolutionary Biology. 2nd Edition. Academic Press, San Diego.

Blake, R. W. 1983. Energetics of leaping in dolphins and other aquatic animals. Journal of the Marine Biological Association of the United Kingdom 63: 61-70.

Boszczyk, B. M., A. A. Boszczyk, and R. Putz. 2001. Comparative and functional anatomy of the mammalian lumbar spine. The Anatomical Record 264: 157-168.

Buchholtz, E. A. 1998. Implications of vertebral morphology for locomotor evolution in early Cetacea. Pp. 325-351 in J. G. M. Thewissen (ed.), The Emergence of Whales: Evolutionary Patterns in the Origin of Cetacea. Plenum Press, New York.

Buchholtz, E. A. 2001. Vertebral osteology and swimming style in living and fossil whales (Order: Cetacea). Journal of Zoology (London) 253: 175-190.

Buchholtz, E. A. 2007. Modular evolution of the cetacean vertebral column. Evolution & Development 9: 278-289.

Buchholtz, E. A., and S. A. Schur. 2004. Vertebral osteology in Delphinidae (Cetacea). Zoological Journal of the Linnean Society 104: 383-401.

Buchholtz, E. A., E. M. Wolkovich, and R. J. Cleary. 2005. Vertebral osteology and complexity in *Lagenorhynchus acutus* (Delphinidae) with comparison to other delphinoid genera. Marine Mammal Science 21: 411-428.

Carus, C. G. 1847. Resultate geologischer, anatomischer und zoologischer Untersuchungen über das unter dem Namen *Hydrarchos* von Dr. A. C. Koch zuerst nach Europa gebrachte und in Dresden angestellte grosse fossile Skelett. Arnoldische Buchhandlung, Dresden and Leipzig, 15 pp.

Clack, J. A. 2009. The fish-tetrapod transition: new fossils and interpretations. Evolution: Education and Outreach 2: 213-223.

Clementz, M. T., A. Goswami, P. D. Gingerich, and P. L. Koch. 2006. Isotopic records from early whales and sea cows: contrasting patterns of ecological transition. Journal of Vertebrate Paleontology 26: 355-370.

Cooper, L. N., J. G. M. Thewissen, and S. T. Hussain. 2009. New middle Eocene archaeocetes (Cetacea: Mammalia) from the Kuldana Formation of northern Pakistan. Journal of Vertebrate Paleontology 29: 1289-1299.

Coughlin, B. L., and F. E. Fish. 2009. Hippopotamus underwater locomotion: reduced-gravity movements for a massive mammal. Journal of Mammalogy 90: 675-679.

Curren, K., N. Bose, and J. Lien. 1994. Swimming kinematics of a harbor porpoise (*Phocoena phocoena*) and an atlantic white-sided dolphin (*Lagenorhynchus acutus*). Marine Mammal Science 10: 485-492.

Dagg, A. I., and D. E. Windsor. 1972. Swimming in northern terrestrial mammals. Canadian Journal of Zoology 50: 117-130.

Dames, W. B. 1894. Über Zeuglodonten aus Aegypten und die Beziehungen der Archaeoceten zu den übrigen Cetaceen. Paläontologische Abhandlungen, Jena, Neue Folge 1: 189-222.

Dehm, R., and T. z. Oettingen-Spielberg. 1958. Palëontologische und geologische Untersuchungen im Tertiär von Pakistan. 2. Die mitteleocänen Säugetiere von Ganda Kas bei Basal in Nordwest-Pakistan. Abhandlungen der Bayerische Akademie der Wissenschaften, Mathematisch-Naturwissenschaftliche Klasse, München, Neue Folge 91: 1-54.

Domning, D. P. 2000. The readaptation of Eocene sirenians to life in water. Historical Biology 14: 115-119.

English, A. W. 1976. Functional anatomy of the hands of fur seals and sea lions. American Journal of Anatomy 147: 1-18.

Feldkamp, S. D. 1987a. Foreflipper propulsion in the California sea lion, *Zalophus californianus*. Journal of Zoology (London) 212: 43-57.

Feldkamp, S. D. 1987b. Swimming in the California sea lion: morphometrics, drag, and energetics. Journal of Experimental Biology 131: 117-135.

Fish, F. E. 1982a. Aerobic energetics of surface swimming in the muskrat *Ondatra zibethicus*. Physiological Zoology 55: 180-189.

Fish, F. E. 1982b. Function of the compressed tail of surface swimming muskrats (*Ondatra zibethicus*). Journal of Mammalogy 63: 591-597.

Fish, F. E. 1984. Mechanics, power output and efficiency of the swimming muskrat (*Ondatra zibethicus*). Journal of Experimental Biology 110: 183-201.

Fish, F. E. 1992. Aquatic locomotion. Pp. 34-63 in T. E. Tomasi and T. H. Horton (eds.), Mammalian Energetics: Interdisciplinary Views of Metabolism and Reproduction. Cornell University Press, Ithaca.

Fish, F. E. 1993a. Comparison of swimming kinematics between terrestrial and semiaquatic opossums. Journal of Mammalogy 74: 275-284.

Fish, F. E. 1993b. Influence of hydrodynamic design and propulsive mode on mammalian swimming energetics. Australian Journal of Zoology 42: 79-101.

Fish, F. E. 1993c. Power output and propulsive efficiency of swimming bottlenose dolphins (*Tursiops truncatus*). Journal of Experimental Biology 185: 179-193.

Fish, F. E. 1994. Association of propulsive swimming mode with behavior in river otters (*Lutra canadensis*). Journal of Mammalogy 75: 989-997.

Fish, F. E. 1996. Transitions from drag-based to lift-based propulsion in mammalian swimming. American Zoologist 36: 628-641.

Fish, F. E. 1998a. Biomechanical perspective on the origin of cetacean flukes. Pp. 303-324 in J. G. M. Thewissen (ed.), The Emergence of Whales: Evolutionary Patterns in the Origin of Cetacea. Plenum Press, New York.

Fish, F. E. 1998b. Comparative kinematics and hydrodynamics of odontocete cetaceans: morphological and ecological correlates with swimming performance. Journal of Experimental Biology 201: 2867-2877.

Fish, F. E. 2000. Biomechanics and energetics in aquatic and semiaquatic mammals: platypus to whale. Physiological and Biochemical Zoology 73: 683-698.

Fish, F. E. 2001. A mechanism for evolutionary transition in swimming mode by mammals. Pp. 261-287 in J.-M. Mazin and V. de Buffrénil (eds.), Secondary Adaptation of Tetrapods to Life in Water. Verlag Dr. Friedrich Pfeil, München.

Fish, F. E. 2002. Balancing requirements for stability and maneuverability in cetaceans. Integrative and Comparative Biology 42: 85-93.

Fish, F. E., and R. V. Baudinette. 1999. Energetics of locomotion by the Australian water rat (*Hydromys chrysogaster*): a comparison of swimming and running in a semi-aquatic mammal. Journal of Experimental Biology 202: 353-363.

Fish, F. E., and R. V. Baudinette. 2008. Energetics of swimming by the ferret: consequences of forelimb paddling. Comparative Biochemistry and Physiology, Part A 150: 136-143.

Fish, F. E., R. V. Baudinette, P. B. Frappell, and M. P. Sarre. 1997. Energetics of swimming by the platypus (*Ornithorhynchus anatinus*): metabolic effort associated with rowing. Journal of Experimental Biology 200: 2647-2652.

Fish, F. E., and C. A. Hui. 1991. Dolphin swimming - A review. Mammal Review 21: 181-195.

Fish, F. E., J. Hurley, and D. P. Costa. 2003a. Maneuverability by the sea lion *Zalophus californianus*: turning performance of an unstable body design. Journal of Experimental Biology 206: 667-674.

Fish, F. E., S. Innes, and K. Ronald. 1988. Kinematics and estimated thrust production of swimming harp and ringed seals. Journal of Experimental Biology 137: 157-173.

Fish, F. E., J. E. Peacock, and J. J. Rohr. 2003b. Stabilization mechanism in swimming odontocete cetaceans by phased movements. Marine Mammal Science 19: 515-528.

Fish, F. E., and J. J. Rohr. 1999. Review of dolphin hydrodynamics and swimming performance. SPAWAR Systems Center Technical Report 1801, San Diego, 137 pp.

Fitzgerald, E. M. G. 2010. The morphology and systematics of *Mammalodon colliveri* (Cetacea: Mysticeti), a toothed mysticete from the Oligocene of Australia. Zoological Journal of the Linnean Society 158: 367-476.

Flower, W. H. 1885. An Introduction to the Osteology of the Mammalia. 3rd Edition. Macmillan and Company, London, 382 pp.

Fordyce, R. E., and C. de Muizon. 2001. Evolutionary history of cetaceans: a review. Pp. 169-233 in J.-M. Mazin and V. de Buffrénil (eds.), Secondary Adaptation of Tetrapods to Life in Water. Verlag Dr. Friedrich Pfeil, München.

Fraas, E. 1904. Neue Zeuglodonten aus dem unteren Mitteleocän vom Mokattam bei Cairo. Geologische und Paläontologische Abhandlungen, Neue Folge 6: 199-220.

Friedman, M., and M. D. Brazeau. 2010. Sequences, stratigraphy and scenarios: what can we say about the fossil record of the earliest tetrapods? Proceedings of the Royal Society B 278: 432-439.

Gál, J. M. 1993. Mammalian spinal biomechanics: I. Static and dynamic mechanical properties of intact intervertebral joints. Journal of Experimental Biology 174: 247-280.

Gatesy, J., and M. A. O'Leary. 2001. Deciphering whale origins with molecules and fossils. Trends in Ecology and Evolution 16: 562-570.

Geisler, J. H. 2001. New morphological evidence for the phylogeny of Artiodactyla, Cetacea, and Mesonychidae. American Museum Novitates 3344: 1-53.

Geisler, J. H., A. E. Sanders, and Z. Luo. 2005. A new protocetid whale (Cetacea: Archaeoceti) from the late middle Eocene of South Carolina. American Museum Novitates 3480: 1-65.

Geisler, J. H., J. M. Theodor, M. D. Uhen, and S. E. Foss. 2007. Phylogenetic relationships of cetaceans to terrestrial artiodactyls. Pp. 19-31 in D. R. Prothero and S. E. Foss (eds.), The Evolution of Artiodactyls. Johns Hopkins University Press, Baltimore.

Geisler, J. H., and M. D. Uhen. 2003. Morphological support for a close relationship between hippos and whales. Journal of Vertebrate Paleontology 23: 991-996.

Geisler, J. H., and M. D. Uhen. 2005. Phylogenetic relationships of extinct cetartiodactyls: results of simultaneous analyses of molecular, morphological, and stratigraphic data. Journal of Mammalian Evolution 12: 145-160.

Getty, R. ed 1975. Sisson and Grossman's the Anatomy of the Domestic Animals. W.B. Saunders Company, Philadelphia.

Gibbes, R. W. 1845. Description of the teeth of a new fossil animal found in the green sand of South Carolina. Proceedings of the Academy of Natural Sciences of Philadelphia 2: 254-256.

Gingerich, P. D. 2003a. Land-to-sea transition in early whales: evolution of Eocene Archaeoceti (Cetacea) in relation to skeletal proportions and locomotion of living semiaquatic mammals. Paleobiology 29: 429-454.

Gingerich, P. D. 2003b. Stratigraphic and micropaleontological constraints on the middle Eocene age of the mammal-bearing Kuldana Formation of Pakistan. Journal of Vertebrate Paleontology 23: 643-651.

Gingerich, P. D. 2005. Cetacea. Pp. 234-252 in K. D. Rose and J. D. Archibald (eds.), The Rise of Placental Mammals: Origins and Relationships of the Major Extant Clades. John Hopkins University Press, Baltimore.

Gingerich, P. D. 2007. *Stromerius nidensis*, new archaeocete (Mammalia, Cetacea) from the upper Eocene Qasr El-Sagha Formation, Fayum, Egypt. Contributions from the Museum of Paleontology, University of Michigan 31: 363-378.

Gingerich, P. D. 2010. Cetacea. Pp. 873-899 in L. Werdelin and W. J. Sanders (eds.), Cenozoic Mammals of Africa. University of California Press, Berkeley.

Gingerich, P. D., M. Arif, M. A. Bhatti, M. Anwar, and W. J. Sanders. 1997. *Basilosaurus drazindai* and *Basiloterus hussaini*, new Archaeoceti (Mammalia, Cetacea) from the middle Eocene Drazinda Formation, with a revised interpretation of ages of whale-bearing strata in the Kirthar Group of the Sulaiman Range, Punjab (Pakistan). Contributions from the Museum of Paleontology, University of Michigan 30: 55-81.

Gingerich, P. D., M. Arif, M. A. Bhatti, and W. C. Clyde. 1998. Middle Eocene stratigraphy and marine mammals (Mammalia: Cetacea and Sirenia) of the Sulaiman Range, Pakistan. Bulletin of the Carnegie Museum of Natural History 34: 239-259.

Gingerich, P. D., M. Arif, and W. C. Clyde. 1995. New archaeocetes (Mammalia, Cetacea) from the middle Eocene Domanda Formation of the Sulaiman Range, Punjab (Pakistan). Contributions from the Museum of Paleontology, University of Michigan 29: 291-330.

Gingerich, P. D., S. M. Raza, M. Arif, M. Anwar, and X. Zhou. 1994. New whale from the Eocene of Pakistan and the origin of cetacean swimming. Nature 368: 844-847.

Gingerich, P. D., and D. E. Russell. 1981. *Pakicetus inachus*, a new archaeocete (Mammalia, Cetacea) from the early-middle Eocene Kuldana Formation of Kohat (Pakistan). Contributions from the Museum of Paleontology, University of Michigan 25: 235-246.

Gingerich, P. D., and M. D. Uhen. 1996. *Ancalecetus simonsi*, a new dorudontine archaeocete (Mammalia, Cetacea) from the early late Eocene of Wadi Hitan, Egypt. Contributions from the Museum of Paleontology, University of Michigan 29: 359-401.

Gingerich, P. D., M. ul-Haq, I. H. Khan, and I. S. Zalmout. 2001a. Eocene stratigraphy and archaeocete whales (Mammalia, Cetacea) of Drug Lahar in the eastern Sulaiman Range, Balochistan (Pakistan). Contributions from the Museum of Paleontology, University of Michigan 30: 269-319.

Gingerich, P. D., M. ul-Haq, W. von Koenigswald, W. J. Sanders, B. H. Smith, and I. S. Zalmout. 2009. New protocetid whale from the middle Eocene of Pakistan: birth on land, precocial development, and sexual dimorphism. PLoS ONE 4: e4366.

Gingerich, P. D., M. ul-Haq, I. S. Zalmout, I. H. Khan, and M. S. Malkani. 2001b. Origin of whales from early artiodactyls: hands and feet of Eocene Protocetidae from Pakistan. Science 293: 2239-2242.

Gingerich, P. D., I. S. Zalmout, M. ul-Haq, and M. A. Bhatti. 2005. *Makaracetus bidens*, a new protocetid archaeocete (Mammalia, Cetacea) from the early middle Eocene of Balochistan (Pakistan). Contributions from the Museum of Paleontology, University of Michigan 31: 197-210.

Gordon, K. R. 1981. Locomotor behaviour of the walrus (*Odobenus*). Journal of Zoology (London) 195: 349-367.

Grand, T. I. 1997. How muscle mass is part of the fabric of behavioral ecology in East African bovids (*Madoqua*, *Gazella*, *Damaliscus*, *Hippotragus*). Anatomy and Embryology 195: 375-386.

Harlan, R. 1834. Notice of fossil bones found in the Tertiary formation of the state of Louisiana. Transactions of the American Philosophical Society 4: 397-403.

Hickman, G. C. 1984. Swimming ability of talpid moles, with particular reference to the semi-aquatic *Condylura cristata*. Mammalia 48: 505-513.

Hildebrand, M. 1959. Motions of the running cheetah and horse. Journal of Mammalogy 40: 481-495.

Howell, A. B. 1944. Speed in Animals: Their Specializations for Running and Leaping. University of Chicago Press, Chicago, 270 pp.

Hulbert, R. C., Jr., R. M. Petkewich, G. A. Bishop, D. Bukry, and D. P. Aleshire. 1998. A new middle Eocene protocetid whale (Mammalia: Cetacea: Archaeoceti) and associated biota from Georgia. Journal of Paleontology 72: 907-927.

Kellogg, R. 1928. The history of whales - Their adaptation to life in the water. The Quarterly Review of Biology 3: 29-76.

Kellogg, R. 1936. A review of the Archaeoceti. Carnegie Institute of Washington Publication 482: 1-366.

Kojeszewski, T., and F. E. Fish. 2007. Swimming kinematics of the Florida manatee (*Trichechus manatus latirostris*): hydrodynamic analysis of an undulatory mammalian swimmer. Journal of Experimental Biology 210: 2411-2418.

Kumar, K., and A. Sahni. 1986. *Remingtonocetus harudiensis*, new combination, a middle Eocene archaeocete (Mammalia, Cetacea) from western Kutch, India. Journal of Vertebrate Paleontology 6: 326-349.

Madar, S. I. 1998. Structural adaptations of early archaeocete long bones. Pp. 353-378 in J. G. M. Thewissen (ed.), The Emergence of Whales: Evolutionary Patterns in the Origin of Cetacea. Plenum Press, New York.

Madar, S. I. 2007. The postcranial skeleton of early Eocene pakicetid cetaceans. Journal of Paleontology 81: 176-200.

Madar, S. I., J. G. M. Thewissen, and S. T. Hussain. 2002. Additional holotype remains of *Ambulocetus natans* (Cetacea, Ambulocetidae), and their implications for locomotion in early whales. Journal of Vertebrate Paleontology 22: 405-422.

Mazin, J.-M., and V. de Buffrénil eds. 2001. Secondary Adaptation of Tetrapods to Life in Water. Verlag Dr. Friedrich Pfeil, München.

McLeod, S. A., and L. G. Barnes. 2008. A new genus and species of Eocene protocetid archaeocete whale (Mammalia, Cetacea) from the Atlantic Coastal Plain. Science Series, Natural History Museum of Los Angeles County 41: 73-98.

Mitchell, E. D. 1989. A new cetacean from the late Eocene La Meseta Formation, Seymour Island, Antarctic Peninsula. Canadian Journal of Fisheries and Aquatic Sciences 46: 2219-2235.

Nummela, S., J. G. M. Thewissen, S. Bajpai, S. T. Hussain, and K. Kumar. 2004. Eocene evolution of whale hearing. Nature 430: 776-778.

Nummela, S., J. G. M. Thewissen, S. Bajpai, S. T. Hussain, and K. Kumar. 2007. Sound transmission in archaic and modern whales: anatomical adaptations for underwater hearing. The Anatomical Record 290: 716-733.

O'Leary, M. A. 1998. Phylogenetic and morphometric reassessment of the dental evidence for a mesonychian and cetacean clade. Pp. 133-161 in J. G. M. Thewissen (ed.), The Emergence of Whales: Evolutionary Patterns in the Origin of Cetacea. Plenum Press, New York.

O'Leary, M. A. 1999. Parsimony analysis of total evidence from extinct and extant taxa and the cetacean-artiodactyl question (Mammalia, Ungulata). Cladistics 15: 315-330.

O'Leary, M. A. 2001. The phylogenetic position of cetaceans: further combined data analyses, comparisons with the stratigraphic record and a discussion of character optimization. American Zoologist 41: 487-506.

O'Leary, M. A., and J. Gatesy. 2008. Impact of increased character sampling on the phylogeny of Cetartiodactyla (Mammalia): combined analysis including fossils. Cladistics 24: 397-442.

O'Leary, M. A., J. Gatesy, and M. J. Novacek. 2003. Are the dental data really at odds with the molecular data? Morphological evidence for whale phylogeny (re)reexamined. Systematic Biology 52: 853-864.

O'Leary, M. A., and J. H. Geisler. 1999. The position of Cetacea within Mammalia: phylogenetic analysis of morphological data from extinct and extant taxa. Systematic Biology 48: 455-490.

O'Leary, M. A., and M. D. Uhen. 1999. The time of origin of whales and the role of behavioral changes in the terrestrial-aquatic transition. Paleobiology 25: 534-556.

Pabst, D. A. 1993. Intramuscular morphology and tendon geometry of the epaxial swimming muscles of dolphins. Journal of Zoology (London) 230: 159-176.

Pabst, D. A. 2000. To bend a dolphin: convergence of force transmission designs in cetaceans and scombrid fishes. American Zoologist 40: 146-155.

Peters, S. E., M. S. M. Antar, I. S. Zalmout, and P. D. Gingerich. 2009. Sequence stratigraphic control on preservation of late Eocene whales and other vertebrates at Wadi Al-Hitan, Egypt. Palaios 24: 290-302.

Reichenbach, H. G. L. 1847. Systematisches. Pp. 13-15 in C. G. Carus (ed.), Resultate geologischer, anatomischer und zoologischer Untersuchungen über das unter dem Namen *Hydrarchos* von Dr. A. C. Koch zuerst nach Europa gebrachte und in Dresden angestellte grosse fossile Skelett. Arnoldische Buchlandlung, Dresden and Leipzig.

Roe, L. J., J. G. M. Thewissen, J. Quade, J. R. O'Neil, S. Bajpai, A. Sahni, and S. T. Hussain. 1998. Isotopic approaches to understanding the terrestrial-to-marine transition of the earliest cetaceans. Pp. 399-422 in J. G. M. Thewissen (ed.), The Emergence of Whales: Evolutionary Patterns in the Origin of Cetacea, New York.

Rohr, J. J., F. E. Fish, and J. W. Gilpatrick, Jr. 2002. Maximum swimming speeds of captive and free-ranging delphinids: critical analysis of extraordinary performance. Marine Mammal Science 18: 1-19.

Sahni, A., and V. P. Mishra. 1972. A new species of *Protocetus* (Cetacea) from the middle Eocene of Kutch, western India. Palaeontology 15: 490-495.

Sahni, A., and V. P. Mishra. 1975. Lower Tertiary vertebrates from western India. Monograph of the Palaeontological Society of India 3: 1-48.

Simpson, G. G. 1945. The principles of classification and a classification of mammals. Bulletin of the American Museum of Natural History 85: 1-350.

Skrovan, R. C., T. M. Williams, P. S. Berry, P. W. Moore, and R. W. Davis. 1999. The diving physiology of bottlenose dolphins (*Tursiops truncatus*). II. Biomechanics and changes in buoyancy at depth. Journal of Experimental Biology 202: 2749-2761.

Slijper, E. J. 1946. Comparative biologic-anatomical investigations on the vertebral column and spinal musculature of mammals. Verhandelingen der Koninklijke Nederlandsche Akademie van Wetenschappen, Afdeling Natuurkunde, Tweede Sectie 42: 1-128.

Slijper, E. J. 1947. Observations on the vertebral column of the domestic animals. The Veterinary Journal 103: 376-387.

Slijper, E. J. 1961. Locomotion and locomotory organs in whales and dolphins (Cetacea). Symposia of the Zoological Society of London 5: 77-94.

Spaulding, M., M. A. O'Leary, and J. Gatesy. 2009. Relationships of Cetacea (Artiodactyla) among mammals: increased taxon sampling alters interpretations of key fossils and character evolution. PLoS ONE 4: e7062.

Spoor, F., S. Bajpai, S. T. Hussain, K. Kumar, and J. G. M. Thewissen. 2002. Vestibular evidence for the evolution of aquatic behavior in early cetaceans. Nature 417: 163-166.

Spoor, F., and J. G. M. Thewissen. 2008. Comparative and functional anatomy of balance in aquatic mammals. Pp. 257-284 in J. G. M. Thewissen and S. Nummela (eds.), Sensory Evolution on the Threshold: Adaptations in Secondarily Aquatic Vertebrates. University of California Press, Berkeley.

Tarasoff, F. J., A. Bisaillon, J. Piérard, and A. P. Whitt. 1972. Locomotory patterns and external morphology of the river otter, sea otter, and harp seal (Mammalia). Canadian Journal of Zoology 50: 915-929.

Thewissen, J. G. M., and S. Bajpai. 2001. Whale origins as a poster child for macroevolution. Bioscience 51: 1037-1049.

Thewissen, J. G. M., and S. Bajpai. 2009. New skeletal material of *Andrewsiphius* and *Kutchicetus*, two Eocene cetaceans from India. Journal of Paleontology 83: 635-663.

Thewissen, J. G. M., and F. E. Fish. 1997. Locomotor evolution in the earliest cetaceans: functional model, modern analogues, and paleontological evidence. Paleobiology 23: 482-490.

Thewissen, J. G. M., and S. T. Hussain. 1998. Systematic review of the Pakicetidae, early and middle Eocene Cetacea (Mammalia) from Pakistan and India. Bulletin of the Carnegie Museum of Natural History 34: 220-238.

Thewissen, J. G. M., and S. T. Hussain. 2000. *Attockicetus praecursor*, a new remingtonocetid cetacean from marine Eocene sediments of Pakistan. Journal of Mammalian Evolution 7: 133-146.

Thewissen, J. G. M., S. T. Hussain, and M. Arif. 1994. Fossil evidence for the origin of aquatic locomotion in archaeocete whales. Science 263: 210-212.

Thewissen, J. G. M., S. I. Madar, and S. T. Hussain. 1996. *Ambulocetus natans*, an Eocene cetacean (Mammalia) from Pakistan. Courier Forschungsinstitut Senckenberg 190: 1-86.

Thewissen, J. G. M., and S. Nummela. 2008. Toward an integrative approach. Pp. 333-340 in J. G. M. Thewissen and S. Nummela (eds.), Sensory Evolution on the Threshold: Adaptations in Secondarily Aquatic Vertebrates. University of California Press, Berkeley.

Thewissen, J. G. M., and E. M. Williams. 2002. The early radiations of Cetacea (Mammalia): evolutionary pattern and developmental correlations. Annual Review of Ecology and Systematics 33: 73-90.

Thewissen, J. G. M., E. M. Williams, L. J. Roe, and S. T. Hussain. 2001. Skeletons of terrestrial cetaceans and the relationship of whales to artiodactyls. Nature 413: 277-281.

Trivedy, A. N., and P. P. Satsangi. 1984. A new archaeocete (whale) from the Eocene of India. Abstracts of the 27th International Geological Congress, Moscow 1: 322-323.

Uhen, M. D. 1998. New protocetid (Mammalia, Cetacea) from the late middle Eocene Cook Mountain Formation of Louisiana. Journal of Vertebrate Paleontology 18: 664-668.

Uhen, M. D. 1999. New species of protocetid archaeocete whale, *Eocetus wardii* (Mammalia: Cetacea) from the middle Eocene of North Carolina. Journal of Paleontology 73: 512-528.

Uhen, M. D. 2004. Form, function, and anatomy of *Dorudon atrox* (Mammalia, Cetacea): an archaeocete from the middle to late Eocene of Egypt. University of Michigan Papers on Paleontology 34: 1-222.

Uhen, M. D. 2005. A new genus and species of archaeocete whale from Mississippi. Southeastern Geology 43: 157-172.

Uhen, M. D. 2007. Evolution of marine mammals: back to sea after 300 million years. The Anatomical Record 290: 514-522.

Uhen, M. D. 2010. The origin(s) of whales. Annual Review of Earth and Planetary Sciences 38: 189-219.

Uhen, M. D., and P. D. Gingerich. 2001. New genus of dorudontine archaeocete (Cetacea) from the middle-to-late Eocene of South Carolina. Marine Mammal Science 17: 1-34.

Walker, J. D., and J. W. Geissman. 2009. 2009 GSA geologic time scale. GSA Today 19: 60.

Weber, P. W., L. E. Howle, M. M. Murray, and F. E. Fish. 2009. Lift and drag performance of odontocete cetacean flippers. Journal of Experimental Biology 212: 2149-2158.

West, R. M. 1980. Middle Eocene large mammal assemblage with Tethyan affinities, Ganda Kas region, Pakistan. Journal of Paleontology 54: 508-533.

Williams, T. M. 1983. Locomotion in the North American mink, a semi-aquatic mammal. I. Swimming energetics and body drag. Journal of Experimental Biology 103: 155-168.

Williams, T. M. 1989. Swimming by sea otters: adaptations for low energetic cost locomotion. Journal of Comparative Physiology A 164: 815-824.

Yazdi, P., A. Kilian, and B. M. Culik. 1999. Energy expenditure of swimming bottlenose dolphins. Marine Biology 134: 601-607.

Zhou, X., W. J. Sanders, and P. D. Gingerich. 1992. Functional and behavioral implications of vertebral structure in *Pachyaena ossifraga* (Mammalia,

Mesonychia). Contributions from the Museum of Paleontology, University of Michigan 28: 289-319.

Chapter 2

Systematic Review of the Remingtonocetidae (Mammalia, Cetacea)

INTRODUCTION

The cetacean family Remingtonocetidae has had a checkered systematic history. Hundreds of archaeocete fossils have been collected from the Eocene of India and Pakistan since the first remingtonocetid specimens were described, revealing much more about the diversity of the earliest whales than was known before. These larger samples have helped to clarify the unusual anatomy of remingtonocetids and their systematic relationships. However, new interpretations of several specimens and changes in taxonomy can be quite confusing.

Four species that are included in Remingtonocetidae were described by Sahni and Mishra (1972, 1975) before the family itself was named by Kumar and Sahni (1986). Since then, three of those species have been synonymized, due in part to key specimens (including a holotype) being misinterpreted for nearly 20 years (Gingerich et al., 2001; Thewissen and Bajpai, 2009). In addition, two other remingtonocetids described in later years appeared to be distinct when known from little more than their holotypes (Gingerich et al., 1995), but they now appear to be, potentially, males and females of a single species (Gingerich et al., 2001; Bebej, 2009).

The purpose of this chapter is to review the systematics of the Remingtonocetidae, in order to clarify which taxa are under analysis in later studies. This involves a brief discussion of their stratigraphic and temporal distribution, followed by a detailed discussion of the taxonomic history and distinguishing characteristics of each remingtonocetid species. This review focuses on the well-known taxa *Dalanistes ahmedi* and *Remingtonocetus domandaensis*, in particular, to evaluate whether these two taxa are different species or possibly males and females of a single species.

AGE OF REMINGTONOCETID-BEARING FORMATIONS

Remingtonocetids are known from four formations in Pakistan and India: the upper Kuldana Formation of northern Pakistan, the Domanda Formation of central Pakistan, the lower Harudi Formation of western India, and the Panandhro Formation of western India. The Kuldana Formation is earliest Lutetian in age (Gingerich, 2003), dating to about 48.0-48.5 million years ago (Ma; Gradstein et al., 2004), and has yielded many fragmentary specimens of pakicetid archaeocetes, including the holotypes of *Ichthyolestes pinfoldi* Dehm and Oettingen-Spielberg, 1958; *Pakicetus attocki* West, 1980; *Pakicetus inachus* Gingerich et al., 1981; *Nalacetus ratimitus* Thewissen and Hussain, 1998; *Pakicetus calcis* Cooper et al., 2009; and *Pakicetus chittas* Cooper et al., 2009, as well as the ambulocetid *Ambulocetus natans* Thewissen et al., 1994, and the possible ambulocetid *Gandakasia potens* Dehm and Oettingen-Spielberg, 1958. The only remingtonocetid known from the Kuldana Formation is *Attockicetus praecursor*

Thewissen and Hussain, 2000, which is known from just two fragmentary specimens (Thewissen and Hussain, 2000; Cooper et al., 2009).

The Domanda Formation has yielded many species of protocetids, including *Rodhocetus kasranii* Gingerich et al., 1994; *Takracetus simus* Gingerich et al., 1995; *Gaviacetus razai* Gingerich et al., 1995; *Qaisracetus arifi* Gingerich et al., 2001; and *Makaracetus bidens* Gingerich et al., 2005, along with three species of remingtonocetids: *Dalanistes ahmedi* Gingerich et al., 1995; *Remingtonocetus domandaensis* Gingerich et al., 2001; and *Andrewsiphius sloani* (Sahni and Mishra, 1972; Gingerich et al., 2001). The formation was formerly thought to represent the late early (Gingerich et al., 1995) to middle Lutetian (Gingerich et al., 1998), but is now interpreted as extending from the late early Lutetian through to the end of the Lutetian (Gingerich et al., 2001), about 40.4-46.0 Ma (Gradstein et al., 2004).

The Harudi Formation has yielded specimens of four protocetid species, including *Indocetus ramani* Sahni and Mishra, 1975; *Babiacetus indicus* Trivedy and Satsangi 1984; *Babiacetus mishrai* Bajpai and Thewissen, 1998; and *Gaviacetus sahnii* Bajpai and Thewissen, 1998, and four remingtonocetid species: *Andrewsiphius sloani* (Sahni and Mishra, 1972; Gingerich et al., 2001); *Remingtonocetus harudiensis* (Sahni and Mishra, 1975; Kumar and Sahni, 1986); *Dalanistes ahmedi* Gingerich et al., 1995 (Thewissen and Bajpai, 2001); and *Kutchicetus minimus* Bajpai and Thewissen, 2000. The formation has long been considered Lutetian in age (e.g., Biswas, 1992), but some workers have suggested a younger Bartonian age for the formation based on nannofossils (e.g., Singh and Singh, 1991). Gingerich et al. (2001) considered the Harudi

Formation to be equivalent in age to the Pir Koh Formation of Pakistan, which overlies the Domanda Formation and represents the earliest Bartonian, about 40.4 Ma (Gradstein et al., 2004).

Thewissen and Bajpai (2009), however, argued for a late Lutetian age for the archaeocetes from Kutch, pointing out that they were collected from the lower part of the Harudi Formation, which has a paucity of microfossils and is below the stratigraphic levels where the nannofossils were collected. This interpretation is consistent with a recent study that suggested a late Lutetian age for the whale-bearing strata (41.0-42.5 Ma) based on $^{87}Sr/^{86}Sr$ ratios from samples of mollusk shells, benthic foraminifera, and a shark tooth from the same level as the cetacean fossils (Ravikant and Bajpai, 2010). This age interpretation makes the lower Harudi Formation roughly correlative in time with the upper Domanda Formation.

Bajpai and Thewissen (2002) regarded archaeocetes recovered from the Panandhro lignite field as coming from the Naredi Formation, making them early Eocene (Ypresian) in age (Biswas, 1992). However, Thewissen and Bajpai (2009) pointed out that the type section of the Naredi Formation has neither lignite deposits nor fossil cetaceans, arguing that the strata near the Panandhro and Akri Lignite Mines where whales were collected are better understood as belonging to the Panandhro Formation. This interpretation makes the beds equivalent in age to the lower Harudi Formation (late Lutetian).

SYSTEMATIC PALEONTOLOGY

Class MAMMALIA Linnaeus, 1758

Order CETACEA Brisson, 1762

Family REMINGTONOCETIDAE Kumar and Sahni, 1986

Type genus. – *Remingtonocetus* Kumar and Sahni, 1986.

Included genera. – *Andrewsiphius* Sahni and Mishra, 1975; *Remingtonocetus* Kumar and Sahni, 1986; *Dalanistes* Gingerich et al., 1995; *Attockicetus* Thewissen and Hussain, 2000; *Kutchicetus* Bajpai and Thewissen, 2000.

Diagnosis. – Remingtonocetidae differ from all other archaeocetes in having extremely long, narrow skulls; relatively narrow supraorbital shields; small orbits; convex palates; palatine-pterygoid surfaces with prominent midline keels; laterally-positioned auditory bullae; long mandibular symphyses extending to the level of P_3 or beyond; relatively long cervical vertebrae; and narrow to closed acetabular notches of the innominates (Gingerich et al., 1998, 2001; Williams, 1998).

Discussion. – When the first remingtonocetid specimens were described, there were only three known non-basilosaurid archaeocetes, all in the family Protocetidae: *Protocetus atavus* (Fraas, 1904), *Eocetus schweinfurthi* (Fraas, 1904), and *Pappocetus lugardi* (Andrews, 1920). In describing their new archaeocete material from India, Sahni and Mishra (1972) designated it as a new species of protocetid (*Protocetus sloani*). They later described three additional new species of fossil cetaceans from Kutch: *Protocetus harudiensis*, which they also placed in Protocetidae, and *Andrewsiphius kutchensis* and *Andrewsiphius minor*, which they placed in the odontocete family Agorophiidae (Sahni

and Mishra, 1975). Fordyce (1981) recognized that *A. kutchensis* and *A. minor* were archaeocetes rather than odontocetes and provisionally placed *Andrewsiphius* in Protocetidae. When better comparative material was recovered, Kumar and Sahni (1986) showed that *P. sloani*, *P. harudiensis*, *A. kutchensis*, and *A. minor* are very similar to one another and also distinctly different in many ways from other non-basilosaurid archaeocetes. They recombined *P. sloani* and *P. harudiensis* into the new genus *Remingtonocetus*, and they erected the archaeocete family Remingtonocetidae to accommodate *R. sloani*, *R. harudiensis*, *A. kutchensis*, and *A. minor*.

Genus *Andrewsiphius* Sahni and Mishra, 1975

Protocetus (in part), Sahni and Mishra, 1972, p. 491; 1975, p. 20.

Andrewsiphius Sahni and Mishra, 1975, p. 23. Thewissen and Bajpai, 2009, p. 636.

Remingtonocetus (in part), Kumar and Sahni, 1986, p. 341.

Andrewsiphius (in part), Bajpai and Thewissen, 1998, p. 221. Gingerich et al., 2001, p. 287.

Type and only species. – *Andrewsiphius sloani* (Sahni and Mishra, 1972).

Diagnosis. – *Andrewsiphius* differs from *Remingtonocetus* and *Dalanistes* in having a smaller body size, a narrower rostrum, eyes positioned near the midline, relatively smaller premolars, a fused mandibular symphysis that extends to or beyond the level of M_2, and infraorbital foramina dorsal to M^2-M^3 rather than P^3 (Gingerich et

al., 2001; Thewissen and Bajpai, 2009; personal observation). It differs from the closely-related, similar-sized *Kutchicetus* in having double-rooted P^2, P^3, P_2, and P_3; lower molars not separated by diastemata; a mandible dorsoventrally taller than the combined width of right and left dentaries near the posterior premolars; and posterior thoracic vertebrae similar in length to lumbar vertebrae (Thewissen and Bajpai, 2009).

Andrewsiphius sloani (Sahni and Mishra, 1972)

Protocetus sloani Sahni and Mishra, 1972, p. 491, Pl. 97: 4-5; 1975, p. 20.

Cetacea indet., Sahni and Mishra, 1975, p. 17, Pl. 5: 5.

Andrewsiphius kutchensis Sahni and Mishra, 1975, p. 23, fig. 3, Pl. 5: 6.

Andrewsiphius minor Sahni and Mishra, 1975, p. 25, Pl. 5: 7.

Remingtonocetus harudiensis (in part), Kumar and Sahni, 1986, p. 330, figs. 7C and 10G.

Remingtonocetus sloani, Kumar and Sahni, 1986, p. 341, fig. 8K.

Andrewsiphius kutchensis (in part), Bajpai and Thewissen, 1998, p. 221, fig. 6G-6H.

Andrewsiphius sloani (in part), Gingerich et al., 2001, p. 287, fig. 14.

Andrewsiphius sloani, Thewissen and Bajpai, 2009, p. 637, figs. 1, 2.1-2.2, 2.8-2.10, 4.1-4.2, 5.1-5.3, 6.4-6.7, 7, 8.1-8.4, 8.6, 8.14, 9.11-9.14, 10.3-10.4, 10.11, and 10.14.

Holotype. – LUVP 11002, mandibular fragment with alveoli for P_3, P_4, and M_1 (Fig. 2.1A).

Type locality. – Chocolate Limestone, Babia Stage, 2 km northwest of Harudi, Kutch, India (23° 34′ 20″ N, 68° 43′ 10″ E).

Diagnosis. – As for genus.

Age and distribution. – *Andrewsiphius sloani* is known from the late Lutetian upper Domanda Formation of Pakistan (Gingerich et al., 2001) and from the late Lutetian Panandhro and lower Harudi Formations of India (Thewissen and Bajpai, 2009).

Etymology. – *Andrewsiphius sloani* is named for Charles W. Andrews, who contributed substantially to our knowledge of the marine mammals of Fayum, Egypt, and Robert E. Sloan, who contributed to knowledge of the Cretaceous-Tertiary boundary and the radiation of Paleocene mammals.

Referred specimens. – See Table 2.1.

Discussion. – When Sahni and Mishra (1975) proposed the genus *Andrewsiphius*, they designated two species, *A. kutchensis* and the slightly smaller *A. minor*, and assigned them to the odontocete family Agorophiidae. Kumar and Sahni (1986) recognized the similarity of these taxa to *Remingtonocetus sloani* and *Remingtonocetus harudiensis* and grouped them all together in the new archaeocete family Remingtonocetidae. Both species of *Andrewsiphius* continued to be recognized (e.g., Bajpai and Thewissen, 1998; Williams, 1998) until Gingerich et al. (2001) interpreted the poorly preserved holotypes of *A. kutchensis* (LUVP 11060), *A. minor* (LUVP 11165), and *R. sloani* (LUVP 11002) as being maxillary rather than mandibular, synonymizing these three species (along with *Kutchicetus minimus*) under the combination *Andrewsiphius sloani*.

Better comparative material, described by Thewissen and Bajpai (2009), demonstrates that the holotype of *Andrewsiphius minor* (LUVP 11165) is indeed maxillary as interpreted by Gingerich et al. (2001), but that the holotypes of *Andrewsiphius kutchensis* (LUVP 11060) and *Remingtonocetus sloani* (LUVP 11002) are mandibular as originally interpreted by Sahni and Mishra (1972, 1975). Maxillary fragments have infraorbital grooves anterior to the infraorbital foramina that run along the dorsoventral middle of the rostrum to accommodate the infraorbital neurovascular group. Mandibular fragments, on the other hand, have grooves to accommodate the mental nerve that runs along the ventral-most edge of the mandible. Thus, maxillary and mandibular fragments can be distinguished by the location of the grooves on their lateral surfaces. The new material of Thewissen and Bajpai (2009) also supports the synonymy of *A. kutchensis*, *A. minor*, and *R. sloani* under the combination *Andrewsiphius sloani*, while demonstrating the distinctness of *Kutchicetus minimus* (see description of *K. minimus* below).

Genus *Remingtonocetus* Kumar and Sahni, 1986

Protocetus (in part), Sahni and Mishra, 1972, p. 491; 1975, p. 21.

Protosiren (in part), Sahni and Mishra, 1972, p. 27.

Remingtonocetus Kumar and Sahni, 1986, p. 330. Gingerich et al., 1995, p. 310; 2001, p. 289.

Indocetus (in part), Gingerich et al., 1993, p. 396.

Remingtonocetus (in part), Bajpai and Thewissen, 1998, p. 215.

Type species. – *Remingtonocetus harudiensis* (Sahni and Mishra, 1975).

Referred species. – *Remingtonocetus domandaensis* Gingerich et al., 2001.

Diagnosis. – *Remingtonocetus* differs from *Andrewsiphius* and *Kutchicetus* in having a larger body size, a wider rostrum, laterally-positioned eyes, a mandibular symphysis that extends to the level of P_3, longer premolars, and infraorbital foramina dorsal to P^3 rather than M^2-M^3 (Gingerich et al., 2001; Thewissen and Bajpai, 2009; personal observation). It is smaller than *Dalanistes* and has less robust premolars and molars, relatively shorter M_2-M_3 (Gingerich et al., 2001), and relatively longer lumbar vertebrae (see below).

Age and distribution. – *Remingtonocetus* is known from the middle to late Lutetian of the middle and upper Domanda Formation throughout the Sulaiman Range of central Pakistan and the late Lutetian Harudi Formation of western India.

Remingtonocetus harudiensis (Sahni and Mishra, 1975)

Protocetus sloani (in part), Sahni and Mishra, 1972, p. 491, Pl. 97: 1-3; 1975, p. 20, Pl. 5: 2.

Protocetus harudiensis Sahni and Mishra, 1975, p. 21, Pl. 4: 4-7.

Protosiren fraasi (in part), Sahni and Mishra, 1975, p. 27, fig. 4, Pl. 6: 1.

Cf. moeritheriid, Sahni and Mishra, 1975, p. 29, fig. 5, Pl. 6: 2.

Remingtonocetus harudiensis Kumar and Sahni, 1986, p. 330, figs. 3-10. Bajpai and Thewissen, 1998, p. 215, figs. 2A-2D and 3A. Das et al., 2009, p. 225, Pl. 1.

Remingtonocetus sloani (in part), Bajpai and Thewissen, 1998, p. 218, figs. 2E-2G, 3B, 4A-4C, and 5A.

Remingtonocetus sp., Thewissen and Bajpai, 2001, p. 464, fig. 1.3-1.5; 2009, p. 636. Spoor et al., 2002, p. 164. Nummela et al., 2004, p. 776, fig. 1e-1g; 2006, p. 749. Bajpai et al., 2009, p. 678, figs. 5 and 10.

Holotype. – LUVP 11037, incomplete skull with roots for P^4-M^3, isolated cusps of upper cheek teeth, left mandibular ramus with roots for P_4-M_3, right mandibular ramus with roots for P_4-M_2, and crowns of left M_1 and M_2 (Fig. 2.1B).

Type locality. – Chocolate Limestone, Babia Stage, Rato Nala, 2 km north of Harudi, Kutch, India (23° 30′ 20″ N, 68° 41′ 15″ E).

Diagnosis. – *Remingtonocetus harudiensis* differs from *Remingtonocetus domandaensis* primarily in molar morphology. The M_1 and M_2 of *R. harudiensis* lack the second apical cusps seen in M_1 and M_2 of *R. domandaensis*. The crests anterior and posterior to the apical cusp of M_2 in *R. harudiensis* are straight and concave respectively, while the corresponding crests are both convex in *R. domandaensis* (Gingerich et al., 2001).

Age and distribution. – *Remingtonocetus harudiensis* is known from the late Lutetian lower Harudi Formation of western India (Kumar and Sahni, 1986; Bajpai and Thewissen, 1998).

Etymology. – *Remingtonocetus* is a contraction of Remington, in honor of Remington Kellogg, the foremost early 20th century expert on archaeocete cetaceans, and *cetus*, the Latin word for whale. The specific epithet *harudiensis* refers to the Harudi Formation, which yielded the type specimen.

Referred specimens. – See Table 2.2. This list includes all *Remingtonocetus* specimens from India mentioned in the literature, but it is almost certainly incomplete. Many specimens of *Remingtonocetus harudiensis* are referred to in various studies (e.g., Spoor et al., 2002; Nummela et al., 2004, 2007; Bajpai et al., 2009; Thewissen and Bajpai, 2009), despite never being adequately described or, in some cases, given a specimen number (e.g., Nummela et al., 2006).

Discussion. – *Remingtonocetus harudiensis* is known from several well-preserved and relatively complete cranial specimens (Kumar and Sahni, 1986; Bajpai and Thewissen, 1998; Bajpai et al., 2009), but its postcranial skeleton is poorly unknown. The pelvic fragment and weathered sacrum referred to the species by Gingerich et al. (1993) and a fragmentary lumbar centrum from the Mikir Hills of northeastern India questionably assigned to Cetacea (and compared to *Remingtonocetus* sp.) by Whiso et al. (2009) represent the only described postcranial elements with any connection to this species. Thewissen and Bajpai (2009, Fig. 13.3-13.4, p. 652) show plots of centrum dimensions for two specimens of *R. harudiensis*, but these specimens have not been described.

Remingtonocetus domandaensis Gingerich et al., 2001

Indocetus ramani (in part), Gingerich et al., 1993, p. 396, figs. 4, 5B, 6-10, 12B, and 13A-13C.

Remingtonocetus cf. *R. harudiensis* (in part), Gingerich et al., 1995, p. 310, figs. 12C-12D, 13-15.

Remingtonocetus domandaensis Gingerich et al., 2001, p. 291, fig. 16.

Holotype. – GSP-UM 3225, partial cranium and anterior rostrum with right dentary possessing C_1-M_3 and partial skeleton, including C1-C2, C3, C6-C7, T2?-T3?, T6?, L2, L5, one caudal vertebra, and several rib fragments (Fig. 2.1C).

Type locality. – Reddish brown shales of the upper part of the middle Domanda Formation, Ander Dabh Shumali, near Drug in easternmost Baluchistan, Pakistan (30° 59.14′ N, 70° 13.18′ E).

Diagnosis. – *Remingtonocetus domandaensis* differs from *Remingtonocetus harudiensis* primarily in molar morphology. The M_1 and M_2 of *R. domandaensis* possess second apical cusps that are absent in *R. harudiensis*. The crests anterior and posterior to the apical cusps of M_2 in *R. domandaensis* are both convex upward, whereas the corresponding crests in *R. harudiensis* are straight and concave respectively (Gingerich et al., 2001).

Age and distribution. – *Remingtonocetus domandaensis* is known from the middle to late Lutetian of the middle and upper Domanda Formation throughout the Sulaiman Range of central Pakistan (Gingerich et al., 2001).

Etymology. – The specific epithet *domandaensis* refers to the Domanda Formation, which has yielded all known specimens of this taxon.

Referred specimens. – See Table 2.3.

Discussion. – When the first specimens of *Remingtonocetus domandaensis* were described (e.g., GSP-UM 3009, 3015), they were thought to belong to the protocetid *Indocetus ramani* (Gingerich et al., 1993). Later comparison with specimens of *Dalanistes ahmedi* demonstrated that these were remingtonocetid, and Gingerich et al. (1995) provisionally assigned them to *Remingtonocetus* cf. *R. harudiensis*. The recovery of more complete cranial and dental material allowed the specimens of *Remingtonocetus* from the Domanda Formation of Pakistan to be distinguished from those of the Harudi Formation of India (Gingerich et al., 2001). Other than the differences in dentition described above, there appear to be few differences in cranial morphology between *R. harudiensis* and *R. domandaensis*, and while a good deal is known about the postcranial morphology of *R. domandaensis* (Gingerich et al., 1995, 2001; Bebej et al., 2007; Bebej, 2008, this volume), it cannot be compared with that of *R. harudiensis*, for which virtually no postcranial elements have been described.

Genus *Dalanistes* Gingerich et al., 1995

Indocetus (in part), Gingerich et al., 1993, p. 396.

Remingtonocetus (in part), Gingerich et al., 1995, p. 310.

Dalanistes Gingerich et al., 1995, p. 317; 2001, p. 294. Thewissen and Bajpai, 2001, p. 463.

Type and only species. – *Dalanistes ahmedi* Gingerich et al., 1995.

Diagnosis. – *Dalanistes* is larger than all other remingtonocetids. It differs from *Andrewsiphius* and *Kutchicetus* in having a large body size, a broader rostrum, relatively longer premolars, and infraorbital foramina dorsal to P^3 rather than M^2-M^3 (Gingerich et al., 2001; personal observation). It is about 15% larger than *Remingtonocetus* in linear dimensions and has more robust premolars and molars, relatively longer M_2-M_3 (Gingerich et al., 2001), and relatively shorter lumbar vertebrae (see below).

Dalanistes ahmedi Gingerich et al., 1995

Indocetus ramani (in part), Gingerich et al., 1993, p. 396, figs. 5A and 12A.

Remingtonocetus cf. *R. harudiensis* (in part), Gingerich et al., 1995, p. 310, fig. 12A-12B.

Dalanistes ahmedi Gingerich et al., 1995, p. 317, figs. 17-20. Thewissen and Bajpai, 2001, p. 463, fig. 1.1-1.2.

Holotype. – GSP-UM 3106, partially articulated skull, dentary, and postcranial skeleton, including centra for C3, C5, T1-T2?, T4?-T6?, L1-L3, and L5-L6; sacrum; partial innominate; femoral head and distal epiphysis; and fragmentary ribs (Fig. 2.1D).

Type locality. – Basti Ahmed, in Dalana Nala drainage just south of Takra Valley, Sulaiman Range, Pakistan (30° 7′ 33″ N, 70° 21′ 55″ E).

Diagnosis. – As for genus.

Age and distribution. – *Dalanistes ahmedi* is known from the middle Lutetian middle Domanda Formation of Pakistan (Gingerich et al., 1995, 1998, 2001) and the late Lutetian lower Harudi Formation of India (Thewissen and Bajpai, 2001).

Etymology. – *Dalanistes* is a contraction of Dalana, referring to the Dalana Nala drainage where the type specimen was found, and *Platanistes*, after the modern Indus River dolphin *Platanista minor*, a cetacean known for its small eyes and long narrow rostrum. The specific epithet *ahmedi* refers to Basti Ahmed, the type locality.

Referred specimens. – See Table 2.4. IITR-SB 2521 was identified as *Dalanistes ahmedi* when it was described by Thewissen and Bajpai (2001). Later authors referring to this specimen identified it as *Remingtonocetus* sp. (Nummela et al., 2007; Thewissen and Bajpai, 2009). The crown lengths of the premolars and molars in IITR-SB 2521 are similar to published measurements of *D. ahmedi* (Gingerich et al., 1995) and markedly greater than those of *Remingtonocetus domandaensis* (Gingerich et al., 2001). Thus, its identification as *D. ahmedi* is favored here.

Discussion. – *Dalanistes ahmedi* was initially described as a genus and species distinct from *Remingtonocetus harudiensis*. Later, after additional specimens of *D. ahmedi* and *Remingtonocetus domandaensis* had been collected, Gingerich et al. (2001) realized that the two taxa were more similar to one another than was previously evident. They suggested that the two taxa could be congeneric or even males and females of a single sexually-dimorphic species. Given differences in the proportions and absolute sizes of cheek teeth, Gingerich et al. (2001) argued that the two taxa should remain distinct, but regarded them as closely related remingtonocetid genera. However, nearly all of the characteristics initially used to distinguish these two taxa are invalid (see below), and other than differences in size, the morphology of homologous postcranial elements is virtually identical. This taxonomic paradigm has not been thoroughly tested, and the question still remains: are *D. ahmedi* and *R. domandaensis* truly separate species, or might they be sexually-dimorphic members of a single species? This question is addressed in the following section.

Genus *Attockicetus* Thewissen and Hussain, 2000

Attockicetus Thewissen and Hussain, 2000, p. 135.

Cf. *Attockicetus*, Cooper et al., 2009, p. 1296.

Type and only species. – *Attockicetus praecursor* Thewissen and Hussain, 2000.

Diagnosis. – *Attockicetus* differs from all other remingtonocetids in retaining large molar protocones on upper molars and orbits positioned dorsal to M^3 rather than posterior to the end of the tooth row.

Attockicetus praecursor Thewissen and Hussain, 2000

Attockicetus praecursor Thewissen and Hussain, 2000, p. 135, figs. 2-3.

Cf. *Attockicetus praecursor*, Cooper et al., 2009, p. 1296, fig. 10.

Holotype. – H-GSP 96232, fragmentary cranium including partial rostrum with supraorbital region and orbits, fragments of left P^3-M^2 and right P^3-M^1, endocast, and poorly preserved braincase and ectotympanic (Fig. 2.1E).

Type locality. – H-GSP Locality 9604, Ganda Kas area, Kala Chitta Hills, northern Pakistan (33° 36′ 55″ N, 72° 11′ 50″ E). Thewissen and Hussain (2000) describe the holotype as coming from either the lowermost Kohat Formation or the uppermost Kuldana Formation. Cooper et al. (2009) describe the specimen as coming from the uppermost Kuldana Formation.

Diagnosis. – As for genus.

Age and distribution. – *Attockicetus praecursor* is known from the early Lutetian upper Kuldana Formation of northern Pakistan (Thewissen and Hussain, 2000; Cooper et al., 2009).

Etymology. – *Attockicetus* is a contraction of Attock, the district where the type specimen was found (Attock District, Punjab Province, Pakistan), and *cetus*, the Latin word for whale. The specific epithet *praecursor* is the Latin word for forerunner, signifying its presumed basal position in remingtonocetid phylogeny.

Referred specimen. – H-GSP 96630, isolated P_3 and P_4 (Cooper et al., 2009).

Discussion. – *Attockicetus praecursor* is known from only two specimens. The fragmentary holotype skull (H-GSP 96232) is from near the boundary between the Kuldana and Kohat formations (Thewissen and Hussain, 2000), and additional dental material attributed to cf. *Attockicetus* (H-GSP 96630) has been recovered from about 40 m lower in the upper Kuldana Formation (Cooper et al., 2009). It is both the oldest known and most plesiomorphic remingtonocetid taxon (Thewissen and Hussain, 2000).

Genus *Kutchicetus* Bajpai and Thewissen, 2000

Andrewsiphius (in part), Bajpai and Thewissen, 1998, p. 221. Gingerich et al., 2001, p. 287.

Kutchicetus Bajpai and Thewissen, 2000, p. 1478; 2002, p. 508. Thewissen and Bajpai, 2009, p. 642.

Type and only species. – *Kutchicetus minimus* Bajpai and Thewissen, 2000.

Diagnosis. – *Kutchicetus* is the smallest known remingtonocetid, based on linear dimensions of vertebral centra and long bones (Thewissen and Bajpai, 2009). It differs

from *Remingtonocetus* and *Dalanistes* in having a smaller body size, a narrower rostrum, eyes positioned closer to the midline, and a fused mandibular symphysis that extends to or past the level of M_2 (Thewissen and Bajpai, 2009). It differs from the similar-sized *Andrewsiphius* in possessing single-rooted P^2, P^3, P_2, and P_3; lower molars separated by diastemata; a mandible that is dorsoventrally shorter than the combined width of right and left dentaries near the posterior premolars and so narrow that it must flare buccally to accommodate the roots of the premolars; and posterior thoracic vertebrae shorter in length than lumbar vertebrae (Bajpai and Thewissen, 2000; Thewissen and Bajpai, 2009).

Kutchicetus minimus Bajpai and Thewissen 2000

Andrewsiphius kutchensis (in part), Bajpai and Thewissen, 1998, p. 221, figs. 4D, 6A-6F, and 7A-7B.

Andrewsiphius sloani (in part), Gingerich et al., 2001, p. 287.

Kutchicetus minimus Bajpai and Thewissen, 2000, p. 1478, figs. 1 and 3; 2002, p. 508, fig. 2o-2p and 2r-2s. Thewissen and Bajpai, 2009, p. 642, figs. 2.3-2.7, 3.4-3.5, 4.3-4.7, 5.4-5.8, 6.1-6.3, 8.5, 8.7-8.13, 9.1-9.8, 10.1-10.2, 10.5-10.10, 10.12-10.13, and 12.

Holotype. – IITR-SB 2647, partial non-articulated skeleton collected over several field seasons including a few small skull and dental fragments, a number of fragmentary

vertebrae (six cervical, nine thoracic, four lumbar, four fused sacral, and 13 caudal), partial limb bones (humerus, two radii, ulna, pelvis, two femora, and tibia), partial innominate, and fragments of ribs (Fig. 2.1F).

Type locality. – Chocolate Limestone of Harudi Formation, 1 km east of Godhatad, Kutch, India (23° 39′ 0″ N, 68° 39′ 30″ E).

Diagnosis. – As for genus.

Age and distribution. – *Kutchicetus minimus* is known from the late Lutetian lower Harudi and Panandhro Formations of western India (Bajpai and Thewissen, 2002; Thewissen and Bajpai, 2009).

Etymology. – *Kutchicetus* is a contraction of Kutch, the district where the type specimen was found (Kutch District, Gujarat State, India), and *cetus*, the Latin word for whale. The specific epithet *minimus*, the Latin word for least, refers to this taxon's distinction as the smallest remingtonocetid.

Referred specimens. – See Table 2.5.

Discussion. – When the holotype of *Kutchicetus minimus* (IITR-SB 2647) was described, it was distinguished from other remingtonocetids primarily on the basis of its small size (Bajpai and Thewissen, 2000), though no comparative measurements were provided. Gingerich et al. (2001) argued that this taxon, as initially described, was not sufficiently different from other previously described remingtonocetids, considering *K. minimus* a junior synonym of *Andrewsiphius sloani*. Additional material attributed to the holotype and several new specimens collected from the Panandhro Formation

(including more complete cranial material) demonstrate that *K. minimus* is distinct from, though probably closely related to, *A. sloani* (Thewissen and Bajpai, 2009).

DISCUSSION

Are Dalanistes *and* Remingtonocetus *males and females of a single species?*

When *Dalanistes* was initially described, Gingerich et al. (1995) differentiated it from *Remingtonocetus* as follows:

1. *Dalanistes* is about 20% larger in size.
2. The external nares of *Dalanistes* open above C^1 rather than P^1.
3. *Dalanistes* has higher sagittal and nuchal crests.
4. The rostrum of *Dalanistes* is angled downward relative to the orientation of the braincase (a condition known as clinorhynchy).
5. *Dalanistes* retains an open mandibular symphysis ending at P_3 rather than P_4.
6. *Dalanistes* possesses right and left mandibular canals that remain separate throughout their length.

Many of these characters are based on comparisons with VPL 15001, a mostly complete, well-preserved skull of *R. harudiensis* described by Kumar and Sahni (1986). In recent years, several additional *Remingtonocetus* specimens have been collected that preserve features not present in VPL 15001 and call nearly all of these distinguishing characters into question.

The difference in size between *Dalanistes* and *Remingtonocetus* is the only original differentiating feature that is still valid. The skull of *Dalanistes* (GSP-UM 3106:

90 cm; Gingerich et al., 1995, p. 320) is about 20% longer than skulls described for *Remingtonocetus harudiensis* (VPL 15001: 75.8 cm; Kumar and Sahni, 1986, p. 333) and *Remingtonocetus domandaensis* (GSP-UM 3415, erroneously referred to as GSP-UM 3408 in the text: 75 cm; Gingerich et al., 2001, p. 292). The C_1-M_3 length in *Dalanistes* (GSP-UM 3106: 41.0 cm, GSP-UM 3165: 40.1; Gingerich et al., 2001, p. 293) is 17% longer on average than that of *R. domandaensis* (GSP-UM 3225: 34.7 cm; Gingerich et al., 2001, p. 293). However, while all cranial and postcranial elements of *Dalanistes* are clearly larger than those of *Remingtonocetus*, the differences in size between homologous postcranial elements are not as consistent as differences between homologous cranial measurements. This suggests that the two taxa may not only be different in size, but also proportioned differently (details are described below).

The external nares of *Dalanistes* open above C^1 (Gingerich et al., 1995, Fig. 17, p. 319). VPL 15001 is notably missing all of the nasals anterior to P^3, and the external nares are reconstructed as opening above P^1 (Kumar and Sahni, 1986, Fig. 4, p. 332). Two specimens of *Remingtonocetus domandaensis* (GSP-UM 3225 and 3415) collected since that time show unequivocally that the external nares open above C^1 in *Remingtonocetus* rather than above P^1 (Gingerich et al., 2001), just as in *Dalanistes*.

The sagittal crest preserved in the holotype of *Dalanistes* (GSP-UM 3106) is indeed higher than that evident in VPL 15001, but VPL 15001 is broken and does not preserve the nuchal crest (Kumar and Sahni, 1986, Fig. 4, p. 332). More complete specimens of *Remingtonocetus domandaensis* preserve a robust sagittal crest and a large, posteriorly-projecting nuchal crest (GSP-UM 3415 and 3552). The clinorhynchy

evident in *Dalanistes* is due to a difference in orientation between the rostrum and the presphenoid. The presphenoid is covered by the pterygoids in most specimens, making this characteristic difficult to measure, but it appears that *R. domandaensis* (GSP-UM 3415) may too have a slight difference in the orientation between its braincase and its rostrum. These features of the cranium appear to be more similar in these two taxa than previously appreciated.

The mandibular symphysis of *Dalanistes* extends to the level of P_3 (Gingerich et al., 1995). The interpretation of the mandibular symphysis extending to P_4 or beyond in *Remingtonocetus* stems from the condition seen in LUVP 11132, which was assigned to *Remingtonocetus harudiensis* by Kumar and Sahni (1986). Gingerich et al. (2001) interpreted LUVP 11132 as being maxillary rather than mandibular and as belonging to *Andrewsiphius*. The comparative material described by Thewissen and Bajpai (2009) indicates that LUVP 11132 belongs to *Andrewsiphius*, but that it is indeed mandibular as originally interpreted. The mandibular symphysis in *Andrewsiphius* extends all the way to between M_1 and M_3 (Thewissen and Bajpai, 2009). The holotype specimen of *Remingtonocetus domandaensis* (GSP-UM 3225) exhibits a mandibular symphysis that extends to the level of P_3 (Gingerich et al., 2001), just as in *Dalanistes*.

The right and left mandibular canals of *Dalanistes* remain separate throughout their length (Gingerich et al., 1995). Kumar and Sahni (1986) describe the right and left mandibular canals of LUVP 11132 as joining to form a single canal anterior to P_2, but it is now clear that this specimen belongs to *Andrewsiphius* rather than *Remingtonocetus*. While the anterior confluence of the mandibular canals is variable in different

specimens of *Andrewsiphius* (Thewissen and Bajpai, 2009), well-preserved mandibles of *Remingtonocetus* (GSP-UM 3225) indicate that right and left canals remain separate as in *Dalanistes*.

Dalanistes and *Remingtonocetus* are clearly more similar than initially described, but are they actually separate taxa, or might they be males and females of a single species? Gingerich et al. (2001) regarded the two as separate taxa pending the recovery of larger samples. The number of remingtonocetids known from the Domanda Formation has since grown to over 100 specimens, of which 42 are identified as *Dalanistes* and 54 as *Remingtonocetus*, thus offering an opportunity to further test this taxonomic paradigm.

A wide range of sexual dimorphism exists in modern mammals, but it can be very challenging to recognize in the fossil record in the absence of discrete, sex-specific morphological characters, such as horns or antlers, or a clearly bimodal sampling distribution (Plavcan, 1994). This can cause serious taxonomic problems: males and females of a single species might be so dissimilar that they could be interpreted as separate taxa, while different, closely-related species might be so similar that they could be regarded as a single species (Kurtén, 1969). Sexual dimorphism in fossil mammals has often been inferred based on differences in overall body size and/or canine size and shape (e.g., Coombs, 1975; Fleagle et al., 1980; Gingerich, 1981a, 1981b; Krishtalka et al., 1990; Gingerich, 1995), including in a number of fossil cetaceans (Gingerich et al., 2009; Antar et al., 2010; Lambert et al., 2010). In order to investigate the possibility that *Dalanistes ahmedi* and *Remingtonocetus domandaensis* were sexually-dimorphic

members of a single species, I assessed their differences in overall body size, canine tooth proportions, and stratigraphic distributions in the Domanda Formation.

Differences in size between homologous postcranial elements — The difference in size between cranial elements of *Dalanistes ahmedi* and *Remingtonocetus domandaensis* (17-20%) is well-established, as described above (Fig. 2.2). However, size differences in postcranial anatomy, though noted, have never been quantified. Cervical, thoracic, and lumbar vertebrae from 18 individuals of *D. ahmedi* and 25 individuals of *R. domandaensis* (totaling 152 total vertebrae) were identified to their position in the vertebral column (e.g., C6, L3, etc.). Centrum lengths were compared among homologous vertebrae to assess the difference in size between *D. ahmedi* and *R. domandaensis* at each position and to determine the pattern of mean size differences in each region of the column. The presacral vertebrae of two modern pinniped species were also analyzed in order to assess whether or not the data from *D. ahmedi* and *R. domandaensis* fit the patterns exhibited by a moderately dimorphic (California sea lion, *Zalophus californianus*) or weakly dimorphic (harbor seal, *Phoca vitulina*) semiaquatic mammal.

Centrum lengths of the cervical, thoracic, and lumbar vertebrae of *Dalanistes ahmedi* and *Remingtonocetus domandaensis* are listed in Tables 2.6 and 2.7 respectively. Cervical and anterior thoracic vertebrae (defined as T1-T7) display the greatest differences in length between taxa. On average, the cervical vertebrae of *D. ahmedi* are 16.3% longer than those of *R. domandaensis*, while the difference in length between anterior thoracic vertebrae is 19.7% (Table 2.8). These differences are similar

in magnitude to those seen between cranial measurements. On the other hand, there is less difference in size between the posterior thoracic (T8-T13) and lumbar vertebrae of these taxa (12.3% and 12.7% respectively). Figure 2.3 illustrates that the size ranges of *D. ahmedi* and *R. domandaensis* remain distinct, with little to no overlap, from C3 to about T10; however, posterior to T10, the upper range of *R. domandaensis* specimens begins to overlap with the lower range of *D. ahmedi* specimens. In other words, *R. domandaensis* has relatively longer posterior thoracic and lumbar vertebrae compared to overall body size than does *D. ahmedi*.

This pattern differs from what is seen in *Zalophus californianus* and *Phoca vitulina*. *Z. californianus* is considered a strongly dimorphic species (Ralls and Mesnick, 2009), with males being about 33% longer and 200% heavier than females (King, 1983). *P. vitulina*, on the other hand, is a weakly dimorphic species, with males being about 20% longer and 23% heavier (King, 1983). Despite the differences in size between the presacral vertebrae of males and females of both species (Tables 2.9-2.10), the anterior-to-posterior pattern of centrum lengths is virtually the same (Fig. 2.4), which is not the case between *Dalanistes ahmedi* and *Remingtonocetus domandaensis*. The mean differences in size across the cervical, anterior thoracic, posterior thoracic, and lumbar vertebrae are very similar in *P. vitulina* (19.7%, 20.2%, 20.0%, and 16.9% respectively; Fig. 2.5), while the mean difference in the cervical vertebrae of *Z. californianus* (31.2%) is noticeably greater than those for the anterior thoracic, posterior thoracic, and lumbar vertebrae (23.2%, 22.5%, and 22.1% respectively; Fig. 2.5).

This disparity in *Zalophus californianus* appears relatively wide but is likely due to an allometric effect (Kurtén, 1969). Because the overall difference in body size of male and female *Z. californianus* is much greater than that between male and female *Phoca vitulina* and that between *Dalanistes ahmedi* and *Remingtonocetus domandaensis*, the relative differences between vertebral regions is greater as well. In order to remove this factor and effectively equalize the relative size difference in these three comparisons, the mean percent differences of *Z. californianus* and *P. vitulina* were scaled down so that their mean percent difference in cervical vertebrae matched that between *D. ahmedi* and *R. domandaensis* (16.3%), which was the best-sampled region for remingtonocetids. After scaling, there is much less variation in size differences across vertebral regions between male and female pinnipeds (Fig. 2.5); this clearly contrasts with the pattern seen between *D. ahmedi* and *R. domandaensis*, in which there is much less size difference between the posterior thoracic and lumbar vertebrae than there is between the cervical and anterior thoracic vertebrae.

Differences in size between canine teeth — Male members of a sexually-dimorphic species often have more robust canine teeth than do females, and this characteristic has often been cited to infer sexual dimorphism in fossil species (Kurtén, 1969; Fleagle et al., 1980; Gingerich, 1981a, 1981b; Krishtalka et al., 1990; Gingerich, 1995). One protocetid archaeocete has been identified as a sexually-dimorphic species due, in part, to this criterion. *Maiacetus inuus* is known from two specimens: GSP-UM 3475, an articulated skull, thorax, and left forelimb with the skull and partial skeleton of a fetus preserved *in utero*, and GSP-UM 3551, a virtually complete skull and skeleton

(Gingerich et al., 2009). The preserved fetus in GSP-UM 3475 indicates with certainty that this specimen is a female. GSP-UM 3551 is about 12% larger than GSP-UM 3475, but possesses canine teeth that are about 20% larger. Gingerich et al. (2009) interpret this specimen as male and note that the degree of sexual dimorphism exhibited in this taxon is moderate compared to the degree of dimorphism exhibited by many modern marine mammals.

The dentition of remingtonocetids is poorly known (Gingerich et al., 2001; Thewissen and Bajpai, 2001), but there are several skulls and jaws that preserve alveoli for upper and lower canines, premolars, and molars. The lengths and widths of alveoli and the crown heights of preserved teeth (when available) were compared between *Dalanistes ahmedi* and *Remingtonocetus domandaensis* in order to assess if the difference in canine size was suggestive of sexual dimorphism (Table 2.11). The canines of *D. ahmedi* average 20.3% larger than the canines of *R. domandaensis*, while the molars and premolars average a 16.6% difference. Though this metric demonstrates that the difference in canine size between *D. ahmedi* and *R. domandaensis* is greater than the differences observed between the premolars and molars of these taxa, all of the differences in dental dimensions fall right in line with size differences observed in other aspects of cranial anatomy. The canine teeth of *D. ahmedi* are not exceptionally larger than those of *R. domandaensis*, as would be expected in a sexually-dimorphic species.

Stratigraphic distributions — Stratigraphic data are also relevant for assessing whether or not *Dalanistes ahmedi* and *Remingtonocetus domandaensis* are two

separate taxa or males and females of a single species. One would expect males and females of a single species to correlate temporally and geographically, and unless there was a strong bias in the sex ratio in the living population and/or some taphonomic bias (Kurtén, 1969), one would expect to find both in roughly equal numbers. The genera *Dalanistes* and *Remingtonocetus* are both known from the Domanda Formation of Pakistan and the Harudi Formation of India, but their distribution within the Domanda Formation is quite telling (Fig. 2.6).

Dalanistes ahmedi is represented by 42 specimens recovered from the middle part of the Domanda Formation, where 40 specimens of *Remingtonocetus domandaensis* have also been recovered. However, no specimens of *D. ahmedi* have been recovered from the upper Domanda Formation, which has yielded 14 specimens of *R. domandaensis* and 4 specimens of *Andrewsiphius sloani*. *D. ahmedi* was not extinct by the late Lutetian, as it is known from the lower Harudi Formation (Thewissen and Bajpai, 2001), but its absence in the upper Domanda Formation suggests that it was not present in that area of Pakistan at the time. It is possible that *D. ahmedi* was present and that there are some factors that prevented it from being preserved. However, given the abundance of both *D. ahmedi* and *R. domandaensis* in the middle Domanda Formation, the similarity of the facies between the middle and upper parts of the formation, and the number of remingtonocetid specimens collected from the upper part of the formation (18), it is likely that at least one specimen of *D. ahmedi* would have been collected from the upper Domanda Formation had it been present when the formation was deposited.

Conclusion:* Dalanistes *and* Remingtonocetus *are distinct taxa — While *Dalanistes ahmedi* and *Remingtonocetus domandaensis* are certainly more similar than initially realized, the two species appear to be separate, closely-related taxa rather than males and females of a single, sexually-dimorphic species. The vertebral length profiles exhibited by these two species indicate that they have different vertebral proportions, which is not the case in two modern sexually-dimorphic semiaquatic mammals. *D. ahmedi* also does not possess the larger, more robust canine teeth often exhibited by males of a sexually-dimorphic species. In addition, while the temporal ranges of *Dalanistes* and *Remingtonocetus* overlap completely, their stratigraphic distributions do not. Considering all of this evidence, it is much more likely that *D. ahmedi* and *R. domandaensis* represent unique taxa rather than males and females of a single species.

Summary

Five valid genera and six valid species are currently recognized in the archaeocete family Remingtonocetidae. All taxa are restricted to the Lutetian of Indo-Pakistan. *Attockicetus* is the oldest taxon and is known only from the early Lutetian Kuldana Formation of northern Pakistan. *Dalanistes* and *Remingtonocetus* are both known from the middle-to-late Lutetian Domanda Formation of central Pakistan and the late Lutetian Harudi Formation of western India. *Andrewsiphius* and *Kutchicetus* are both known from the late Lutetian Panandhro and Harudi Formations of western India, though *Andrewsiphius* is also known from the late Lutetian upper Domanda Formation of Pakistan.

The family is typically recognized as a monophyletic group, though most phylogenetic analyses have included only one (O'Leary, 1999; O'Leary and Geisler, 1999; O'Leary and Uhen, 1999; Geisler and Uhen, 2005) or two (Uhen, 1999, 2004; Uhen and Gingerich, 2001; Geisler et al., 2005) remingtonocetid genera: typically *Remingtonocetus*, and occasionally *Dalanistes*. Thewissen and Hussain (2000) conducted a small-scale phylogenetic analysis that included *Andrewsiphius*, *Attockicetus*, *Dalanistes*, and *Remingtonocetus*, but their analysis included few other archaeocetes. Their study supported remingtonocetid monophyly and demonstrated that *Attockicetus* is the most plesiomorphic member of the family. Their analysis also suggested that *Andrewsiphius* and *Remingtonocetus* were the most derived remingtonocetid genera. However, given the highly derived skull and mandibular characteristics shared by *Andrewsiphius* and *Kutchicetus*, which Thewissen and Hussain (2009) placed together in the subfamily Andrewsiphiinae, it is likely that those two taxa represent the most derived remingtonocetids.

The best known taxa skeletally are *Dalanistes ahmedi* and *Remingtonocetus domandaensis*, which both include a number of partial skeletons. While few limb elements have been recovered for these species, several specimens include well-preserved and reasonably complete vertebral series. GSP-UM 3552, a specimen of *R. domandaensis* collected in 2004, preserves the most complete series of remingtonocetid vertebral elements known to date. This exceptional specimen allows remingtonocetid vertebral morphology and function to be studied in depth for the first time and provides the key to identifying a large number of isolated remingtonocetid

vertebrae. The morphology and function of the remingtonocetid vertebral column are described in the following chapter.

Figure 2.1. Holotype specimens of remingtonocetid species. For some specimens, not all elements are pictured. See the text for complete descriptions of each specimen. A. *Andrewsiphius sloani* (LUVP 11002), mandibular fragment in occlusal view (anterior to the right; modified from Sahni and Mishra, 1972). B. *Remingtonocetus harudiensis* (LUVP 11037), left maxilla (top) and left mandible (bottom left) in occlusal view (anterior to the left), left M_2 (bottom right) in labial view (modified from Sahni and Mishra, 1975). C. *Remingtonocetus domandaensis* (GSP-UM 3225), right dentary and anterior rostrum in right lateral view (modified from Gingerich et al., 2001). D. *Dalanistes ahmedi* (GSP-UM 3106), skull cast in ventral view (modified from Gingerich et al., 1995). E. *Attockicetus praecursor* (H-GSP 96232), fragmentary cranium (left) in dorsal view and fragmentary rostrum (right) in palatal view (anterior to the right; modified from Thewissen and Hussain, 2000). F. *Kutchicetus minimus* (IITR-SB 2647), partial non-articulated skeleton in right lateral view (modified from Bajpai and Thewissen, 2000).

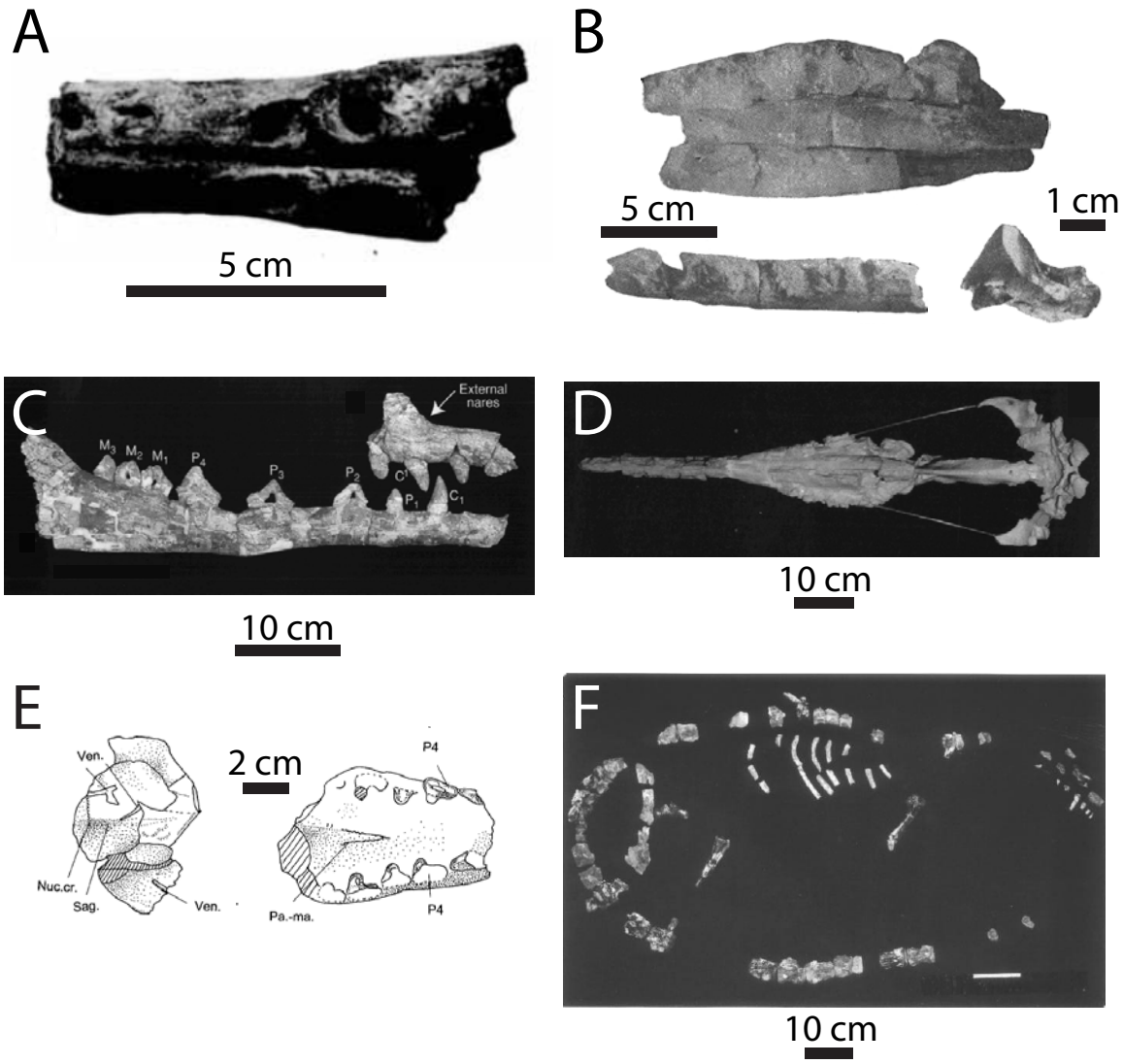

Figure 2.2. Cranial material of *Remingtonocetus domandaensis* and *Dalanistes ahmedi*. A. Skulls of *R. domandaensis* (top) and *D. ahmedi* (bottom) in palatal view (modified from Gingerich et al., 1998). B. Right dentaries of *R. domandaensis* (top; GSP-UM 3225) and *D. ahmedi* (bottom; GSP-UM 3165) in lateral view.

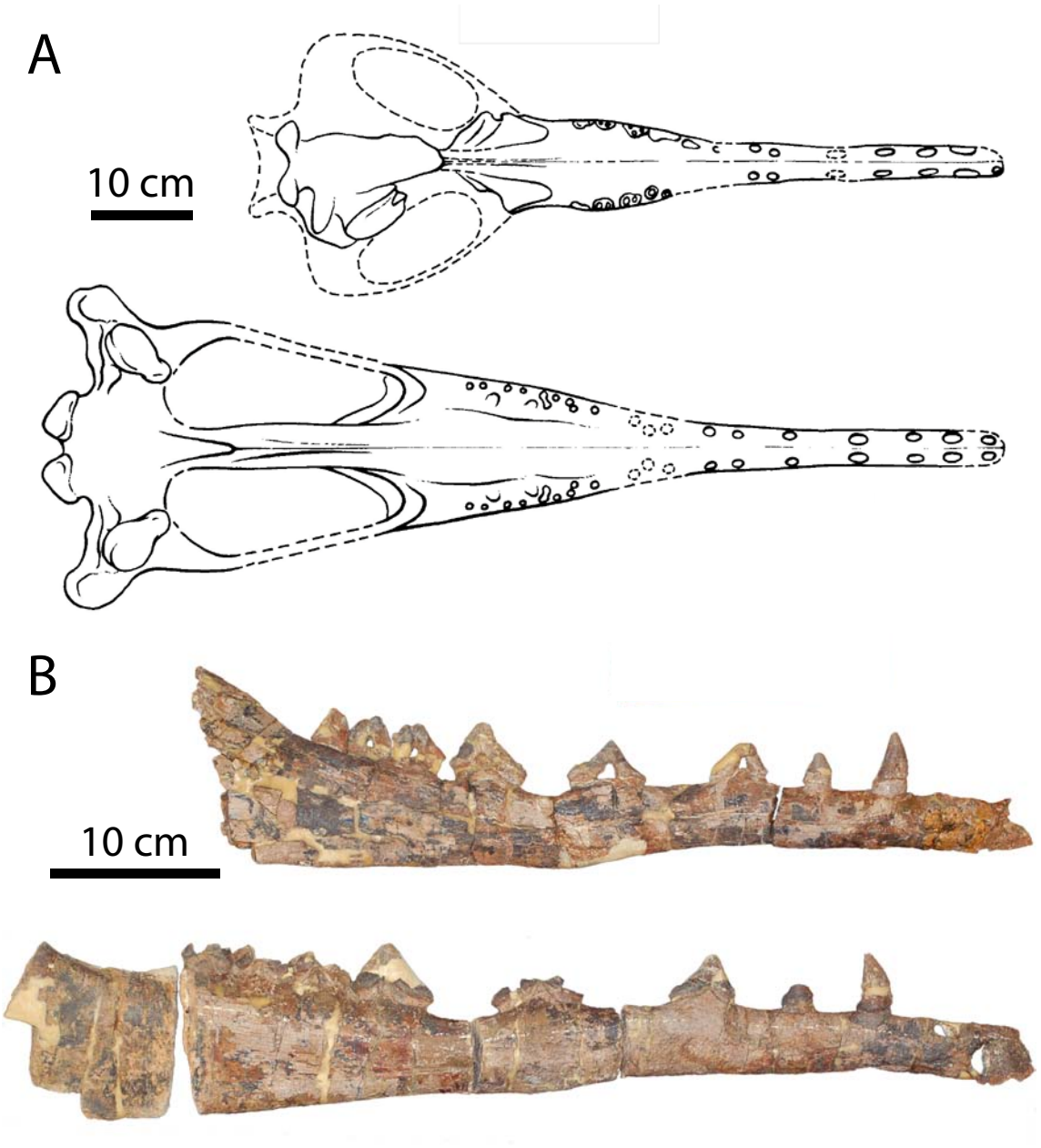

Figure 2.3. Centrum length profiles for presacral vertebral columns of *Dalanistes ahmedi* and *Remingtonocetus domandaensis*. Navy and yellow shadings mark the hypothesized size ranges of *D. ahmedi* and *R. domandaensis* respectively. In most cases, the upper and lower bounds of these envelopes are defined by the largest and smallest sampled elements at each position, but in cases where only one specimen was available at a position, the upper and lower bounds were estimated by comparison with adjacent vertebral positions. Note the difference in the shape of these profiles. The posterior thoracic and lumbar vertebrae of *R. domandaensis* are relatively longer (compared to cervical and anterior thoracic vertebrae) than those of *D. ahmedi*.

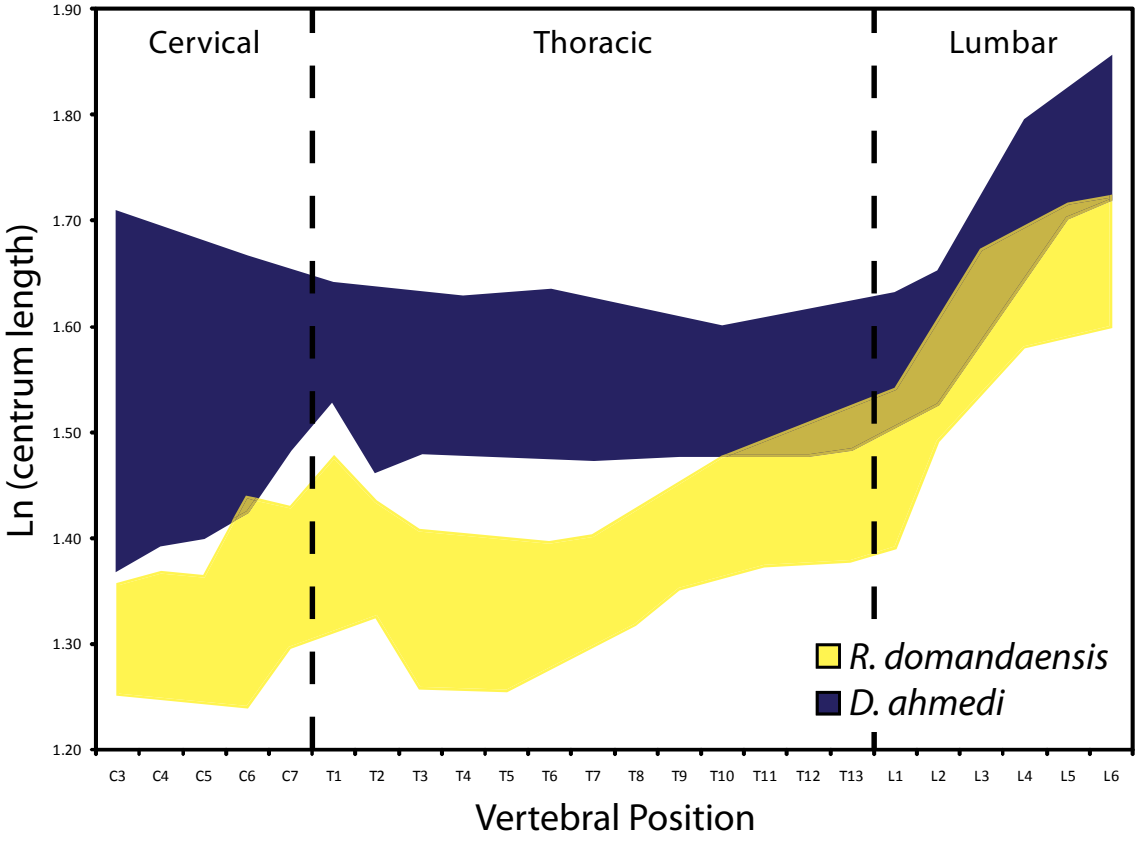

Figure 2.4. Centrum length profiles for presacral vertebral columns of the California sea lion (*Zalophus californianus*) and harbor seal (*Phoca vitulina*). Navy and yellow shadings mark the ranges of sampled males and females respectively. Note the consistent shape of the vertebral profiles between males and females, despite the differences in overall size.

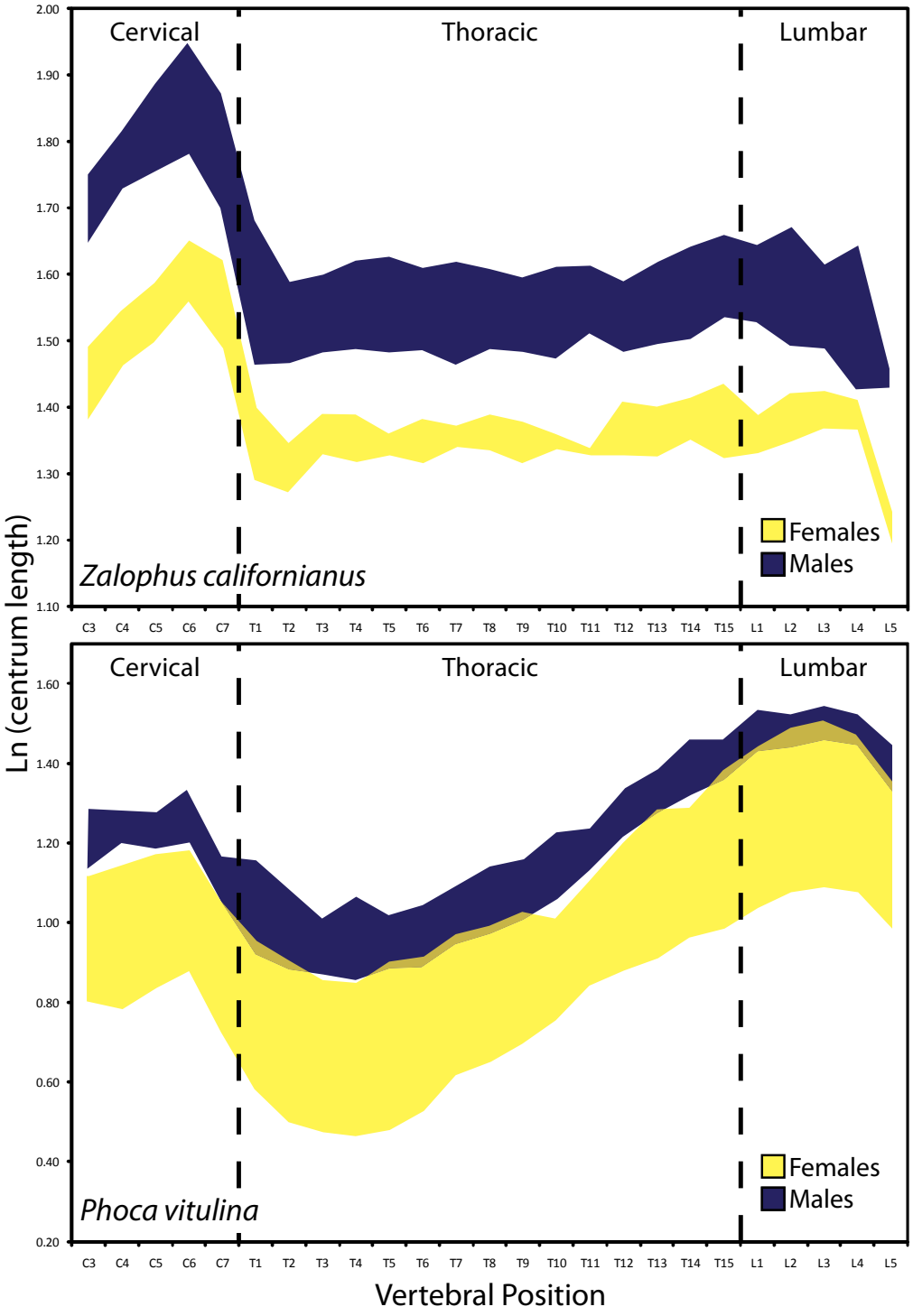

Figure 2.5. Mean percent differences in centrum length between *Dalanistes ahmedi* and *Remingtonocetus domandaensis*, male and female California sea lions (*Zalophus californianus*), and male and female harbor seals (*Phoca vitulina*) by presacral vertebral region. Note the greater size disparity among cervical and anterior thoracic vertebrae than among posterior thoracic and lumbar vertebrae between *D. ahmedi* and *R. domandaensis*.

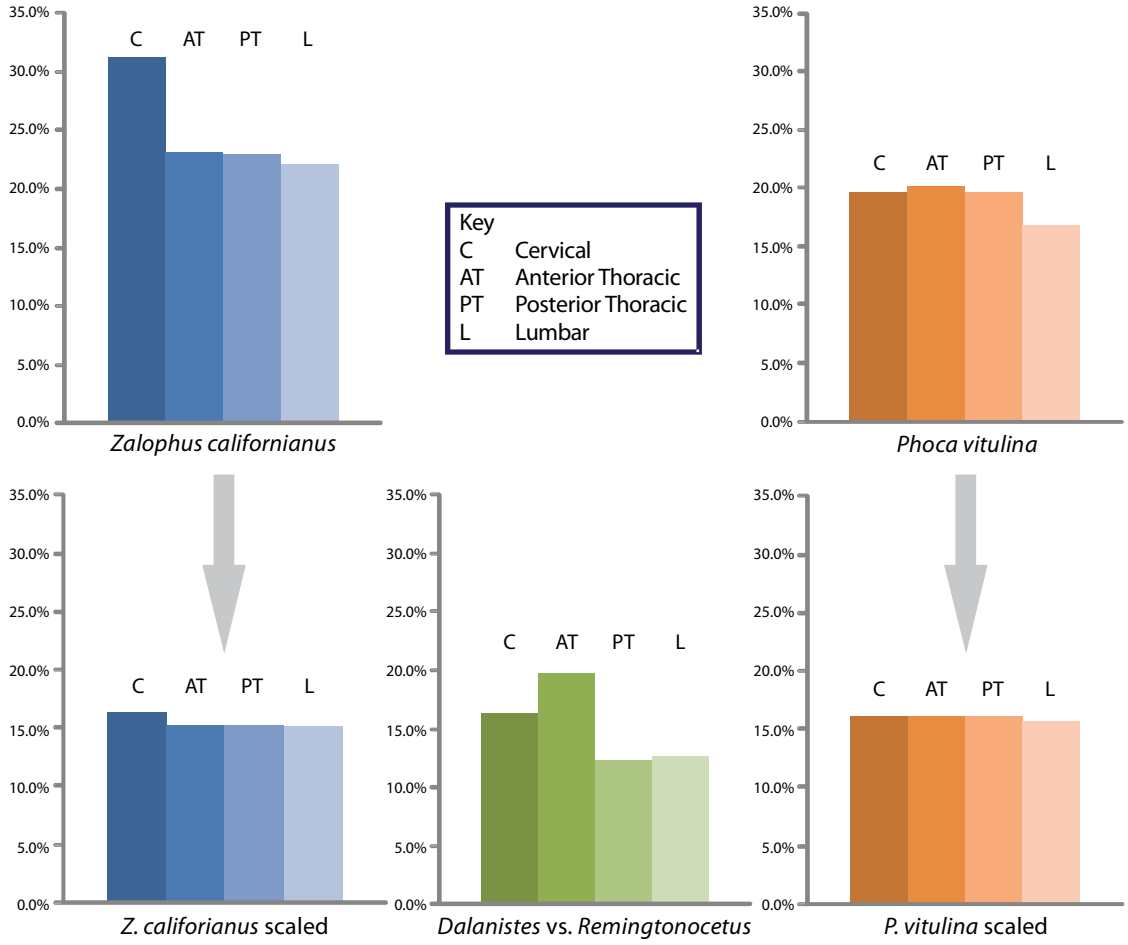

Figure 2.6. Distribution of *Andrewsiphius sloani*, *Remingtonocetus domandaensis*, and *Dalanistes ahmedi* specimens from the middle and upper parts of the Domanda Formation. Note the absence of *D. ahmedi* from the upper Domanda Formation.

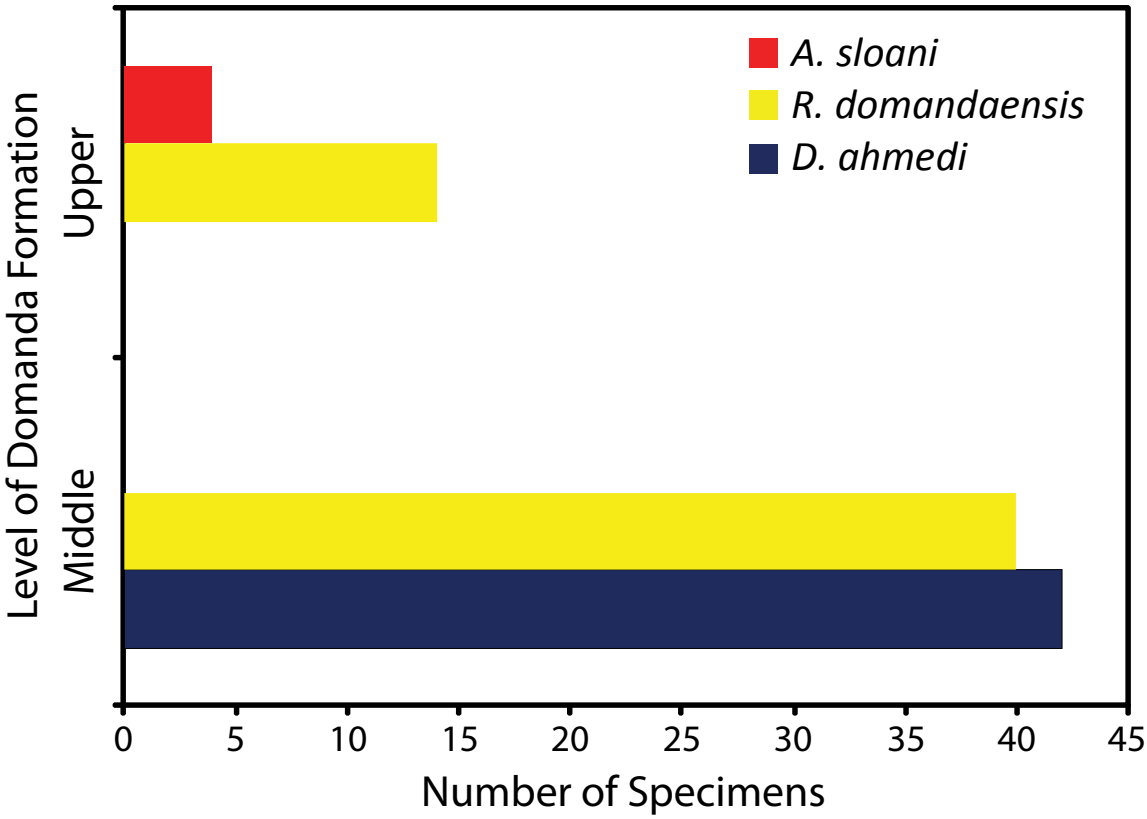

Table 2.1. Complete specimen list of *Andrewsiphius sloani*.

Specimen No.	References	Description
GSP-UM 3307	Gingerich et al., 2001	Three skull pieces, including partial mandible with alveoli for P_1-P_3
GSP-UM 3335	none	Fragmentary thoracic centrum
GSP-UM 3344	none	Fragmentary sacral centrum
GSP-UM 3393	Gingerich et al., 2001	Partial braincase with natural endocast
IITR-SB 2021	Bajpai and Thewissen, 1998	Palatal fragment with alveolus for right P^4 and roots for left and right M^1-M^3 (referred by Thewissen and Bajpai, 2009)
IITR-SB 2031	Thewissen and Bajpai, 2009	Maxilla with alveoli for left and right C^1-P^4
IITR-SB 2517	Thewissen and Bajpai, 2009	Rostrum fragment alveolus for right I^3, remnant or left dI^3?, and left and right C^1
IITR-SB 2526	Thewissen and Bajpai, 2009	Mandibular fragment with left and right P_4-M_1 and right alveolus for M_2
IITR-SB 2534	Thewissen and Bajpai, 2009	Gypsified braincase with left and right bullae, paroccipital processes, and occipital condyles; tentatively referred
IITR-SB 2600	Thewissen and Bajpai, 2009	Paroccipital process
IITR-SB 2648	Thewissen and Bajpai, 2009	Mandibular fragment with alveoli for P_4-M_1
IITR-SB 2650	Thewissen and Bajpai, 2009	Mandibular fragment with right ramus and alveoli for left P_3-M_3
IITR-SB 2701	Thewissen and Bajpai, 2009	Maxilla with roots for left and right P^2-P^3
IITR-SB 2712	Thewissen and Bajpai, 2009	Mandibular fragment with alveoli for left and right I_2-I_3
IITR-SB 2723	Thewissen and Bajpai, 2009	Mandibular fragment with alveoli and partial-to-complete crowns for P_3-M_3
IITR-SB 2724	Thewissen and Bajpai, 2009	Rostrum fragment with alveoli for left and right P^1-M^3 and some fragmentary molar crowns
IITR-SB 2725	Thewissen and Bajpai, 2009	Rostrum fragment with alveoli for left C^1-P^2 and right C^1-P^3 and a fragmentary crown for right C^1
IITR-SB 2742	Thewissen and Bajpai, 2009	Associated skull fragments
IITR-SB 2751	Thewissen and Bajpai, 2009	Two large skull fragments, including a well-preserved basicranium
IITR-SB 2786	Thewissen and Bajpai, 2009	Associated skull fragments
IITR-SB 2787	Thewissen and Bajpai, 2009	Mandibular fragment with incisor alveoli
IITR-SB 2793	Thewissen and Bajpai, 2009	Gypsified maxilla fragment with fragmentary M^2-M^3
IITR-SB 2794	Thewissen and Bajpai, 2009	Mandibular fragment with two unidentified alveoli on right and left sides
IITR-SB 2827	Thewissen and Bajpai, 2009	Mandibular fragment with alveoli for left and right I_2
IITR-SB 2833	Thewissen and Bajpai, 2009	Mandibular fragment with alveoli for left and right P_2 and unerupted crowns for P_3; tentatively referred

Table 2.1. Continued.

Specimen No.	References	Description
IITR-SB 2846	Thewissen and Bajpai, 2009	Maxillary fragment with alveoli for I^2 and I^3
IITR-SB 2866	Thewissen and Bajpai, 2009	Gypsified maxilla with roots for right P^3-M^3 and left P^1-P^2
IITR-SB 2869	Thewissen and Bajpai, 2009	Mandibular fragment with alveoli for left and right P_3-M_2
IITR-SB 2871	Thewissen and Bajpai, 2009	Associated skeletal elements, including skull material, vertebrae, and limb bones
IITR-SB 2879	Thewissen and Bajpai, 2009	Gypsified braincase; tentatively referred
IITR-SB 2907	Thewissen and Bajpai, 2009	Partial skull with complete sagittal and nuchal crests
IITR-SB 2923	Thewissen and Bajpai, 2009	Maxillary fragment with roots for P^2-M^2
IITR-SB 2930	Thewissen and Bajpai, 2009	Gypsified braincase; tentatively referred
IITR-SB 2951	Thewissen and Bajpai, 2009	Maxillary fragment with alveoli or roots for P^4-M^3
IITR-SB 2979	Thewissen and Bajpai, 2009	Cranial fragments including orbits and part of maxilla
IITR-SB 3093	Thewissen and Bajpai, 2009	Gypsified rostrum fragment with alveoli for P^1-P^3
IITR-SB 3153	Thewissen and Bajpai, 2009	Partial braincase with rostrum fragment
LUVP 11002	Sahni and Mishra, 1972	Mandibular fragment with alveoli for left and right P_4 and M_1 and right M_2; **holotype**
LUVP 11060	Sahni and Mishra, 1975	Mandible with alveoli for left and right I_3-M_2; holotype of *A. kutchensis* (referred by Thewissen and Bajpai, 2009)
LUVP 11132	Kumar and Sahni, 1986	Mandibular fragment with alveoli for left and right P_4-M_2 (referred by Thewissen and Bajpai, 2009)
LUVP 11165	Sahni and Mishra, 1975	Maxillary fragment with alveoli and roots for left and right P^4-M^1 and poor left M^2-M^3 crowns; holotype of *A. minor* (referred by Thewissen and Bajpai, 2009)
VPL 1019	Bajpai and Thewissen, 1998	Rostrum in two fragments with crown/roots for C^1-P^2 and alveoli for P^3-M^3 (referred by Thewissen and Bajpai, 2009)

Table 2.2. Complete published specimen list of *Remingtonocetus harudiensis*.

Specimen No.	References	Description
IITR-SB 2016	Bajpai and Thewissen, 1998	Fragmentary posterior maxilla with M^2-M^3 and partial orbit
IITR-SB 2017	Bajpai and Thewissen, 1998	Fragmentary braincase with left occipital condyle
IITR-SB 2018	Bajpai and Thewissen, 1998	Rostrum fragment with right P^2
IITR-SB 2019	Bajpai and Thewissen, 1998	Premaxilla with roots for I^1-I^3
IITR-SB 2020	Bajpai and Thewissen, 1998	Fragmentary maxilla with bases of left M^2-M^3 and endocasts of paranasal sinuses
IITR-SB 2022	Bajpai and Thewissen, 1998	Rostrum with partial orbits and bases of C^1-M^1
IITR-SB 2025	Bajpai and Thewissen, 1998	Left maxillary fragment with bases for M^1-M^3 and endocasts of paranasal sinuses
IITR-SB 2026	Bajpai and Thewissen, 1998	Fragmentary rostrum with bases for left and right P^2
IITR-SB 2529	Spoor et al., 2002	Partial cranium with ear region
IITR-SB 2592	Thewissen and Bajpai, 2001	Left mandible with mandibular foramen and M_1
IITR-SB 2630	Thewissen and Bajpai, 2001	Partial maxilla with crowns for left M^1-M^3
IITR-SB 2653	Thewissen and Bajpai, 2009	Two cervical, five thoracic, and two lumbar vertebrae (has not been described)
IITR-SB 2704	Thewissen and Bajpai, 2009	Mandible (has not been described)
IITR-SB 2770	Bajpai et al., 2009	Virtually complete skull
IITR-SB 2781	Nummela et al., 2007	Partial cranium including right ear region with parts of the squamosal, periotic, parietal, supraoccipital, and exoccipital
IITR-SB 2811	Thewissen and Bajpai, 2009	Mandible (has not been described)
IITR-SB 2812	Thewissen and Bajpai, 2009	Mandible (has not been described)
IITR-SB 2814	Thewissen and Bajpai, 2009	Mandible (has not been described)
IITR-SB 2828	Nummela et al., 2004	Partial braincase with left ear region
IITR-SB 2906	Thewissen and Bajpai, 2009	Two cervical, five thoracic, three lumbar, and three sacral vertebrae (has not been described)
IITR-SB 2914	Nummela et al., 2004	Partial braincase with left ear region
IITR-SB 3018	Das et al., 2009	Partial mandible
K60/996	Das et al., 2009	Skull preserved in articulation with the mandible
LUVP 11001	Sahni and Mishra, 1972	Partial skull (referred by Thewissen and Bajpai, 2009)

Table 2.2. Continued.

Specimen No.	References	Description
LUVP 11037	Sahni and Mishra, 1975	Incomplete skull with roots for P^4-M^3, isolated cusps of upper cheek teeth, left mandibular ramus with roots for P_4-M_3, right mandibular ramus with roots for P_4-M_2, and crowns for left M_1-M_2; **holotype**
LUVP 11038	Sahni and Mishra, 1975	Left innominate fragment including the acetabulum (referred by Gingerich et al., 2001)
LUVP 11069	Sahni and Mishra, 1975	Partial weathered sacrum (referred by Gingerich et al., 2001)
LUVP 11146	Sahni and Mishra, 1975	Partial gypsified braincase (referred by Thewissen and Bajpai, 2009)
VPL 1001	Bajpai and Thewissen, 1998	Poorly preserved skull
VPL 1004	Bajpai and Thewissen, 1998	Partial braincase
VPL 1010	Thewissen and Bajpai, 2009	Mandible (has not been described)
VPL 15001	Kumar and Sahni, 1986	Relatively complete skull with partial dentition
VPL 15002	Kumar and Sahni, 1986	Fragmentary skull
VPL 15003	Kumar and Sahni, 1986	Gypsified skull

Table 2.3. Complete specimen list of *Remingtonocetus domandaensis*.

Specimen No.	References	Description
GSP-UM 3	none	Vertebral fragment?
GSP-UM 9	Gingerich et al., 1993	Two proximal caudal vertebrae
GSP-UM 13	none	Partial cranium
GSP-UM 19	Gingerich et al., 1993	C5 centrum; initially identified as *Indocetus ramani*
GSP-UM 20	Gingerich et al., 1993	L4 posterior endplate; initially identified as *Indocetus ramani*
GSP-UM 77	Gingerich et al., 1993	Partial sacrum (S1-S2); initially identified as *Indocetus ramani*
GSP-UM 3009	Gingerich et al., 1993	Cranial fragments, vertebral fragments (C2, C7?), partial sacrum (S2-S3), fragmentary acetabulum (referred by Gingerich et al., 1995)
GSP-UM 3015	Gingerich et al., 1993	Cranial fragments, centra for C2-C4, C6, T2?-T3?, T7?, T9?, T13?, L1, L3, L5, two caudal vertebrae, proximal femur, partial tibia (referred by Gingerich et al., 1995)
GSP-UM 3054	Gingerich et al., 1995	Left femur missing only distal epiphysis, patella, proximal epiphysis of tibia
GSP-UM 3057	Gingerich et al., 1995	Cranial fragment (exoccipital), complete C2, centra for C3-C7, T3?, L2-L4, fragmentary sacrum (S1-S2), rib fragments, other fragments
GSP-UM 3101	Gingerich et al., 1995	Fragmentary skull, including frontal sinus and part of orbit
GSP-UM 3111	none	Fragmentary sacrum (S1-S2)
GSP-UM 3131	none	18 vertebral centra (including C6, C7, three other cervical fragments, T1-T4, T5?-T9?, L1)
GSP-UM 3155	none	L4 centrum
GSP-UM 3160	none	L6 centrum
GSP-UM 3166	none	Atlas, two fragmentary cervical centra, thoracic centrum; juvenile individual
GSP-UM 3169	none	T5? centrum
GSP-UM 3171	none	Tip of rostrum
GSP-UM 3180	none	C3 centrum
GSP-UM 3223	none	Anterior dentary fragment
GSP-UM 3225	Gingerich et al., 2001	Partial cranium and anterior rostrum, right dentary (including C_1-M_3), C1-C2, C3 centrum, C6 centrum, C7, T2?-T3?, T6?, L2, L5 centrum, one caudal vertebra, partial ribs; **holotype**
GSP-UM 3229	none	Maxilla fragment
GSP-UM 3232	none	Rostrum fragment; initially identified as *Dalanistes ahmedi*
GSP-UM 3241	none	Cervical centrum (either C3 or C4)
GSP-UM 3262	none	Pelvic fragment?
GSP-UM 3264	none	5 non-associated vertebral fragments (including C3 or C4 centrum)
GSP-UM 3267	none	Fragmentary centrum of caudal vertebra
GSP-UM 3274	none	L3 centrum
GSP-UM 3290	none	Two thoracic centra (including T5?), other fragments; initially identified as *Dalanistes ahmedi*
GSP-UM 3299	none	T7? centrum and partial neural spine
GSP-UM 3303	none	C6 centrum
GSP-UM 3304	none	Back of cranium

Table 2.3. Continued.

Specimen No.	References	Description
GSP-UM 3310	none	Ca1 centrum
GSP-UM 3313	none	Fragmentary ilium, centra for C6, L1, one caudal vertebra, other fragments
GSP-UM 3325	none	C5 centrum; initially identified as *Andrewsiphius sloani*
GSP-UM 3338	none	Fragmentary sacrum (S1)
GSP-UM 3340	none	Distal femur, miscellaneous fragments
GSP-UM 3345	none	T11? centrum
GSP-UM 3353	none	T3? centrum
GSP-UM 3361	none	Atlas, axis fragment, C5-C6 centra, dentary fragment; likely an immature individual
GSP-UM 3376	none	T1 centrum
GSP-UM 3383	none	Femur fragment, centra for C7, T10?, L3, L5-L6, one caudal vertebra, other fragments
GSP-UM 3390	none	Partial cervical centrum (C3, C4, or C5?)
GSP-UM 3408	Gingerich et al., 2001	Centra for C3, T11?-T12?, L2-L3, L5, complete L6, sacrum (S1-S4), four mostly complete caudal vertebrae, partial innominates (acetabula, ilium, ischium)
GSP-UM 3412	none	Partial sacrum (S1), fragmentary humerus, vertebral fragments
GSP-UM 3414	none	L1 centrum
GSP-UM 3415	Gingerich et al., 2001	Cranium and rostrum with complete right P^1, P^3, M^1-M^3
GSP-UM 3416	none	Centrum of caudal vertebra
GSP-UM 3418	none	Partial axis centrum and dens
GSP-UM 3419	none	Scapula fragment?
GSP-UM 3420	none	T7? centrum
GSP-UM 3422	none	Proximal femur
GSP-UM 3423	none	Proximal femur fragment, tooth row fragments
GSP-UM 3552	Bebej et al., 2007, Bebej, 2008	Partial skull, dentary, C1-T4, T5?, fragmentary centra of T6? and T10?, T11-S3, partial innominate (ilium, acetabulum, partial ischium, partial pubis)

Table 2.4. Complete specimen list of *Dalanistes ahmedi*.

Specimen No.	References	Description
GSP-UM 11	Gingerich et al., 1993, 1995	Partial sacrum (S2-S3); initially identified as *Indocetus ramani*, but referred to *D. ahmedi* by Gingerich et al., 1995
GSP-UM 12	Gingerich et al., 1993	Lumbar vertebral fragments; initially identified as *Indocetus ramani*
GSP-UM 14	Gingerich et al., 1993	Atlas fragments; initially identified as *Indocetus ramani*
GSP-UM 18	Gingerich et al., 1993	Partial innominate with acetabulum; initially identified as *Indocetus ramani*
GSP-UM 1856	Gingerich et al., 1995, 2001	Partial skull, rostrum fragment; initially identified as *Remingtonocetus* but recognized as immature *D. ahmedi* by Gingerich et al., 2001
GSP-UM 3045	Gingerich et al., 1995	Partial L4
GSP-UM 3052	Gingerich et al., 1995	Cranium
GSP-UM 3089	Gingerich et al., 1995	Partial innominate with ilium and acetabulum; initially identified as *Indocetus ramani*
GSP-UM 3096	Gingerich et al., 1995	C3 centrum
GSP-UM 3097	Gingerich et al., 1995	L6 centrum
GSP-UM 3099	Gingerich et al., 1995	Partial cranium, Ca1?, Ca4?
GSP-UM 3102	Gingerich et al., 1995	Sacrum (S1-S4), miscellaneous fragments
GSP-UM 3106	Gingerich et al., 1995	Partial skull, partial dentary, C2?, centra for C3, C5, T1, T2?, T4?-T6?, L1-L3, L5-L6, sacrum (S1-S4), partial innominate with ilium and acetabulum, femoral head and distal epiphysis; **holotype**
GSP-UM 3109	Gingerich et al., 1995	Mostly complete L5
GSP-UM 3115	Gingerich et al., 1995	Distal femur
GSP-UM 3126	none	Rostral fragment
GSP-UM 3146	none	Dentary fragments, six vertebral centra (T12?-T13?, L2, L4, S2 or S3, one caudal), miscellaneous fragments
GSP-UM 3159	none	C3 centrum, fragmentary C5, fragmentary lumbar centrum (L4 or L5), miscellaneous fragments
GSP-UM 3165	none	Dentary with full to partial C_1-M_3, centra for C2-C7, T1?-T3?, T5?-T6?, T8?-T10?, one caudal, various rib and vertebral fragments
GSP-UM 3176	none	C7 centrum; initially identified as *Remingtonocetus*
GSP-UM 3215	none	Distal femur
GSP-UM 3252	none	Presphenoid, partial T4?
GSP-UM 3263	none	Maxillary fragment
GSP-UM 3269	none	Metapodial fragment?
GSP-UM 3273	none	Distal tibia
GSP-UM 3276	none	Dentary fragments, centra for C7, T1?, T3?, T6?-T7?, T10?
GSP-UM 3279	none	Sacrum (S1-S4), centra for C3, C6, T1?, T3?, T7?-T10?, L4, Ca1?
GSP-UM 3289	none	Partial innominate with fragmentary acetabulum

Table 2.4. Continued.

Specimen No.	References	Description
GSP-UM 3291	none	Centrum of caudal vertebra
GSP-UM 3295	Gingerich et al., 2001	Immature skull and dentary with partially erupted M^3
GSP-UM 3296	none	Partial innominate with acetabulum
GSP-UM 3297	none	Centra for C6, two thoracics (including T10?), other vertebral fragments, scapula fragment?; initially identified as *Remingtonocetus*
GSP-UM 3320	none	Skull and dentary fragments
GSP-UM 3368	none	Centra for C3, L2, L6
GSP-UM 3369	none	Partial innominate with acetabulum
GSP-UM 3371	none	Distal femur, T2? centrum
GSP-UM 3372	none	Rostral fragment, dentary fragment, centra for C5, T2?, T4?, T6?, L1, S1-S3, one caudal; likely a juvenile individual
GSP-UM 3401	none	L2? centrum
GSP-UM 3417	none	Caudal centrum; initially identified as *Remingtonocetus*
GSP-UM 3421	none	T2? centrum; initially identified as *Remingtonocetus*
GSP-UM 3424	none	Presphenoid, T11? centrum
GSP-UM 3489	none	Partial sacrum (S1-S3)
IITR-SB 2521	Thewissen and Bajpai, 2001	Partial left and right dentaries with left I_2 and P_2-M_3 and right P_4-M_2 and an associated thoracic vertebra
IITR-SB 2938	Thewissen and Bajpai, 2009	Mandible (has not been described)
NHML M50719	Gingerich et al., 1995	Occiput with partial rostrum and associated C6 centrum

Table 2.5. Complete specimen list of *Kutchicetus minimus*.

Specimen No.	References	Description
IITR-SB 2541	Thewissen and Bajpai, 2009	Mandibular fragment with alveoli for left and right M_1
IITR-SB 2590	Thewissen and Bajpai, 2009	Left P^1; tentatively referred
IITR-SB 2617	Thewissen and Bajpai, 2009	Mandibular fragment with alveoli for right P_4-M_1 and left P_4-M_2
IITR-SB 2618	Thewissen and Bajpai, 2009	Mandibular fragment with alveoli for left and right I_1-C_1
IITR-SB 2629	Thewissen and Bajpai, 2009	Mandibular fragment with alveoli for left P_2-M_3 and right P_2-P_4; tentatively referred
IITR-SB 2636	Thewissen and Bajpai, 2009	Complete mandibular rami and alveoli for left and right I_1-M_3
IITR-SB 2647	Bajpai and Thewissen, 2000	Partial non-articulated skeleton including skull and dental fragments, numerous partial vertebrae, partial limb bones partial innominate, and rib fragments; **holotype**
IITR-SB 2780	Thewissen and Bajpai, 2009	Mandible with alveoli for left and right P_2-M_1
IITR-SB 2791	Thewissen and Bajpai, 2009	Rostrum with partial orbit, alveoli for I^3-M^3, and partial I^1-I^3
IITR-SB 2949	Thewissen and Bajpai, 2009	Mandibular fragment with base of left and right M_1 and alveoli for M_2-M_3
IITR-SB 3100	Thewissen and Bajpai, 2009	Rostrum fragment with alveoli for M^1-M^2
VPL 1007	Bajpai and Thewissen, 1998	Associated braincase and rostral fragments with alveoli and crown for left M^3 (referred by Bajpai and Thewissen, 2009)

Table 2.6. Centrum lengths of presacral vertebrae in *Dalanistes ahmedi*. Measurements are in cm.

Specimen No.	C3	C4	C5	C6	C7	T1	T2	T3	T4	T5	T6	T7	T8	T9	T10	T11	T12	T13	L1	L2	L3	L4	L5	L6
GSP-UM 3045	-	-	-	-	-	-	-	-	-	-	-	-	-	-	-	-	-	-	-	-	-	6.24	-	-
GSP-UM 3096	5.49	-	-	-	-	-	-	-	-	-	-	-	-	-	-	-	-	-	-	-	-	-	-	-
GSP-UM 3097	-	-	-	-	-	-	-	-	-	-	-	-	-	-	-	-	-	-	-	-	-	-	-	6.39
GSP-UM 3106	5.51	-	4.93	-	-	5.15	4.69	-	4.96	4.95	5.13	-	-	-	-	-	-	-	5.10	5.07	5.25	-	5.70	5.92
GSP-UM 3109	-	-	-	-	-	-	-	-	-	-	-	-	-	-	-	-	-	-	-	-	-	-	5.49	-
GSP-UM 3146	-	-	-	-	-	-	-	-	-	-	-	-	-	-	-	-	4.39	4.42	-	4.92	-	5.90	-	-
GSP-UM 3159	4.94	-	4.56	-	-	-	-	-	-	-	-	-	-	-	-	-	-	-	-	-	-	-	-	-
GSP-UM 3165	3.93	4.02	4.05	4.16	4.40	4.62	4.32	4.39	-	4.58	4.58	-	4.63	4.70	4.84	-	-	-	-	-	-	-	-	-
GSP-UM 3176	-	-	-	-	4.67	-	-	-	-	-	-	-	-	-	-	-	-	-	-	-	-	-	-	-
GSP-UM 3252	-	-	-	-	-	-	-	-	5.09	-	-	-	-	-	-	-	-	-	-	-	-	-	-	-
GSP-UM 3276	-	-	-	-	4.41	4.75	-	4.69	-	-	4.66	4.80	-	-	4.45	-	-	-	-	-	-	-	-	-
GSP-UM 3279	4.60	-	-	4.62	-	4.84	-	4.40	-	-	-	4.37	4.50	4.39	4.47	-	-	-	-	-	-	6.03	-	-
GSP-UM 3297	-	-	-	4.24	-	-	-	-	-	-	-	-	-	-	4.95	-	-	-	-	-	-	-	-	-
GSP-UM 3368	4.46	-	-	-	-	-	-	-	-	-	-	-	-	-	-	-	-	-	-	4.60	-	-	-	5.60
GSP-UM 3371	-	-	-	-	-	-	4.68	-	-	-	-	-	-	-	-	-	-	-	-	-	-	-	-	-
GSP-UM 3401	-	-	-	-	-	-	-	-	-	-	-	-	-	-	-	-	-	-	-	5.22	-	-	-	-
GSP-UM 3424	-	-	-	-	-	-	-	-	-	-	-	-	-	-	-	4.58	-	-	-	-	-	-	-	-
NHML M50719	-	-	-	5.29	-	-	-	-	-	-	-	-	-	-	-	-	-	-	-	-	-	-	-	-
Sample Size	6	1	3	4	3	4	3	3	2	2	3	2	2	2	4	1	1	1	1	4	1	3	2	3
Mean	4.82	4.02	4.51	4.58	4.49	4.84	4.56	4.49	5.03	4.77	4.79	4.59	4.57	4.55	4.68	4.58	4.39	4.42	5.10	4.95	5.25	6.06	5.60	5.97

Table 2.7. Centrum lengths of presacral vertebrae in *Remingtonocetus domandaensis*. Measurements are in cm.

Specimen No.	C3	C4	C5	C6	C7	T1	T2	T3	T4	T5	T6	T7	T8	T9	T10	T11	T12	T13	L1	L2	L3	L4	L5	L6
GSP-UM 19	-	-	3.91	-	-	-	-	-	-	-	-	-	-	-	-	-	-	-	-	-	-	-	-	-
GSP-UM 3009	-	-	-	-	4.07	-	-	-	-	-	-	-	-	-	-	-	-	-	-	-	-	-	-	-
GSP-UM 3015	3.88	3.69	-	3.98	-	-	4.15	4.09	-	-	-	3.87	-	3.86	-	-	-	3.97	4.10	-	4.76	4.97	5.13	-
GSP-UM 3057	3.89	3.84	3.67	3.46	3.65	-	-	3.52	-	-	-	-	-	-	-	-	-	-	-	4.53	4.76	4.85	-	-
GSP-UM 3131	-	-	-	3.63	3.77	4.04	3.76	3.86	3.88	3.70	3.75	3.77	3.74	4.01	-	-	-	-	4.02	-	-	-	-	-
GSP-UM 3155	-	-	-	-	-	-	-	-	-	-	-	-	-	-	-	-	-	-	-	-	-	5.04	-	-
GSP-UM 3160	-	-	-	-	-	-	-	-	-	-	-	-	-	-	-	-	-	-	-	-	-	-	-	4.95
GSP-UM 3169	-	-	-	-	-	-	-	-	-	3.77	-	-	-	-	-	-	-	-	-	-	-	-	-	-
GSP-UM 3180	3.50	-	-	-	-	-	-	-	-	-	-	-	-	-	-	-	-	-	-	-	-	-	-	-
GSP-UM 3225	3.77	-	-	3.75	3.84	-	4.20	4.05	-	-	4.04	-	-	-	-	-	-	-	-	4.44	-	-	5.13	-
GSP-UM 3241	3.60	-	-	-	-	-	-	-	-	-	-	-	-	-	-	-	-	-	-	-	-	-	-	-
GSP-UM 3274	-	-	-	-	-	-	-	-	-	-	-	-	-	-	-	-	-	-	-	-	4.84	-	-	-
GSP-UM 3290	-	-	-	-	-	-	-	-	-	3.51	-	-	-	-	-	-	-	-	-	-	-	-	-	-
GSP-UM 3299	-	-	-	-	-	-	-	-	-	-	-	4.06	-	-	-	-	-	-	-	-	-	-	-	-
GSP-UM 3303	-	-	-	4.04	-	-	-	-	-	-	-	-	-	-	-	-	-	-	-	-	-	-	-	-
GSP-UM 3313	-	-	-	4.18	-	-	-	-	-	-	-	-	-	-	-	-	-	-	4.28	-	-	-	-	-
GSP-UM 3325	-	-	3.86	-	-	-	-	-	-	-	-	-	-	-	-	-	-	-	-	-	-	-	-	-
GSP-UM 3345	-	-	-	-	-	-	-	-	-	-	-	-	-	-	-	4.12	-	-	-	-	-	-	-	-
GSP-UM 3353	-	-	-	-	-	-	-	4.08	-	-	-	-	-	-	-	-	-	-	-	-	-	-	-	-
GSP-UM 3376	-	-	-	-	-	4.38	-	-	-	-	-	-	-	-	-	-	-	-	-	-	-	-	-	-
GSP-UM 3383	-	-	-	-	4.15	-	-	-	-	-	-	-	-	-	4.38	-	-	-	-	-	5.32	-	5.57	5.61
GSP-UM 3408	3.86	-	-	-	-	-	-	-	-	-	-	-	-	-	-	4.08	4.05	-	-	4.73	4.85	-	5.14	5.23
GSP-UM 3414	-	-	-	-	-	-	-	-	-	-	-	-	-	-	-	-	-	-	4.67	-	-	-	-	-
GSP-UM 3420	-	-	-	-	-	-	-	-	-	-	-	3.75	-	-	-	-	-	-	-	-	-	-	-	-
GSP-UM 3552	4.04	3.98	3.87	4.25	4.15	4.27	4.16	4.09	4.00	3.86	-	-	-	-	-	4.00	4.05	4.20	4.23	4.67	4.85	5.12	5.18	5.29
Sample Size	7	3	4	7	6	3	4	6	2	4	2	4	1	2	1	3	2	2	5	4	6	4	5	4
Mean	3.79	3.84	3.83	3.90	3.94	4.23	4.07	3.95	3.94	3.71	3.90	3.86	3.74	3.94	4.38	4.07	4.05	4.09	4.26	4.59	4.90	5.00	5.23	5.27

Table 2.8. Percent differences in mean centrum lengths of *Dalanistes ahmedi* and *Remingtonocetus domandaensis*. Percent differences were calculated for each vertebral position by dividing the value for *D. ahmedi* by the value for *R. domandaensis* and subtracting one. For calculating mean differences by vertebral region, T1-T7 are identified as anterior thoracic vertebrae, while T8-13 are identified as posterior thoracic vertebrae.

Species	C3	C4	C5	C6	C7	T1	T2	T3	T4	T5	T6	T7
D. ahmedi	4.82	4.02	4.51	4.58	4.49	4.84	4.56	4.49	5.03	4.77	4.79	4.59
R. domandaensis	3.79	3.84	3.83	3.90	3.94	4.23	4.07	3.95	3.94	3.71	3.90	3.86
Percent Difference	27.2%	4.8%	17.9%	17.4%	14.1%	14.4%	12.2%	13.8%	27.5%	28.4%	23.0%	18.7%

Species	T8	T9	T10	T11	T12	T13	L1	L2	L3	L4	L5	L6
D. ahmedi	4.57	4.55	4.68	4.58	4.39	4.42	5.10	4.95	5.25	6.06	5.60	5.97
R. domandaensis	3.74	3.94	4.38	4.07	4.05	4.09	4.26	4.59	4.90	5.00	5.23	5.27
Percent Difference	22.1%	15.5%	6.8%	12.6%	8.4%	8.2%	19.7%	7.8%	7.2%	21.3%	7.0%	13.3%

Mean Differences	
Cervicals	16.3%
Anterior Thoracics	19.7%
Posterior Thoracics	12.3%
Lumbars	12.7%

Table 2.9. Centrum lengths of presacral vertebrae in the California sea lion (*Zalophus californianus*) and percent differences between males and females. Measurements are in cm. Percent differences were calculated for each vertebral position by dividing the mean centrum length of males by the mean centrum length of females and subtracting one. For calculating mean differences by vertebral region, T1-T8 are identified as anterior thoracic vertebrae, while T9-T15 are identified as posterior thoracic vertebrae.

Specimen No.	Sex	C3	C4	C5	C6	C7	T1	T2	T3	T4	T5	T6	T7	T8
USNM 200847	M	5.19	5.64	5.79	5.94	5.46	4.32	4.33	4.39	4.41	4.38	4.41	4.32	4.41
USNM A14410	M	5.75	6.14	6.61	7.01	6.50	5.36	4.90	4.95	5.06	5.09	5.00	5.05	5.00
USNM 252144	F	4.43	4.67	4.87	5.19	5.04	4.04	3.84	4.00	4.01	3.88	3.97	3.93	3.99
USNM 504203	F	3.98	4.31	4.47	4.73	4.41	3.63	3.55	3.78	3.73	3.89	3.87	3.84	3.84
USNM 504991	F	4.15	4.35	4.56	4.83	4.68	3.71	3.65	3.76	3.84	3.75	3.71	3.82	3.80
Male Mean		5.47	5.89	6.20	6.48	5.98	4.84	4.61	4.67	4.73	4.73	4.71	4.68	4.70
Female Mean		4.18	4.44	4.63	4.92	4.71	3.79	3.68	3.85	3.86	3.84	3.85	3.86	3.87
Percent Difference		30.7%	32.5%	33.8%	31.7%	27.0%	27.7%	25.3%	21.4%	22.7%	23.3%	22.3%	21.4%	21.3%

Specimen No.	Sex	T9	T10	T11	T12	T13	T14	T15	L1	L2	L3	L4	L5
USNM 200847	M	4.40	4.35	4.51	4.41	4.46	4.49	4.64	4.60	4.44	4.41	4.16	-
USNM A14410	M	4.93	5.01	5.02	4.90	5.05	5.16	5.25	5.18	5.31	5.02	5.17	4.29
USNM 252144	F	3.97	3.89	3.75	4.07	4.04	4.11	4.18	3.99	3.90	4.15	4.08	3.45
USNM 504203	F	3.82	3.79	3.79	3.84	3.80	3.85	3.76	3.78	3.85	3.91	3.91	3.35
USNM 504991	F	3.71	3.81	3.78	3.76	3.76	3.84	3.88	3.86	4.12	4.02	4.03	3.30
Male Mean		4.67	4.68	4.76	4.65	4.75	4.82	4.95	4.89	4.88	4.72	4.66	4.29
Female Mean		3.83	3.83	3.77	3.89	3.87	3.93	3.94	3.87	3.96	4.03	4.01	3.37
Percent Difference		21.7%	22.2%	26.2%	19.6%	22.9%	22.7%	25.6%	26.2%	23.2%	17.2%	16.4%	27.3%

Mean Differences	
Cervicals	31.2%
Anterior Thoracics	23.2%
Posterior Thoracics	22.5%
Lumbars	22.1%

Table 2.10. Centrum lengths of presacral vertebrae in the harbor seal (*Phoca vitulina*) and percent differences between males and females. Measurements are in cm. Percent differences were calculated for each vertebral position by dividing the mean centrum length of males by the mean centrum length of females and subtracting one. For calculating mean differences by vertebral region, T1-T8 are identified as anterior thoracic vertebrae, while T9-T15 are identified as posterior thoracic vertebrae.

Specimen No.	Sex	C3	C4	C5	C6	C7	T1	T2	T3	T4	T5	T6	T7	T8
USNM 504298	M	3.10	3.31	3.35	3.32	2.86	2.52	2.41	2.37	2.34	2.44	2.42	2.68	2.84
USNM 504526	M	3.27	3.31	3.28	3.35	2.97	2.69	2.43	2.39	2.38	2.42	2.44	2.57	2.65
USNM 219876	M	3.59	3.59	3.59	3.79	3.21	3.16	2.92	2.75	2.91	2.76	2.82	2.97	3.11
USNM 504299	F	2.22	2.18	2.31	2.41	2.06	1.79	1.65	1.60	1.59	1.62	1.70	1.84	1.92
USNM 250712	F	3.06	3.13	3.21	3.25	2.79	2.48	2.38	2.34	2.34	2.45	2.50	2.63	2.68
USNM 250713	F	2.96	2.98	3.05	3.23	2.85	2.59	2.46	2.28	2.21	2.36	2.33	2.56	2.49
Male Mean		3.32	3.40	3.41	3.49	3.02	2.79	2.59	2.50	2.54	2.54	2.56	2.74	2.87
Female Mean		2.75	2.76	2.86	2.96	2.57	2.28	2.16	2.07	2.05	2.14	2.17	2.34	2.36
Percent Difference		20.9%	23.1%	19.3%	17.7%	17.6%	22.2%	19.7%	20.9%	24.3%	18.4%	17.8%	16.9%	21.2%

Specimen No.	Sex	T9	T10	T11	T12	T13	T14	T15	L1	L2	L3	L4	L5
USNM 504298	M	2.97	3.08	3.29	3.52	3.71	3.83	3.90	4.19	4.23	4.30	4.24	4.24
USNM 504526	M	2.74	2.89	3.09	3.36	3.56	3.75	3.87	4.33	4.40	4.50	4.39	3.95
USNM 219876	M	3.19	3.39	3.43	3.81	4.01	4.28	4.28	4.61	4.56	4.66	4.56	3.78
USNM 504299	F	2.00	2.12	2.31	2.41	2.49	2.61	2.68	2.82	2.94	2.98	2.92	2.68
USNM 250712	F	2.79	2.68	3.00	3.31	3.51	3.61	3.96	4.24	4.41	4.53	4.36	3.85
USNM 250713	F	2.62	2.73	2.97	3.21	3.58	3.44	3.80	4.16	4.15	4.13	4.05	3.40
Male Mean		2.97	3.12	3.27	3.56	3.76	3.95	4.02	4.37	4.40	4.49	4.40	3.99
Female Mean		2.47	2.51	2.76	2.98	3.19	3.22	3.48	3.74	3.83	3.88	3.77	3.31
Percent Difference		20.2%	24.2%	18.4%	19.6%	17.7%	22.9%	15.3%	17.0%	14.6%	15.7%	16.5%	20.4%

Mean Differences	
Cervicals	19.7%
Anterior Thoracics	20.2%
Posterior Thoracics	20.0%
Lumbars	16.9%

Table 2.11. Differences in dimensions of alveoli and crown heights for upper and lower canines, premolars, and molars in *Dalanistes ahmedi* and *Remingtonocetus domandaensis*. Measurements are in cm. Percent differences were calculated for each measurement by dividing the mean for *D. ahmedi* (*D. ahm.*) by the mean for *R. domandaensis* (*R. dom.*) and subtracting one.

			C^1			P^1			P^2			P^3			P^4			M^1			M^2			M^3		
Species	**Spec. No.**	**Side**	**L**	**W**	**H**	**L**	**W**	**H**	**L**	**W**	**H**	**L**	**W**	**H**	**L**	**W**	**H**	**L**	**W**	**H**	**L**	**W**	**H**	**L**	**W**	**H**
R. dom.	GSP-UM 3225	R	2.95	1.47	-	2.19	1.58	-	-	-	-	-	-	-	-	-	-	-	-	-	-	-	-	-	-	-
		L	2.06	0.96	-	-	1.56	-	-	-	-	-	-	-	-	-	-	-	-	-	-	-	-	-	-	-
R. dom.	GSP-UM 3415	R	2.68	1.69	-	1.77	1.25	-	4.04	1.26	-	4.24	1.04	-	3.06	1.57	-	2.33	0.82	-	2.45	0.99	-	2.23	0.90	-
		L	2.55	1.34	-	1.83	1.35	-	3.79	1.19	-	4.15	1.39	-	-	-	-	-	-	-	-	-	-	-	-	-
D. ahm.	GSP-UM 3165	R	-	-	-	-	-	-	-	-	-	-	-	-	-	-	-	-	-	-	-	-	-	-	-	-
		L	-	-	-	-	-	-	-	-	-	-	-	-	-	-	-	-	-	-	-	-	-	-	-	-
D. ahm.	GSP-UM 3106	R	2.99	1.94	-	2.54	1.36	-	5.16	1.30	-	-	-	-	4.15	1.41	-	2.66	1.03	-	3.13	0.98	-	2.57	1.02	-
		L	2.89	2.17	-	2.19	1.20	-	5.03	1.04	-	-	-	-	3.80	1.67	-	-	-	-	-	-	-	-	-	-
D. ahm.	NHML M50719	R	-	-	-	-	-	-	-	-	-	-	-	-	-	-	-	-	-	-	2.37	1.29	-	2.63	1.18	-
		L	-	-	-	-	-	-	-	-	-	-	-	-	-	-	-	-	-	-	-	-	-	-	-	-
***R. domandaensis* Mean**			2.56	1.37	-	1.93	1.44	-	3.92	1.23	-	4.20	1.22	-	3.06	1.57	-	2.33	0.82	-	2.45	0.99	-	2.23	0.90	-
***D. ahmedi* Mean**			2.94	2.06	-	2.37	1.28	-	5.10	1.17	-	-	-	-	3.98	1.54	-	2.66	1.03	-	2.75	1.14	-	2.60	1.10	-
Percent Difference			15%	51%	-	23%	-11%	-	30%	-4%	-	-	-	-	30%	-2%	-	14%	26%	-	12%	15%	-	17%	22%	-

			C_1			P_1			P_2			P_3			P_4			M_1			M_2			M_3		
Species	**Spec. No.**	**Side**	**L**	**W**	**H**	**L**	**W**	**H**	**L**	**W**	**H**	**L**	**W**	**H**	**L**	**W**	**H**	**L**	**W**	**H**	**L**	**W**	**H**	**L**	**W**	**H**
R. dom.	GSP-UM 3225	R	2.29	1.47	2.77	1.84	1.11	-	3.50	0.90	1.90	4.43	0.82	-	3.78	0.80	2.80	2.81	1.00	-	2.58	0.89	-	2.04	0.85	-
		L	-	-	-	-	-	-	-	-	-	-	-	-	-	-	-	-	-	-	-	-	-	-	-	-
R. dom.	GSP-UM 3415	R	-	-	-	-	-	-	-	-	-	-	-	-	-	-	-	-	-	-	-	-	-	-	-	-
		L	-	-	-	-	-	-	-	-	-	-	-	-	-	-	-	-	-	-	-	-	-	-	-	-
D. ahm.	GSP-UM 3165	R	2.41	1.58	3.56	2.16	1.19	-	3.78	0.92	2.12	4.78	0.90	-	4.57	1.18	2.90	3.23	0.92	-	3.02	1.01	-	2.75	0.96	-
		L	-	-	-	-	-	-	-	-	-	-	-	-	-	-	-	-	-	-	-	-	-	-	-	-
D. ahm.	GSP-UM 3106	R	2.37	1.45	-	2.18	1.18	-	4.77	0.95	-	5.19	0.97	-	4.54	1.48	-	3.07	1.15	-	3.11	1.18	-	2.88	1.07	-
		L	-	-	-	-	-	-	-	-	-	-	-	-	-	-	-	-	-	-	-	-	-	-	-	-
D. ahm.	NHML M50719	R	-	-	-	-	-	-	-	-	-	-	-	-	-	-	-	-	-	-	-	-	-	-	-	-
		L	-	-	-	-	-	-	-	-	-	-	-	-	-	-	-	-	-	-	-	-	-	-	-	-
***R. domandaensis* Mean**			2.29	1.47	2.77	1.84	1.11	-	3.50	0.90	1.90	4.43	0.82	-	3.78	0.80	2.80	2.81	1.00	-	2.58	0.89	-	2.04	0.85	-
***D. ahmedi* Mean**			2.39	1.52	3.56	2.17	1.19	-	4.28	0.94	2.12	4.99	0.94	-	4.56	1.33	2.90	3.15	1.04	-	3.07	1.10	-	2.82	1.02	-
Percent Difference			4%	3%	29%	18%	7%	-	22%	4%	12%	13%	14%	-	21%	66%	4%	12%	3%	-	19%	23%	-	38%	19%	-

Mean Difference in Canine Dimensions	20.3%
Mean Difference in Premolar and Molar Dimensions	16.6%
Median Difference in Canine Dimensions	14.8%
Median Difference in Premolar and Molar Dimensions	15.6%

REFERENCES

Andrews, C. W. 1920. A description of new species of zeuglodont and of leathery turtle from the Eocene of southern Nigeria. Proceedings of the Zoological Society of London for 1919 (no volume number): 309-319.

Antar, M. S., I. S. Zalmout, and P. D. Gingerich. 2010. Sexual dimorphism in hind limbs of late Eocene *Basilosaurus isis* (Mammalia, Cetacea), Wadi Al Hitan World Heritage Site, Egypt. Journal of Vertebrate Paleontology, SVP Program and Abstracts Book: 54A-55A.

Bajpai, S., and J. G. M. Thewissen. 1998. Middle Eocene cetaceans from the Harudi and Subathu Formations of India. Pp. 213-233 in J. G. M. Thewissen (ed.), The Emergence of Whales: Evolutionary Patterns in the Origin of Cetacea. Plenum Press, New York.

Bajpai, S., and J. G. M. Thewissen. 2000. A new, diminutive Eocene whale from Kachchh (Gujarat, India) and its implications for locomotor evolution of cetaceans. Current Science 79: 1478-1482.

Bajpai, S., and J. G. M. Thewissen. 2002. Vertebrate fauna from Panandhro lignite field (lower Eocene), District Kachchh, western India. Current Science 82: 507-509.

Bajpai, S., J. G. M. Thewissen, and A. Sahni. 2009. The origin and early evolution of whales: macroevolution documented on the Indian subcontinent. Journal of Biosciences 34: 673-686.

Bebej, R. M. 2008. Lumbar spine of *Remingtonocetus* (Mammalia, Cetacea, Archaeoceti) and implications for aquatic locomotion. Journal of Vertebrate Paleontology 28: 49A.

Bebej, R. M. 2009. Possible sexual dimorphism in Remingtonocetidae (Mammalia, Cetacea, Archaeoceti) from the Domanda Formation of Pakistan. Journal of Vertebrate Paleontology, SVP Program and Abstracts Book: 60A.

Bebej, R. M., M. ul-Haq, I. S. Zalmout, and P. D. Gingerich. 2007. Functional interpretation of the neck in Eocene *Remingtonocetus* from Pakistan (Mammalia, Cetacea, Archaeoceti). Journal of Vertebrate Paleontology 27: 45A.

Biswas, S. K. 1992. Tertiary stratigraphy of Kutch. Journal of the Palaeontological Society of India 37: 1-29.

Coombs, M. C. 1975. Sexual dimorphism in chalicotheres (Mammalia, Perissodactyla). Systematic Zoology 24: 55-62.

Cooper, L. N., J. G. M. Thewissen, and S. T. Hussain. 2009. New middle Eocene archaeocetes (Cetacea: Mammalia) from the Kuldana Formation of northern Pakistan. Journal of Vertebrate Paleontology 29: 1289-1299.

Dehm, R., and T. z. Oettingen-Spielberg. 1958. Palëontologische und geologische Untersuchungen im Tertiär von Pakistan. 2. Die mitteleocänen Säugetiere von Ganda Kas bei Basal in Nordwest-Pakistan. Abhandlungen der Bayerische Akademie der Wissenschaften, Mathematisch-Naturwissenschaftliche Klasse, München, Neue Folge 91: 1-54.

Fleagle, J. G., R. F. Kay, and E. L. Simons. 1980. Sexual dimorphism. Nature 287: 328-330.

Fordyce, R. E. 1981. Systematics of the odontocete whale *Agorophius pygmaeus* and the family Agorophiidae (Mammalia: Cetacea). Journal of Paleontology 55: 1028-1045.

Fraas, E. 1904. Neue Zeuglodonten aus dem unteren Mitteleocän vom Mokattam bei Cairo. Geologische und Paläontologische Abhandlungen, Neue Folge 6: 199-220.

Geisler, J. H., A. E. Sanders, and Z. Luo. 2005. A new protocetid whale (Cetacea: Archaeoceti) from the late middle Eocene of South Carolina. American Museum Novitates 3480: 1-65.

Geisler, J. H., and M. D. Uhen. 2005. Phylogenetic relationships of extinct cetartiodactyls: results of simultaneous analyses of molecular, morphological, and stratigraphic data. Journal of Mammalian Evolution 12: 145-160.

Gingerich, P. D. 1981a. Cranial morphology and adaptations in Eocene Adapidae. I. Sexual dimorphism in *Adapis magnus* and *Adapis parisiensis*. American Journal of Physical Anthropology 56: 217-234.

Gingerich, P. D. 1981b. Variation, sexual dimorphism, and social structure in the early Eocene horse *Hyracotherium* (Mammalia, Perissodactyla). Paleobiology 7: 443-455.

Gingerich, P. D. 1995. Sexual dimorphism in earliest Eocene *Cantius torresi* (Mammalia, Primates, Adapoidea). Contributions from the Museum of Paleontology, University of Michigan 29: 185-199.

Gingerich, P. D. 2003. Stratigraphic and micropaleontological constraints on the middle Eocene age of the mammal-bearing Kuldana Formation of Pakistan. Journal of Vertebrate Paleontology 23: 643-651.

Gingerich, P. D., M. Arif, M. A. Bhatti, and W. C. Clyde. 1998. Middle Eocene stratigraphy and marine mammals (Mammalia: Cetacea and Sirenia) of the Sulaiman Range, Pakistan. Bulletin of the Carnegie Museum of Natural History 34: 239-259.

Gingerich, P. D., M. Arif, and W. C. Clyde. 1995. New archaeocetes (Mammalia, Cetacea) from the middle Eocene Domanda Formation of the Sulaiman Range, Punjab (Pakistan). Contributions from the Museum of Paleontology, University of Michigan 29: 291-330.

Gingerich, P. D., S. M. Raza, M. Arif, M. Anwar, and X. Zhou. 1993. Partial skeletons of *Indocetus ramani* (Mammalia, Cetacea) from the lower middle Eocene Domanda shale in the Sulaiman Range of Punjab (Pakistan). Contributions from the Museum of Paleontology, University of Michigan 28: 393-416.

Gingerich, P. D., S. M. Raza, M. Arif, M. Anwar, and X. Zhou. 1994. New whale from the Eocene of Pakistan and the origin of cetacean swimming. Nature 368: 844-847.

Gingerich, P. D., D. E. Russell, and N. A. Wells. 1981. Origin of whales (Mammalia, Cetacea) in epicontinental remnant seas: evidnce from the Eocene of Pakistan. Geological Society of America Abstracts with Programs 13: 459.

Gingerich, P. D., M. ul-Haq, I. H. Khan, and I. S. Zalmout. 2001. Eocene stratigraphy and archaeocete whales (Mammalia, Cetacea) of Drug Lahar in the eastern Sulaiman Range, Balochistan (Pakistan). Contributions from the Museum of Paleontology, University of Michigan 30: 269-319.

Gingerich, P. D., M. ul-Haq, W. von Koenigswald, W. J. Sanders, B. H. Smith, and I. S. Zalmout. 2009. New protocetid whale from the middle Eocene of Pakistan: birth on land, precocial development, and sexual dimorphism. PLoS ONE 4: e4366.

Gingerich, P. D., I. S. Zalmout, M. ul-Haq, and M. A. Bhatti. 2005. *Makaracetus bidens*, a new protocetid archaeocete (Mammalia, Cetacea) from the early middle Eocene of Balochistan (Pakistan). Contributions from the Museum of Paleontology, University of Michigan 31: 197-210.

Gradstein, F. M., J. G. Ogg, and A. G. Smith. 2004. A Geologic Time Scale 2004. Cambridge University Press, New York, 589 pp.

King, J. E. 1983. Seals of the World. 2nd Edition. Cornell University Press, Ithaca, 240 pp.

Krishtalka, L., R. K. Stucky, and K. C. Beard. 1990. The earliest fossil evidence for sexual dimorphism in primates. Proceedings of the National Academy of Sciences of the United States of America 87: 5223-5226.

Kumar, K., and A. Sahni. 1986. *Remingtonocetus harudiensis*, new combination, a middle Eocene archaeocete (Mammalia, Cetacea) from western Kutch, India. Journal of Vertebrate Paleontology 6: 326-349.

Kurtén, B. 1969. Sexual dimorphism in fossil mammals. Pp. 226-233 in G. E. G. Westermann (ed.), Sexual Dimorphism in Fossil Metazoa and Taxonomic Implications. E. Schweizerbart'sche Verlagsbuchhandlung, Stuttgart.

Lambert, O., G. Bianucci, and K. Post. 2010. Tusk-bearing beaked whales from the Miocene of Peru: sexual dimorphism in fossil ziphiids? Journal of Mammalogy 91: 19-26.

Nummela, S., S. T. Hussain, and J. G. M. Thewissen. 2006. Cranial anatomy of Pakicetidae (Cetacea, Mammalia). Journal of Vertebrate Paleontology 26: 746-759.

Nummela, S., J. G. M. Thewissen, S. Bajpai, S. T. Hussain, and K. Kumar. 2004. Eocene evolution of whale hearing. Nature 430: 776-778.

Nummela, S., J. G. M. Thewissen, S. Bajpai, S. T. Hussain, and K. Kumar. 2007. Sound transmission in archaic and modern whales: anatomical adaptations for underwater hearing. The Anatomical Record 290: 716-733.

O'Leary, M. A. 1999. Parsimony analysis of total evidence from extinct and extant taxa and the cetacean-artiodactyl question (Mammalia, Ungulata). Cladistics 15: 315-330.

O'Leary, M. A., and J. H. Geisler. 1999. The position of Cetacea within Mammalia: phylogenetic analysis of morphological data from extinct and extant taxa. Systematic Biology 48: 455-490.

O'Leary, M. A., and M. D. Uhen. 1999. The time of origin of whales and the role of behavioral changes in the terrestrial-aquatic transition. Paleobiology 25: 534-556.

Plavcan, J. M. 1994. Comparison of four simple methods for estimating sexual dimorphism in fossils. American Journal of Physical Anthropology 94: 465-476.

Ralls, K., and S. L. Mesnick. 2009. Sexual dimorphism. Pp. 1005-1011 in W. F. Perrin, B. Würsig, and J. G. M. Thewissen (eds.), Encyclopedia of Marine Mammals, 2nd Edition. Academic Press, San Diego.

Ravikant, V., and S. Bajpai. 2010. Strontium isotope evidence for the age of Eocene fossil whales of Kutch, western India. Geological Magazine 147: 473-477.

Sahni, A., and V. P. Mishra. 1972. A new species of *Protocetus* (Cetacea) from the middle Eocene of Kutch, western India. Palaeontology 15: 490-495.

Sahni, A., and V. P. Mishra. 1975. Lower Tertiary vertebrates from western India. Monograph of the Palaeontological Society of India 3: 1-48.

Singh, P., and M. P. Singh. 1991. Nannofloral biostratigraphy of the late middle Eocene strata of Kachchh region, Gujarat State, India. Geoscience Journal 12: 17-51.

Spoor, F., S. Bajpai, S. T. Hussain, K. Kumar, and J. G. M. Thewissen. 2002. Vestibular evidence for the evolution of aquatic behavior in early cetaceans. Nature 417: 163-166.

Thewissen, J. G. M., and S. Bajpai. 2001. Dental morphology of Remingtonocetidae (Cetacea, Mammalia). Journal of Paleontology 75: 463-465.

Thewissen, J. G. M., and S. Bajpai. 2009. New skeletal material of *Andrewsiphius* and *Kutchicetus*, two Eocene cetaceans from India. Journal of Paleontology 83: 635-663.

Thewissen, J. G. M., and S. T. Hussain. 1998. Systematic review of the Pakicetidae, early and middle Eocene Cetacea (Mammalia) from Pakistan and India. Bulletin of the Carnegie Museum of Natural History 34: 220-238.

Thewissen, J. G. M., and S. T. Hussain. 2000. *Attockicetus praecursor*, a new remingtonocetid cetacean from marine Eocene sediments of Pakistan. Journal of Mammalian Evolution 7: 133-146.

Thewissen, J. G. M., S. T. Hussain, and M. Arif. 1994. Fossil evidence for the origin of aquatic locomotion in archaeocete whales. Science 263: 210-212.

Trivedy, A. N., and P. P. Satsangi. 1984. A new archaeocete (whale) from the Eocene of India. Abstracts of the 27th International Geological Congress, Moscow 1: 322-323.

Uhen, M. D. 1999. New species of protocetid archaeocete whale, *Eocetus wardii* (Mammalia: Cetacea) from the middle Eocene of North Carolina. Journal of Paleontology 73: 512-528.

Uhen, M. D. 2004. Form, function, and anatomy of *Dorudon atrox* (Mammalia, Cetacea): an archaeocete from the middle to late Eocene of Egypt. University of Michigan Papers on Paleontology 34: 1-222.

Uhen, M. D., and P. D. Gingerich. 2001. New genus of dorudontine archaeocete (Cetacea) from the middle-to-late Eocene of South Carolina. Marine Mammal Science 17: 1-34.

West, R. M. 1980. Middle Eocene large mammal assemblage with Tethyan affinities, Ganda Kas region, Pakistan. Journal of Paleontology 54: 508-533.

Whiso, K., B. N. Tiwari, S. Bajpai, L. N. Cooper, and J. G. M. Thewissen. 2009. A fossil mammal from marine Eocene strata (Jaintia Group) of the Mikir Hills, Assam, northeastern India. Journal of the Palaeontological Society of India 54: 111-114.

Williams, E. M. 1998. Synopsis of the earliest cetaceans. Pp. 1-28 in J. G. M. Thewissen (ed.), The Emergence of Whales: Evolutionary Patterns in the Origin of Cetacea. Plenum Press, New York.

Chapter 3

Vertebral Morphology and Function of *Remingtonocetus domandaensis*

INTRODUCTION

Aquatic locomotion in archaeocete cetaceans is constrained by vertebral morphology and function. While archaeocetes in the family Remingtonocetidae have been known for several decades (e.g., Sahni and Mishra, 1972, 1975; Kumar and Sahni, 1986), very few vertebral elements have been described. Gingerich et al. (1993, 1995, 2001) described partial vertebrae of *Remingtonocetus domandaensis* and *Dalanistes ahmedi*, but because they were mostly centra from non-articulated vertebral columns, they provided little functional information. Partial vertebrae have also been described for *Kutchicetus minimus* (Bajpai and Thewissen, 2000; Thewissen and Bajpai, 2009), but these too offer little functional information due to their fragmentary nature.

GSP-UM 3552 is the most complete specimen of *Remingtonocetus domandaensis* known and has yet to be described. It preserves a partial cranium and dentary, all seven cervical vertebrae, ten partial to complete thoracic vertebrae, all six lumbar vertebrae, a partial sacrum, and much of a left innominate. Many of the vertebrae are virtually complete and exceptionally well-preserved, allowing the first in-depth functional interpretation of the remingtonocetid vertebral column. In addition,

many of the vertebrae were preserved in articulation, enabling their position in the column to be known with certainty. This allows the vertebral formula for *R. domandaensis* to be estimated with confidence, while also permitting dozens of vertebrae from other remingtonocetid specimens to be accurately identified. GSP-UM 3552 serves as the basis for the first postcranial reconstruction of *R. domandaensis* (Fig. 3.1) and provides key insights into the locomotor behavior of this taxon and the earliest stages in the evolution of swimming in cetaceans.

In this chapter, I begin with a review of vertebral formulae in early archaeocetes and propose a precaudal vertebral count for *Remingtonocetus domandaensis*. Most of the chapter is devoted to detailed descriptions of vertebral morphology for each position in the spine. The chapter concludes with functional interpretations of the vertebral column in *R. domandaensis*, especially with regard to locomotor behavior. These interpretations focus on the probable anatomy of the soft tissues of the spine (e.g., epaxial muscles and ligaments) as inferred from vertebral morphology. Interpretation of the lumbar region, in particular, provides the basis for alternative hypotheses of lumbar function tested in Chapters 4 and 5.

VERTEBRAL COUNTS

Knowledge of the number of vertebrae present in fossil cetaceans is crucial for understanding function because high vertebral counts increase the number of intervertebral joints, thereby increasing the flexibility of the column in the absence of other constraints (Buchholtz, 2001; Madar et al., 2002; Buchholtz and Schur, 2004).

Vertebral formulae of three fossil artiodactyls and nine archaeocete cetaceans are summarized in Table 3.1. No complete vertebral column has been recovered for any remingtonocetid, but vertebral formulas have been postulated for several remingtonocetid taxa. Gingerich et al. (1993) estimated a precaudal vertebral count in *Remingtonocetus domandaensis* (though these specimens were initially described as belonging to *Indocetus ramani*) as C7: T14: L5: S4 based on scant remains. Gingerich (1998) postulated a precaudal vertebral formula of C7: T13: L6: S4 for *Dalanistes ahmedi*, based on several partial specimens (GSP-UM 3099, 3106, 3165, and NHML 50719). Bajpai and Thewissen (2000) proposed a vertebral formula of C7: T15: L8: S4: Ca20-25 for *Kutchicetus minimus*. However, the holotype specimen (IITR-SB 2647) preserved only three cervical, eight thoracic, four lumbar, four sacral, and 13 caudal vertebrae (Thewissen and Bajpai, 2009).

The elevated number of thoracic and lumbar vertebrae estimated for *Kutchicetus minimus* was based largely on the count proposed for *Ambulocetus natans*. The initial description of the *A. natans* holotype (H-GSP 18507) included only four cervical, five thoracic, one lumbar, and two referred (H-GSP 18472 and field number 92148) caudal vertebrae (Thewissen et al., 1996). New material collected in a subsequent excavation was later attributed to the holotype, and Madar et al. (2002) described a precaudal vertebral count of C7: T16: L8: S4 for *A. natans*, noting that the thoracic count may be as high as 17. This estimate later led to the proposal that pakicetids, including *Pakicetus attocki*, *Ichthyolestes pinfoldi*, and *Nalacetus ratimitus*, possessed as many as 8-9 lumbar vertebrae (Madar, 2007).

These elevated thoracolumbar vertebral counts are equivocal for several reasons. First, the specimen upon which these elevated counts are based, the holotype of *Ambulocetus natans* (H-GSP 18507), was not preserved in articulation. Many of the vertebrae that were later assigned to the holotype were indeed preserved in close association, including the sacrum and 17 thoracolumbar vertebrae (Madar et al., 2002, Fig. 1, p. 406). But all other vertebrae assigned to this specimen were found as isolated, disarticulated elements. All of these skeletal elements plausibly belong to *A. natans*, but their attribution to a single individual is questionable. Madar et al. (2002) described the new holotypic material as coming from "a single block of indurated siltstone, approximately 30 cm below the central block of the original in situ specimens" (p. 405), so it is possible that the holotype specimen as currently defined represents two individuals of *A. natans* rather than one. But even if that is not the case, the vertebral formula of *A. natans* should be treated as tentative until a complete, articulated vertebral column is recovered, and it should certainly not be the basis for estimating vertebral counts in other archaeocetes whose vertebral columns are even more poorly known (e.g. *Pakicetus attocki*, *Kutchicetus minimus*).

Second, later semiaquatic archaeocetes, whose precaudal vertebral counts are known with certainty, possess fewer vertebrae than postulated for *Ambulocetus natans*. *Maiacetus inuus* (GSP-UM 3551) is the only known archaeocete specimen to preserve a complete vertebral column, yielding a formula of C7: T13: L6: S4: Ca21 (Gingerich et al., 2009). Other protocetids, however, possess complete precaudal vertebral columns that were preserved in articulation. *Rodhocetus kasranii* (Gingerich et al., 1994) and

Qaisracetus arifi (Gingerich et al., 2001) both possess unequivocal precaudal counts of C7: T13: L6: S4. The only direct evidence for elevated vertebral counts in archaeocetes comes from fully aquatic basilosaurids. *Dorudon atrox* and *Basilosaurus isis* are among the archaeocetes whose vertebral columns are well-characterized, though neither is known from a single complete specimen). Both species have elevated vertebral counts similar to those of many modern cetaceans. If the 'sacral lumbar' vertebrae of Buchholtz (1998) are counted here as sacral vertebrae, *D. atrox* has an estimated vertebral count of C7: T17: L16: S4: Ca21 (Uhen, 2004), while *B. isis* has an estimated vertebral count of C7: T16: L19: S4: Ca20 (Gingerich et al., in prep).

Buchholtz (2007) proposed a precaudal count of C7: T13: L6: S4 to be ancestral for cetaceans. Modern artiodactyls typically have precaudal counts of either C7: T13: L6: S4 or occasionally C7: T14: L5: S4 due to homeotic changes in gene expression (Buchholtz, 2007). Several Eocene artiodactyls, including *Archaeomeryx* (Colbert, 1941), *Messelobunodon* (Franzen, 1981), and possibly *Diacodexis* (Rose, 1985), also possessed a precaudal count of C7: T13: L6: S4. Given the information from fossil artiodactyls and early protocetids, it is most parsimonious to reconstruct early archaeocetes with a precaudal vertebral count of C7: T13: L6: S4 until well-preserved, articulated, and complete specimens dictate otherwise. It is possible that pakicetids, ambulocetids, and remingtonocetids experienced meristic increases in thoracic and lumbar counts that were autapomorphic or subsequently lost in protocetids (Buchholtz, 2007), but there is no unequivocal evidence for this.

No remingtonocetid specimen preserves a complete precaudal column, though GSP-UM 3552 (*Remingtonocetus domandaensis*) preserves more pre-caudal vertebrae than any known individual. C1-T3 were preserved in articulation, as were the two most posterior thoracic vertebrae through the lumbars and sacrum. Isolated elements of the mid-thoracic region were recovered, and it is clear that the thorax preserved in this specimen (comprising 10 partial to complete vertebrae) is incomplete. Thus, the exact thoracic count is not known. The lumbar count, however, is known with certainty. Six lumbar vertebrae were preserved in articulation between two posterior thoracic vertebrae and the sacrum in GSP-UM 3552. This number contrasts with the elevated lumbar counts proposed for some basal archaeocetes, but is consistent with the vertebral counts known in early protocetids. Based on this, the precaudal vertebral count of *R. domandaensis* is conservatively estimated to be the same as that of Eocene artiodactyls and early protocetid cetaceans: C7: T13: L6: S4. The identification of individual vertebral elements below follows this hypothesis, though the precise position of the thoracic vertebrae should be treated as tentative until a complete remingtonocetid thorax is recovered.

MORPHOLOGICAL DESCRIPTIONS

An individual vertebra is composed of two primary parts: a body and a neural arch. The cylindrical vertebral body or *centrum* lies ventral to the spinal cord. Adjacent vertebrae articulate via the anterior and posterior ends of the centrum known as endplates or *epiphyses*. Centra may have several associated processes. If present,

hypapophyses project ventrally from the midline of the centrum. *Transverse processes*, which are sometimes referred to as *pleurapophyses* (e.g., Owen, 1848; Cave, 1975), project laterally from either the centrum or the base of the neural arch. Ribs articulate with thoracic vertebrae via two facets. The facet that articulates with the head of the rib is called the *capitular facet* or *parapophysis*, while the facet that articulates with the tubercle of the rib is called the *tubercular facet* or *diapophysis*.

The *neural arch* lies lateral and dorsal to the spinal cord and defines the *neural canal*. The neural canal is flanked laterally by left and right *pedicles*, which rise dorsally from the centrum, and dorsally by left and right *laminae*, which arise from the pedicles and meet on the midline. In most cases, the neural arch possesses left and right articular facets known as *prezygapophyses* (on the anterior aspect) and *postzygapophyses* (on the posterior aspect) that articulate between adjacent vertebrae. In the lumbar regions of the spine, zygapophyses are often flanked by *mammillary processes* or *metapophyses*. In some cases, *accessory processes* or *anapophyses* project posteriorly from the lateral aspects of the laminae. A *spinous process* or *neural spine* projects dorsally from the neural arch at the midline.

When possible, the morphology of each vertebral position is described as follows. First, previously described specimens are summarized. Then, the morphology of the centrum and its associated processes is described. Finally, the morphology of the neural arch and its associated processes is described. Most of the descriptions are based on GSP-UM 3552, though certain positions (e.g., Ca1-Ca4) rely heavily on other

specimens (e.g., GSP-UM 3408). Measurements of vertebrae from GSP-UM 3408 and 3552 are listed in Tables 3.2-3.3.

Cervical Vertebrae

The cervical vertebrae of *Remingtonocetus domandaensis* have long been known from well-preserved centra (Gingerich et al., 1993, 1995) and several exceptionally-complete vertebrae (Gingerich et al., 1995, 2001). These specimens show some unusual features in remingtonocetids. Cervical centra are longer than they are in early protocetids, indicating that the neck was fairly long for an archaeocete. Further, the centra are rhomboidal or trapezoidal in lateral view, indicating that the head was habitually raised above the level of the rest of the body. However, it was not until GSP-UM 3552 was found that it became clear just how unusual the necks of remingtonocetids were. The following descriptions are based primarily on C1-C7 of GSP-UM 3552, whose cervical vertebrae were found virtually complete and in articulation.

C1 (Atlas) — As in all mammals, the first cervical vertebra, the atlas, possesses a unique morphology compared to all other vertebrae. As such, its description does not follow the pattern prescribed above. The atlas of *Remingtonocetus domandaensis* was very briefly described by Gingerich et al. (2001, p. 293). Two specimens include a partial atlas (GSP-UM 3166 and 3361), and two specimens include a virtually complete atlas (GSP-UM 3225 and 3552). The atlas of GSP-UM 3552 (Fig. 3.2) is slightly wider (21.2 cm) and taller (7.2 cm) than that of GSP-UM 3225 (18.9 cm in width and 6.9 cm in height). The entire element is flexed ventrally in the sagittal plane, indicating that there was

significant angulation between the long axes of the skull and neck (Gingerich et al., 2001). C-shaped cranial articular facets form deeply concave fossae for articulation with the occipital condyles of the skull.

The neural canal is shaped like a very rounded, ventrally-pointing triangle. The dorsal arch, which forms the dorsal border of the neural canal, is thicker anteriorly, tapering to a thin edge at its posterior margin, and possesses a small dorsal tubercle closer to its anterior margin. The anterior margin of the dorsal arch, in dorsal view, is marked by a broad supracondylar notch at the midline (terminology follows Geisler et al., 2005). The ventral arch, which forms the ventral margin of the neural canal, is slightly thicker than the dorsal arch and is marked by a prominent, posteriorly-projecting hypapophysis. The dorsal surface of the ventral arch forms a shallow, smooth odontoid fossa (for articulation with the dens or odontoid process of the axis), which is bordered by a sharp lip anteriorly and two pits laterally to accommodate the transverse ligament (GSP-UM 3225 possesses two sets of these pits). The posterior articular facets are ovoid with slightly concave surfaces. The facets are defined by sharp edges laterally and edges that blend smoothly into the odontoid fossa medially.

Broad wings project posterolaterally and are marked by two portions that meet at the level of the dorsal margin of the posterior articular facets. The dorsal portions extend obliquely from the dorsal arch, and the ventral portions extend almost vertically from the ventral arch, forming a deeply concave atlantal fossa. The margins of the dorsal portions are thinner and rounder than the margins of the ventral portions, which come to more prominent points ventrolaterally. Lateral to the posterior articular facets,

the ventral portions of the wings are perforated by transverse foramina. Anterodorsal to the anterior openings of the transverse foramina are the alar foramina. These foramina perforate the dorsal portions of the wings and lead to the lateral vertebral foramina, which pass through the anterior part of the dorsal arch just posterior to the cranial articular facets. These three sets of foramina accommodate the vertebral arteries, which pass first through the transverse foramina, then through the alar foramina, and finally through the lateral vertebral foramina, before entering the skull by way of the neural canal and foramen magnum (Gingerich et al., 2001).

C2 (Axis) — The axis was figured and briefly described by Gingerich et al. (1993, GSP-UM 3009 and 3015, Fig. 6, p. 401; 1995, GSP-UM 3057, Figs. 13-14, pp. 313-315). A number of specimens include parts of the axis (GSP-UM 3009, 3015, 3225, 3361, and 3418); however, few are complete. The axis of GSP-UM 3057 is mostly complete, but lacks the lateral parts of the cranial articular surfaces and the dorsal extent of the neural spine. The axis of GSP-UM 3552 is totally complete (Figs. 3.3-3.4). The dens (also known as the odontoid process) is thumb-shaped, with a flatter dorsal surface and rounder ventral surface, and projects anteriorly from the centrum. It is flanked laterally by two pits to accommodate the alar ligaments.

The oval-shaped cranial articular facets are lateral to these alar pits and possess surfaces that are gently concave medially before becoming convex out to the lateral margins. Large transverse foramina, obscured anteriorly by the articular facets, pass through thin, triangular transverse processes posterior to the articular facets. The transverse processes project ventrolaterally, tapering to a point, and possess flat,

broader surfaces that face caudally. The posterior epiphysis of the centrum is mostly circular in shape and depressed in the center. The ventral surface of the centrum is divided into two concave fossae by a prominent midline keel that begins at the posterior margin of the dens and terminates posteriorly in a robust, bifid hypapophysis. In lateral view, the centrum and dens are notably flexed in the sagittal plane and have a profile shaped like an obtuse triangle.

The pedicles of the neural arch are robust and define a neural canal that is circular in cross-section anteriorly and hemi-oval posteriorly. The postzygapophyses are flat, shaped like rounded parallelograms, and face ventrolaterally. The neural spine is robust, blade-like, and very thick at its base. A tuberosity for attachment of the dorsal atlanto-axial ligament is present dorsal to the neural canal on the anterior margin of the neural spine. The spine projects posteriorly and tapers very little anteroposteriorly along its length. The distal-most portion of the neural spine hooks ventrally and includes a dorsoventrally tall posterior margin in order to accommodate the nuchal ligament.

C3 — Centra for C3 were figured and briefly described by Gingerich et al. (1993, GSP-UM 3015, Fig. 6, pp. 401-402; 1995, GSP-UM 3057, Figs. 13-14, pp. 313-315; 2001, p. 293) and are known from many specimens (GSP-UM 3015, 3057, 3131, 3166, 3180, 3225, 3241, 3264, 3390, and 3408). Only GSP-UM 3552 preserves a complete C3 (Figs. 3.3-3.4). The centrum is longer than it is high or wide and has a rhombus-shaped profile when viewed laterally (described as "trapezoidal" by Gingerich et al., 1995). The anterior epiphysis is shield-shaped, while the posterior epiphysis is shaped like a broad

teardrop. Both epiphyses possess central depressions. The ventral surface of the centrum has a well-developed midline keel that terminates posteriorly at a robust hypapophysis, that may (e.g., GSP-UM 3057 and 3225) or may not (GSP-UM 3552) be bifid.

Large, oval transverse foramina flank the centrum laterally and reside dorsal to robust transverse processes, which measure 7.0 cm from the anterior-most point to the posterior-most point. The transverse processes are quadrilateral-shaped, with gently concave margins, and project ventrolaterally from the centrum. They are composite structures with two components connected by a thin lamina: a posterodorsal (or posterior) component, arising from the pedicle just ventral to the zygapophyses, and an anteroventral (or anterior) component, arising from the ventrolateral aspect of the centrum (Cave, 1975). The anterior component projects more than 2.0 cm in front of the anterior epiphysis of the centrum before merging distally with the thicker posterior component. The posterior component angles ventrolaterally with a very slight posterior inclination and possesses a distinct posterior projection distally.

The pedicles are very thick and define a circular neural canal. The pre- and postzygapophyses are flat, oval-shaped, and angled dorsomedially and ventrolaterally respectively. Slight depressions are present in the lateral aspect of the pedicles just anterior to the postzygapophyses. The neural spine is very short and rounded.

C4 — Centra for C4 were figured and briefly described by Gingerich et al. (1993, GSP-UM 3015, Fig. 6, pp. 401-402; 1995, GSP-UM 3057, Figs. 13-14, pp. 313-315) and are known from several specimens (GSP-UM 3015, 3057, 3131, 3166, 3241, 3264, and

3390). Only GSP-UM 3552 preserves a complete C4 (Figs. 3.3-3.4). C4 is very similar in morphology to C3, making it difficult to distinguish the two based on centra alone. The centrum of C4 is longer than it is high or wide and has a rhombus-shaped lateral profile. It is shorter anteroposteriorly than C3, but it is relatively longer compared to its height and width. The anterior epiphysis is nearly circular, while the posterior epiphysis is shaped like a broad teardrop. Both epiphyses possess central depressions, with that of the posterior epiphysis being relatively shallow. The ventral midline keel and non-bifid hypapophysis of C4 are less developed those of C3, but are still prominent.

The centrum is flanked by two oval transverse foramina and robust, ventrolaterally-projecting transverse processes. The transverse processes are similar in shape to those of C3, but are substantially larger and more robust, with a maximum anteroposterior length of 8.0 cm. The anterior component of the transverse process is more developed than that of C3, extending more than 3.0 cm in front of the anterior face of the centrum and resulting in a more expanded lamina connecting the anterior and posterior components. The distal corner of the posterior component forms a robust tuberosity.

The pedicles are even thicker than those of C3 and form a circular neural canal. The pre- and postzygapophyses are flat and oval-shaped with straighter medial edges; they face dorsomedially and ventrolaterally respectively. Slight depressions are present in the lateral aspect of the pedicles just anterior to the postzygapophyses. The neural spine is very short and rounded as in C3.

C5 — A centrum for C5 was figured and briefly described by Gingerich et al. (1993, GSP-UM 19, Fig. 5, pp. 401-402; 1995, GSP-UM 3057, Figs. 13-14, pp. 313-315). Only GSP-UM 3552 preserves a mostly complete C5 (missing only the distal-most portion of the right transverse process; Figs. 3.3-3.4), though centra are known from a number of specimens (GSP-UM 19, 3057, 3131, 3325, 3361, and 3390). The centrum is longer than it is high or wide and has a rhombus-shaped outline in lateral view. Anterior and posterior epiphyses possess central depressions and are mostly circular, though the lateral edges of the posterior epiphysis form rounded corners just ventral to the posterior openings of the oval-shaped transverse foramina. The ventral midline keel and non-bifid hypapophysis are less developed than in C3 and C4.

The plate-like transverse processes are smaller and less robust than those of C4, with a maximum anteroposterior length of 6.5 cm, and more triangular in shape. They are oriented more obliquely to the long axis of the vertebra and project less anteriorly and posteriorly when compared with C3 and C4. The posterior component of the transverse process is thick and forms a prominent ridge separating it from the thin lamina that connects it to the anterior component.

The pedicles are robust and form a circular neural canal. The pre- and postzygapophyses are similar in size, shape, and orientation to those of C4, and there are slight depressions anterior to the postzygapophyses. The neural spine is thicker and more developed than in C3 and C4, though it is still relatively short.

C6 — Centra for C6 were figured and/or briefly described by Gingerich et al. (1993, GSP-UM 3015, Fig. 6, pp. 401-402; 1995, GSP-UM 3057, Figs. 13-14, pp. 313-315;

2001, GSP-UM 3225, p. 293). Many C6 centra have been collected (GSP-UM 3015, 3057, 3131, 3303, 3313, and 3361), including some with transverse processes intact (GSP-UM 3225), but only GSP-UM 3552 preserves a complete C6 (Figs. 3.3-3.4). The centrum is easy to distinguish from the centra of other cervical vertebrae. The centrum is longer than it is high or wide, with a length greater than C3, C4, or C5. In lateral view, the centrum appears trapezoidal rather than rhomboidal in profile, as the planes defined by the anterior and posterior epiphyses form more of an acute angle dorsally rather than being parallel. Both epiphyses are circular and have shallow central depressions. There is a very small, weakly-developed ridge discernible on the ventral surfaces on some centra (e.g., GSP-UM 3552), but this is totally absent in others (e.g., GSP-UM 3225). C6 lacks a hypapophysis.

The ventrolaterally-projecting transverse processes are massive, reaching to over 7.0 cm below the ventral margin of the centrum, but are shaped differently than those of C3-C5, resembling a narrow sector of a circle. Anterior and posterior margins of the transverse processes begin roughly parallel, but steadily flare away from one another until reaching the ventral margin, which forms a shallow convex curve. The proximal part of the transverse process is marked by laterally-projecting, anteroposteriorly-facing flanges just lateral to the ovoid transverse foramina.

The pedicles are thick and form an oval neural canal. Zygapophyses are similar in size, shape, and orientation to those of C5. However, no depressions are apparent anterior to the postzygapophyses. The neural spine is broken in GSP-UM 3552, but it appears to be similar in height, but less robust, than that of C5.

C7 — Centra for C7 were figured and/or briefly described by Gingerich et al. (1995, GSP-UM 3057, Figs. 13-14, pp. 313-315; 2001, GSP-UM 3225, p. 293) and are preserved in a number of specimens (GSP-UM 3009, 3057, 3131, and 3383). Two complete C7 vertebrae are known (GSP-UM 3225 and 3552; Figs. 3.3-3.4). The centrum is longer than it is high or wide and has a rhomboidal outline in lateral profile like C3-C5. The anterior epiphysis is circular, while the posterior epiphysis is wider than it is high, giving it an oval shape. Both epiphyses possess shallow central depressions. The posterior epiphysis may (GSP-UM 3552) or may not (GSP-UM 3225) display obvious capitular facets on the lateral margin of the centrum. The ventral aspect of the centrum has neither a keel nor a hypapophysis.

Transverse processes are knob-like and project laterally from the centrum, curving ventrally. Small pits are present on the dorsal aspect of the transverse processes near where the ventral margins of the processes meet the centrum. Transverse foramina are absent.

Pedicles are thinner and outline a semicircular to triangular neural canal. Pre- and postzygapophyses are flat, roughly oval, and face dorsomedially and ventrolaterally respectively. Prominent pits are present in the pedicles just anterior to the postzygapophyses. The thin neural spine is taller than in all other cervical vertebrae and projects posteriorly.

Thoracic Vertebrae

No known remingtonocetid specimens include a full complement of thoracic vertebrae. GSP-UM 3131 includes nine fairly well-preserved centra that appear to be consecutive (T1-T9), while GSP-UM 3552 preserves the first six and last four thoracic vertebrae (T1-T6, T10-T13). GSP-UM 3225 preserves only three anterior thoracic vertebrae (T2-T3, T6), but they are virtually complete. Thoracic elements (primarily centra) from other specimens of *Remingtonocetus domandaensis* were identified to position by comparison with GSP-UM 3131, 3225 and 3552, along with some noteworthy specimens of *Dalanistes ahmedi* (GSP-UM 3106, 3165, 3276, and 3279).

T1 — Several specimens include T1 (GSP-UM 3131 and 3376), though only in GSP-UM 3552 is it mostly complete (Figs. 3.5-3.6). Overall, its morphology is similar to that of C7. The centrum is longer than it is wide or high anteriorly, but has a posterior epiphysis that is significantly wider than its anterior face. The anterior epiphysis approaches a pentagonal shape, as it possesses capitular facets ventrolaterally. The posterior epiphysis is broad and short, giving it an oval shape, and has capitular facets laterally. Transverse processes project laterally, coming off the centrum more dorsally than in C7, and possess curved tubercular facets; they lack developed metapophyses.

Pedicles are about the same width as in C7 and outline a more triangular and shorter neural canal. Prezygapophyses are oval, slightly curved, and face dorsomedially, though with more of a dorsal component than C7. Postzygapophyses are oval and face almost entirely ventrally. The neural spine is long and thin, projecting posteriorly at a 132° angle to the horizontal (in GSP-UM 3552).

T2 — Two centra (GSP-UM 3015 and 3131) and two mostly complete specimens (GSP-UM 3225 and 3552) are known for T2 (Figs. 3.5-3.6). GSP-UM 3552 preserves everything except for the neural spine, postzygapophyses, and left transverse process, while GSP-UM 3225 is nearly complete, missing only the prezygapophyses. The centrum is nearly identical in size and shape to that of T1. The transverse processes of T2 are similar in size and shape to those of T1, but notably differ in projecting laterally from the pedicles rather than from the centrum and possessing small, dorsally-projecting metapophyses

The neural canal is semicircular (GSP-UM 3225) to triangular (GSP-UM 3552) in shape and smaller in cross-sectional area than the neural canal of T1. Prezygapophyses are curved and face mostly dorsally with a small medial component. Postzygapophyses are flat and face totally ventrally. The neural spine is thin and long and projects more posteriorly than T1. The postzygapophyses and neural spine define a broad, triangular fossa in the posterior aspect of the neural arch, termed here the supraneural fossa.

T3 — A centrum of T3 was figured by Gingerich et al. (1995, GSP-UM 3057, Fig. 13, p. 314). Virtually complete T3 are known for GSP-UM 3225 and 3552 (Figs. 3.5-3.6), while centra are known from several other specimens (GSP-UM 3015, 3131, and 3353). Centra are similar in size and shape to those of T1 and T2. Transverse processes arise from the pedicles and project dorsolaterally, but are shorter, project more dorsally, and have more prominent metapophyses than those of T2.

The neural canal is more circular in cross-section. Pre- and postzygapophyses are flat and broadly set, facing dorsally and ventrally respectively. The neural spine is

long and thin, projecting slightly more dorsally than that of T2, and may possess a prominent keel along its posterior midline (GSP-UM 3225). A supraneural fossa is present like in T2.

T4-T10 — The middle thoracic vertebrae are poorly known in *Remingtonocetus domandaensis*. Because few preserve zygapophyses, neural arches, or neural spines, precise identification of vertebral position for these specimens is more tentative than for other thoracic vertebrae. Size and shape vary little in this region of the vertebral column, but because vertebral positions are known with confidence for GSP-UM 3131, 3225, and 3552, reasonable identifications for isolated centra were able to be proposed. Middle thoracic vertebrae have been identified for GSP-UM 3015 (T7, T9), 3131 (T4-T9), 3169 (T5), 3225 (T6), 3290 (T5), 3299 (T7), 3383 (T10), 3420 (T7), and 3552 (T4-T6, T10). Specimens that include partial neural arches are T5 of GSP-UM 3169, T6 of GSP-UM 3225 (which is mostly complete), and T4 of GSP-UM 3552 (Figs. 3.5-3.6).

Centra are as wide as (or wider than) they are long and change very little in size or shape from T4-T10. Epiphyses are heart- to shield-shaped and possess prominent capitular facets. Transverse processes project laterally from the pedicles as in T3, though they may become shorter in more posterior vertebrae.

Moderately thick pedicles define oval-shaped neural canals. Pre- and postzygapophyses face dorsally and ventrally respectively as in T3. A neural spine is preserved in T6 of GSP-UM 3225, and compared to T1-T3, it is relatively thicker, shorter, and more posteriorly-projecting. Postzygapophyses and a partial neural arch were preserved in articulation with T11 of GSP-UM 3552, indicating that T10 had

postzygapophyses oriented like other middle thoracic vertebrae and a neural spine that was inclined posteriorly.

T11 — Two centra (GSP-UM 3345 and 3408) and one specimen preserving prezygapophyses, transverse processes, and a partial neural arch (GSP-UM 3552) are known for T11 (Figs. 3.5-3.6). Centra are about the same length and height as anterior and middle thoracic vertebrae but are noticeably wider. Anterior and posterior epiphyses are more reniform than heart-shaped and possess distinct capitular facets. The lateral aspect of the centrum has a prominent ridge running between anterior and posterior capitular facets. Transverse processes are short and project slightly laterally from the pedicles. Tubercular facets are absent, but dorsal to the anterior capitular facets, there are pronounced lateral pits to accommodate costovertebral ligaments. These pits are bounded by three small projections: anteriorly by laterally-projecting transverse processes, dorsally by dorsal-projecting metapophyses, and posteriorly by caudally-projecting anapophyses.

The neural arch of GSP-UM 3552 is incomplete, but preserves an ovate neural canal that is wider than tall. Excavations in anterior laminae dorsal to the neural canal indicate fairly robust ligamenta flava. The orientation of the base of the neural spine suggests a slight posterior inclination. Prezygapophyses are flat, widely-set, and face dorsally and slightly laterally. Postzygapophyses have not been preserved, but the orientation of the posterior margins of the pedicles in GSP-UM 3552 is more vertical those of more anterior thoracic vertebrae, which have ventrally-oriented postzygapophyses. This suggests that T11 may have had higher-set, ventrolaterally-

oriented postzygapophyses like those of lumbar vertebrae. The combination of dorsally-oriented prezygapophyses and ventrolaterally-oriented postzygapophyses would define T11 as the diaphragmatic vertebra. This interpretation is favored here, but requires a more well-preserved specimen to be confirmed.

T12 — One fairly well-preserved centrum (GSP-UM 3408) and one specimen that includes a partial neural arch, but is more poorly preserved (GSP-UM 3552), are all that is known of T12 (Figs. 3.5-3.6). Centra are longer and wider than T11 and have strongly reniform anterior and posterior epiphyses. Capitular facets are present on the lateral margins of both anterior and posterior faces and are connected by a pronounced ridge as in T11. Transverse processes are not preserved in either specimen.

The neural canal is ovate with a greater width than height, and ligamentous pits are present in anterior laminae dorsal to the neural canal. Prezygapophyses are not preserved, but postzygapophyses are slightly curved, widely set, and face ventrolaterally. (Given the absence of prezygapophyses, it is possible that T12 may have dorsally-oriented prezygapophyses, thereby making it the diaphragmatic vertebra rather than T11. But for the reasons described above, it appears that T11 had ventrolaterally-oriented postzygapophyses, which necessitates T12 having dorsomedially-oriented prezygapophyses, thus precluding it from being diaphragmatic.) The neural spine is thin anteriorly, widens posteriorly, and projects dorsally at nearly a 90° angle to the plane of the centrum, defining T12 as the anticlinal vertebra.

T13 — One centrum (GSP-UM 3015) and one mostly complete specimen (GSP-UM 3552) are known for T13 (Figs. 3.5-3.6). Centra are longer and wider than T11 or

T12 and possess strongly reniform epiphyses. Anterior epiphyses have laterally-placed capitular facets, but the posterior epiphyses do not. Transverse processes are not preserved.

Neural canals are similar in size and shape to that of T12, and laminae dorsal to the neural canal are marked by ligamentous pits. Prezygapophyses are poorly preserved and broken, but it is clear that they are curved and face dorsomedially. Postzygapophyses are narrow, curved, and face ventrolaterally. The neural spine is incomplete and broken in GSP-UM 3552. The proximal part of the neural spine is oriented anteriorly at an angle of about 84.5° to the long axis of the centrum, whereas the distal part of the neural spine forms a much more obtuse angle. This change in orientation is attributed to breakage of the specimen, and the former measurement is taken to be a more accurate estimation of the neural spine angle in life.

Lumbar Vertebrae

Lumbar centra have long been known for *Remingtonocetus domandaensis* (Gingerich et al., 1993, 1995), but have remained undescribed because these specimens preserve virtually no additional features. GSP-UM 3552 preserves a full, articulated lumbar series (L1-L6), in which every vertebra is virtually complete. The following descriptions are based primarily on this specimen and comparison with complete lumbar vertebrae from GSP-UM 3225 and 3408, along with the holotype of *Dalanistes ahmedi* (GSP-UM 3106).

L1 — A centrum of L1 was figured by Gingerich et al. (1993, GSP-UM 3015, Figs. 7-8, pp. 402-403). Several centra have been collected (GSP-UM 3015, 3131, 3313, and 3414), but only GSP-UM 3552 preserves a complete L1 (Figs. 3.7-3.8). Centra have the shortest anteroposterior lengths among lumbar vertebrae, but are longer than posterior thoracic vertebrae. Anterior and posterior epiphyses are broad and reniform. Complete transverse processes are not preserved, but it is clear that they project laterally from the anterolateral aspect of the centrum. This condition differs from that of more posterior lumbar vertebrae, in which the transverse processes project from the anteroposterior middle of the centrum rather than from closer to its anterior margin.

Thick pedicles define a semicircular neural canal. Prominent ligamentous pits are present in the anterior laminae dorsal to the neural canal. Pre- and postzygapophyses are not revolute, but are curved rather than flat and face medially and laterally respectively. Robust metapophyses project dorsolaterally from the prezygapophyses. The neural spine is not complete, but it appears to be relatively short dorsoventrally and rather long anteroposteriorly. It angles anteriorly at approximately 86.0° to the horizontal, which is the least acute neural spine angle compared to other lumbar vertebrae.

L2 — A centrum of L2 was figured by Gingerich et al. (1995, GSP-UM 3057, Fig. 13, p. 314), though was mistakenly identified as L5. L2 is known from two centra (GSP-UM 3057 and 3408) and two nearly complete specimens (GSP-UM 3225 and 3552; Figs. 3.7-3.8). Centra are anteroposteriorly longer than L1. Anterior and posterior epiphyses are broad and reniform, though the posterior epiphysis is notably wider. Transverse

processes project laterally from the centrum, forming near right angles with respect to the neural spine. Their anteroposterior placement on the centrum is more posterior than in L1, but more anterior than in L3-L6. They are relatively short and dorsoventrally thin with rounded distal margins.

Ligamentous pits are present in anterior laminae dorsal to the semicircular neural canal, with the deepest pockets positioned laterally. Pre- and postzygapophyses are similar in size, shape, and orientation to those of L1 and are flanked dorsally by robust metapophyses. The neural spine is mostly complete in both GSP-UM 3225 and 3552. It is relatively short dorsoventrally (though the spine of GSP-3225 is comparatively longer) and long anteroposteriorly, and it angles anteriorly at a more acute angle than the neural spine of L1. The apex of the neural spine is laterally expanded along both its dorsal and posterior margins.

L3 — A centrum of L3 was figured by Gingerich et al. (1995, GSP-UM 3057, Fig. 13, p. 314), though was incorrectly identified as L4. While several centra have been identified (GSP-UM 3015, 3057, 3274, 3383, and 3408), there is only one mostly complete specimen (GSP-UM 3552; Figs. 3.7-3.8). Centra are longer than those of L1-L2 and possess reniform anterior and posterior epiphyses, though posterior epiphyses exhibit slightly less concavity along their dorsal margins. A complete left transverse process is preserved in GSP-UM 3552, projecting nearly horizontally from the lateral aspect of the centrum and with an anteroposterior position nearer to the middle of the centrum. The posterior margin of the transverse process is straight, while the anterior

margin is convexly curved, thus causing the transverse process to taper laterally. It is longer than the transverse processes of L2, but still relatively short.

Deep excavations in the laminae to accommodate ligamentous attachments are present dorsal to the semicircular neural canal, with the deepest excavations laterally. Zygapophyses and metapophyses are similar in size, shape, and orientation to those of L2. The neural spine is not complete, but is angled more anteriorly than that of L2.

L4 — A centrum of L4 was figured by Gingerich et al. (1995, GSP-UM 3015, Fig. 13, p. 314), but was identified as L3. There are a few known L4 centra (GSP-UM 3015, 3057, and 3155), but only one mostly complete specimen (GSP-UM 3552; Figs. 3.7-3.8). Centra are anteroposteriorly longer than those of L1-L3. Anterior and posterior epiphyses are reniform, though posterior epiphyses exhibit less concavity along their dorsal margins (like seen in L3). Transverse processes are positioned near the anteroposterior center of the centrum and project ventrolaterally, with the distal halves of the transverse processes curving anteriorly. They are longer, wider, and thicker than the transverse processes of L1-L3.

Deep ligamentous pits, marked by prominent lateral pockets, are present in the anterior laminae dorsal to the semicircular neural canal. Prezygapophyses are highly curved, face medially, and are bordered by large, dorsally-projecting metapophyses. Postzygapophyses are curved, but slightly flatter, and face laterally. The neural spine is not complete, but it clearly thickens posteriorly and includes an obvious keel along the midline on its posterior margin. It is angled more anteriorly than the neural spines of L1-L3.

L5 — A centrum of L5 was figured by Gingerich et al. (1993, GSP-UM 3015, Figs. 7-8, pp. 402-403). GSP-UM 3552 preserves the only known complete L5 (Figs. 3.7-3.8), but several specimens include centra (GSP-UM 3015, 3383, and 3408), including some with partial transverse processes (GSP-UM 3225). Centra are anteroposteriorly longer than centra of L1-L4. Anterior epiphyses are reniform, while posterior epiphyses are more elliptical, with lateral corners at the level of the transverse processes. Transverse processes project ventrolaterally from the anteroposterior middle of the centrum, with the distal halves of the transverse processes curving anteriorly. They are less broad than those of L4, but they are marked by a prominent ridge extending from the base of the metapophyses down to their posterior margins.

Prominent excavations with deep lateral pits mark the anterior laminae dorsal to a neural canal that is semicircular to triangular in cross-section. Prezygapophyses are curved, face medially, and are flanked dorsally by dorsally-projecting metapophyses. Postzygapophyses are curved and face laterally. The neural spine is relatively short, but longer than the spinous processes of L1-L4. It is thin along its anterior margin, but expands at its dorsal apex and along its posterior margin. At its base, the neural spine is angled anteriorly more so than in L1-L4, but it begins to curve vertically about halfway along its extent.

L6 — Four specimens of L6 are known, including two centra (GSP-UM 3160 and 3383), one specimen with a partial neural arch (GSP-UM 3408), and one complete specimen (GSP-UM 3552; Figs. 3.7-3.8). L6 centra are the longest centra among lumbar vertebrae. Anterior epiphyses are reniform, and posterior epiphyses are elliptical with

less prominent lateral corners than L5. L6 is the only lumbar vertebra in which anterior epiphyses are wider than posterior epiphyses. Transverse processes extend ventrolaterally from the anteroposterior middle of the centrum and curve slightly anteriorly. They are very short laterally, in order to accommodate the ilia of the innominates.

Pedicles are thick, and laminae with prominent ligamentous pits surround the semicircular-to-triangular neural canal. Prezygapophyses are curved, face dorsomedially, and are bordered by less robust metapophyses than seen in more anterior lumbar vertebrae. Postzygapophyses are flat rather than curved and face ventrolaterally. The neural spine is angled anteriorly at its base, before curving more vertically. It is expanded slightly along its dorsal and posterior margins, but less so than in more anterior lumbar vertebrae.

Sacral Vertebrae

Sacral vertebrae have been briefly described and figured by Gingerich et al. (1993, GSP-UM 77 and 3009, Figs. 9-10, pp. 404-405; 1995, GSP-UM 3057, Fig. 13, p. 314; 2001), but no complete sacra have been thoroughly described. Partial sacral are known from many specimens (GSP-UM 77: S1-S2, 3009: S2-S3, 3057: S1-S2, 3111: S1-S2, 3340: S1, and 3352: S1-S3), but only one specimen of *Remingtonocetus domandaensis* preserves all four sacral vertebrae (GSP-UM 3408; Fig. 3.9). In all cases, the first three sacral vertebrae are solidly fused to one another across centra, pleurapophyses, zygapophyses, and neural spines. The fourth sacral vertebra is not at all fused to the

rest of the sacrum, but contributes to the continuous pleurapophyseal shelf running from S1-S4. This condition mirrors that seen in three specimens of *Dalanistes ahmedi* (GSP-UM 3106, 3279, and 3372), but contrasts with the condition seen in *Kutchicetus minimus* (Thewissen and Bajpai, 2009) and other specimens of *D. ahmedi* (GSP-UM 3102), in which S1-S4 are solidly fused.

The sacrum is long, reaching some 20.2 cm in length from S1-S4 (GSP-UM 3408). The lengths of individual centra appear to change little from S1-S4, despite the concomitant decreases in both centrum height and width. The anterior epiphysis of S1 is fairly reniform, but with little concavity along its dorsal margin, and the posterior epiphysis of S4 is smaller and elliptical. Broad auricular processes for articulation with the ilia of the innominates project ventrolaterally from S1 and are marked by rugose, quadrilateral-shaped surfaces. The auricular processes project some 2 cm in front of the anterior epiphysis of S1 and extend onto the pleurapophyses of S2. The remaining pleurapophyses comprise a continuous, relatively narrow shelf extending laterally from the centra. The pleurapophyses of S4 increase in width posteriorly, akin to the shapes of the transverse processes of anterior caudal vertebrae. The junctions of S1-S2 and S2-S3 are marked by large dorsal and ventral sacral foramina, averaging 0.95 cm in diameter in GSP-UM 3552, and the articulation between S3 and S4 forms two large dorsoventrally-oriented foramina between their respective centra and pleurapophyses.

The neural canal is triangular in cross-section and is notably smaller than in the lumbar vertebrae. Ligamentous pits are present in anterior laminae dorsal to the neural canal, but are not nearly as deep as those present in lumbar vertebrae.

Prezygapophyses of S1 are mostly flat and face dorsomedially, while the postzygapophyses of S4 (which are not complete in any specimen) appear to be closely set and face ventrolaterally. The neural spine of S1 is similar in height to that of L6 and thickens distally. GSP-UM 3552 demonstrates that the neural spine of S2 is fully fused with the neural spine of S1, forming a broad, vertical wall of bone.

Caudal Vertebrae

Caudal vertebrae are poorly known in *Remingtonocetus domandaensis*. A total of 14 caudal vertebrae have been recovered, but most are isolated elements. GSP-UM 3267, 3310, 3313, 3416, and one vertebra from GSP-UM 3015 are fragmentary centra that contribute no new information to that which can be gleaned from more complete specimens. GSP-UM 3383 preserves a partial neural arch, while GSP-UM 3225 and a second vertebra from GSP-UM 3015 are virtually complete. GSP-UM 9 preserves two complete caudal vertebrae in articulation. But the most informative specimen is GSP-UM 3408, which preserves four consecutive caudal vertebrae (Fig. 3.10). Ca1 and Ca2 lack complete neural arches, but Ca3 and Ca4 are virtually complete. This specimen provides the basis for the following descriptions.

Ca1 — Ca1 preserves a complete centrum with intact transverse processes and a partial neural arch. The centrum is similar in length to mid-lumbar vertebrae, but is notably narrower. The anterior epiphysis is oval in shape and wider than tall. The posterior epiphysis is wider than the anterior epiphysis, more pentagonal in shape, and possesses two facets along its ventral margin for articulation with a hemal arch (or

chevron), which is not preserved. Transverse processes project laterally from the centrum and possess a slight ventral curve distally. They are roughly triangular in shape in dorsal view, as wide as the centrum is long and tapering to a rounded, knob-like process laterally. Pedicles are less robust than in more anterior vertebrae and define a semicircular neural canal.

Ca2 — Ca2 is slightly more complete than Ca1, as it possesses left pre- and postzygapophyses. The centrum is longer, wider, and higher than that of Ca1, and epiphyseal morphology differs only in being slightly more circular. Prominent ridges are present on the ventral aspect of the centrum, anterior to the hemal arch facets. The transverse processes are identical in morphology to those of Ca1, but are less wide and less robust.

The pedicles are relatively thin and define a semicircular neural canal. The left prezygapophysis is curved, faces dorsomedially (though with a greater dorsal component), and projects more than 1.0 cm in front of the anterior epiphysis of the centrum. The left postzygapophysis is curved, faces ventrolaterally, and projects very little past the posterior epiphysis of the centrum.

Ca3 — Ca3 is virtually complete, missing only the distal portions of the transverse processes. The centrum is longer and higher than Ca1 and Ca2, but it is notably narrower, thus resulting in epiphyses that are nearly equal in height and width. The anterior epiphysis is circular in cross-section, while the posterior epiphysis is more pentagonal due to the hemal arch facets. Ridges on the ventral aspect of the centrum anterior to the hemal arch facets are even more prominent than in Ca2. Compared to

more anterior caudal vertebrae, the transverse processes of Ca3 are less robust, less wide, and have bases that encompass less of the centrum length.

Pedicles are thin and define a relatively small semicircular neural canal. Dorsomedially-facing prezygapophyses are narrowly-set, curved, and sit medial to prominent, dorsolaterally-projecting metapophyses. Postzygapophyses are narrowly-set and face ventrolaterally. The neural spine is relatively tall, but very thin anteroposteriorly. It is triangular-shaped in dorsal view with broader posterior margin. It is nearly vertical, but with a slight anterior inclination.

Ca4 — Ca4 is complete. The centrum is longer and narrower than more anterior caudal vertebrae. The anterior and posterior epiphyses are circular and pentagonal in cross-section respectively, and there are prominent ridges anterior to the hemal arch facets on the ventral aspect of the centrum. Transverse processes are similar in morphology to the processes of more anterior caudal vertebrae, but they are smaller and more posteriorly-positioned on the centrum.

Pedicles are thin and define an even smaller semicircular neural canal. Curved prezygapophyses face dorsomedially and are more narrowly-set than in Ca3. Metapophyses project dorsolaterally and are fairly robust. Postzygapophyses are narrowly-set and face ventrolaterally. The neural spine is similar in size and morphology to that of Ca3.

FUNCTIONAL MORPHOLOGY

The following functional interpretation of the vertebral column focuses primarily on the cervical and lumbosacral regions. These regions are the most complete parts of the spine known for *Remingtonocetus domandaensis*, and they represent the areas with the most relevance for reconstructing aquatic locomotion. The origins, insertions, actions, and names of muscles in the following discussion come from Getty (1975) and Evans (1993) unless otherwise noted.

Cervical Region

The cervical region of *Remingtonocetus domandaensis* is unlike that of any known cetacean, fossil or modern. One of the most notable differences is its length. Modern cetaceans have very short necks that contribute to their streamlined body shape and help to stabilize the head during caudally-propelled swimming (Buchholtz, 1998, 2001; Fish, 2002; Fish et al., 2003). Modern cetaceans retain seven cervical vertebrae like nearly all other mammals and achieve a short, stiff neck by reducing the relative lengths of cervical centra and frequently fusing many of them together (Buchholtz, 2001). The cervical centra of all archaeocetes are long in comparison to modern forms, but the neck of *R. domandaensis* stands out even among archaeocetes.

One way to quantify the relative length of cervical centra across taxa of different body sizes is to compare the ratio of centrum length to anterior centrum height. This ratio is listed in Table 3.4 for C3-C7 of 15 archaeocetes and five modern cetaceans. The cervical centra of the five extant taxa are all demonstrably shorter than those of the

archaeocetes, although the cervical vertebrae of basilosaurids approach the foreshortening seen in some modern forms. Non-basilosaurid archaeocetes have comparatively longer necks, but exhibit a trend of decreasing cervical lengths from earlier to later taxa. The cervical centra of *Remingtonocetus domandaensis* are longer, compared to their respective heights, than those of any known cetacean, even older and more primitive species like *Pakicetus attocki* and *Ichthyolestes pinfoldi*. This suggests that the neck of *R. domandaensis* may have been capable of more movement than those of other cetaceans (Long et al., 1997; Buchholtz, 1998; Buchholtz and Schur, 2004); however, other features of the cervical vertebrae suggest that motion between vertebrae may have been limited to certain planes.

The most unusual features of the cervical column of *Remingtonocetus domandaensis* are the robust transverse processes. The wing-like transverse processes of C6 are not uncommon among early archaeocetes (e.g., Gingerich et al., 1994, 2009), but the plate-like transverse processes of C3-C5 are unlike those of any extinct or extant mammal. Several different epaxial muscles originate and/or insert on these transverse processes, offering insight into the neck's function. The most posterior of these muscles are the superficial and deep portions of the *m. scalenus*, which extend from the ribs to the lateral surfaces of the transverse processes. These muscles draw the neck ventrally when right and left sides act together or bend the neck sideward when the muscles act unilaterally.

The *mm. intertransversarii* are deep, short segments of muscle that run between adjacent vertebrae. The *mm. intertransversarii dorsales cervicis* run between the

zygapophyses of more posterior vertebrae and insert on the lateral surfaces of more anterior transverse processes. The *mm. intertransversarii ventrales cervicis* lie ventral to the *m. scalenus* and run between the lateral surfaces of adjacent transverse processes. These muscles are primarily used to fix the cervical column, though they may aid in laterally bending the neck.

The *m. longus capitis* and *m. longus colli* lie ventral to the cervical vertebrae. The *m. longus capitis* originates on the ventromedial surfaces of the transverse processes and extends all the way to the base of the skull, where it inserts on the tubercles of the basioccipital, which are prominent in *Remingtonocetus domandaensis* (e.g., GSP-UM 3552). The *m. longus colli* is enclosed by the *m. longus capitis* and runs from the transverse processes of more posterior vertebrae to the hypapophyses of vertebrae one to two positions craniad of where it originated. These two muscles primarily serve to draw the head and neck ventrally (Wickland et al., 1991). Laterally, the primary muscle that inserts on the transverse processes is the *m. longissimus cervicis*, which consists of several bundles that originate on the zygapophyses of anterior thoracic vertebrae. This muscle extends the neck when right and left sides act together and inclines the neck sideways when one side acts unilaterally.

The size of the cervical transverse processes in *Remingtonocetus domandaensis* indicates that the muscles attached there were substantial, especially the *m. longus capitis* (as suggested by prominent tubercles on the basioccipital) and the *m. longus colli* (indicated by the robust hypapophyses on C2-C5). Most of the muscles described above (excluding the *m. longissimus cervicis*) serve primarily to flex the head and neck ventrally

or to bend the neck laterally. There are no modern analogues with the exact same cervical morphology as *R. domandaensis*, but sea lions and fur seals (Order Carnivora, Family Otariidae) possess a similar morphology.

Otariids hold their heads above the level of their body and possess cervical vertebrae considered long for semiaquatic mammals (Buchholtz, 1998, 2001), with large, ventrally-projecting transverse processes. During terrestrial locomotion, they utilize lateral swings of their heads and necks to alter the position of their center-of-mass and to help them lift their forelimbs off the ground (English, 1976; Beentjes, 1990). This lateral movement is executed primarily by the *m. longissimus cervicis*, which has enhanced leverage on otariid cervical vertebrae due to lateral projections on the proximal blades of the transverse processes. The flexibility of the neck is also achieved in part because the transverse processes do not at all imbricate, allowing the vertebrae ample space to flex laterally in relation to one another.

The cervical vertebrae of *Remingtonocetus domandaensis* lack lateral projections, thereby indicating reduced leverage for lateral rotation by the *m. longissimus cervicis*, and when the cervical vertebrae are articulated, the transverse processes strongly imbricate (Fig. 3.11), thus reducing the potential for lateral flexion or axial rotation. Given the apparent robustness of the muscles attached to the transverse processes and the limited potential for lateral bending of the neck, it follows that the primary function of these muscles in *R. domandaensis* was to flex the neck ventrally.

One potential explanation for this relates to hydrodynamic streamlining. Several lines of evidence indicate that the neutral position of the neck in *Remingtonocetus*

domandaensis had the head elevated above the level of the rest of the body. The rhomboidal lateral cross-sections of the cervical centra indicate this (Gingerich et al., 1993, 1995), as does the inference that *R. domandaensis* had a large nuchal ligament running between the blade-like neural spine of C2 and the tall neural spines of C7-T1, which would have passively acted to support the head (Slijper, 1946; Gellman et al., 2002). This posture is likely a sign of some degree of terrestriality and is rarely seen in predominantly aquatic mammals, which typically hold their head in line with the rest of their body to give them a more streamlined body shape.

If *Remingtonocetus domandaensis* had maintained the neutral posture of its neck underwater while swimming, it would have experienced increased drag compared to other aquatic mammals. Its robust lateral and ventral neck muscles would have been able to flex the neck ventrally, pulling it more in line with the rest of the body. But in order to achieve a streamlined body shape, the skull must have been simultaneously extended (or dorsiflexed) to reduce the significant angulation between the long axes of the skull and neck during neutral posture. There are several indications that *R. domandaensis* had the musculature to do just that. One of its most notable skull features is a large, posteriorly-projecting nuchal crest (or lambdoidal ridge) that defines a large supraoccipital fossa for supporting musculature that originates on the cervical and anterior thoracic vertebrae and inserts on the back of the skull.

The *m. splenius*, which serves primarily to support the head and extend the atlanto-occipital joint (Slijper, 1946), is the most superficial of these muscles, originating on the neural spines of T1-T2 and inserting all along the nuchal crest, from the mastoid

processes to the midline (Wickland et al., 1991). The *m. semispinalis capitis* (or *m. biventer cervicis*) also extends the head, originating on the dorsal aspect of the posterior cervical and anterior thoracic vertebrae and inserting near the nuchal crest (Wickland et al., 1991). Lastly, the robust neural spine of the axis and the dorsal tubercle of the atlas would have supported the three branches of the *m. rectus capitis dorsalis*, which extend between the back of the skull and the dorsal aspects of the atlas and axis, serving almost exclusively to raise or extend the head (Wickland et al., 1991). The size and orientation of the nuchal crest and supraoccipital bone in *Remingtonocetus domandaensis* provided much surface area for the attachment of these muscles, indicating that the muscles used for extending the atlanto-occipital joint in this animal were robust. This supports the idea that *R. domandaensis* was capable of simultaneously flexing its cervical vertebrae and extending its atlanto-occipital joint to integrate the head and neck with the rest of its body to give it a hydrodynamically favorable body shape for swimming.

It is clear that the cervical spine of *Remingtonocetus domandaensis* lacks many of the adaptations for passive stabilization of the head that are evident in most cetaceans. Yet, it appears that this species still stabilized its head and neck, just in different ways given its lifestyle and peculiar anatomy. There are inherent trade-offs in retaining such a long neck. The shortened cervical vertebrae possessed by most cetaceans passively stabilize the head and neck, which helps to decrease the drag experienced during swimming by limiting pitching of the rostrum (Fish, 2002; Fish et al., 2003). However, reduction of cervical length in *R. domandaensis* would have made it difficult to support the musculature necessary for controlling its large skull. The long

neck of *R. domandaensis* preserved the surface area to support this musculature, but it also required novel methods for stabilization of the head and neck during swimming.

The imbricated transverse processes offered the head of *Remingtonocetus domandaensis* some passive lateral stability, while simultaneously providing the surface area for musculature to pull the neck in line with the rest of the body and actively stabilize it in multiple planes during swimming. The robust dorsal cervical musculature enabled the extension of the atlanto-occipital joint, which, in conjunction with the flexion of the neck, would have given *R. domandaensis* a more streamlined body shape during submerged swimming to reduce drag, thereby increasing propulsive efficiency. This active stabilization of the head and neck during locomotion was undoubtedly more costly energetically than the passive stabilization utilized by most other cetaceans, but it also allowed *R. domandaensis* to retain its posture and unique cranial morphology, which were undoubtedly critical for this animal's feeding niche.

Thoracic Region

Compared to other regions of the spine, the thoracic region of *Remingtonocetus domandaensis* is rather poorly known. However, while little can be said about the muscles and ligaments in this region, known specimens shed some light on the role of the thorax during locomotion. The anterior and middle thoracic regions were likely rigid due to stabilization by the ribs and sternum, thus playing no direct role in locomotor movements other than as muscle attachment sites (Filler, 1986; Pabst, 1993; Long et al., 1997; Buchholtz, 2001; Fish et al., 2003; Buchholtz and Schur, 2004). Posterior thoracic

vertebrae were likely comparatively more flexible (Slijper, 1946), which means they could have played some role in locomotion.

The diaphragmatic and anticlinal vertebrae signal the transition between the functional thorax and the functional lumbus (Zhou et al., 1992). Thoracic vertebrae posterior to the diaphragmatic vertebra have shapes and functions more like lumbar vertebrae. The anticlinal vertebra marks the area of greatest sagittal flexibility due to the shape and orientation of its neural spine (Slijper, 1946; Zhou et al., 1992). Dorsomobile mammals that utilize flexion and extension of the lumbar spine during locomotion are often marked by diaphragmatic and anticlinal vertebrae several positions anterior to the thoracolumbar junction (Slijper, 1946; Hildebrand, 1959; Zhou et al., 1992). The anterior placement of these landmarks enables them to incorporate more of their thorax into their sagittal movements. This effectively increases the length of their lumbus, thereby increasing its total displacement during locomotion.

In *Remingtonocetus domandaensis*, T11 appears to be the diaphragmatic vertebra, and T12 is the anticlinal vertebra. Only two thoracic vertebrae (T12-T13) lie posterior to the diaphragmatic vertebra, demonstrating that very little of the thorax was recruited into the functional lumbus. This suggests that the posterior thorax of *R. domandaensis* was not significantly flexed or extended during locomotion as it often is in modern dorsomobile mammals. If *R. domandaensis* flexed and extended its precaudal spine to any significant degree during locomotion, it would have been almost entirely restricted to the lumbar region.

Lumbosacral Region

Elucidation of the degree of mobility of the lumbosacral region in *Remingtonocetus domandaensis* is crucial for reconstructing its locomotor mode. The lumbar centra of *R. domandaensis* are relatively long. In Chapter 2, I demonstrated that its vertebral proportions differed from those of its remingtonocetid contemporary *Dalanistes ahmedi*, primarily in having much longer posterior thoracic and lumbar vertebrae in comparison to cervical and anterior thoracic vertebrae. Its lumbar vertebrae are even long compared to other groups of archaeocetes (Fig. 3.12). When relative lengths are calculated by dividing the centrum length of each lumbar vertebra by the mean heights of T1-T3 centra (method modified from Gingerich, 1998), the lumbar vertebrae of *R. domandaensis* are longer than those of the basilosaurid *Dorudon atrox* (Uhen, 2004) and the early protocetids *Rodhocetus kasranii* (Gingerich et al., 1994), *Qaisracetus arifi* (Gingerich et al., 2001), and *Maiacetus inuus* (Gingerich et al., 2009). This greater relative length increases the maximum potential displacement of the vertebral column in this region of the spine and suggests greater movement during locomotion compared to taxa with shorter lumbar vertebrae (Buchholtz, 1998, 2001; Buchholtz and Schur, 2004).

However, any increase in potential displacement of the column afforded by longer centra can be easily constrained by other aspects of vertebral anatomy (Buchholtz and Schur, 2004). One key osteological feature relevant for inferring mobility of the spine is the shape of the zygapophyses. The lumbar vertebrae of modern ungulates possess revolute (or 'embracing') zygapophyses that drastically limit

intervertebral movement (Howell, 1944; Slijper, 1947; Zhou et al., 1992); Slijper (1946, p. 38) described these joints in artiodactyls as "practically immovable." Mammals with more mobile lumbar spines, such as otters (Tarasoff et al., 1972; Williams, 1989; Fish, 1994), pinnipeds (Tarasoff et al., 1972; Berta and Adam, 2001), and many terrestrial carnivores (Hildebrand, 1959; Alexander et al., 1985; Walter and Carrier, 2009), possess flatter, non-revolute zygapophyses, allowing for more dorsoventral mobility during locomotion, especially in extension (Gál, 1993b).

The lumbar zygapophyses of *Remingtonocetus domandaensis* are curved (essentially intermediate between revolute and flat) and face mediolaterally. This condition indicates greater potential intervertebral flexion and extension than is possible in lumbar spines exhibiting revolute zygapophyses (like most artiodactyls), but would still limit both axial and lateral rotation. Compared to other archaeocetes, the zygapophyseal morphology of *R. domandaensis* would have likely permitted more dorsoventral movement than possible in *Pakicetus attocki* and *Ambulocetus natans*, both of which possessed restrictive revolute zygapophyses (Thewissen et al., 2001; Madar et al., 2002; Madar, 2007), but less movement than in protocetids like *Maiacetus inuus*, which had flatter zygapophyses (Gingerich et al., 2009).

The anteroposterior length of the neural spine is another osteological feature that limits vertebral mobility. Impaction of neural spines limits intervertebral extension and occurs at lesser degrees of angular rotation when the anteroposterior lengths of the neural spines approach the lengths of their centra (Zhou et al., 1992; Buchholtz and Schur, 2004). Like those of *Ambulocetus natans* (Madar et al., 2002), the lumbar neural

spines of *Remingtonocetus domandaensis* are anteroposteriorly long, which would have limited extension, especially in comparison with other archaeocetes like *Maiacetus innus*, whose lumbar neural spines were dorsoventrally taller, but anteroposteriorly shorter (Gingerich et al., 2009), presumably allowing a greater degree of extension.

Many non-osteological features contribute significantly to the flexibility of the lumbar column, and their functions can be inferred from the morphology of the lumbar vertebrae themselves. The primary extensor muscles of the lumbar spine are commonly called the erector spinae (Macintosh and Bogduk, 1987) and include principally the *m. iliocostalis lumborum* and the *m. longissimus lumborum*. The *m. iliocostalis lumborum* runs between the posterior ribs and the iliac crest of the innominate, picking up muscle fascicles from the lumbar transverse processes along its length. In some cases, it assists in extending the lumbar spine (Carlson, 1978), but because it is reduced in most mammals (Slijper, 1946; Schilling and Carrier, 2010), it serves primarily to stabilize it (English, 1980).

The principal extensor of the lower back is the *m. longissimus lumborum* (Carlson, 1978; Alexander et al., 1985; Pabst, 2000), which arises from the iliac crest, ventral surface of the ilium, and lateral surfaces of neural spines of posterior lumbar vertebrae, inserting on the lateral surfaces of more anterior vertebrae, including on the anapophyses and transverse processes (Slijper, 1946; English, 1980). There are no anapophyses present in the lumbar spine of *Remingtonocetus domandaensis*, and while the transverse processes are robust, they are short and project very little anteriorly or ventrally, especially in L1-L3 where the transverse processes project straight laterally

from the centrum. These features indicate that the erector spinae musculature had diminished leverage for performing dorsoventral movements compared to the spines of dorsomobile mammals (Zhou et al., 1992), which are marked by long, anteroventrally-projecting transverse processes and prominent, posteriorly-projecting anapophyses (Howell, 1944; Slijper, 1946). This supports the interpretation that the erector spinae musculature in *R. domandaensis* served more of a rheostatic function, stabilizing the lumbar spine more than mobilizing it (Zhou et al., 1992).

Another epaxial muscle that serves primarily to stabilize the lumbar spine is the *m. multifidus*. The *m. multifidus lumborum* is composed of numerous individual segments that run between the metapophyses and zygapophyses of one vertebra and the neural spine of a vertebra one to two positions craniad. Due to its orientation, the *m. multifidus lumborum* has some potential to extend intervertebral joints (Schilling and Carrier, 2010), but its primary action is to fix or stabilize the lumbar spine (English, 1980; Schilling and Carrier, 2010). In modern dolphins, the caudal extension of the *m. multifidus* (*m. extensor caudae medialis*) actively extends the tailstock, but the thoracolumbar branch of the *m. multifidus* serves primarily to stabilize the joints and deep tendon where the *m. longissimus* originates (Pabst, 1993). The metapophyses of *Remingtonocetus domandaensis* are robust like those of *Ambulocetus natans* (Madar et al., 2002), indicating a strong *m. multifidus* that would have acted to stabilize the column.

The intervertebral ligaments also play a critical role in determining the relative mobility of the lumbar spine. To what degree these ligaments serve as spring-like elastic

structures to harness, store, and release kinetic energy during locomotion is debatable (Alexander et al., 1985; Pabst, 1996; Roberts and Azizi, 2011), but they undoubtedly serve as some of the primary means of resisting bending in the spine (Slijper, 1946; Gál, 1993a, 1993b; Long et al., 1997; Gillespie and Dickey, 2004). The three ligaments that routinely exhibit the most resistance to flexion of the lumbar spine are the supraspinous ligament, the interspinous ligament, and the ligamenta flava.

The supraspinous ligament is essentially a posterior continuation of the nuchal ligament, running along and between the apices of adjacent neural spines (Slijper, 1946; Gál, 1993a). The interspinous ligaments form a sheet in the sagittal plane, connecting the blades of adjacent neural spines (Evans, 1993; Long et al., 1997). The ligamenta flava (or yellow ligaments) are oriented anteroposteriorly and connect the neural arches of neighboring vertebrae, essentially forming a roof over the epidural space; these are frequently the ligaments that are the most resistant to ventral flexion (Dumas et al., 1987; Gál, 1993b; Ponseti, 1995). Each of these ligaments appears to have been well-developed in *Remingtonocetus domandaensis*. Both the apices and posterior margins of the neural spines are expanded, offering an increased surface area for attachment of the supraspinous and interspinous ligaments. Deep ligamentous pits in the anterior laminae dorsal to the neural canal indicate robust ligamenta flava. These ligaments would have all worked together to resist ventral flexion in the lumbar spine of *R. domandaensis*.

In sum, while certain features suggest some degree of dorsoventral mobility in the lumbus of *Remingtonocetus domandaensis*, most features signal that the lumbus

was not especially mobile, suggesting that undulation of the lumbar region was not utilized to generate propulsion during swimming, as has been suggested for other early archaeocetes (Thewissen et al., 1994, 1996; Madar et al., 2002). This interpretation is further supported by the morphology of the sacrum in *R. domandaensis*, which would have disrupted any continuity of function between lumbar and caudal vertebrae, thereby limiting the potential for undulatory swimming (Gingerich et al., 1995, 2001). Yet, the sacrum would have also provided a strong base for foot-powered swimming.

Pelvic paddling is a mode of swimming utilized by a wide variety of semiaquatic mammals (e.g., Hickman, 1984; Stein, 1988; Fish, 1993b, 1993a; Thewissen and Fish, 1997; Fish and Baudinette, 1999). The hind limbs of these mammals are typically marked by short femora (Fish, 1996, 2001) and large hind feet with long digits (Howell, 1930; Thewissen and Fish, 1997). While the absence of any hind limb elements distal to the tibia prevents the pedal morphology of *Remingtonocetus domandaensis* from being evaluated, there are a number of indications that this species was well-built for powerful pelvic paddling. All forms of paddling are drag-based modes of locomotion, marked by stroke cycles with both power and recovery phases (Fish, 1984, 1996). The power stroke in a pelvic paddler involves retraction of the hind limb, which generates drag that is resolved into forward thrust. The primary retractor muscles in the mammalian hind limb include the *m. gluteus medius*, *m. gluteus superficialis*, and *m. adductor magnus* (Schilling et al., 2009), and it is clear that these muscles were powerful in *R. domandaensis*.

The *m. gluteus medius* originates on the lateral surface of the ilium and inserts on the greater trochanter of the femur. The broad, fan-like ilium and high greater trochanter (Gingerich et al., 1995, Fig. 15, p. 316) of *Remingtonocetus domandaensis* indicate that its *m. gluteus medius* must have been powerful. Likewise, the smooth, concave surface between the pleurapophyseal shelf and the fused neural spines of the sacrum would have supported a robust *m. gluteus superficialis*, which would have inserted on a rudimentary third trochanter distal to the greater trochanter. The *m. adductor magnus*, which extends and adducts the hip joint, originates along the pubic symphysis, which is unknown in *R. domandaensis*, and inserts along the lateral surface of the femur. The femur of *R. domandaensis* possesses a distinctive lateral keel (Gingerich et al., 1995) that indicates a well-developed *m. adductor magnus*.

In addition, the deep trochanteric fossa of the femur in *Remingtonocetus domandaensis* (Gingerich et al., 1995) indicates robust *m. obturator internus* and *m. obturator externus* for rotating the hip joint. Also, the round femoral head suggests that rotation of the femur was not limited to the parasagittal plane. Rather, the hip joint was likely flexible in a number of different planes. The morphological features of the sacrum, innominate, and femur suggest that the hind limbs of *R. domandaensis* were well-suited to serve as powerful and flexible propulsors during swimming.

This interpretation also makes sense of the inferred function of the lumbar column. Powerful retraction of the hind limbs introduces instability into the spine. When the femur is retracted, it causes anteversion of the pelvis, which in turn causes sagittal flexion of the lumbar region (Gray, 1968; Schilling and Carrier, 2009, 2010).

During this action, the *m. multifidus lumborum* and *m. longissimus lumborum* could have acted to stabilize the lumbar column, acting in opposition to the flexion of the lumbus induced by hind limb retraction. This would have allowed *Remingtonocetus domandaensis* to maintain a more rigid axis during paddling, which would have provided a steady base for the movement of the hind limbs while simultaneously allowing the animal to maintain a stable body axis. Thus, when taken together with evidence from the sacrum, innominate, and femur, the morphology of the lumbar region is most consistent with an animal that swam primarily by powerful movements of its hind limbs rather than dorsoventral undulations of its body axis.

Anterior Caudal Region

Very little can be said about the tail of *Remingtonocetus domandaensis* since so few caudal vertebrae have been recovered. Thewissen and Bajpai (2009) suggested that the greater tapering of the sacrum in *Remingtonocetus* compared to *Kutchicetus minimus* indicates that the tail of the former may have been comparatively shorter and less muscular. But given the size of the known anterior caudal vertebrae, it is clear that *R. domandaensis* had a heavy tail and probably used it during swimming in some way. The nearly circular cross-sections of anterior caudal centra signal a reduction in the relative width of the vertebrae and a decrease in the resistance of the centra to lateral bending. But whether the tail was used primarily as a dorsoventrally-undulating propulsive surface or more of a laterally-moving rudder (or possibly both) cannot be ascertained until specimens of middle and distal caudal vertebrae are recovered.

DISCUSSION

The postcranial anatomy of *Remingtonocetus domandaensis* is unlike that of any known cetacean. Its long neck held above the level of the body and retention of a fused four-vertebra sacrum with robust hind limbs would seem to be obvious hallmarks of terrestrial competence, but upon closer inspection, *R. domandaensis* appears uniquely adapted for moving through an aquatic environment. Early ideas about the lifestyle of *R. domandaensis* suggested a semiaquatic life, spending significant time on land and possibly hunting in the shallows as an ambush predator (Gingerich et al., 1995, 1998), but it now appears that its terrestrial abilities may have been limited.

Gingerich et al. (2001) pointed out that the shallow fovea capitis on the femur and the closure of the acetabular notch of the pelvis indicate the reduction of the round ligament, which may have reduced the weight-bearing capabilities of its hind limbs. Additional evidence for reduced terrestrial competence comes from the cortical architecture of the femur and tibia (Madar, 1998), the reduced surface area between the auricular process of the sacrum and the ilium (Madar et al., 2002), and the difficulty of terrestrial locomotion with a reduced semicircular canal system (Spoor et al., 2002; Spoor and Thewissen, 2008; Spoor, 2009). Thus, though it likely could have hauled itself out onto land, *Remingtonocetus domandaensis* is envisioned here as a semiaquatic cetacean that was much more at home in the water, utilizing its muscular body axis to stabilize the vertebral column for hydrodynamic reasons and to counteract the forces exerted on it by powerful movements of the hind limbs.

But while close inspection of bone morphology and reconstruction of inferred ligaments and musculature can offer us much insight into the lifestyles and behaviors of extinct animals, additional analyses are often required. Different researchers may interpret the same morphology differently; thus, objective, quantitative analyses are needed in order to assess which interpretation (if either) should be favored. The interpretation of the lumbar region here is noteworthy because it differs from the functional interpretations of the lumbar spine in other early cetaceans that have very similar lumbar morphology. The following chapters set out to test this functional interpretation utilizing two different methods: multivariate analysis of lumbar proportions (Chapter 4) and three-dimensional rigid-body modeling simulations (Chapter 5).

Figure 3.1. Composite skeletal reconstruction of *Remingtonocetus domandaensis*. The skull and anterior two-thirds of the dentary are based on GSP-UM 3415 and 3225 respectively. The posterior-most extent of the dentary, C1-C7, T1-T4, T11-T13, L1-L6, S1-S3, and the innominate are based on GSP-UM 3552. Middle thoracic vertebrae are based on GSP-UM 3131, 3290, and 3383, while S4-Ca4 represent GSP-UM 3408. The femur and tibia are based on GSP-UM 3054 and 3015 respectively. Dotted lines indicate reconstructed elements. Diagonal hatching indicates broken edges, while cross-hatching indicates areas that have been filled in. (Illustrated by Bonnie Miljour)

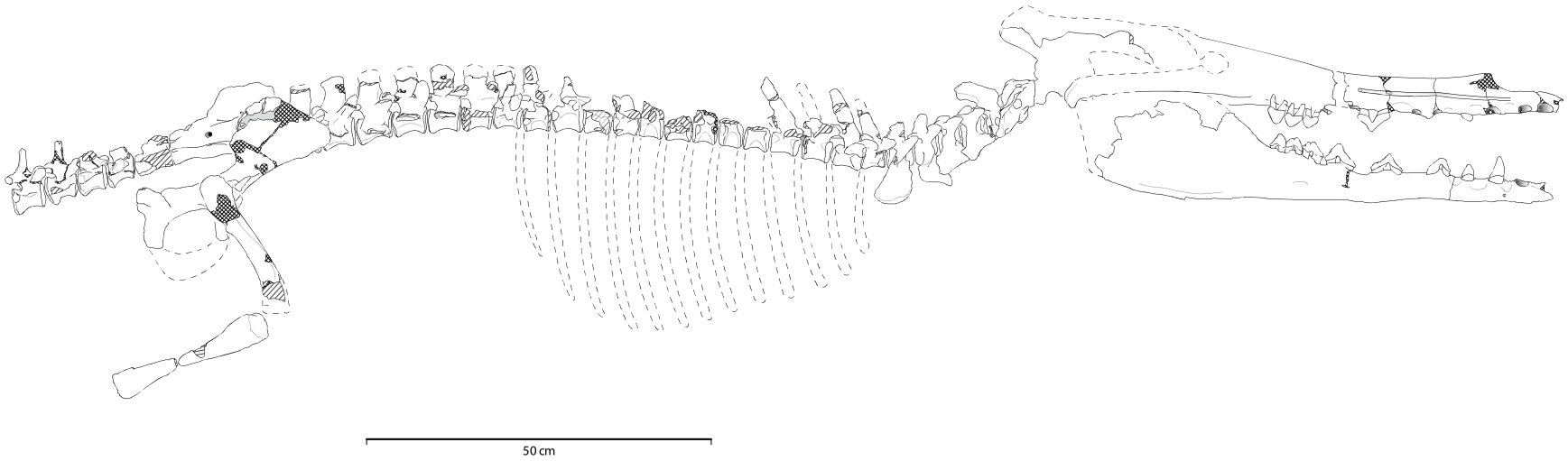

Figure 3.2. Atlas (C1) of *Remingtonocetus domandaensis* GSP-UM 3552 in anterior (top) and dorsal (bottom) view. Note the broad wings and deep atlantal fossae for the attachment of musculature to support the long skull.

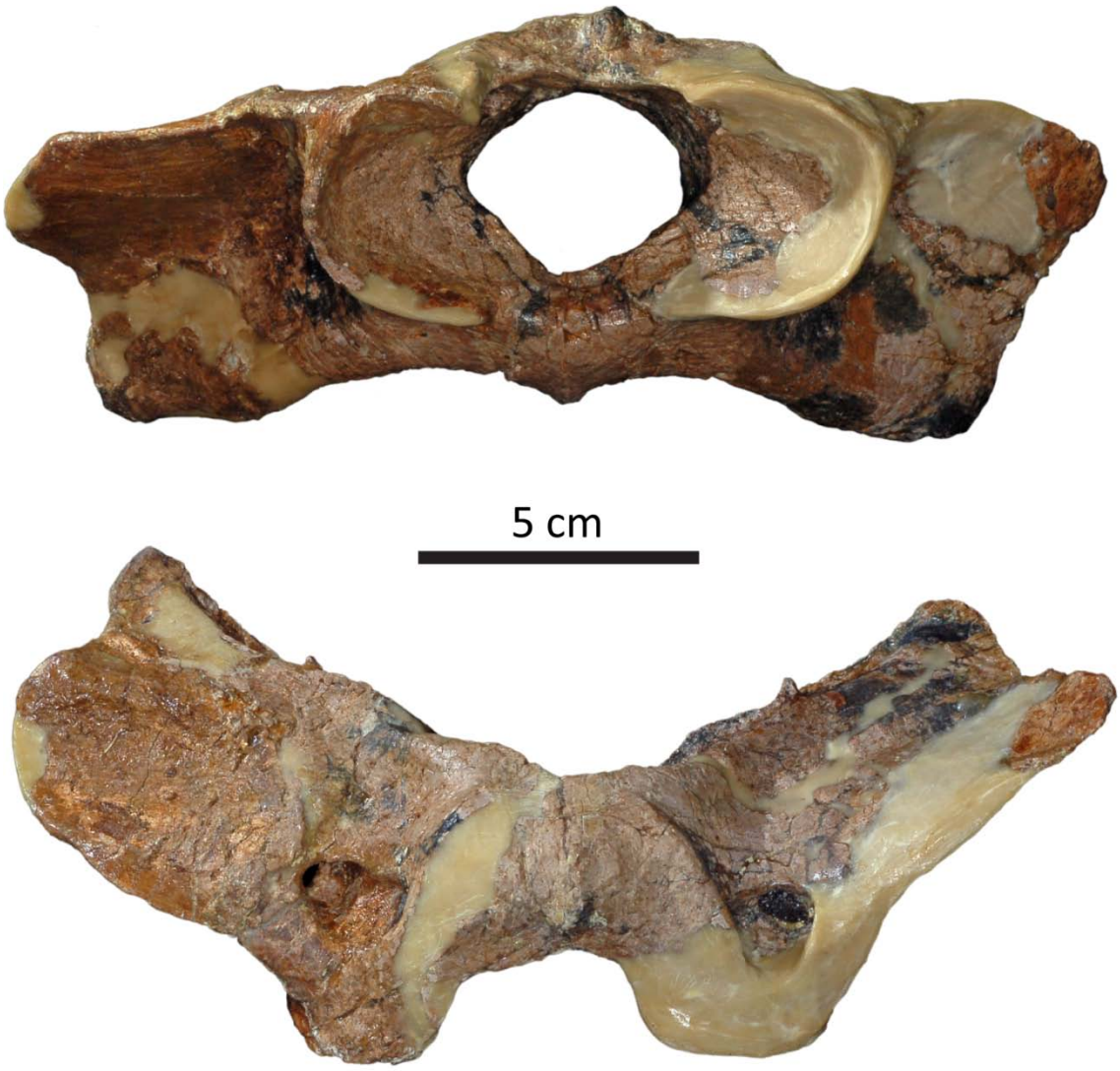

Figure 3.3. Cervical vertebrae (C2-C7) of *Remingtonocetus domandaensis* GSP-UM 3552 in anterior view. The right transverse process of C3 is broken and would have projected more laterally in life. Note the robust hypapophyses on C2-C4 and the massive transverse processes of C3-C6.

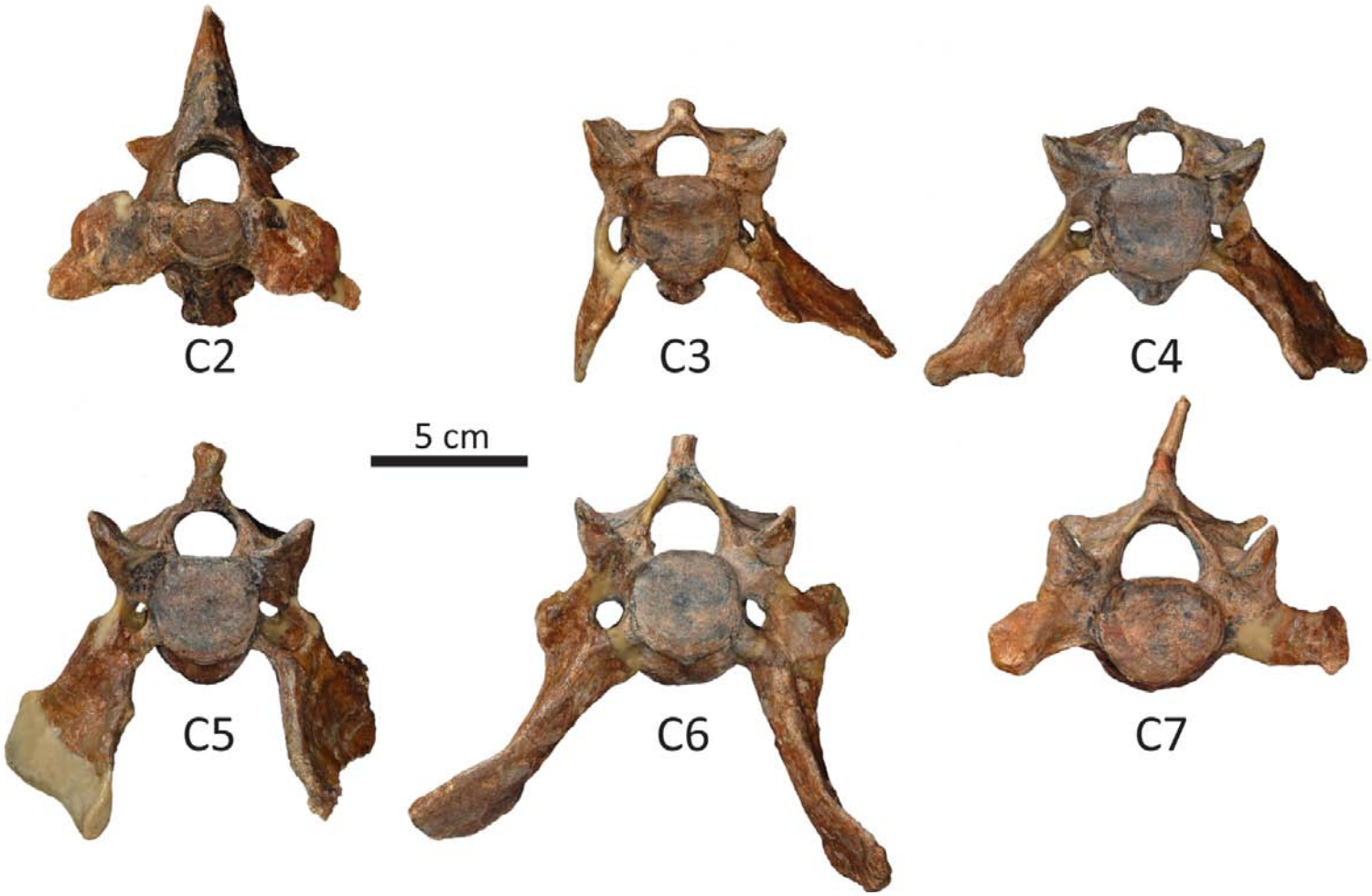

Figure 3.4. Cervical vertebrae (C2-C7) of *Remingtonocetus domandaensis* GSP-UM 3552 in left lateral view. Note the shapes of the centra in C2-C6 that indicate that the neutral posture of the neck held the head above the level of the rest of the body.

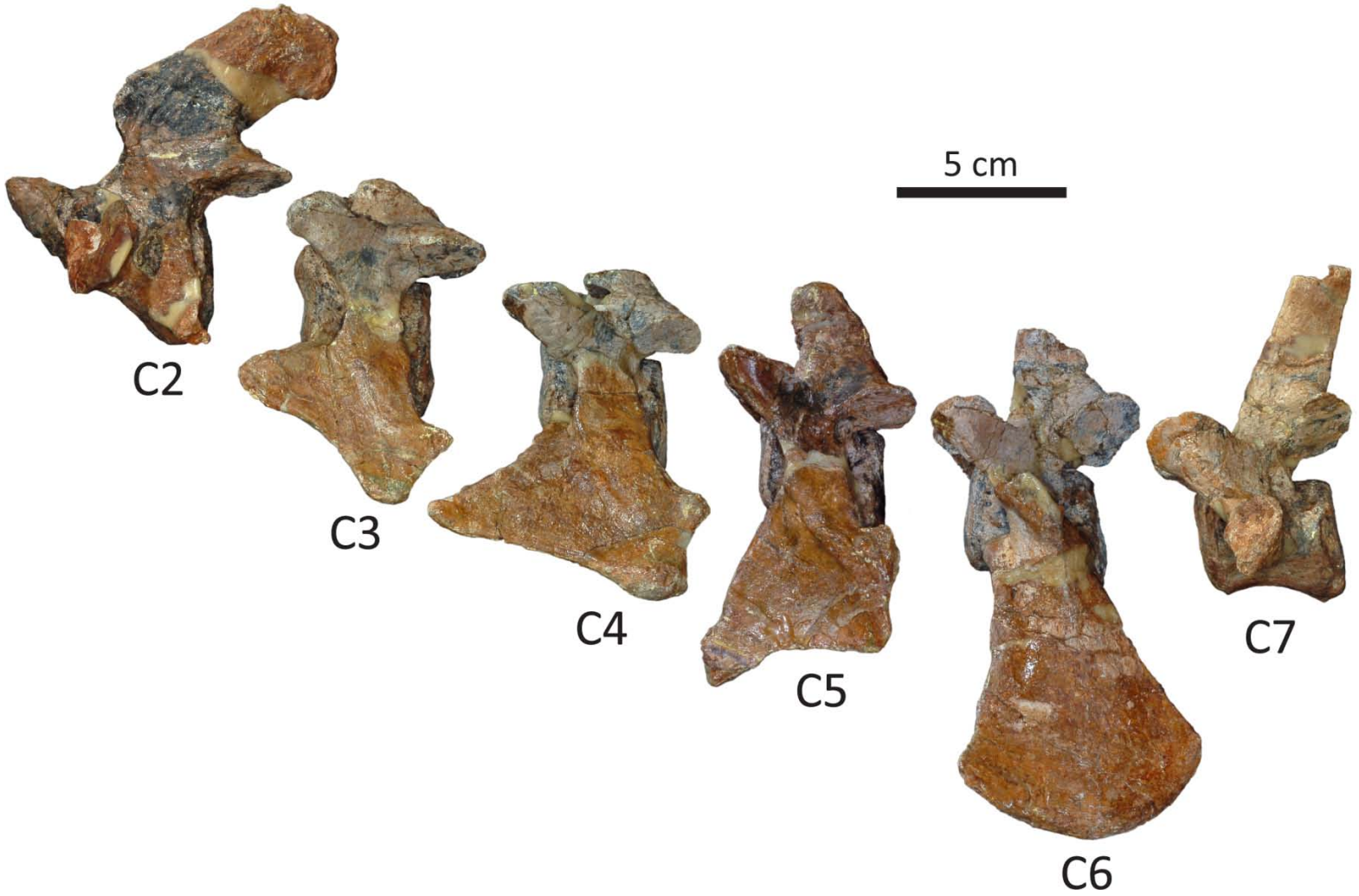

Figure 3.5. Anterior (T1-T4) and posterior (T11-T13) thoracic vertebrae of *Remingtonocetus domandaensis* GSP-UM 3552 in anterior view. T1-T3 were preserved in articulation posterior to C1-C7, and T12-T13 were preserved in articulation anterior to L1-L6.

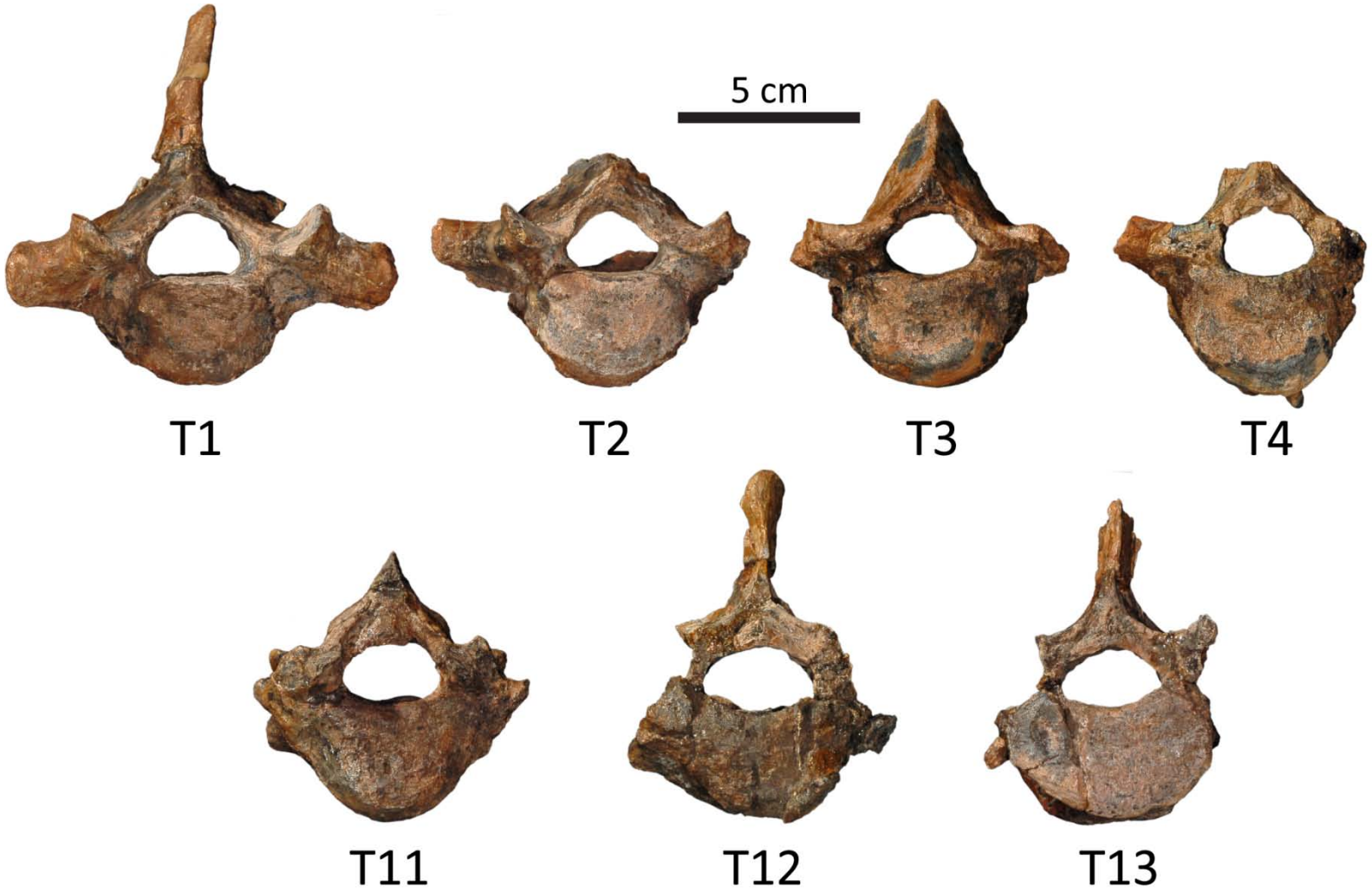

Figure 3.6. Anterior (T1-T4) and posterior (T11-T13) thoracic vertebrae of *Remingtonocetus domandaensis* GSP-UM 3552 in left lateral view. Note the dorsally-facing prezygapophyses of T11 (suggesting it is the diaphragmatic vertebra) and the vertical neural spine of T12 (making it the anticlinal vertebra). The neural spine of T13 had an anterior inclination prior to breakage (as evidenced by the angle at its base).

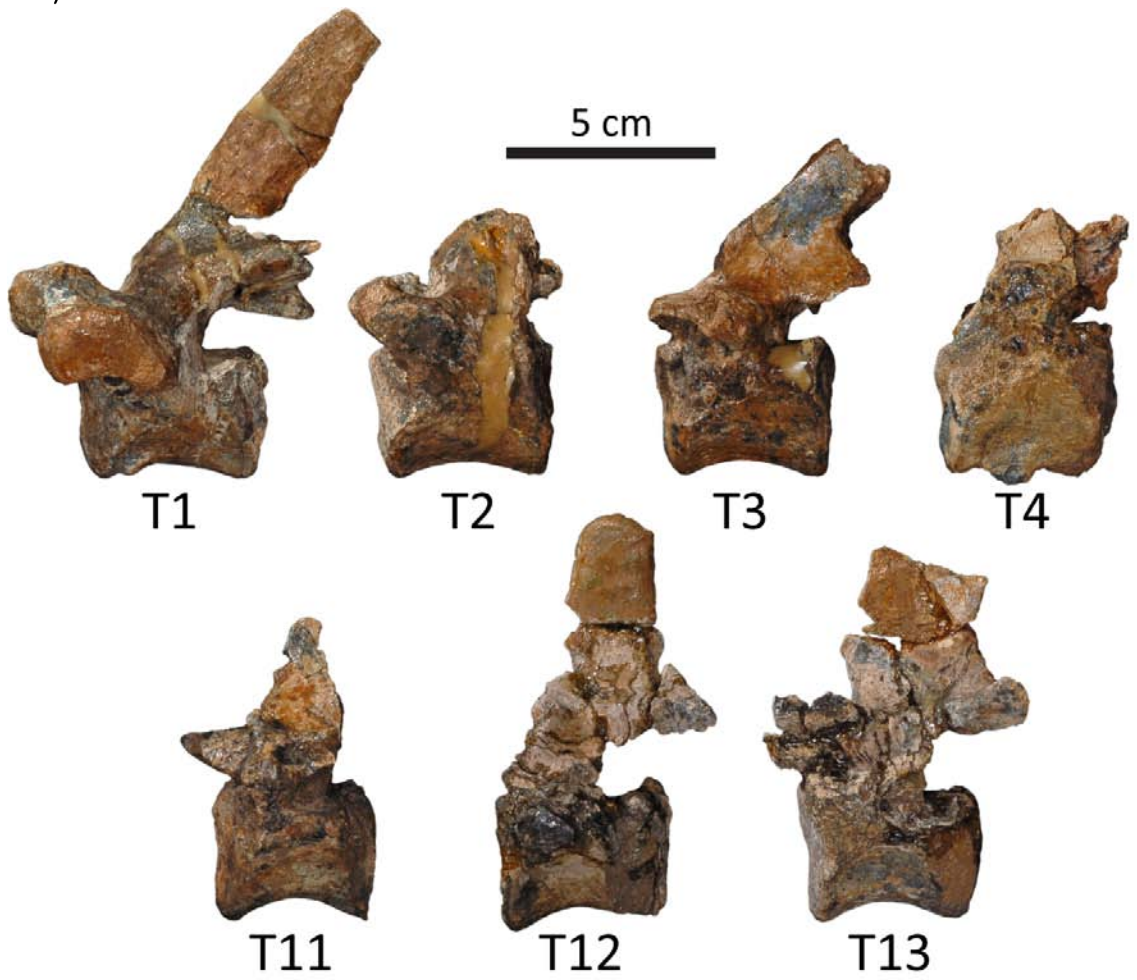

Figure 3.7. Lumbar vertebrae (L1-L6) of *Remingtonocetus domandaensis* GSP-UM 3552 in anterior view. Note the curved prezygapophyses, the robust metapophyses, the short and robust neural spines, and the laterally-projecting transverse processes of L1-L3. The right transverse process of L6 is severely broken and irreparable.

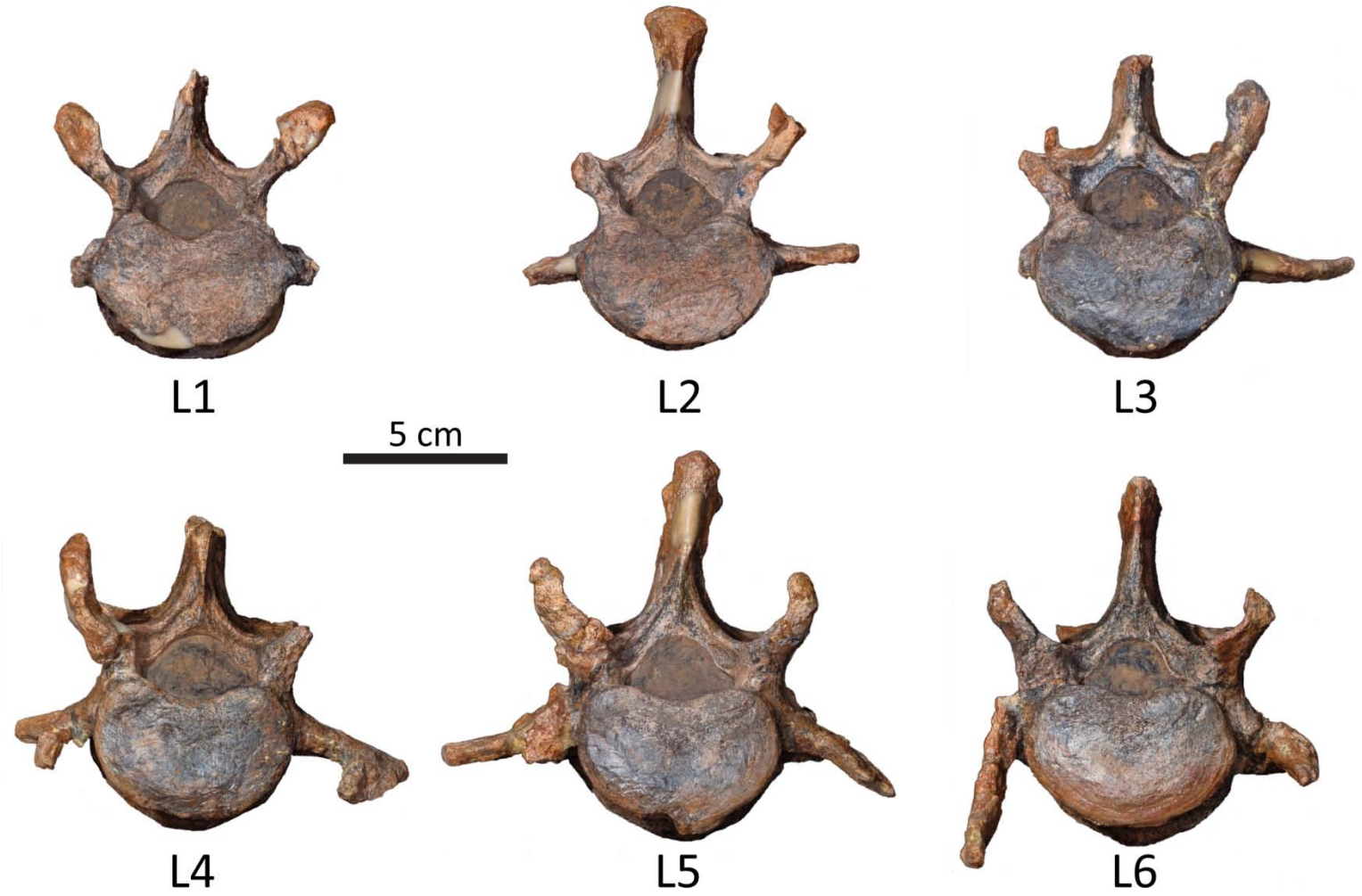

Figure 3.8. Lumbar vertebrae (L1-L6) of *Remingtonocetus domandaensis* GSP-UM 3552 in left lateral view. Note the relatively long centra, the anteroposteriorly long neural spines, and the minimal anterior inclination of the transverse processes.

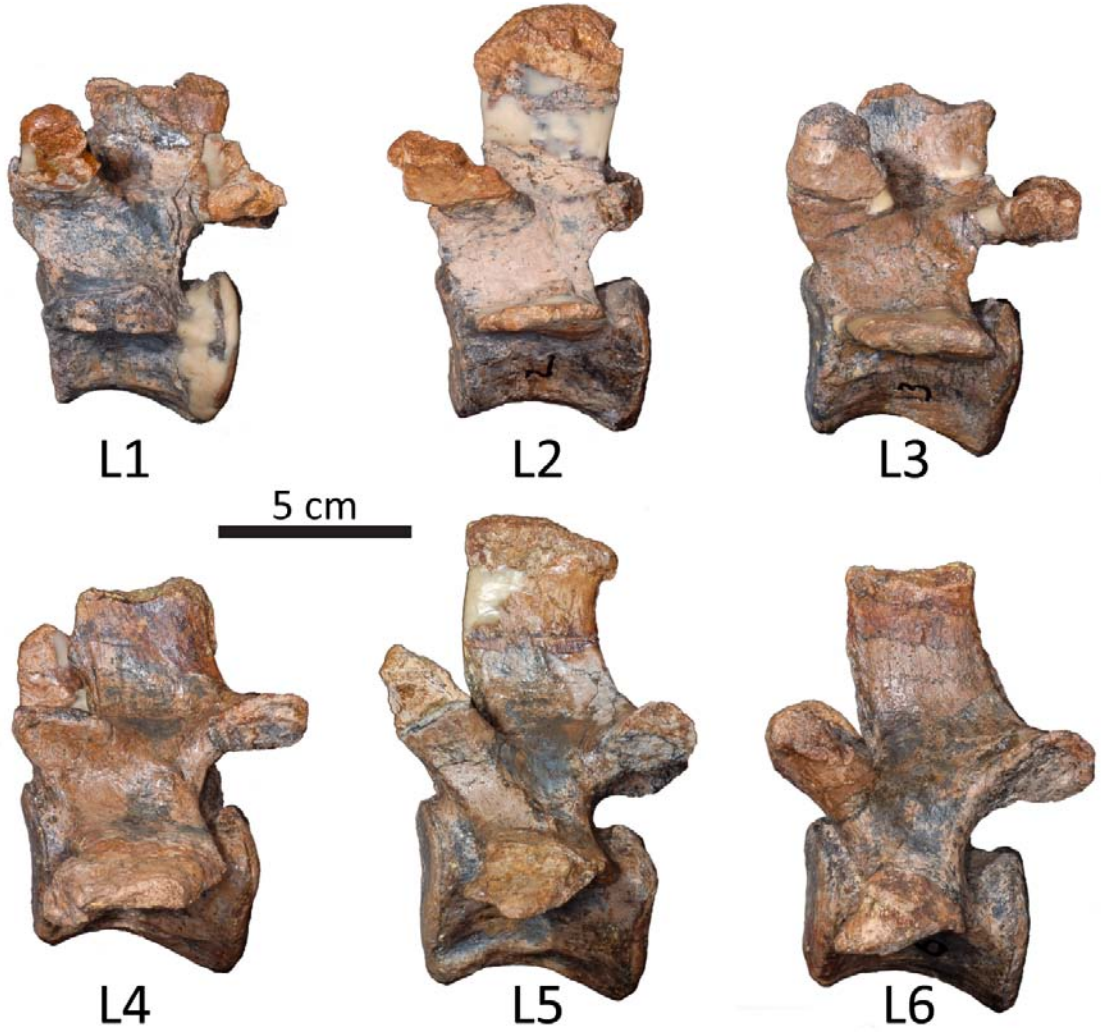

Figure 3.9. Sacral vertebrae of *Remingtonocetus domandaensis* GSP-UM 3552 (top; S1-S3) and 3408 (bottom; S1-S4) in anterior (left) and left lateral (right) views. Note the broad auricular surface for articulation with the ilium, the flat prezygapophyses of S1, and the lack of fusion between S3 and S4.

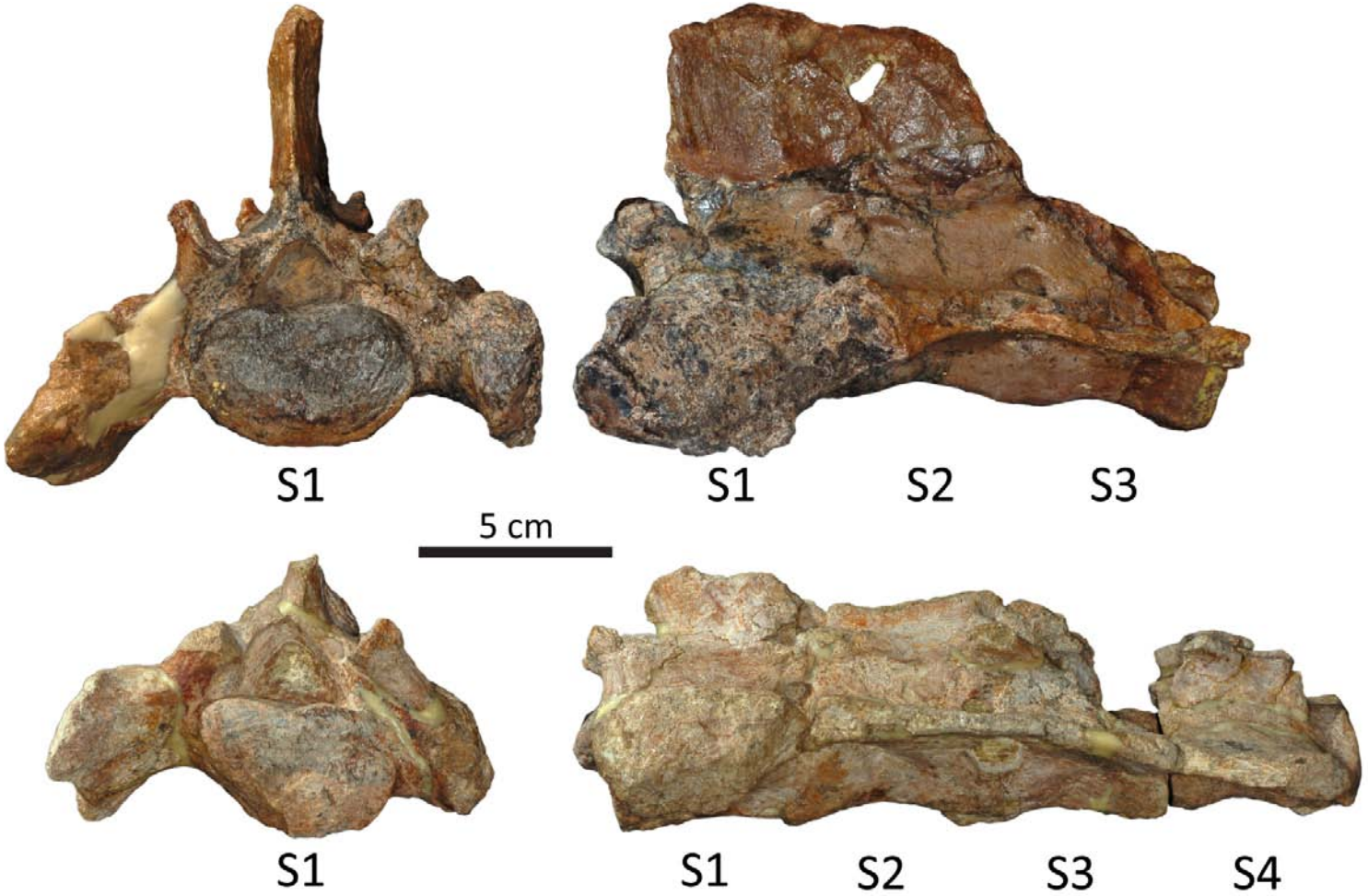

Figure 3.10. Caudal vertebrae (Ca1-Ca4) of *Remingtonocetus domandaensis* GSP-UM 3408 in anterior (top) and left lateral (bottom) views. Note the increasingly circular cross-sections of the anterior epiphyses.

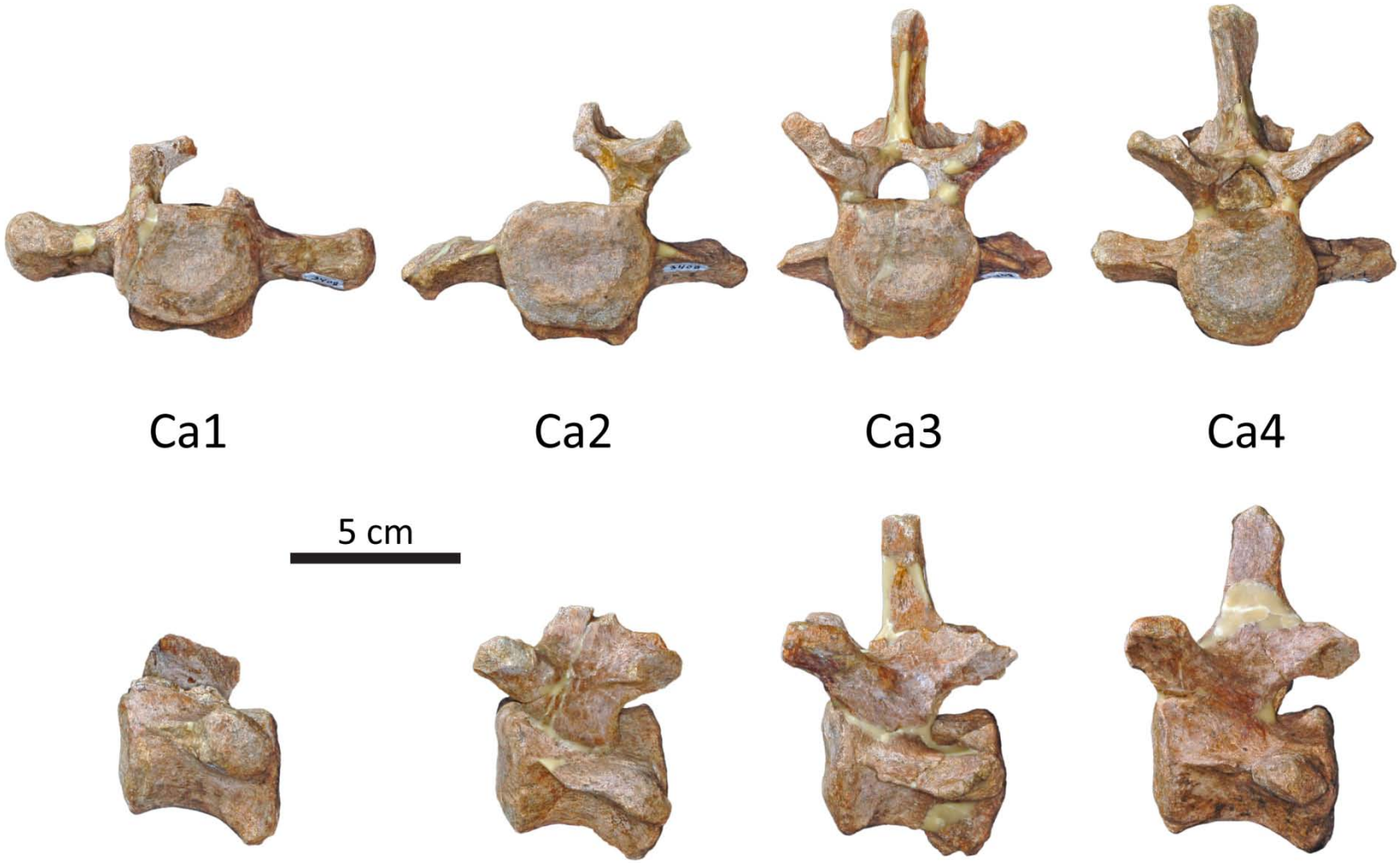

Figure 3.11. Three-dimensional models of C1-C7 of *Remingtonocetus domandaensis* GSP-UM 3552 in articulation in left lateral view. Note the inclination of the neck and the imbrications of the transverse processes of C3-C5 that would have limited lateral flexion and restricted most movement to the sagittal plane.

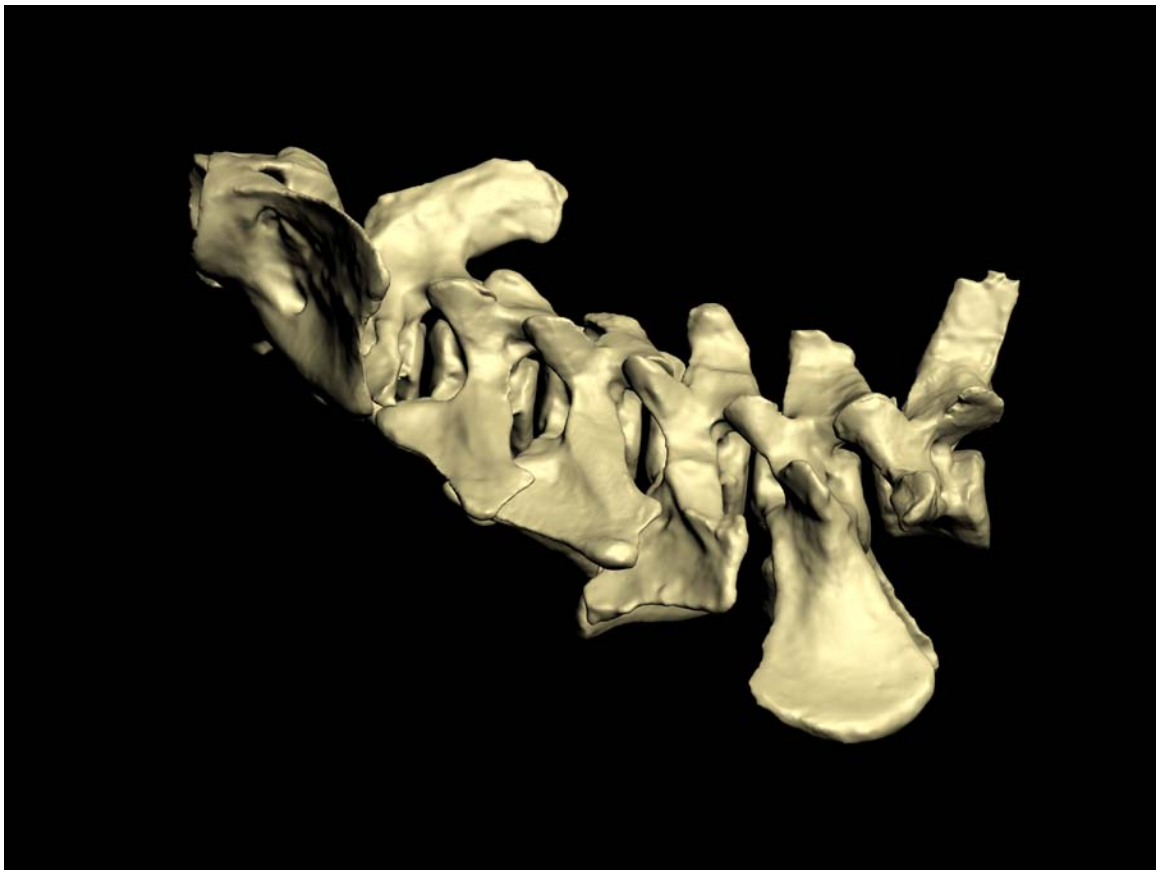

Figure 3.12. Comparisons of L1-L6 in *Remingtonocetus domandaensis*, *Maiacetus inuus*, *Rodhocetus kasranii*, *Qaisracetus arifi*, and *Dorudon atrox*. A. Natural-log transformed centrum lengths by vertebral position. B. Relative centrum length standardized by the mean centrum height of T1-T3 (method modified from Gingerich, 1998). Note how *R. domandaensis* has the greatest relative lumbar length of taxa included here.

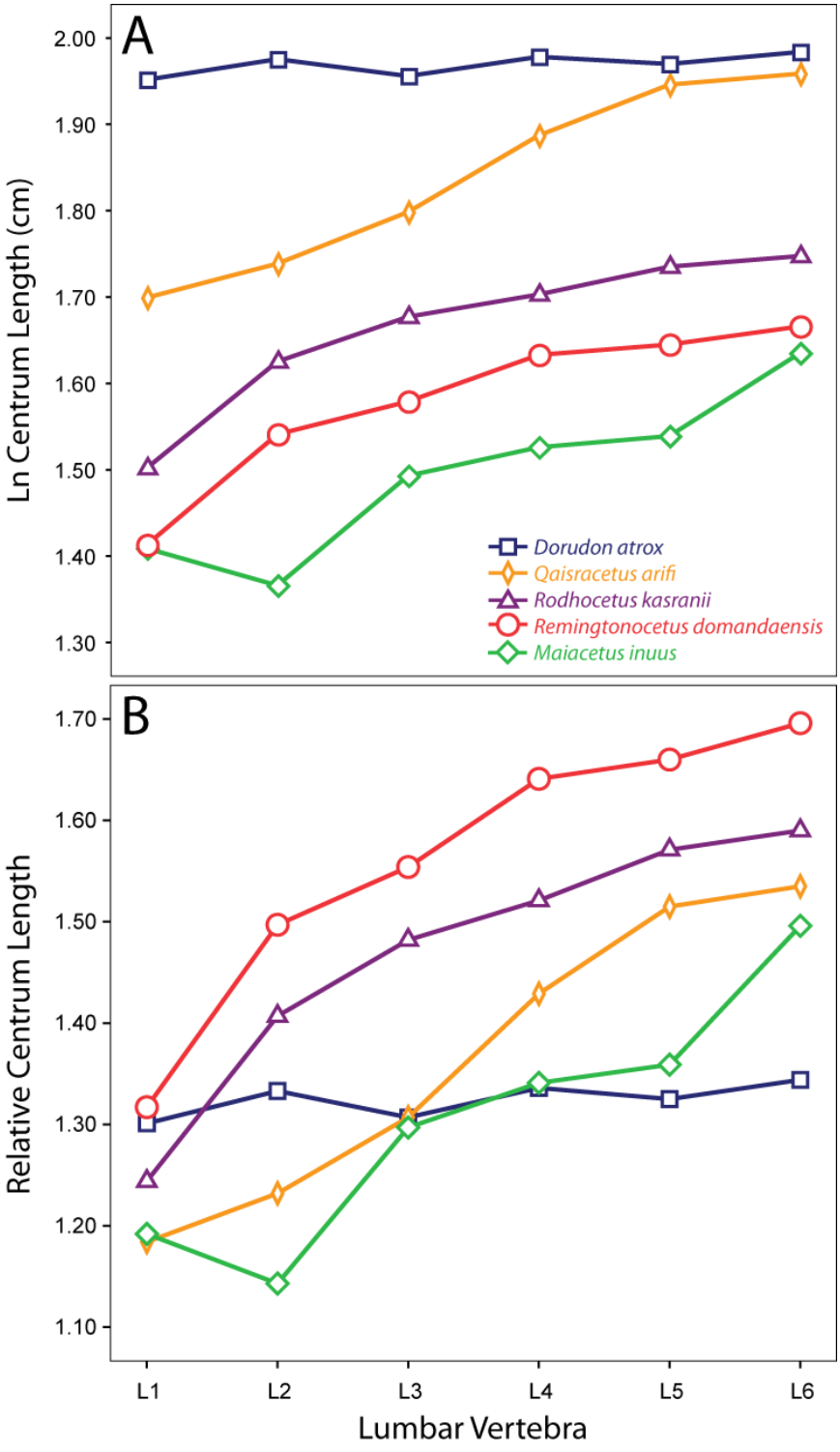

Table 3.1. Estimated counts of cervical (C), thoracic (T), lumbar (L), sacral (S), and caudal (Ca) vertebrae for three extinct artiodactyls and nine archaeocete cetaceans. Reliable estimates are in **bold**. Estimates for *P. attocki*, *A. natans*, and *K. minimus* are based on composite, incomplete, or non-articulated skeletons, whereas counts for *D. metsiacus*, *M. schaeferi*, *A. optatus*, *M. inuus*, *R. kasranii*, *Q. arifi*, *D. atrox*, and *B. isis* are based on mostly complete, articulated skeletons. The estimated count for *R. domandaensis* is based on GSP-UM 3552, which preserved most precaudal vertebrae in articulation (excluding middle thoracic vertebrae and S4).

Family and Species	C	T	L	S	Ca	Reference
Dichobunidae						
Diacodexis metsiacus	**7**	**13?**	**6**	**3**	**19+**	**Rose, 1985**
Messelobunodon schaeferi	**7**	**13**	**6**	**3?**	**24**	**Franzen, 1981**
Hypertragulidae						
Archaeomeryx optatus	**7**	**13**	**6**	**2-4**	**?**	**Colbert, 1941**
Pakicetidae						
Pakicetus attocki	7	?	8-9	4	20+	Madar, 2007
Ambulocetidae						
Ambulocetus natans	7	16-17	8	4	20+	Madar et al., 2002
Remingtonocetidae						
Kutchicetus minimus	7	15	8	4	20-25	Bajpai and Thewissen, 2000
Remingtonocetus domandaensis	**7**	**13?**	**6**	**4**	**?**	**This study**
Protocetidae						
Maiacetus inuus	**7**	**13**	**6**	**4**	**21**	**Gingerich et al., 2009**
Qaisracetus arifi	**7**	**13**	**6**	**4**	**?**	**Gingerich et al., 2001**
Rodhocetus kasranii	**7**	**13**	**6**	**4**	**?**	**Gingerich et al., 1994**
Basilosauridae						
Basilosaurus isis	**7**	**16**	**19**	**4**	**20**	**Gingerich et al., in prep**
Dorudon atrox	**7**	**17**	**16**	**4**	**21**	**Uhen, 2004**

Table 3.2. Measurements of vertebrae in *Remingtonocetus domandaensis* GSP-UM 3408. Measurements are in cm, except for neural spine angle, which is measured in degrees from the horizontal (angles <90° indicate neural spines angled anteriorly, whereas angles >90° indicate neural spines angled posteriorly). Asterisks (*) indicate estimates, and "np" indicates that the vertebra was not preserved in this specimen. Centrum posterior height of C3 includes hypapophysis. Abbreviations: *Ant. Hgt.*, anterior height; *Ant. Wid.*, anterior width; *Pos. Hgt.*, posterior height; *Pos. Wid.*, posterior width; *Ven. Len.*, ventral length.

		Centrum					Neural Canal		Neural Spine	
Vertebra		Ven. Len.	Ant. Wid.	Ant. Hgt.	Pos. Wid.	Pos. Hgt.	Ant. Wid.	Ant. Hgt.	Ant. Hgt.	Angle (°)
C1	(np)	-	-	-	-	-	-	-	-	-
C2	(np)	-	-	-	-	-	-	-	-	-
C3		3.86	3.64	3.52	4.10	3.49	-	-	-	-
C4	(np)	-	-	-	-	-	-	-	-	-
C5	(np)	-	-	-	-	-	-	-	-	-
C6	(np)	-	-	-	-	-	-	-	-	-
C7	(np)	-	-	-	-	-	-	-	-	-
T1	(np)	-	-	-	-	-	-	-	-	-
T2	(np)	-	-	-	-	-	-	-	-	-
T3	(np)	-	-	-	-	-	-	-	-	-
T4	(np)	-	-	-	-	-	-	-	-	-
T5	(np)	-	-	-	-	-	-	-	-	-
T6	(np)	-	-	-	-	-	-	-	-	-
T7	(np)	-	-	-	-	-	-	-	-	-
T8	(np)	-	-	-	-	-	-	-	-	-
T9	(np)	-	-	-	-	-	-	-	-	-
T10	(np)	-	-	-	-	-	-	-	-	-
T11		4.08	4.73	3.29	-	3.25	-	-	-	-
T12		4.05	-	3.18	-	3.24	2.65	-	-	-
T13	(np)	-	-	-	-	-	-	-	-	-
L1	(np)	-	-	-	-	-	-	-	-	-
L2		4.73	-	-	5.66	3.62	-	-	-	-
L3		4.85	5.30	3.65	5.64	3.73	-	-	-	-
L4	(np)	-	-	-	-	-	-	-	-	-
L5		5.14	5.41	4.23	5.88	4.23	-	-	-	-
L6		5.23	5.32	4.14	5.31	4.05	2.53	1.75	-	-
S1		5.25*	5.52	3.85*	4.05	-	2.35	1.86	-	-
S2		5.10*	4.05	-	3.70	-	-	-	-	-
S3		4.75*	3.70	-	3.80*	1.04	-	-	-	-
S4		5.14	3.88	3.23	4.85	-	2.23	-	-	-
Ca1		4.91	4.39	3.64	5.15	4.08	2.09	1.62	-	-
Ca2		5.11	4.72	3.84	4.96	4.37	-	1.75	-	-
Ca3		5.20	4.62	4.21	4.80	4.33	2.05	1.42	5.00*	79.3
Ca4		5.65	4.25	4.19	4.81	4.43	1.93	1.36	4.98	91.9

Table 3.3. Measurements of vertebrae in *Remingtonocetus domandaensis* GSP-UM 3552. Measurements are in cm, except for neural spine angle, which is measured in degrees from the horizontal (angles <90° indicate neural spines angled anteriorly, whereas angles >90° indicate neural spines angled posteriorly). Asterisks (*) indicate estimates, and "np" indicates that the vertebra was not preserved in this specimen. Centrum length and anterior width of C2 include the dens and cranial articular facets respectively. Centrum posterior heights of C2-C5 include hypapophyses. Abbreviations follow Table 3.2.

	Centrum					Neural Canal		Neural Spine	
Vertebra	Ven. Len.	Ant. Wid.	Ant. Hgt.	Pos. Wid.	Pos. Hgt.	Ant. Wid.	Ant. Hgt.	Ant. Hgt.	Angle (°)
C1	2.74	-	1.77	-	1.49	4.52	3.32	-	-
C2	7.50	8.63	2.12	3.99	3.63	2.11	2.38	7.31	133.9
C3	4.04	3.59	3.76	3.89	4.05	1.91	1.55	1.20	-
C4	3.98	3.54	3.50	3.82	4.01	1.91	1.33	-	-
C5	3.87	3.57	3.50	3.81	4.06	2.12	1.56	2.13	61.0
C6	4.25	3.48	3.48	4.21	3.77	2.34	2.18	-	-
C7	4.15	4.10	3.45	4.59	3.58	2.72	2.27	4.70*	112.6
T1	4.27	4.20	3.04	5.56	3.16	2.70	1.94	8.70*	132.1
T2	4.16	4.20	3.11	5.50*	3.22	2.54	1.76	-	-
T3	4.09	4.22	3.07	5.55	3.18	2.53	1.86	-	135.0
T4	4.00	4.20*	3.32	5.50*	3.29	2.50	1.89	-	-
T5?	3.86	4.38	3.27	-	-	-	-	-	-
T6?	-	-	-	-	-	-	-	-	-
T7 (np)	-	-	-	-	-	-	-	-	-
T8 (np)	-	-	-	-	-	-	-	-	-
T9 (np)	-	-	-	-	-	-	-	-	-
T10?	-	-	-	-	3.28	-	-	-	-
T11	4.00*	4.55	3.26	5.70*	3.29	2.67	1.64	-	-
T12	4.10*	5.25*	3.13	-	3.04	3.06	1.93	5.33	92.3
T13	4.15*	5.55	3.08	5.25*	3.10	2.80	1.75	-	84.5
L1	4.23	5.49	3.16	5.76	3.29	2.68	1.70	5.09	86.0
L2	4.67	5.60	3.23	6.09	3.45	2.75	1.92	5.26	85.3
L3	4.85	5.82	3.39	6.05	3.58	2.95	1.95	5.28	83.1
L4	5.12	5.68	3.44	6.20	3.74	3.07	1.95	5.30	83.8
L5	5.18	5.76	3.78	6.47	3.84	3.15	2.04	5.41	75.5
L6	5.29	5.98	3.69	5.79	3.85	2.93	1.74	5.60	68.3
S1	5.25*	5.87	3.56	4.30	-	2.79	1.79	5.62	-
S2	4.95*	4.30	-	4.24	-	-	-	-	-
S3	4.80*	4.24	-	4.19	2.53	-	-	-	-
S4 (np)	-	-	-	-	-	-	-	-	-
Ca1 (np)	-	-	-	-	-	-	-	-	-
Ca2 (np)	-	-	-	-	-	-	-	-	-
Ca3 (np)	-	-	-	-	-	-	-	-	-
Ca4 (np)	-	-	-	-	-	-	-	-	-

Table 3.4. Ratio of centrum length to anterior centrum height in C3-C7 of select archaeocete and modern cetaceans. Species are sorted by mean relative length. Daggers (†) indicate extinct taxa. Remingtonocetids have the longest cervical vertebrae, followed by pakicetids and protocetids. Basilosaurids have the shortest cervical vertebrae among archaeocetes, although they are not quite as foreshortened as those of modern cetaceans.

Species	Family	Specimen No.	C3	C4	C5	C6	C7	Mean
Remingtonocetus domandaensis †	Remingtonocetidae	GSP-UM 3552	1.07	1.14	1.11	1.22	1.20	**1.15**
Dalanistes ahmedi †	Remingtonocetidae	GSP-UM 3165	0.96	1.00	1.07	1.18	1.23	**1.09**
[a] *Ichthyolestes pinfoldi* †	Pakicetidae	H-GSP 96251, 96598	1.23	0.93	-	-	-	**1.08**
[a] *Pakicetus attocki* †	Pakicetidae	H-GSP 96383, 96218, 92082, 91043, 96382	1.02	1.05	1.10	1.14	0.99	**1.06**
[b] *Maiacetus inuus* †	Protocetidae	GSP-UM 3551	0.83	0.83	0.80	0.88	0.94	**0.86**
[c] *Qaisracetus arifi* †	Protocetidae	GSP-UM 3410	0.76	0.73	-	0.82	-	**0.77**
Rodhocetus kasranii †	Protocetidae	GSP-UM 3012	0.74	0.73	0.71	0.77	0.81	**0.75**
[d] *Carolinacetus gingerichi* †	Protocetidae	ChM PV5401	0.75	-	-	0.77	0.67	**0.73**
[e] *Protocetus atavus* †	Protocetidae	SMNS 11087	0.73	-	-	0.69	0.58	**0.67**
[f] *Georgiacetus vogtlensis* †	Protocetidae	GSM 350	-	0.63	0.68	-	0.62	**0.65**
[g] *Basilosaurus cetoides* †	Basilosauridae	USNM 4675	0.47	0.43	0.53	0.60	0.67	**0.54**
[h] *Cynthiacetus maxwelli* †	Basilosauridae	MMNS VP 445	0.51	0.50	-	-	-	**0.51**
[i] *Chrysocetus healyorum* †	Basilosauridae	SCSM 87.195	0.52	-	0.46	0.48	0.54	**0.50**
Dorudon atrox †	Basilosauridae	UMMP 101222	0.47	0.45	0.42	0.46	0.53	**0.47**
[g] *Zygorhiza kochii* †	Basilosauridae	USNM 4678	0.47	0.43	0.49	-	-	**0.46**
Inia geoffrensis	Iniidae	USNM 239667	0.33	0.33	0.37	0.43	0.53	**0.40**
Balaenoptera physalus	Balaenopteridae	USNM 16045	0.26	0.28	0.29	0.32	0.37	**0.30**
Megaptera novaeangliae	Balaenopteridae	USNM 301636	0.23	0.19	0.19	0.25	0.22	**0.21**
Delphinus delphis	Delphinidae	USNM 572980	0.17	0.18	0.18	0.23	0.28	**0.21**
Tursiops truncatus	Delphinidae	USNM 571414	0.12	0.13	0.13	0.14	0.19	**0.14**

Data sources: [a] Madar (2007), [b] Gingerich et al. (2009), [c] Gingerich et al. (2001), [d] Geisler et al. (2005), [e] Fraas (1904), [f] Hulbert (1998), [g] Kellogg (1936), [h] Uhen (2005), [i] Uhen and Gingerich (2001)

REFERENCES

Alexander, R. M., N. J. Dimery, and R. F. Ker. 1985. Elastic structures in the back and their role in galloping in some mammals. Journal of Zoology (London) 207: 467-482.

Bajpai, S., and J. G. M. Thewissen. 2000. A new, diminutive Eocene whale from Kachchh (Gujarat, India) and its implications for locomotor evolution of cetaceans. Current Science 79: 1478-1482.

Beentjes, M. P. 1990. Comparative terrestrial locomotion of the Hooker's sea lion (*Phocarctos hookeri*) and the New Zealand fur seal (*Arctocephalus forsteri*): evolutionary and ecological implications. Zoological Journal of the Linnean Society 98: 307-325.

Berta, A., and P. J. Adam. 2001. Evolutionary biology of pinnipeds. Pp. 235-260 in J.-M. Mazin and V. de Buffrénil (eds.), Secondary Adaptation of Tetrapods to Life in Water. Verlag Dr. Friedrich Pfeil, München.

Buchholtz, E. A. 1998. Implications of vertebral morphology for locomotor evolution in early Cetacea. Pp. 325-351 in J. G. M. Thewissen (ed.), The Emergence of Whales: Evolutionary Patterns in the Origin of Cetacea. Plenum Press, New York.

Buchholtz, E. A. 2001. Vertebral osteology and swimming style in living and fossil whales (Order: Cetacea). Journal of Zoology (London) 253: 175-190.

Buchholtz, E. A. 2007. Modular evolution of the cetacean vertebral column. Evolution & Development 9: 278-289.

Buchholtz, E. A., and S. A. Schur. 2004. Vertebral osteology in Delphinidae (Cetacea). Zoological Journal of the Linnean Society 104: 383-401.

Carlson, H. 1978. Morphology and contraction properties of cat lumbar back muscles. Acta Physiologica Scandinavica 103: 180-197.

Cave, A. J. E. 1975. The morphology of the mammalian cervical pleurapophysis. Journal of Zoology (London) 177: 377-393.

Colbert, E. H. 1941. The osteology and relationships of *Archaeomeryx*, an ancestral ruminant. American Museum Novitates 1135: 1-24.

Dumas, G. A., L. Beaudoin, and G. Drouin. 1987. *In situ* mechanical behavior of posterior spinal ligaments in the lumbar region. An *in vitro* study. Journal of Biomechanics 20: 301-310.

English, A. W. 1976. Limb movements and locomotor function in the California sea lion (*Zalophus californianus*). Journal of Zoology (London) 178: 341-364.

English, A. W. 1980. The functions of the lumbar spine during stepping in the cat. Journal of Morphology 165: 55-66.

Evans, H. E. 1993. Miller's Anatomy of the Dog. 3rd Edition. Saunders, Philadelphia.

Filler, A. G. 1986. Axial character seriation in mammals: an historical and morphological exploration of the origin, development, use, and current collapse of the homology paradigm. Ph.D. dissertation, Department of Anthropology, Harvard University, Cambridge, MA, 349 pp.

Fish, F. E. 1984. Mechanics, power output and efficiency of the swimming muskrat (*Ondatra zibethicus*). Journal of Experimental Biology 110: 183-201.

Fish, F. E. 1993a. Comparison of swimming kinematics between terrestrial and semiaquatic opossums. Journal of Mammalogy 74: 275-284.

Fish, F. E. 1993b. Influence of hydrodynamic design and propulsive mode on mammalian swimming energetics. Australian Journal of Zoology 42: 79-101.

Fish, F. E. 1994. Association of propulsive swimming mode with behavior in river otters (*Lutra canadensis*). Journal of Mammalogy 75: 989-997.

Fish, F. E. 1996. Transitions from drag-based to lift-based propulsion in mammalian swimming. American Zoologist 36: 628-641.

Fish, F. E. 2001. A mechanism for evolutionary transition in swimming mode by mammals. Pp. 261-287 in J.-M. Mazin and V. de Buffrénil (eds.), Secondary Adaptation of Tetrapods to Life in Water. Verlag Dr. Friedrich Pfeil, München.

Fish, F. E. 2002. Balancing requirements for stability and maneuverability in cetaceans. Integrative and Comparative Biology 42: 85-93.

Fish, F. E., and R. V. Baudinette. 1999. Energetics of locomotion by the Australian water rat (*Hydromys chrysogaster*): a comparison of swimming and running in a semi-aquatic mammal. Journal of Experimental Biology 202: 353-363.

Fish, F. E., J. E. Peacock, and J. J. Rohr. 2003. Stabilization mechanism in swimming odontocete cetaceans by phased movements. Marine Mammal Science 19: 515-528.

Fraas, E. 1904. Neue Zeuglodonten aus dem unteren Mitteleocän vom Mokattam bei Cairo. Geologische und Paläontologische Abhandlungen, Neue Folge 6: 199-220.

Franzen, J. L. 1981. Das erste Skelett eines Dichobuniden (Mammalia, Artiodactyla), geborgen aus mitteleozänen Ölschiefern der „Grube Messel" bei Darmstadt (Deutschland, S-Hessen). Senckenbergiana Lethaea 61: 299-353.

Gál, J. M. 1993a. Mammalian spinal biomechanics: I. Static and dynamic mechanical properties of intact intervertebral joints. Journal of Experimental Biology 174: 247-280.

Gál, J. M. 1993b. Mammalian spinal biomechanics: II. Intervertebral lesion experiments and mechanisms of bending resistance. Journal of Experimental Biology 174: 281-297.

Geisler, J. H., A. E. Sanders, and Z. Luo. 2005. A new protocetid whale (Cetacea: Archaeoceti) from the late middle Eocene of South Carolina. American Museum Novitates 3480: 1-65.

Gellman, K. S., J. E. A. Bertram, and J. W. Hermanson. 2002. Morphology, histochemistry, and function of epaxial cervical musculature in the horse (*Equus caballus*). Journal of Morphology 251: 182-194.

Getty, R. ed 1975. Sisson and Grossman's the Anatomy of the Domestic Animals. W.B. Saunders Company, Philadelphia.

Gillespie, K. A., and J. P. Dickey. 2004. Biomechanical role of lumbar spine ligaments in flexion and extension: determination using a parallel linkage robot and a porcine model. Spine 29: 1208-1216.

Gingerich, P. D. 1998. Paleobiological perspectives on Mesonychia, Archaeoceti, and the origin of whales. Pp. 423-449 in J. G. M. Thewissen (ed.), The Emergence of Whales: Evolutionary Patterns in the Origin of Cetacea. Plenum Press, New York.

Gingerich, P. D., M. Arif, M. A. Bhatti, and W. C. Clyde. 1998. Middle Eocene stratigraphy and marine mammals (Mammalia: Cetacea and Sirenia) of the Sulaiman Range, Pakistan. Bulletin of the Carnegie Museum of Natural History 34: 239-259.

Gingerich, P. D., M. Arif, and W. C. Clyde. 1995. New archaeocetes (Mammalia, Cetacea) from the middle Eocene Domanda Formation of the Sulaiman Range, Punjab (Pakistan). Contributions from the Museum of Paleontology, University of Michigan 29: 291-330.

Gingerich, P. D., S. M. Raza, M. Arif, M. Anwar, and X. Zhou. 1993. Partial skeletons of *Indocetus ramani* (Mammalia, Cetacea) from the lower middle Eocene Domanda shale in the Sulaiman Range of Punjab (Pakistan). Contributions from the Museum of Paleontology, University of Michigan 28: 393-416.

Gingerich, P. D., S. M. Raza, M. Arif, M. Anwar, and X. Zhou. 1994. New whale from the Eocene of Pakistan and the origin of cetacean swimming. Nature 368: 844-847.

Gingerich, P. D., M. ul-Haq, I. H. Khan, and I. S. Zalmout. 2001. Eocene stratigraphy and archaeocete whales (Mammalia, Cetacea) of Drug Lahar in the eastern Sulaiman Range, Balochistan (Pakistan). Contributions from the Museum of Paleontology, University of Michigan 30: 269-319.

Gingerich, P. D., M. ul-Haq, W. von Koenigswald, W. J. Sanders, B. H. Smith, and I. S. Zalmout. 2009. New protocetid whale from the middle Eocene of Pakistan: birth on land, precocial development, and sexual dimorphism. PLoS ONE 4: e4366.

Gray, J. 1968. Animal Locomotion. Norton, New York, 479 pp.

Hickman, G. C. 1984. Swimming ability of talpid moles, with particular reference to the semi-aquatic *Condylura cristata*. Mammalia 48: 505-513.

Hildebrand, M. 1959. Motions of the running cheetah and horse. Journal of Mammalogy 40: 481-495.

Howell, A. B. 1930. Aquatic Mammals. Charles C. Thomas, Springfield, IL, 338 pp.

Howell, A. B. 1944. Speed in Animals: Their Specializations for Running and Leaping. University of Chicago Press, Chicago, 270 pp.

Hulbert, R. C., Jr. 1998. Postcranial osteology of the North American middle Eocene protocetid *Georgiacetus*. Pp. 235-267 in J. G. M. Thewissen (ed.), The Emergence of Whales: Evolutionary Patterns in the Origin of Cetacea. Plenum Press, New York.

Kellogg, R. 1936. A review of the Archaeoceti. Carnegie Institute of Washington Publication 482: 1-366.

Kumar, K., and A. Sahni. 1986. *Remingtonocetus harudiensis*, new combination, a middle Eocene archaeocete (Mammalia, Cetacea) from western Kutch, India. Journal of Vertebrate Paleontology 6: 326-349.

Long, J. H., Jr., D. A. Pabst, W. R. Shepherd, and W. A. McLellan. 1997. Locomotor design of dolphin vertebral columns: bending mechanics and morphology of *Delphinus delphis*. Journal of Experimental Biology 200: 65-81.

Macintosh, J. E., and N. Bogduk. 1987. The morphology of the lumbar erector spinae. Spine 12: 658-668.

Madar, S. I. 1998. Structural adaptations of early archaeocete long bones. Pp. 353-378 in J. G. M. Thewissen (ed.), The Emergence of Whales: Evolutionary Patterns in the Origin of Cetacea. Plenum Press, New York.

Madar, S. I. 2007. The postcranial skeleton of early Eocene pakicetid cetaceans. Journal of Paleontology 81: 176-200.

Madar, S. I., J. G. M. Thewissen, and S. T. Hussain. 2002. Additional holotype remains of *Ambulocetus natans* (Cetacea, Ambulocetidae), and their implications for locomotion in early whales. Journal of Vertebrate Paleontology 22: 405-422.

Owen, R. 1848. On the Archetype and Homologies of the Vertebrate Skeleton. John Van Voorst, Paternoster Row, London.

Pabst, D. A. 1993. Intramuscular morphology and tendon geometry of the epaxial swimming muscles of dolphins. Journal of Zoology (London) 230: 159-176.

Pabst, D. A. 1996. Springs in swimming animals. American Zoologist 36: 723-735.

Pabst, D. A. 2000. To bend a dolphin: convergence of force transmission designs in cetaceans and scombrid fishes. American Zoologist 40: 146-155.

Ponseti, I. V. 1995. Differences in ligamenta flava among some mammals. Iowa Orthopaedic Journal 15: 141-146.

Roberts, T. J., and E. Azizi. 2011. Flexible mechanisms: the diverse roles of biological springs in vertebrate movement. Journal of Experimental Biology 214: 353-361.

Rose, K. D. 1985. Comparative osteology of North American dichobunid artiodactyls. Journal of Paleontology 59: 1203-1226.

Sahni, A., and V. P. Mishra. 1972. A new species of *Protocetus* (Cetacea) from the middle Eocene of Kutch, western India. Palaeontology 15: 490-495.

Sahni, A., and V. P. Mishra. 1975. Lower Tertiary vertebrates from western India. Monograph of the Palaeontological Society of India 3: 1-48.

Schilling, N., and D. R. Carrier. 2009. Function of the epaxial muscles during trotting. Journal of Experimental Biology 212: 1053-1063.

Schilling, N., and D. R. Carrier. 2010. Function of the epaxial muscles in walking, trotting and galloping dogs: implications for the evolution of epaxial muscle function in tetrapods. Journal of Experimental Biology 213: 1490-1502.

Schilling, N., T. Fischbein, E. P. Yang, and D. R. Carrier. 2009. Function of the extrinsic hindlimb muscles in trotting dogs. Journal of Experimental Biology 212: 1036-1052.

Slijper, E. J. 1946. Comparative biologic-anatomical investigations on the vertebral column and spinal musculature of mammals. Verhandelingen der Koninklijke Nederlandsche Akademie van Wetenschappen, Afdeling Natuurkunde, Tweede Sectie 42: 1-128.

Slijper, E. J. 1947. Observations on the vertebral column of the domestic animals. The Veterinary Journal 103: 376-387.

Spoor, F. 2009. Balance. Pp. 76-78 in W. F. Perrin, B. Würsig, and J. G. M. Thewissen (eds.), Encyclopedia of Marine Mammals, 2nd Edition. Academic Press, San Diego.

Spoor, F., S. Bajpai, S. T. Hussain, K. Kumar, and J. G. M. Thewissen. 2002. Vestibular evidence for the evolution of aquatic behavior in early cetaceans. Nature 417: 163-166.

Spoor, F., and J. G. M. Thewissen. 2008. Comparative and functional anatomy of balance in aquatic mammals. Pp. 257-284 in J. G. M. Thewissen and S. Nummela (eds.), Sensory Evolution on the Threshold: Adaptations in Secondarily Aquatic Vertebrates. University of California Press, Berkeley.

Stein, B. R. 1988. Morphology and allometry in several genera of semiaquatic rodents (*Ondatra*, *Nectomys*, and *Oryzomys*). Journal of Mammalogy 69: 500-511.

Tarasoff, F. J., A. Bisaillon, J. Piérard, and A. P. Whitt. 1972. Locomotory patterns and external morphology of the river otter, sea otter, and harp seal (Mammalia). Canadian Journal of Zoology 50: 915-929.

Thewissen, J. G. M., and S. Bajpai. 2009. New skeletal material of *Andrewsiphius* and *Kutchicetus*, two Eocene cetaceans from India. Journal of Paleontology 83: 635-663.

Thewissen, J. G. M., and F. E. Fish. 1997. Locomotor evolution in the earliest cetaceans: functional model, modern analogues, and paleontological evidence. Paleobiology 23: 482-490.

Thewissen, J. G. M., S. T. Hussain, and M. Arif. 1994. Fossil evidence for the origin of aquatic locomotion in archaeocete whales. Science 263: 210-212.

Thewissen, J. G. M., S. I. Madar, and S. T. Hussain. 1996. *Ambulocetus natans*, an Eocene cetacean (Mammalia) from Pakistan. Courier Forschungsinstitut Senckenberg 190: 1-86.

Thewissen, J. G. M., E. M. Williams, L. J. Roe, and S. T. Hussain. 2001. Skeletons of terrestrial cetaceans and the relationship of whales to artiodactyls. Nature 413: 277-281.

Uhen, M. D. 2004. Form, function, and anatomy of *Dorudon atrox* (Mammalia, Cetacea): an archaeocete from the middle to late Eocene of Egypt. University of Michigan Papers on Paleontology 34: 1-222.

Uhen, M. D. 2005. A new genus and species of archaeocete whale from Mississippi. Southeastern Geology 43: 157-172.

Uhen, M. D., and P. D. Gingerich. 2001. New genus of dorudontine archaeocete (Cetacea) from the middle-to-late Eocene of South Carolina. Marine Mammal Science 17: 1-34.

Walter, R. M., and D. R. Carrier. 2009. Rapid acceleration in dogs: ground forces and body posture dynamics. Journal of Experimental Biology 212: 1930-1939.

Wickland, C. R., J. F. Baker, and B. W. Peterson. 1991. Torque vectors of neck muscles in the cat. Experimental Brain Research 84: 649-659.

Williams, T. M. 1989. Swimming by sea otters: adaptations for low energetic cost locomotion. Journal of Comparative Physiology A 164: 815-824.

Zhou, X., W. J. Sanders, and P. D. Gingerich. 1992. Functional and behavioral implications of vertebral structure in *Pachyaena ossifraga* (Mammalia, Mesonychia). Contributions from the Museum of Paleontology, University of Michigan 28: 289-319.

Chapter 4

Multivariate Analysis of Lumbar Proportions in Modern Mammals and Implications for Relative Mobility of the Lumbar Spine in Early Cetaceans

INTRODUCTION

Functional interpretations of fossil species rely on detailed knowledge of the anatomy and lifestyle of modern forms. For fossil cetaceans, the functional implications of the vertebral column, in particular, are crucial for understanding the locomotor capabilities and ecology of extinct taxa. As whales became increasingly well-adapted to a fully aquatic lifestyle, their spines were "dramatically reconfigured" compared to those of terrestrial mammals (Buchholtz and Schur, 2004, p. 392). However, study of vertebral evolution in early whales has been inhibited by the fact that little work has been done to correlate vertebral osteology and function in modern mammals to provide a framework for interpreting the spines of fossil specimens (Buchholtz, 2001).

Assertions about the locomotor mode of the earliest cetaceans have often relied on inferences of musculature and ligaments, without any explicit comparisons to the anatomies of modern forms (e.g., Thewissen et al., 1994, 1996; Bajpai and Thewissen, 2000; Madar et al., 2002; Madar, 2007). In some cases, these interpretations may indeed be accurate. However, when different functional hypotheses can be derived

from a given morphology, additional justification for a particular interpretation is needed. Quantitative analyses of morphology of living species can shed light on how skeletal features should be interpreted in fossil taxa.

Principal components analysis (PCA) can be used to analyze a large set of quantitative morphological data simultaneously, allowing the variation in the data to be represented on a small number of compound axes that often yield meaningful patterns. For example, Gingerich (2003) utilized PCA of 14 trunk and limb measurements from 50 modern semiaquatic mammals to generate a morphospace for interpreting the lifestyles of two exceptional archaeocetes: *Rodhocetus balochistanensis* and *Dorudon atrox*. The PCA allowed most of the variation in the dataset to be represented on three interpretable compound axes. PC-I represented body size, separating small taxa from large taxa. PC-II separated more aquatic animals from more terrestrial animals. PC-III separated hind limb-dominated swimmers from forelimb-dominated swimmers.

On a bivariate plot of PC-II and PC-III scores for each taxon, *Rodhocetus balochistanensis* plotted nearest to *Desmana moschata* (desman), indicating that it is an intermediately aquatic, hind limb-dominated swimmer. *Dorudon atrox* plotted nearest to *Ornithorhynchus anatinus* (platypus), which raised questions about whether or not the fossil taxa were accurately represented in the morphospace defined by the 50 modern semiaquatic mammals. Consequently, a second PCA was carried out that included the fossil taxa in the initial assessment of variance in the dataset. PC-I and PC-II were similar to those of the first PCA, but PC-III was notably different, separating

lumbus-dominated swimmers (like *D. atrox*) from hind limb-dominated swimmers (like *R. balochistanensis*).

Gingerich's (2003) analysis was ground-breaking in that it objectively demonstrated which modern semiaquatic mammals are most similar in postcranial proportions to *Rodhocetus balochistanensis* and *Dorudon atrox*, providing insight into their degree of aquatic adaptation and swimming behavior. This approach has since provided the basis for interpreting degree of terrestriality and swimming mode in fossil desmostylians (Gingerich, 2005), pantolestids (Rose and von Koenigswald, 2005), and pinnipeds (Bebej, 2009). However, it is insufficient for interpreting the locomotor mode of many other archaeocetes for two reasons.

First, it requires a skeleton that is nearly complete. This is a fairly rare occurrence, and *Rodhocetus balochistanensis* and *Dorudon atrox* were exceptional in this regard. Other archaeocete cetaceans, including some that are known from dozens of specimens, lack many of the elements needed for such an analysis. For example, *Remingtonocetus domandaensis* is known from well over 50 partial specimens, yet only five of the 14 postcranial measurements utilized by Gingerich (2003) can be measured or estimated with any confidence in this taxon. The same holds true for many other archaeocetes, which are known from good vertebral columns, but lack complete fore- and hind limbs.

Second, utilization of the lumbus during locomotion is not adequately addressed by this dataset. The extremely long lumbus and reduced hind limbs of *Dorudon atrox* dominate the variance on PC-III, resulting in insufficient differentiation between other

taxa that do and do not utilize movements of their lumbus during swimming. For example, some modern taxa, such as hippos, possess negative PC-II scores, placing them on the lumbus-dominated side of the axis, despite the fact they do not utilize movements of their lumbar region during swimming (Coughlin and Fish, 2009). Likewise, several phocid pinnipeds have positive PC-II scores, placing them on the limb-dominated side of the PC-II axis, despite the fact that lateral movements of the lumbar spine play a crucial role in their locomotion (Tarasoff et al., 1972; Fish et al., 1988).

One approach to address both of these problems is to focus exclusively on the anatomy of the lumbar vertebrae, rather than on the entire postcranial skeleton. Modern mammals exhibit a wide range of mobility in the lumbar region, ranging from being dorsostable at one extreme to dorsomobile at the other. Dorsostable mammals, including nearly all living artiodactyls and perissodactyls (Howell, 1944; Hildebrand, 1959; Alexander et al., 1977, 1985; Grand, 1997; Boszczyk et al., 2001), limit excursions of the lumbar spine during locomotion. While there is usually a good deal of movement possible at the lumbosacral joint (Slijper, 1946, 1947; Gál, 1993), the remaining lumbar joints are mostly immobilized. They possess anteroposteriorly-expanded neural spines that limit extension at intervertebral joints and revolute zygapophyses that limit excursions in all planes (Zhou et al., 1992).

The lumbar vertebrae of dorsomobile mammals lack the osteological constraints evident in the vertebrae of dorsostable mammals. Instead, they possess features that increase the mobility of intervertebral joints, allowing them to utilize movements of their lumbar spine during locomotion. Felids and canids, for example, flex and extend

their lumbar region during running, increasing their speed by lengthening each stride (Howell, 1944; Hildebrand, 1959; Alexander et al., 1985; Schilling and Carrier, 2010). Many semiaquatic mammals move their lumbar spine during swimming. Phocid pinnipeds swim by pelvic oscillation, which involves lateral bending of the lumbar region coupled with lateral sweeps of the hind flippers (Tarasoff et al., 1972; Fish et al., 1988). Otters bend their lumbar column to varying degrees depending on the swimming mode they utilize. Near the surface of the water, they combine pelvic paddling with dorsoventral movements of the lumbar spine to increase the length of their power stroke (Tarasoff et al., 1972; Williams, 1989; Fish, 1994), but during submerged swimming, they often swim exclusively using dorsoventral undulation of their lumbar, sacral, and caudal vertebrae (Williams, 1989; Fish, 1994).

In this study, I utilize the methodology of Gingerich (2003), but with a dataset tailored specifically to address lumbar mobility in early cetaceans. PCAs of lumbar proportions from a range of modern dorsostable and dorsomobile mammals are used to define a series of morphospaces for interpreting the function of the lumbar spine in early whales. Because the measurements are taken from individual lumbar vertebrae, taxa lacking complete skeletons can be included. Lumbar vertebrae for *Remingtonocetus domandaensis*, *Maiacetus inuus*, *Qaisracetus arifi*, and others are included in various analyses. These results provide insight into the relative functional capabilities of each taxon individually (thus, providing an independent test of the lumbar interpretation espoused for *R. domandaensis* in Chapter 3), while also providing

information about the evolution of the lumbar column and locomotion in the earliest cetaceans.

MATERIALS AND METHODS

Specimens

Twenty-five species of modern mammals were chosen to provide the raw data for the PCAs (Table 4.1). Dorsostable mammals are represented by members of the families Antilocapridae, Bovidae, Cervidae, and Equidae, while dorsomobile mammals are represented by members of Canidae, Felidae, Leporidae, Mustelidae (including otters in the subfamily Lutrinae), and Phocidae. Modern cetaceans were excluded from the initial dataset because their derived lumbar morphology lacks morphological landmarks (e.g., zygapophyses) critical for some of the measurements (Slijper, 1946; Boszczyk et al., 2001); however, two modern cetaceans were later included in one PCA (described below) for comparison with fossil cetaceans. Archaeocetes studied in one or more analyses include *Remingtonocetus domandaensis* (L1-LZ); *Maiacetus inuus* (L1-LZ); *Qaisracetus arifi* (L1-LZ); *Rodhocetus kasranii* (LX); GSP-UM 3357, an undescribed species of protocetid (L1-L2); *Dorudon atrox* (L3); and *Basilosaurus isis* (L3).

Measurements

Seventeen measurements were collected from each lumbar vertebra of every specimen. The 17 measurements are summarized in Fig. 4.1, and the raw measurements for each specimen are listed in Tables 4.2-4.7. For measurements in

which both right and left sides could be measured, both measurements were collected and subsequently averaged. Linear measurements were collected with digital calipers. Angles were measured in degrees with respect to a defined axis from digital photographs using ImageJ, a public domain Java-based program for image processing and analysis developed by the National Institutes of Health.

Centrum length (CL) was measured from the middle of the anterior epiphysis to the middle of the posterior epiphysis. Centrum widths (CWa, CWp) were measured as the maximum width across the anterior and posterior epiphyses, while centrum heights (CHa, CHp) were measured at the midline. The neural canal was measured at its anterior opening; its width (NCW) represents the maximum width (typically where the pedicle meets the centrum), and its height (NCH) was measured at the midline.

Neural spine height (NSH) was measured from the dorsal border of the neural canal to the dorsal-most tip of the neural spine. Neural spine length (NSL) was measured as the anteroposterior length of the neural spine at its apex. Pre- and postzygapophyseal widths (PreW, PosW) were measured as the maximum distance between articulating surfaces. (For the modern cetaceans included in the L3 PCA, PreW and PosW were measured across the metapophyses.) Pedicle width (PedW) was measured anteriorly where the pedicle joins the centrum; pedicle length (PedL) was measured at the same level, but anteroposteriorly. Maximum width (MaxW) was measured as the maximum mediolateral distance across transverse processes.

The anteroposterior angle of the neural spine (APAngNS) was measured from photographs in left-lateral view. The horizontal ray of this angle was defined by the top

of the centrum, and the vertical ray was defined by the central axis of the neural spine. Thus, vertebrae with anteriorly-inclined neural spines have APAngNS of <90°, while vertebrae with posteriorly-inclined neural spines have APAngNS of >90°.

The craniocaudal angle of the transverse processes (CCAngTP) was measured from photographs in ventral view and represents the cranial angle between the midline and the central axis of the transverse process. Transverse processes that are angled cranially have CCAngTP of <90°, while transverse processes that project almost straight laterally from the vertebral body have CCAngTP closer to 90°.

The dorsoventral angle of the transverse processes (DVAngTP) was measured from photographs in anterior view and represents the ventral angle between the midline and the central axis of the transverse process. Transverse processes that are angled ventrally have DVAngTP of <90°, while transverse processes that project almost straight laterally from the vertebral body have DVAngTP closer to 90°.

Principal Components Analyses

Principal components analyses were carried out using the statistical analysis software SPSS 13.0 (SPSS, Inc.), following the methodology described in detail by Gingerich (2003). Separate PCAs were performed for each vertebral position using the correlation matrices of the 17 lumbar measurements of the 25 modern taxa. Because early archaeocetes possessed six lumbar vertebrae, six PCAs were carried out, here termed L1, L2, L3, LX, LY, and LZ. L1, L2, and L3 represent the first three lumbar vertebrae in each taxon; LX, LY, and LZ represent the last three lumbar vertebrae in each

taxon. For taxa with six lumbar vertebrae (including most of the taxa in the dataset), LX, LY, and LZ represent L4, L5, and L6. For taxa with more or less than six lumbar vertebrae, LX, LY, and LZ represent the three most posterior lumbar vertebrae (e.g., L5, L6, and L7 for *Canis lupus familiaris*; L3, L4, and L5 for *Phoca vitulina*).

PC scores were calculated for each taxon by multiplying the eigenvector coefficients (loadings) for each PC by the respective normalized, ln-transformed measurements and summing across all 17 variables. Normalization for each measurement was carried out by subtracting the all-species mean from the ln-transformed measurement and dividing that difference by the all-species standard deviation. Following the treatment of fossil taxa in previous analyses (Gingerich, 2003, 2005; Rose and von Koenigswald, 2005; Bebej, 2009), cetaceans were not included in the initial PCAs. Their PC scores were calculated using the loadings generated by the PCA, and they were then plotted in the same morphospace as the modern taxa.

RESULTS

Principal Axes

The results of the six PCAs are so similar that their general results can be described together. The variance in each PCA (Fig. 4.2) is structured nearly identically, with two interpretable components (following the scree plot approach as described by Jackson, 1993). Eigenvalues and loadings for PCs I and II in each analysis are listed in Table 4.8. Loadings of PCs I and II are shown graphically in Figs. 4.3-4.8.

PC-I accounts for 75.2-78.6% of the variance in each analysis. The loadings of the 14 linear measurements are all positive and of a similar magnitude, indicating that they contributed equally to the variance on this axis. The loadings of the three angular measurements are significantly less than those of the linear measurements and closer to zero, indicating that they contributed relatively little to the variance on this axis.

PC-II accounts for less of the variance than PC-I (10.7-12.5%), but still notably more than PCs III-XVII (0.0-4.6%). For the L1-LY PCAs, the most negative PC-II loadings include centrum length, pedicle length, and centrum height. The anteroposterior angle of the neural spine is the most negative loading on PC-II of the LZ PCA. The most positive loadings on PC-II in all six PCAs are the craniocaudal angle of the transverse processes, the dorsoventral angle of the transverse processes, and the anteroposterior length of the neural spine. The absolute values of the loadings for the angles of the transverse processes (minimum: 0.539; maximum: 0671) are two to three times the absolute values of other loadings, indicating that differences in these measurements account for the most variance on this axis. The highest contrast on PC-II is thus between taxa whose lumbar vertebrae are relatively long, with anteroposteriorly shorter neural spines and cranioventrally-angled transverse processes (with negative scores), and taxa whose lumbar vertebrae are relatively short with anteroposteriorly long neural spines and transverse processes with little to no cranial or ventral angulation (with positive scores).

PC Scores

PC-I and PC-II scores for each taxon are listed in Table 4.9 and shown graphically in Figs. 4.3-4.8. The positions of taxa on PC-I are generally consistent in all six PCAs. The taxa with the most negative scores are routinely *Lepus californicus* (black-tailed jackrabbit), *Madoqua kirkii* (Kirk's dik-dik), and many Mustelidae (including otters). The taxa with the most positive scores include *Equus burchellii* (Burchell's zebra), Phocidae, and most Cetacea. The positions of taxa on PC-II are also generally consistent, though the scores of some taxa change from L1-LZ. Artiodactyla and Perissodactyla tend to have the most positive PC-II scores, while *L. californicus*, Phocidae, and cursorial Carnivora (Felidae and Canidae in various analyses) tend to have the most negative scores.

Remingtonocetus domandaensis routinely has the greatest PC-II score among the archaeocete cetaceans, ranging from a minimum of 0.126 (LY) to a maximum of 1.383 (LZ). *Maiacetus inuus* has lower PC-II scores, ranging from -1.371 (LY) to 0.557 (LZ). *Qaisracetus arifi* generally has the lowest PC-II score among cetaceans included in all six PCAs (except at LY and LZ), ranging from -2.492 (LX) to 1.094 (LZ). In the L1 and L2 PCAs, protocetid GSP-UM 3357 has PC-II scores in the range of *Q. arifi* (L1: -0.610; L2: -1.634). L4 of *Rodhocetus kasranii* yields a PC-II score intermediate between those of *R. domandaensis* and *M. inuus* (-0.466). L3 vertebrae of the basilosaurids *Dorudon atrox* and *Basilosaurus isis* have two of the most negative PC-II scores of all taxa in the dataset (*D. atrox*: -2.058; *B. isis*: -3.839). The L3 vertebra of the modern odontocete *Delphinus delphis* (short-beaked saddleback dolphin) exhibited one of the most positive PC-II

scores in the dataset (2.025), while the L3 vertebra of the modern mysticete *Balaenoptera acutorostrata* (common minke whale) possessed a PC-II score of 0.070.

INTERPRETATIONS

PC-I

The loadings of PC-I in each of the six PCAs are similar to the results of previous studies, in which PC-I represented overall size (e.g., Gingerich, 2003; Bebej, 2009). The 14 linear measurements contribute equally to the variance on PC-I, while the three angular measurements, with loadings closer to zero, contribute relatively little. This makes sense if PC-I represents size because all linear measurements should be correlated with overall size, while there should be no correlation between overall size and angles of vertebral processes. Regression of PC-I scores from the L1 analysis on ln-transformed body masses available for 23 of the 25 non-cetacean species (Smith et al., 2003) yields a coefficient of determination (r^2) of 0.849 and a significant regression coefficient (β) of 5.073 ($p < 10^{-9}$). This confirms that PC-I is a good indicator of size, separating lumbar vertebrae of smaller taxa (with negative scores) from lumbar vertebrae of larger taxa (with positive scores).

PC-II

PC-II contrasts taxa based primarily on centrum length, the anteroposterior length of the neural spine, and the craniocaudal and dorsoventral inclinations of the

transverse processes. Comparison of specimens with scores on opposite ends of PC-II sheds light on how this axis can be interpreted (Fig. 4.9).

The L1 vertebra of *Cephalophus zebra* (zebra duiker) has the most positive PC-II score in the L1 PCA (2.126). Its transverse processes extend straight laterally from the centrum at angles approaching 90° with respect to the midline. The L1 vertebra of *Acinonyx jubatus* (cheetah) has the most negative PC-II score (-2.497). Its transverse processes are angled cranially and ventrally at angles much less than 90° with respect to the midline. The horizontally-oriented transverse processes of *C. zebra* align the *m. iliocostalis* and *m. longissimus* in such a manner that maintains the structural integrity of the back, impeding flexion or extension of the lumbus (Zhou et al., 1992). In contrast, the cranioventrally-oriented transverse processes of *A. jubatus* provide increased leverage for these muscles to flex and extend the spine (Zhou et al., 1992).

The elongate neural spine of L1 in *Cephalophus zebra*, which also contributes to its positive PC-II score, provides osteological limits to extension. The anteroposteriorly shorter neural spine of L1 in *Acinonyx jubatus*, on the other hand, allows for much more angular displacement between adjacent vertebrae (Zhou et al., 1992; Buchholtz and Schur, 2004). In addition, the relatively short L1 centrum of *C. zebra* indicates a less flexible region of the spine (Zhou et al., 1992; Long et al., 1997; Buchholtz, 2001), while the greater relative length of the L1 centrum in *A. jubatus*, which contributes significantly to its negative PC-II score, indicates greater spinal mobility (Buchholtz, 1998, 2001). Thus, when the implications of all of these features are considered, PC-II

appears to separate vertebrae of more mobile spines (with negative scores) from vertebrae of more stable spines (with positive scores).

However, interpretation of PC-II in the LZ PCA may not be as straightforward. Interpretation of this axis as separating more mobile spines from more stable spines is complicated by the fact that the lumbosacral joint is one of the few locations in the vertebral columns of ungulates that allows for significant mobility (Slijper, 1946, 1947; Gál, 1993). This greater mobility is achieved, in part, by greater anterior inclination of the neural spine in the terminal lumbar vertebra of ungulates, allowing for a greater degree of extension at the lumbosacral joint than possible with a more vertical neural spine. This difference makes sense of why the anteroposterior angle of the neural spine is the most negative loading on PC-II in this analysis. It is possible that PC-II separates more mobile lumbosacral joints (with negative scores) from less mobile lumbosacral joints (with positive scores), but it should be understood that all of these joints are relatively mobile compared to other intervertebral joints in the lumbar region.

PC Scores of Non-Cetaceans

In the PCAs conducted here, the artiodactyls and perissodactyls tend to have the most positive PC-II scores, suggesting that they have the most stable lumbar spines. Analyses of their locomotion describe them as dorsostable runners (Alexander et al., 1977, 1985; Grand, 1997), thus corroborating this interpretation. *Madoqua kirkii* (Kirk's dik-dik) stands out from the other ungulates in the L1 and LZ PCAs because it has PC-II scores near or less than zero (e.g., L1: 0.089; LZ: -0.519), suggesting that it has a

comparatively more mobile anterior and posterior lumbar spine. This, too, is corroborated by the literature, as Grand (1997) describes the vertebral column of *M. kirkii* as being dorsomobile compared to other artiodactyls. The scores of most of the ungulates (excluding *M. kirkii*) changed little from L1 to LZ. This pattern is exemplified by *Cephalophus zebra* (Fig. 4.10), whose minimum PC-II score is at the LZ position, where its lumbar spine has the greatest mobility (Slijper, 1946, 1947; Gál, 1993).

Lepus californicus, phocids, felids, and canids tend to have the most negative PC-II scores, suggesting that they have the most mobile lumbar spines. Each of these taxa utilize movements of their lumbar columns during locomotion (Howell, 1944; Hildebrand, 1959; Tarasoff et al., 1972; Alexander et al., 1985; Fish et al., 1988; Grauer et al., 2000; Schilling and Carrier, 2010). In addition, biomechanical studies of intact lumbar spines of rabbits and seals have demonstrated that they take relatively little force to bend (Gál, 1993) , which is energetically favorable for a mammal that frequently bends its spine. Thus, functional studies of the vertebral columns of these mammals support the interpretation that they had mobile lumbar spines.

Felids and canids, exemplified by *Acinonyx jubatus* (cheetah) and *Canis lupus familiaris* (greyhound), exhibited contrasting patterns of change in their PC-II scores from L1 to LZ (Fig. 4.10). *A. jubatus* has lower PC-II scores in more anterior lumbar vertebrae, before a sharp increase at LZ, while *C. lupus familiaris* has higher PC-II scores anteriorly with much lower scores at LY and LZ. This pattern suggests that the most flexible area of the lumbar spine is located more anteriorly in felids than it is in canids. While this relationship has not been verified experimentally, this idea has been

supported by estimates of the force required to bend these spines based on the structure of intervertebral ligaments. The anterior lumbar vertebrae of felids appear to require less force to bend than the posterior lumbar vertebrae, indicating that the anterior lumbus is likely more mobile, while the opposite appears to be true in canids (A. R. Wood, unpublished data, personal communication).

Mustelids occupy the middle of the PC-II morphospace, with scores between -1.0 and 1.0 in most analyses. This result is surprising since both aquatic and non-aquatic mustelids seem to have flexible spines. Otters, in particular, utilize undulation of their lumbar, sacral, and caudal vertebrae during swimming (Tarasoff et al., 1972; Williams, 1989; Fish, 1994), yet their PC-II scores were significantly greater than many of the other dorsomobile mammals. It is possible that in a larger dataset representing a wider range of mammalian lifestyles, including more generalized forms, otters could shift downward (more negative) in the PC-II morphospace.

But an alternative explanation is that the range of motion at lumbar joints in otters is indeed less than in the other dorsomobile mammals studied here. This is suggested by the lumbar vertebrae of *Aonyx cinerea* (Oriental small-clawed otter) and *Pteronura brasiliensis* (giant otter), the otters with the greatest PC-II scores. Their lumbar vertebrae possess relatively short transverse processes that project little cranially or ventrally, suggesting decreased leverage for the epaxial muscles that flex and extend the spine. If this is true, it suggests that the lumbar regions of otters may not play as large of a role as the anterior caudal region in undulatory movements,

though this has never been quantified. In either case, further study is necessary to clarify the otters' placement on PC-II.

PC Scores of Cetaceans

The archaeocete cetaceans studied in these analyses exhibit a wide range of PC-II scores. Following the interpretation that more stable lumbar spines yield greater PC-II scores, *Remingtonocetus domandaensis* has the most stable (or least mobile) lumbar column of the archaeocete taxa included here, with a mean PC-II score of 0.567. In the L1 and LZ PCAs, its PC-II scores fall within the lower part of the range occupied by artiodactyls. At other positions, however, its PC-II scores are lower, falling within the range occupied by mustelids. Thus, while its lumbar spine does not appear as immobile as those of ungulates, it is definitely the least mobile of the early archaeocetes studied here. This is consistent with the interpretation of the lumbar vertebrae of *R. domandaensis* described in the previous chapter.

The protocetids *Rodhocetus kasranii*, *Maiacetus inuus*, *Qaisracetus arifi*, and GSP-UM 3357 appear to have comparatively mobile lumbar regions. *R. kasranii* has a greater PC-II score (-0.466) in the LX PCA than *M. inuus* (-0.904) or *Q. arifi* (-2.492), suggesting that it had the least mobile lumbar region of the three. Buchholtz (1998) interpreted *R. kasranii* as undulating its spine during swimming, but at the time, little of the appendicular skeleton was known. Recovery of hind limbs in the slightly smaller *Rodhocetus balochistanensis* demonstrated that the feet of *Rodhocetus* were elongated (Gingerich et al., 2001b), and Gingerich (2003) interpreted a composite skeleton of

Rodhocetus as a highly specialized, hind limb-dominated swimmer. Its unfused sacrum (Gingerich et al., 1994) suggests that *R. kasranii* undulated its vertebral column to some degree during locomotion, but given that its centrum lengths peak in the posterior sacral vertebrae (Buchholtz, 1998), it is likely that its undulatory peak occurred in the sacral or caudal regions rather than in the lumbus. Thus, it is possible that it utilized dorsoventral undulation during swimming to a greater degree than evident from study of its lumbar region alone.

The mean PC-II score of *Maiacetus inuus* is -0.527, implying that it possessed a slightly more flexible lumbus than *Rodhocetus kasranii*. Because it possessed a sacrum composed of four fused vertebrae, however, it likely could not have incorporated the lumbus, sacrum, and anterior tail into a single undulatory unit during swimming. Gingerich et al. (2009) suggested that *M. inuus* was a less specialized foot-powered swimmer than *Rodhocetus* and demonstrated that it is similar in postcranial proportions to *Pteronura brasiliensis* (giant otter). Modern otters couple flexion and extension of the lumbus with pelvic paddling to increase the length of their power stroke during swimming (Tarasoff et al., 1972; Williams, 1989; Fish, 1994), and *M. inuus* may have used this technique. Because the results of the PCAs suggest that the lumbus of *M. inuus* was comparatively more flexible than the lumbar spines of otters, it may have potentially used this technique to even greater effect.

Protocetid GSP-UM 3357 (-1.122) and *Qaisracetus arifi* (-1.081) have the lowest average PC-II scores of all the protocetids studied here, typically plotting within or below the morphospace occupied by phocids. This implies a very mobile lumbar spine.

Q. arifi has a unique sacral morphology, with S1 and S2 fused, a free S3, and a "partially caudalized" S4 (Gingerich et al., 2001a). This raises the possibility that *Q. arifi* had a greater capacity for smooth undulation across its trunk and tail than *Maiacetus inuus*, suggesting that undulation played a more dominant role in its swimming. The only hind limb element known for *Q. arifi* is a left innominate, making it difficult to speculate about the relative contribution of its limbs during aquatic locomotion. But it is clear that the lumbus of *Q. arifi* appears more flexible than the lumbar regions of *Rodhocetus kasranii* and *M. inuus*.

All six lumbar vertebrae of *Remingtonocetus domandaensis*, *Maiacetus inuus*, and *Qaisracetus arifi* were analyzed here. Each taxon displays the same pattern of change in PC-II score from L1 to LZ. Their greatest PC-II scores occur at the L1 and LZ positions (Fig. 4.10), a pattern most similar to that of *Acinonyx jubatus*. This suggests that the area of greatest flexibility in the lumbar spines of these taxa is the middle lumbus. It is interesting to speculate whether or not this pattern would also be exhibited by *Rodhocetus kasranii*. All six lumbar vertebrae are known for this taxon; however, five of them were unable to be included here due to post-mortem deformation affecting the accuracy of most measurements. Given its sacral morphology and the hypothesis that its undulatory peak may have been located more posteriorly, it may have had its lowest PC-II scores in more posterior lumbar vertebrae compared to the protocetids studied here. Recovery of an undeformed lumbar region of *R. kasranii* is necessary to test this hypothesis.

The basilosaurids *Dorudon atrox* and *Basilosaurus isis* were included in the L3 PCA in order to demonstrate where fully aquatic archaeocetes would plot in this morphospace. Both taxa possess strongly negative PC-II scores, indicating that they had highly mobile lumbar spines. Because all basilosaurids have reduced hind limbs and reduced forelimb mobility (Uhen, 1998), they must rely exclusively on their axial skeletons for generating propulsion during locomotion. Centrum dimensions of terminal caudal vertebrae indicate that several basilosaurids possessed tail flukes like modern cetaceans (Gingerich et al., 1990; Buchholtz, 1998, 2001; Uhen, 2004), suggesting that some form of caudally-propelled swimming had already evolved by the late Eocene. However, because most taxa lack a well-defined peduncle anterior to the fluke, it is likely that undulations of the body axis played a more prominent role in generating forward thrust during swimming than rapid oscillation of a fluke (Buchholtz, 2001).

This is especially true for *Basilosaurus isis*. The L3 vertebra of *B. isis* yields the most negative PC-II score (-3.839) of any of the six analyses, due primarily to its extreme elongation. It, too, possessed a small tail fluke, but given the size of the fluke relative to the length of the animal, it likely contributed very little to thrust production during locomotion (Buchholtz, 1998). This animal clearly utilized sinusoidal undulations of its long, serpentine body to swim, though whether these undulations occurred primarily in the dorsoventral (Buchholtz, 1998, 2001) or lateral (Gingerich et al., 1997; Gingerich, 1998) planes has yet to be resolved.

The modern cetaceans *Balaenoptera acutorostrata* (common minke whale) and *Delphinus delphis* (short-beaked saddleback dolphin) were also included in the L3 PCA in order to demonstrate where two representative modern cetaceans would plot in this morphospace. These taxa represent two different patterns of swimming. *B. acutorostrata* and other mysticetes retain a moderately flexible torso, undulating nearly all of the spine posterior to the thorax during swimming (Buchholtz, 2001). The anterior lumbar vertebrae are incorporated into the undulatory unit, but the degree of sagittal excursion at intervertebral joints is limited by reduction of relative centrum length. Instead, flexibility is achieved by higher vertebral counts (Buchholtz, 2001). The intermediate PC-II score (0.070) yielded by L3 of *B. acutorostrata* is consistent with these observations.

Delphinus delphis is like most delphinids and phocoenids in having a very rigid anterior torso. Propulsive movements in most modern dolphins are restricted to the posterior third of the body (Fish and Hui, 1991; Fish, 1993; Pabst, 1993, 2000; Fish et al., 2003), with motion limited to the synclinal point anterior to the tail stock and the caudal peduncle anterior to the fluke (Buchholtz and Schur, 2004; Buchholtz et al., 2005). The lumbar and anterior caudal vertebrae are marked by high intervertebral joint stiffness (Slijper, 1946; Long et al., 1997; Fish, 2002) and serve as a rigid origination for epaxial muscles acting on the tailstock (Pabst, 2000). Thus, the L3 vertebra of *D. delphis* is expected to have a relatively high PC-II score. Its score of 2.025 is greater than the scores of all but two ungulates, indicating that it came from a very immobile region of

the spine. This is fully consistent with what is known about the biomechanics of the lumbar vertebrae in modern delphinids.

DISCUSSION

Evolution of Lumbar Mobility in Archaeocetes

The PCAs conducted here represent a quantitative comparison of lumbar morphology in mammals with very different biomechanics, providing insight into vertebral function in fossils with no clear modern analogues. The loadings of PC-II in these analyses indicate that the anteroposterior lengths of the centrum and neural spine and the craniocaudal and dorsoventral angles of the transverse processes are strongly indicative of the functional movements of the lumbar column. This information can provide a sound rationale for interpreting the function of the lumbar region in taxa not explicitly studied here, including specimens that are disarticulated or incomplete. Lumbar vertebrae have been recovered for several other early archaeocetes that I was unable to access and measure for this study. Despite this, the results of the PCAs performed here offer insight into how the vertebral biomechanics of these taxa should be interpreted.

Lumbar vertebrae have been attributed to three pakicetid taxa: *Pakicetus attocki*, *Ichthyolestes pinfoldi*, and *Nalacetus ratimitus*. Thewissen et al. (2001) characterized pakicetids as having highly immobile lumbar spines, while Madar (2007) described the lumbar region of pakicetids as powerful, yet stable, suggesting that the lumbar, sacral, and caudal vertebrae were consistent with undulation of the spine

during locomotion. The revolute zygapophyses of the lumbar vertebrae argue against the latter interpretation, as do the transverse processes, which project laterally from the centra with very little cranial or ventral inclination, and the neural spines, which are anteroposteriorly long (Madar, 2007, Fig. 2, p. 182). These features are most consistent with an animal that had a rigid lumbar spine, and it is unlikely that any of these pakicetids undulated their lumbar vertebrae during locomotion.

Ambulocetus natans was initially reconstructed as having a mobile lumbar spine that it flexed and extended during swimming (Thewissen et al., 1994, 1996; Thewissen and Fish, 1997), but at the time, only one lumbar vertebra was known. Additional elements discovered in a subsequent excavation led Madar et al. (2002) to interpret *A. natans* as possessing a powerful lumbar spine that it undulated during locomotion. In many ways, the lumbar vertebrae of *A. natans* are very similar to those of *Remingtonocetus domandaensis* (Madar et al., 2002, Fig. 3, p. 410). Anterior lumbar vertebrae have relatively short transverse processes that project straight laterally from the centrum, while more posterior lumbar vertebrae have larger transverse processes angled cranioventrally. Zygapophyses are curved, but not quite revolute, and neural spines are anteroposteriorly long, providing osteological limits to extension. Compared to pakicetids, *A. natans* likely had a more mobile lumbar spine, but given its similarity to *R. domandaensis*, it was likely less mobile than all later archaeocetes.

The protocetid *Georgiacetus vogtlensis* is among the most derived protocetids (Uhen, 2004, 2008) and has been interpreted as utilizing primarily its axial skeleton for aquatic propulsion (Buchholtz, 1998; Hulbert, 1998; Hulbert et al., 1998; Uhen, 2008). It

has been reconstructed as possessing eight lumbar vertebrae, though only six were recovered with the holotype GSM 350 (Hulbert, 1998; Hulbert et al., 1998). Anterior lumbar vertebrae are marked by curved zygapophyses and cranioventrally-angled transverse processes, while posterior lumbar vertebrae possess flatter zygapophyses and transverse processes with a strong ventral and slight cranial inclination (Hulbert, 1998, Figs. 5-8, pp. 247-252). Relative centrum length increases in more posterior lumbar vertebrae, while anteroposterior length of the neural spine appears to decrease. These features are all consistent with a lumbar spine more mobile than those of the protocetids studied here. Given the lack of fusion in the sacral vertebrae and the decoupling of the pelvis and the sacrum (Hulbert, 1998; Hulbert et al., 1998), *G. vogtlensis* likely had a highly flexible spine that it undulated during aquatic locomotion.

When these interpretations are combined with the results of the PCAs performed here, a very interesting picture of lumbar evolution in early cetaceans emerges. The earliest whales (Pakicetidae) possessed relatively inflexible lumbar spines like those of their artiodactyl ancestors. Later semiaquatic archaeocetes that still retained functional hind limbs (Ambulocetidae, Remingtonocetidae, and some Protocetidae) exhibited a modest increase in lumbar mobility, likely to increase the length of the power stroke during pelvic paddling. Reduction of the sacrum (in later Protocetidae and Basilosauridae) allowed functional continuity to be achieved across lumbar, sacral, and anterior caudal vertebrae, enabling these regions to be incorporated into a single, flexible undulatory unit and signaling a reduction in the contribution of the hind limbs to generating propulsion.

Like fully aquatic archaeocetes, modern cetaceans use solely their axial skeletons to generate thrust; however, they have further modified the biomechanics of the vertebral column in ways to increase energetic and propulsive efficiency. Motion in most extant cetaceans is restricted to the middle and posterior caudal vertebrae. While there is some motion in the lumbar spine of certain species, this region serves primarily as a stable anchor point for the attachment of epaxial muscles that flex and extend the tailstock. In a way, this highly rigid lumbar region is reminiscent of the condition in the earliest whales, but it is achieved in a completely different way and for a completely different purpose.

Lumbar rigidity in artiodactyls and early cetaceans is achieved through revolute zygapophyses, anteroposteriorly-expanded neural spines, and alignment of epaxial musculature to promote a rheostatic function. Modern cetaceans typically lack zygapophyses, but instead possess elevated metapophyses that can overlap with the neural spines of adjacent vertebrae to restrict movement (Long et al., 1997; Buchholtz and Schur, 2004). In addition, their high vertebral counts and foreshortened centra (Buchholtz, 2001) give them a stable spinal configuration with the potential for elastic energy storage due to an increased proportion of intervertebral disc to bone (Buchholtz, 2007). Thus, while both early cetaceans and modern cetaceans share mostly inflexible lumbar regions, those of the earliest cetaceans were holdovers from ancestors adapted for efficient terrestrial locomotion, while those of modern species are an adaptation related to a derived and efficient mode of aquatic locomotion.

When exactly in cetacean history the lumbar region began to "re-stabilize" is currently not clear. The locomotor modes of early neocete cetaceans have not been studied, but given the variety of swimming modes utilized by modern cetaceans (Buchholtz, 2001), it is likely that the lumbar region was modified in different ways and at different times in different lineages. Further investigation is needed to clarify the transition from primarily undulatory swimming modes to primarily oscillatory swimming modes in the crown-group radiation of cetaceans.

Conclusions

The PCAs conducted here successfully differentiate the lumbar spines of modern mammals based on relative mobility, providing a quantitative context in which to interpret the lumbar columns of early cetaceans. Based on PC-II scores, *Remingtonocetus domandaensis* had the least mobile lumbar spine of the archaeocetes studied here. Early protocetids, including *Rodhocetus balochistanensis*, *Maiacetus inuus*, and *Qaisracetus arifi*, possessed increasingly mobile lumbar spines. The basilosaurids *Dorudon atrox* and *Basilosaurus isis* had the most mobile lumbar spines of any of the taxa analyzed here. The modern cetaceans *Balaenoptera acutorostrata* and *Delphinus delphis* had less mobile lumbar spines than fully aquatic archaeocetes, with that of *D. delphis* appearing especially rigid.

These results suggest that the evolution of the lumbar spine in cetaceans was marked by an increase in mobility early on, followed by a later decrease in mobility. The lumbar spines of the earliest whales appear to have been relatively stable, with a

significant increase in mobility not evident until early protocetids. Fully aquatic basilosaurids possessed the most mobile lumbar spines of any archaeocetes, which they undulated with sacral and caudal vertebrae to generate propulsion during swimming. However, as locomotion became increasingly refined in later cetaceans, this lumbar mobility was largely lost, with the vertebral region of most mobility displaced to the middle and posterior caudal vertebrae.

The methods employed here provide justification for functional interpretations of the vertebral column in fossil taxa by quantitatively comparing their morphologies with those of modern forms. While these methods certainly yield helpful insights into vertebral function, they do not deal directly with the actual mechanics of the spine. In the following chapter, I attempt to do just that, utilizing three-dimensional rigid body modeling to compare the estimated ranges of motion at the L4-L5 joints of *Remingtonocetus domandaensis* and *Maiacetus inuus*. This novel approach provides a further test of the functional hypotheses described here and in the previous chapter, while also providing a method for quantifying how much motion might have been possible at intervertebral joints of fossil taxa.

Figure 4.1. Schematic of 14 linear and three angular measurements superimposed on the L1 vertebra of a saluki (*Canis lupus familiaris*). Measurements are described in detail in the text. Measurement abbreviations are used throughout subsequent figures and tables.

Key/Abbreviations

1. CL	ventral centrum length
2. CWa	anterior centrum width
3. CHa	anterior centrum height
4. CWp	posterior centrum width
5. CHp	posterior centrum height
6. NCW	neural canal width
7. NCH	neural canal height
8. NSH	neural spine height
9. NSL	neural spine length
10. PreW	prezygapophyses width
11. PosW	postzygapophyses width
12. PedW	pedicle width
13. PedL	pedicle length
14. MaxW	maximum width
15. APAngNS	anteroposterior angle of neural spine
16. CCAngTP	craniocaudal angle of transverse processes
17. DVAngTP	dorsoventral angle of transverse processes

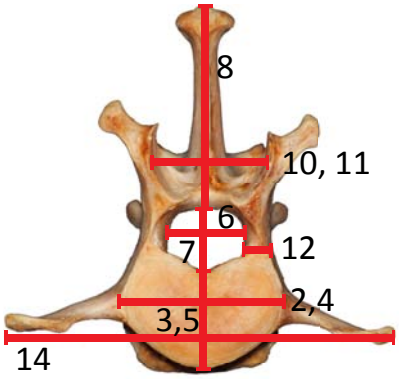

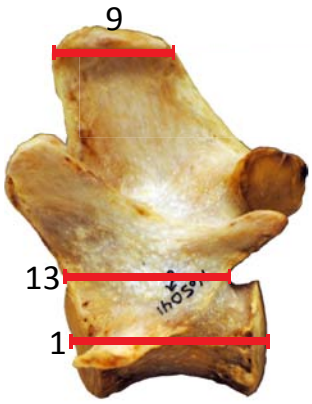

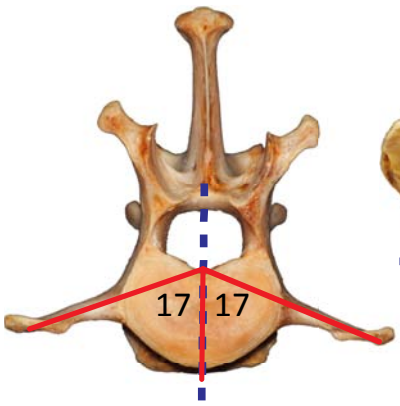

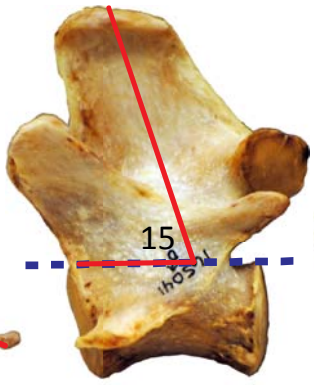

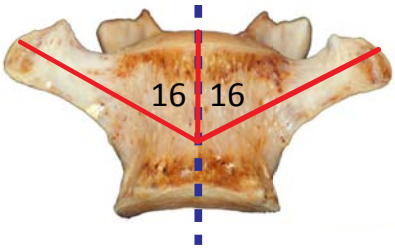

Figure 4.2. Eigenvalues for all six PCAs. Note the similarity in the structure of the variance for each analysis. In each PCA, PC-I encompassed 75-80% of the variance, while PC-II included 10-15%. Remaining PCs accounted for negligible amounts of the overall variance.

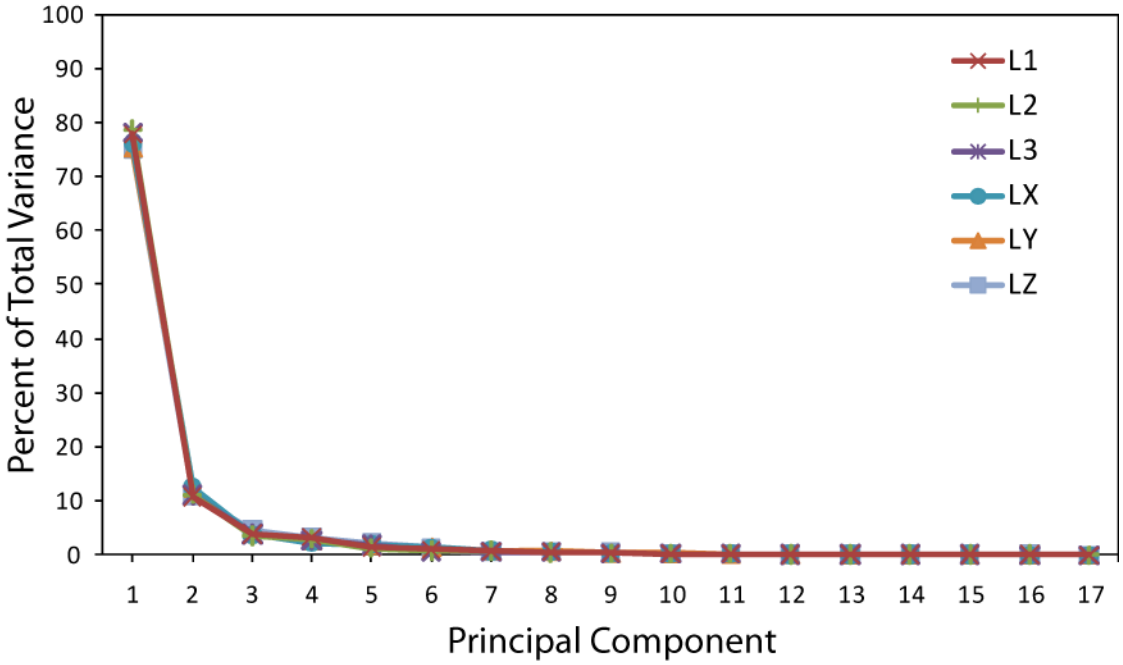

Figure 4.3. Scores and loadings of PCs I and II in the L1 PCA. PC-II scores are plotted against PC-I scores for each taxon. Symbols indicate the family of each species (left), abbreviations of select taxa follow Table 4.1, and abbreviations of measurement loadings follow Figure 4.1. PC-I is interpreted as a size axis, separating smaller taxa (with negative scores) from larger taxa (with positive scores). PC-II is interpreted as separating dorsomobile taxa (with negative scores) from dorsostable taxa (with positive scores). Note the relative placements of the four archaeocete taxa.

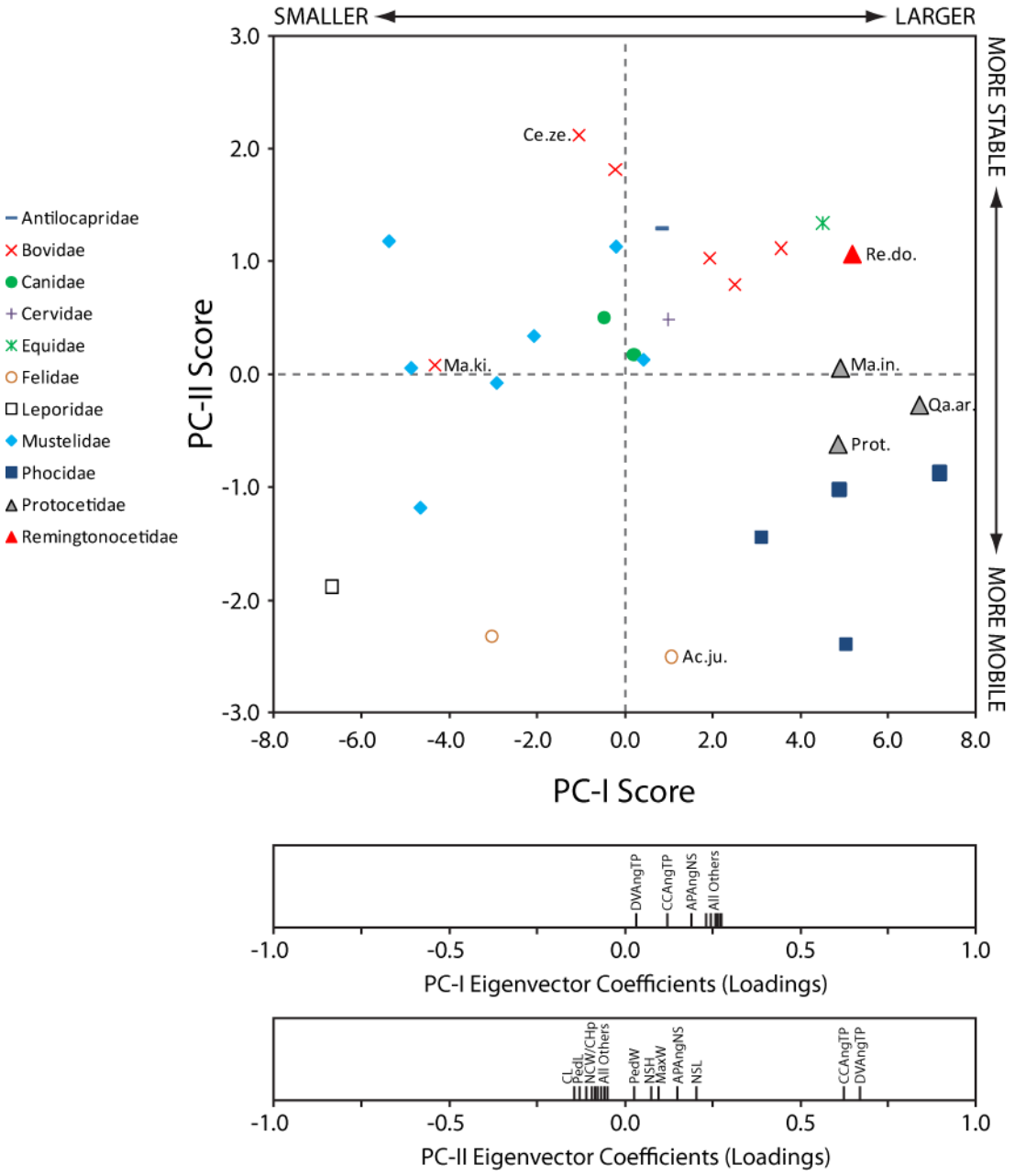

Figure 4.4. Scores and loadings of PCs I and II in the L2 PCA. PC-II scores are plotted against PC-I scores for each taxon. Symbols indicate the family of each species (left), abbreviations of select taxa follow Table 4.1, and abbreviations of measurement loadings follow Figure 4.1. PC-I is interpreted as a size axis, separating smaller taxa (with negative scores) from larger taxa (with positive scores). PC-II is interpreted as separating dorsomobile taxa (with negative scores) from dorsostable taxa (with positive scores). Note the relative placements of the four archaeocete taxa.

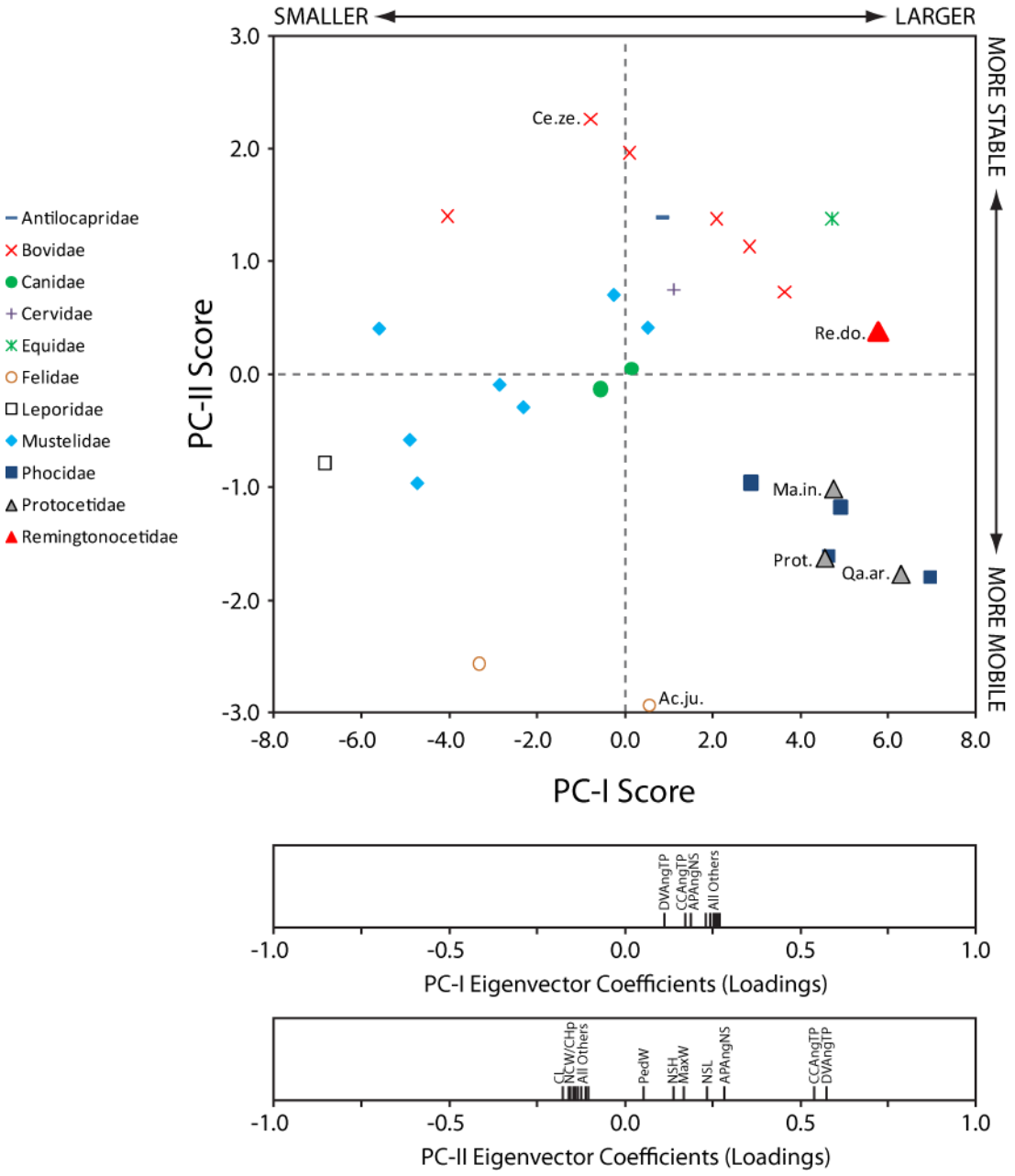

Figure 4.5. Scores and loadings of PCs I and II in the L3 PCA. PC-II scores are plotted against PC-I scores for each taxon. Symbols indicate the family of each species (left), abbreviations of select taxa follow Table 4.1, and abbreviations of measurement loadings follow Figure 4.1. PC-I is interpreted as a size axis, separating smaller taxa (with negative scores) from larger taxa (with positive scores). PC-II is interpreted as separating dorsomobile taxa (with negative scores) from dorsostable taxa (with positive scores). Note placement of the seven cetacean taxa. Also note that the scales of the axes are different from other figures, in order to accommodate the PC scores of *Balaenoptera acutorostrata* and *Basilosaurus isis*.

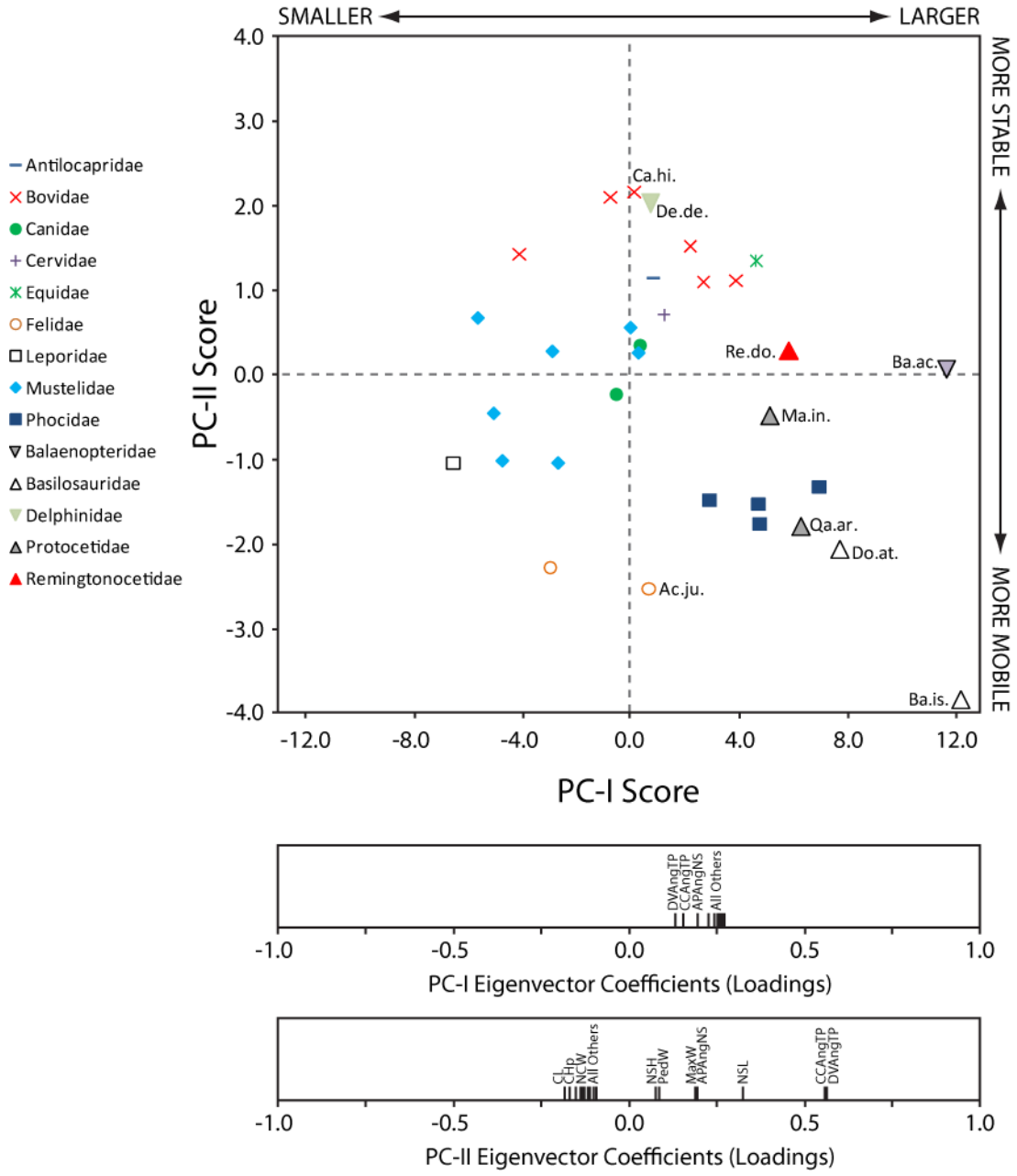

Figure 4.6. Scores and loadings of PCs I and II in the LX PCA. PC-II scores are plotted against PC-I scores for each taxon. Symbols indicate the family of each species (left), abbreviations of select taxa follow Table 4.1, and abbreviations of measurement loadings follow Figure 4.1. PC-I is interpreted as a size axis, separating smaller taxa (with negative scores) from larger taxa (with positive scores). PC-II is interpreted as separating dorsomobile taxa (with negative scores) from dorsostable taxa (with positive scores). Note the relative placements of the four archaeocete taxa.

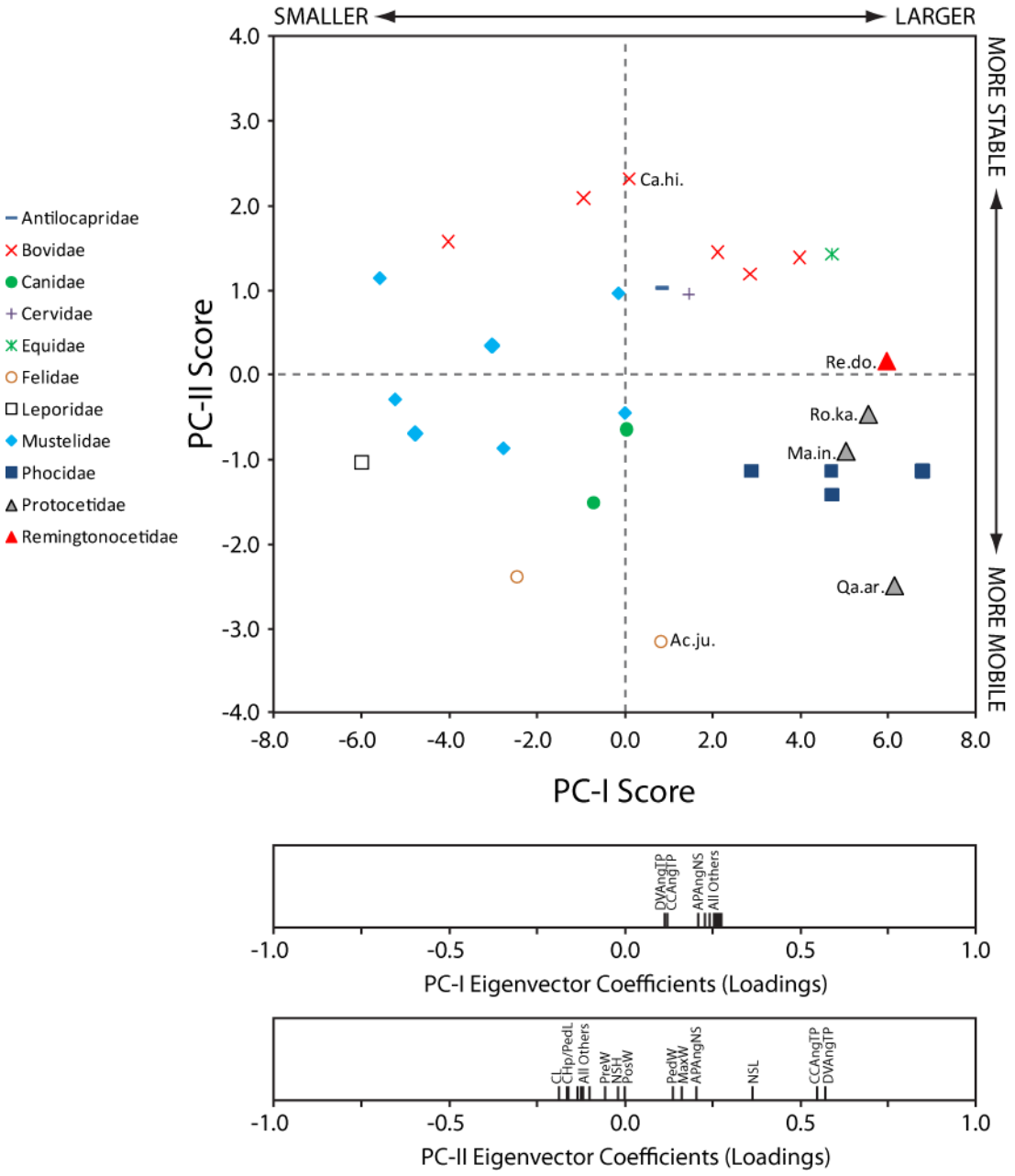

Figure 4.7. Scores and loadings of PCs I and II in the LY PCA. PC-II scores are plotted against PC-I scores for each taxon. Symbols indicate the family of each species (left), abbreviations of select taxa follow Table 4.1, and abbreviations of measurement loadings follow Figure 4.1. PC-I is interpreted as a size axis, separating smaller taxa (with negative scores) from larger taxa (with positive scores). PC-II is interpreted as separating dorsomobile taxa (with negative scores) from dorsostable taxa (with positive scores). Note the relative placements of the three archaeocete taxa.

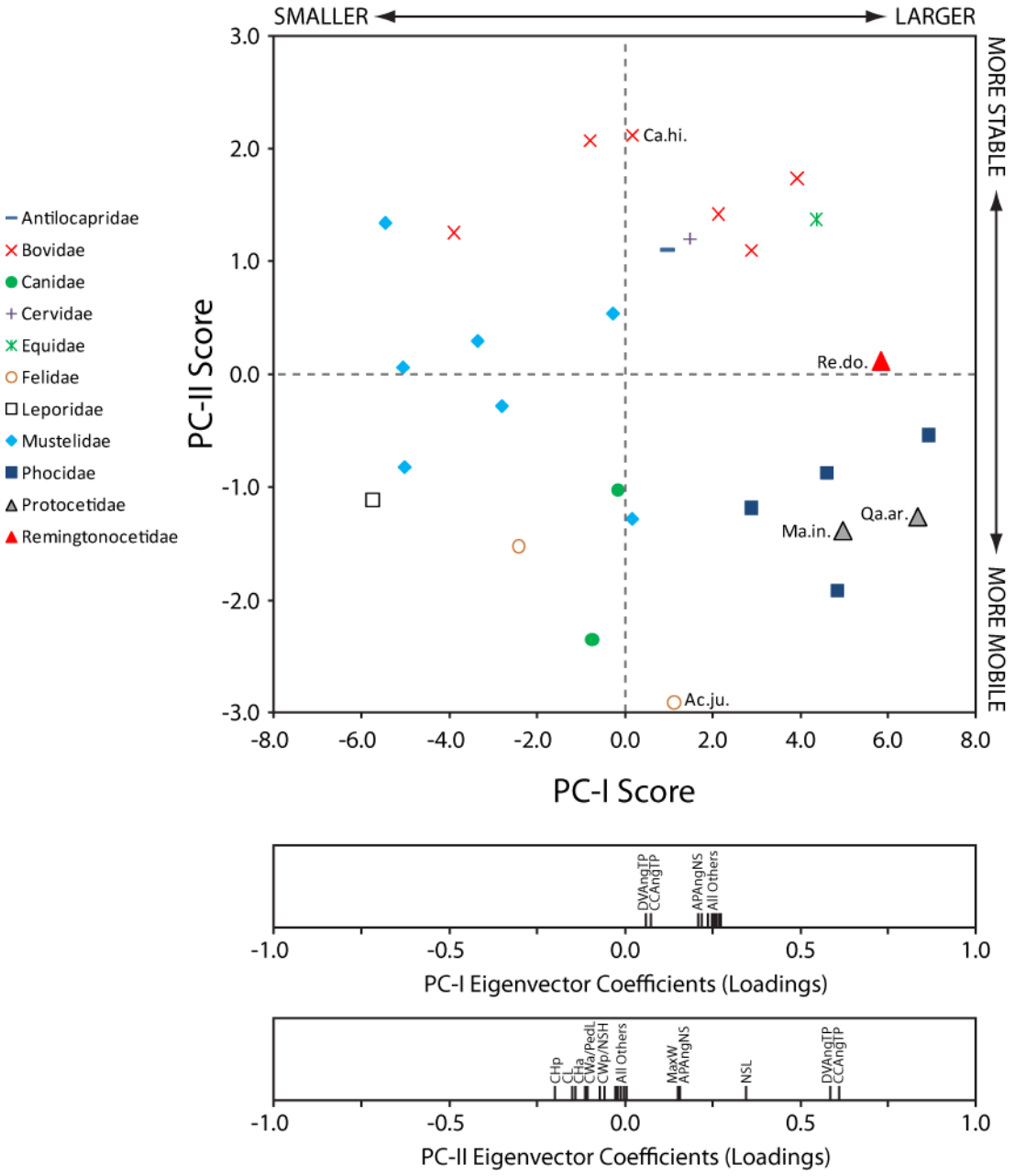

Figure 4.8. Scores and loadings of PCs I and II in the LZ PCA. PC-II scores are plotted against PC-I scores for each taxon. Symbols indicate the family of each species (left), abbreviations of select taxa follow Table 4.1, and abbreviations of measurement loadings follow Figure 4.1. PC-I is interpreted as a size axis, separating smaller taxa (with negative scores) from larger taxa (with positive scores). PC-II is interpreted as separating dorsomobile taxa (with negative scores) from dorsostable taxa (with positive scores), though this interpretation is more complicated than for the other PCAs (see the text for details). Note the relative placements of the four archaeocete taxa and the different spread of data points compared to the other PCAs.

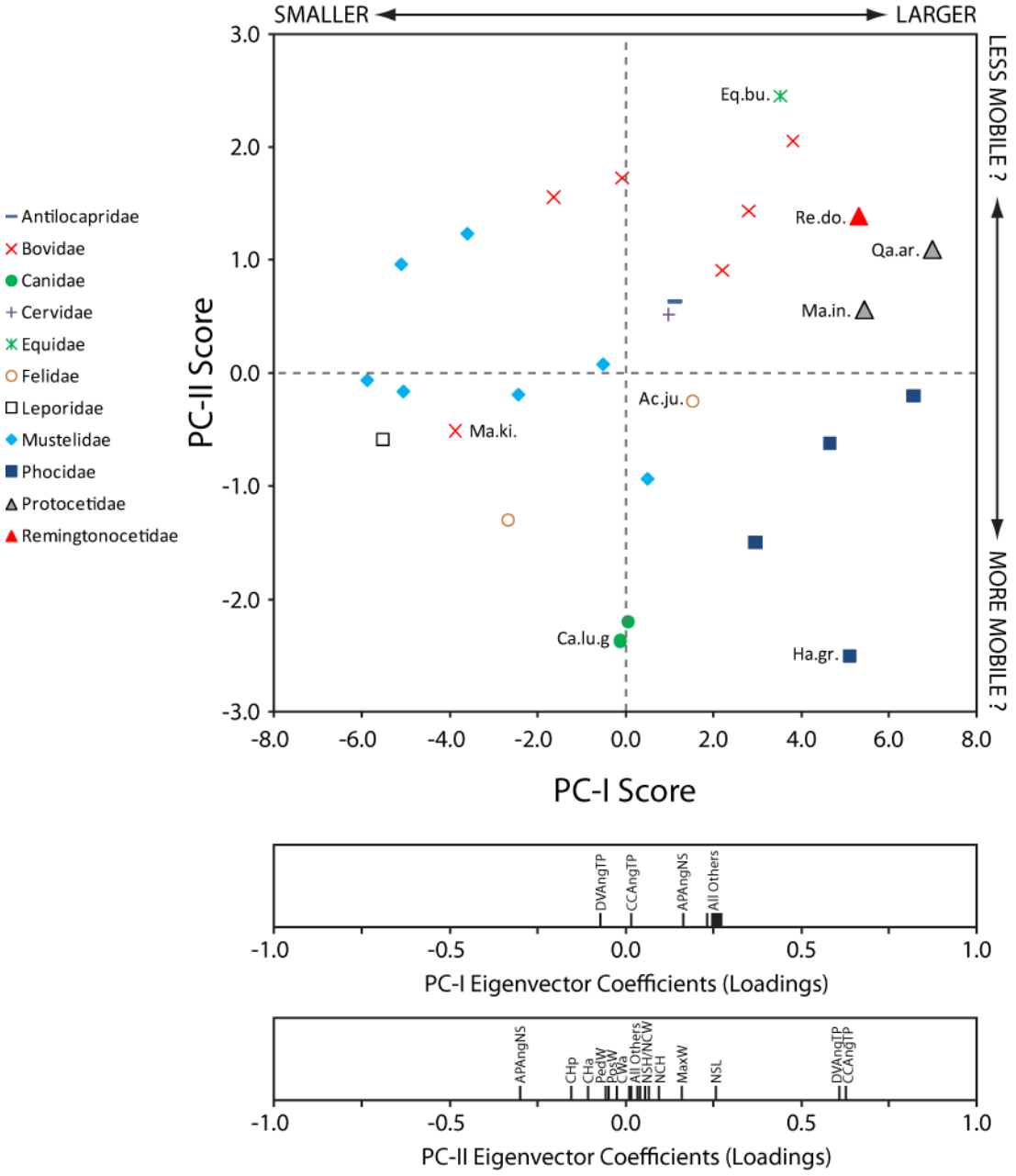

Figure 4.9. L1 vertebrae of the zebra duiker (*Cephalophus zebra*) and cheetah (*Acinonyx jubatus*). A. The L1 vertebra of *C. zebra* had the most positive PC-II score; it is marked by transverse processes that project straight laterally, with very little cranial or ventral inclination, and an anteroposteriorly long neural spine. B. The L1 vertebra of *A. jubatus* had the most negative PC-II score; it is marked by a long centrum, an anteroposteriorly shorter neural spine, and transverse processes that project cranioventrally from the centrum.

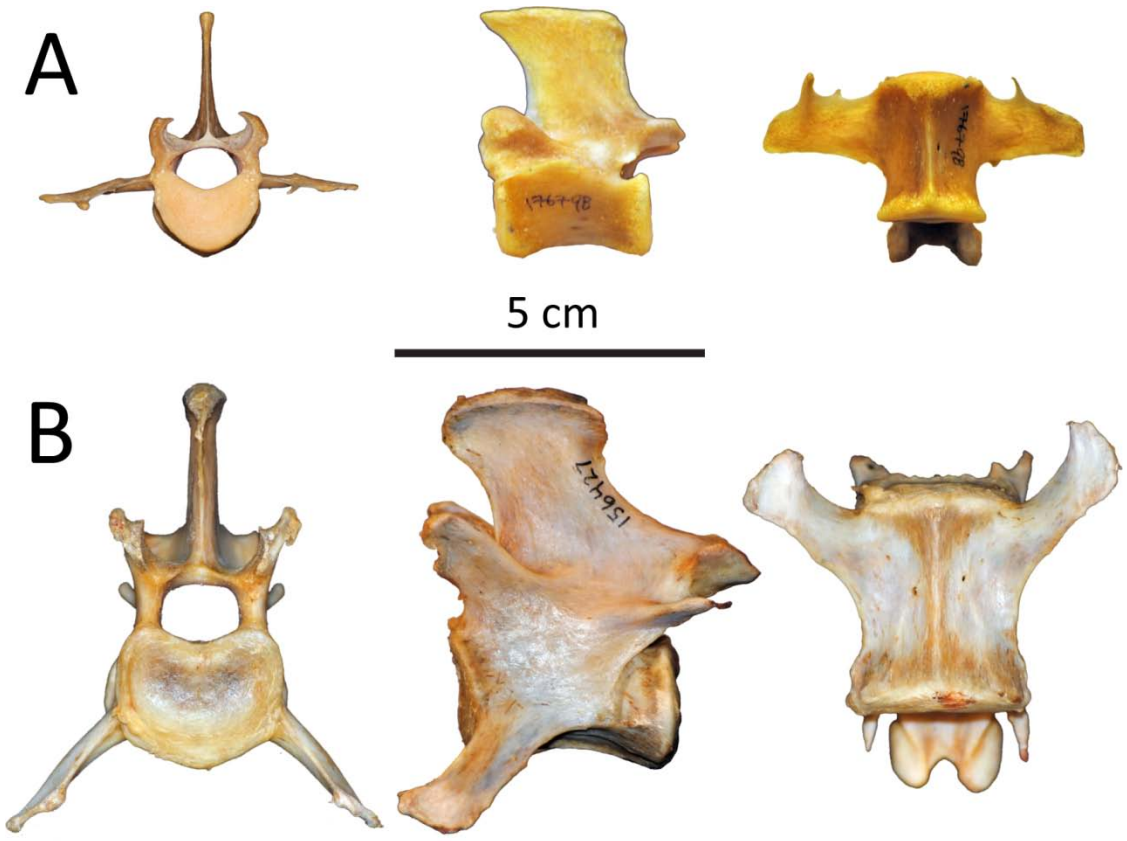

Figure 4.10. PC-II scores by vertebral position for select taxa. The zebra duiker (Ce.ze.) displays the pattern exhibited by most dorsostable mammals. The greyhound (Ca.lu.g) and cheetah (Ac.ju.) exhibit contrasting patterns for dorsomobile mammals. The three archaeocete taxa *Remingtonocetus domandaensis* (Re.do.), *Maiacetus inuus* (Ma.in.), and *Qaisracetus arifi* (Qa.ar.) display a pattern from L1 to LZ that is similar to that of the cheetah, but their scores are markedly greater.

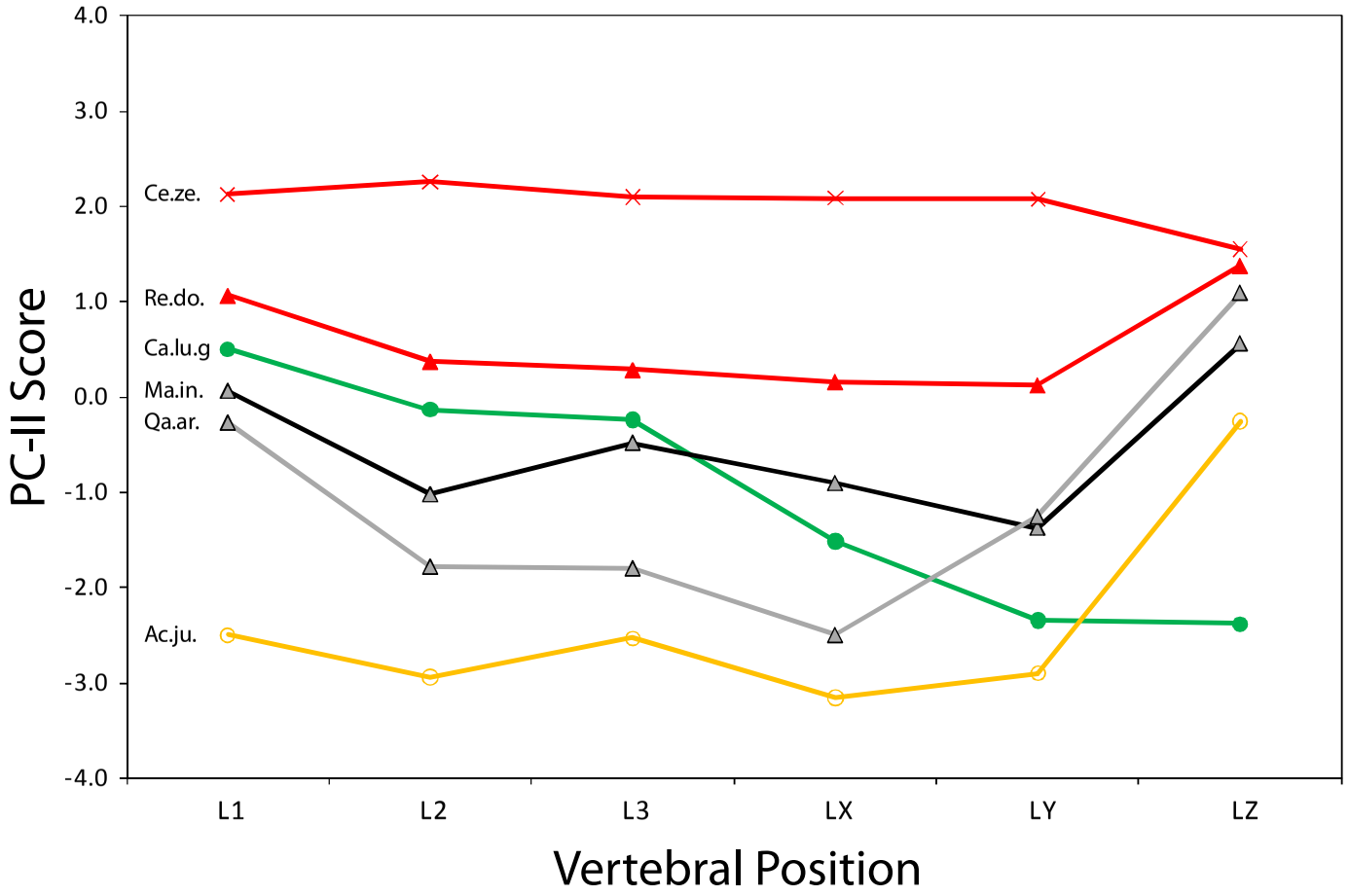

Table 4.1. Taxa and specimens used in PCAs of lumbar vertebrae. Abbreviations are utilized throughout subsequent figures and tables. The dagger (†) indicates extinct taxa.

Species	Abbrev.	Family	Specimen Number
Non-Cetacea			
Antilocapra americana	An.am.	Antilocapridae	UMMZ 65026
Capra hircus	Ca.hi.	Bovidae	USNM A00720
Cephalophus zebra	Ce.ze.	Bovidae	UMMZ 176798
Gazella granti	Ga.gr.	Bovidae	USNM 163083
Hippotragus niger	Hi.ni.	Bovidae	USNM 218780
Madoqua kirkii	Ma.ki.	Bovidae	USNM 538106
Ovis canadensis	Ov.ca.	Bovidae	UMMZ 102446
Canis lupus familiaris (greyhound)	Ca.lu.g	Canidae	USNM A25880
Canis lupus familiaris (saluki)	Ca.lu.s	Canidae	UMMZ 165041
Odocoileus virginianus	Od.vi.	Cervidae	UMMZ 64097
Equus burchellii	Eq.bu.	Equidae	USNM 162960
Acinonyx jubatus	Ac.ju.	Felidae	UMMZ 156427
Lynx rufus	Ly.ru.	Felidae	UMMZ 157265
Lepus californicus	Le.ca.	Leporidae	UMMZ 54480
Aonyx cinerea	Ao.ci.	Mustelidae	USNM 396645
Enhydra lutris	En.lu.	Mustelidae	UMMZ 156623
Gulo gulo	Gu.gu.	Mustelidae	UMMZ 98108
Lontra canadensis	Lo.ca.	Mustelidae	UMMZ 84058
Lontra felina	Lo.fe.	Mustelidae	USNM 512791
Martes pennanti	Ma.pe.	Mustelidae	UMMZ 100796
Pteronura brasiliensis	Pt.br.	Mustelidae	USNM 304663
Halichoerus grypus	Ha.gr.	Phocidae	USNM 504481
Hydrurga leptonyx	Hy.le.	Phocidae	USNM 396931
Monachus schauinslandi	Mo.sc.	Phocidae	USNM 395996
Phoca vitulina	Ph.vi.	Phocidae	USNM 504526
Cetacea			
Balaenoptera acutorostrata	Ba.ac.	Balaenopteridae	UMMZ 176885
Basilosaurus isis †	Ba.is.	Basilosauridae	WH 074
Dorudon atrox †	Do.at.	Basilosauridae	WH 210
Delphinus delphis	De.de.	Delphinidae	UMMZ 177437
Maiacetus inuus †	Ma.in.	Protocetidae	GSP-UM 3551
Protocetid GSP-UM 3357†	Prot.	Protocetidae	GSP-UM 3357
Qaisracetus arifi †	Qa.ar.	Protocetidae	GSP-UM 3410
Rodhocetus kasranii †	Ro.ka.	Protocetidae	GSP-UM 3012
Remingtonocetus domandaensis †	Re.do.	Remingtonocetidae	GSP-UM 3552

Table 4.2. Seventeen L1 measurements of 25 non-cetaceans and four cetaceans. Species abbreviations follow Table 4.1. Measurement abbreviations follow Figure 4.1. Linear measurements are in mm; angular measurements are in degrees. Asterisks (*) indicate estimates.

Species	Family	CL	CWa	CHa	CWp	CHp	NCW	NCH	NSH	NSL	PreW	PosW	PedW	PedL	MaxW	APAngNS	CCAngTP	DVAngTP
An.am.	Antilocapridae	31.69	20.88	15.71	21.87	15.17	12.44	9.35	37.00	29.94	16.93	17.76	2.72	23.55	99.71	88.55	75.77	74.84
Ca.hi.	Bovidae	27.46	19.56	12.68	20.03	12.36	11.72	7.88	17.54	*23.00	15.37	15.48	3.55	20.57	66.43	90.79	79.79	84.94
Ce.ze.	Bovidae	23.87	16.75	9.65	17.54	9.62	11.00	7.11	21.48	21.64	14.45	14.87	2.82	19.22	51.40	81.21	83.98	86.75
Ga.gr.	Bovidae	34.50	24.63	19.66	25.32	20.04	15.47	9.85	44.59	36.54	19.02	19.51	4.79	26.49	114.38	78.53	72.31	76.18
Hi.ni.	Bovidae	45.85	31.98	25.59	34.82	26.03	19.18	14.27	42.74	27.96	*25.80	25.90	8.06	29.80	113.18	88.53	77.75	85.32
Ma.ki.	Bovidae	16.42	10.74	5.93	10.52	6.25	7.79	5.87	14.69	14.75	8.86	9.37	1.00	12.60	37.42	82.68	56.12	55.55
Ov.ca.	Bovidae	39.21	30.99	20.96	32.44	20.32	13.89	10.01	45.49	33.74	21.75	21.90	6.65	30.35	105.54	77.45	67.25	80.74
Ca.lu.g	Canidae	26.56	24.93	16.02	24.07	16.00	11.10	9.00	27.40	13.72	12.27	12.85	2.25	24.29	47.86	71.24	65.65	76.78
Ca.lu.s	Canidae	27.73	24.13	14.80	25.45	14.66	13.15	9.47	30.82	17.41	16.34	17.64	2.76	24.06	59.30	75.70	60.32	73.15
Od.vi.	Cervidae	33.11	23.19	15.63	23.54	14.17	12.99	11.48	35.50	29.15	17.76	18.46	2.99	25.49	80.52	85.34	66.68	68.46
Eq.bu.	Equidae	44.20	42.27	32.85	40.01	31.16	17.16	16.98	57.82	36.31	31.23	29.58	7.34	34.68	*184.00	73.00	77.51	95.24
Ac.ju.	Felidae	37.47	26.42	20.84	30.10	21.00	12.77	9.59	30.72	27.66	19.44	18.96	4.06	29.71	60.38	68.23	42.51	44.03
Ly.ru.	Felidae	24.79	16.41	9.50	17.65	10.02	10.22	7.49	14.17	12.73	12.07	12.45	1.57	19.17	31.76	36.31	44.81	45.81
Le.ca.	Leporidae	16.20	8.95	4.40	10.27	5.20	5.62	3.80	10.16	4.15	5.51	6.35	0.95	14.60	28.79	55.73	41.28	45.17
Ao.ci.	Mustelidae	12.96	11.09	5.81	10.30	6.29	8.00	4.74	7.26	8.26	9.84	9.58	1.36	9.93	21.73	57.44	66.93	77.65
En.lu.	Mustelidae	28.53	22.17	14.84	24.19	15.80	15.10	10.75	31.16	17.43	19.95	20.51	3.57	19.45	51.64	79.68	56.77	76.47
Gu.gu.	Mustelidae	21.92	20.30	9.96	20.79	11.08	12.31	10.14	14.73	11.42	14.14	13.71	1.64	15.56	32.14	50.74	61.17	81.45
Lo.ca.	Mustelidae	19.64	14.06	8.07	15.17	8.09	10.44	6.16	10.68	12.81	14.31	16.01	2.10	17.50	27.42	61.71	55.10	69.46
Lo.fe.	Mustelidae	14.30	11.61	6.30	11.40	6.59	7.87	5.90	7.78	5.22	12.49	12.43	1.88	10.84	21.66	66.78	46.69	81.89
Ma.pe.	Mustelidae	18.60	12.11	6.30	12.28	6.78	7.12	5.13	11.71	8.93	9.62	11.88	1.78	15.40	22.67	46.63	44.15	58.41
Pt.br.	Mustelidae	26.30	23.30	14.25	24.96	15.10	15.52	7.63	16.99	18.53	20.80	20.73	2.23	18.04	42.72	76.63	67.84	91.20
Ha.gr.	Phocidae	52.60	46.10	37.56	45.67	38.94	27.23	14.00	42.00	25.38	38.50	36.05	7.96	34.95	118.90	116.15	55.53	63.49
Hy.le.	Phocidae	82.40	61.70	48.54	61.30	51.02	46.61	24.30	37.64	39.12	61.02	54.58	9.33	44.40	147.73	92.19	75.89	60.44
Mo.sc.	Phocidae	68.91	44.36	34.59	42.25	36.87	34.05	23.35	34.14	21.12	44.55	37.34	7.35	40.05	106.36	95.18	47.67	54.40
Ph.vi.	Phocidae	43.30	36.33	27.66	35.84	31.33	25.65	14.66	30.03	14.96	29.01	26.73	4.01	27.18	83.73	120.50	59.93	50.17
Ma.in.	Protocetidae	40.11	48.03	36.68	51.06	38.58	21.68	18.59	86.23	29.70	39.11	44.99	9.16	26.53	87.82	67.05	81.75	64.08
Prot.	Protocetidae	41.41	51.11	38.68	55.11	41.59	23.62	15.17	82.11	31.31	38.50	39.00	6.88	32.62	87.40	71.78	66.85	63.02
Qa.ar.	Protocetidae	53.80	61.57	49.50	68.97	58.40	30.00	15.30	110.76	43.99	55.18	53.44	8.83	41.31	113.00	74.57	85.05	59.43
Re.do.	Remingtonocetidae	42.53	54.86	31.59	57.55	32.91	26.83	17.00	50.90	35.46	48.47	50.00	8.26	22.85	103.89	85.98	84.89	83.57

Table 4.3. Seventeen L2 measurements of 25 non-cetaceans and four cetaceans. Species abbreviations follow Table 4.1. Measurement abbreviations follow Figure 4.1. Linear measurements are in mm; angular measurements are in degrees.

Species	Family	CL	CWa	CHa	CWp	CHp	NCW	NCH	NSH	NSL	PreW	PosW	PedW	PedL	MaxW	APAngNS	CCAngTP	DVAngTP
An.am.	Antilocapridae	32.29	20.86	15.60	22.16	15.60	11.28	9.49	37.47	29.10	19.08	19.17	3.64	24.64	99.53	90.08	67.48	72.42
Ca.hi.	Bovidae	29.57	19.35	12.75	19.81	12.56	11.47	9.34	20.47	27.20	16.49	16.75	4.82	19.98	80.63	88.78	72.03	84.43
Ce.ze.	Bovidae	23.97	16.30	10.41	17.90	9.34	10.62	7.34	21.78	26.96	16.02	15.98	3.32	19.86	70.30	83.59	80.23	77.85
Ga.gr.	Bovidae	34.55	23.38	20.54	26.01	20.05	15.34	9.66	43.40	42.80	20.41	20.47	5.56	27.17	135.27	90.98	71.61	70.87
Hi.ni.	Bovidae	47.03	31.44	28.04	35.80	26.66	19.80	15.70	42.96	33.62	27.85	28.03	4.45	35.42	142.50	84.76	71.52	84.46
Ma.ki.	Bovidae	17.46	10.18	6.24	11.09	6.52	8.18	5.66	15.14	17.43	9.60	9.94	1.60	13.17	44.08	90.40	55.51	53.98
Ov.ca.	Bovidae	40.98	32.24	21.95	32.17	21.29	14.91	10.01	44.62	37.69	23.21	23.00	8.44	31.38	124.03	84.41	71.99	77.00
Ca.lu.g	Canidae	28.22	23.67	17.09	24.06	16.48	12.11	9.14	32.45	16.59	13.04	13.31	2.37	24.32	56.42	67.82	47.88	65.82
Ca.lu.s	Canidae	29.44	23.62	15.74	26.60	15.92	13.49	9.02	32.49	17.68	17.95	18.59	2.76	24.86	67.58	73.22	50.61	69.12
Od.vi.	Cervidae	34.48	22.44	16.32	23.84	15.18	13.72	11.28	35.18	31.45	19.31	21.06	3.17	26.26	92.81	90.11	63.28	64.91
Eq.bu.	Equidae	46.15	37.70	30.32	41.87	31.18	19.48	17.37	60.13	36.57	28.13	29.15	8.41	35.90	216.00	81.74	87.75	91.15
Ac.ju.	Felidae	40.43	27.21	20.99	30.13	21.65	12.62	10.24	33.25	24.46	19.48	20.63	4.18	30.65	62.39	66.11	32.36	33.81
Ly.ru.	Felidae	27.87	16.70	9.59	17.86	11.08	10.48	8.11	10.49	11.53	12.83	14.41	1.51	21.52	36.77	35.89	33.99	42.77
Le.ca.	Leporidae	17.41	8.21	5.12	10.53	5.65	5.43	4.08	9.81	3.67	5.95	7.45	1.13	14.50	31.28	52.91	36.76	43.24
Ao.ci.	Mustelidae	13.37	10.53	5.91	11.07	6.20	8.76	5.03	8.53	7.90	9.78	10.30	1.20	10.00	24.20	64.39	45.17	58.32
En.lu.	Mustelidae	30.56	21.65	15.48	23.26	16.41	14.68	11.07	35.46	17.46	20.67	21.95	4.41	19.95	54.52	78.56	56.81	72.18
Gu.gu.	Mustelidae	22.37	20.38	10.66	20.38	11.74	12.35	8.94	16.28	10.83	14.05	12.26	1.89	17.10	35.79	49.50	50.02	68.03
Lo.ca.	Mustelidae	20.70	13.96	8.35	15.68	8.71	11.83	6.81	13.05	10.67	16.55	15.94	2.08	17.28	32.49	66.12	46.22	62.79
Lo.fe.	Mustelidae	15.05	11.16	6.97	11.92	6.87	9.20	6.56	9.00	5.43	12.87	12.60	1.89	11.26	23.84	64.71	41.75	49.97
Ma.pe.	Mustelidae	19.44	12.27	6.57	12.69	6.65	7.44	6.06	13.12	9.20	10.52	11.71	1.72	16.10	24.33	47.82	42.48	43.93
Pt.br.	Mustelidae	26.96	24.33	16.03	24.30	15.87	14.56	6.76	17.98	17.28	21.96	21.95	2.96	17.71	46.61	75.60	57.30	84.35
Ha.gr.	Phocidae	55.17	45.44	39.16	44.01	43.66	26.84	15.10	41.80	24.78	39.57	40.57	10.47	37.77	127.32	103.23	56.12	57.88
Hy.le.	Phocidae	86.19	60.00	49.27	60.80	53.41	42.50	24.27	36.67	40.51	59.57	56.14	9.45	51.65	152.17	92.71	67.30	56.24
Mo.sc.	Phocidae	67.60	45.27	34.05	43.14	35.89	33.64	21.54	30.69	23.15	40.90	38.47	6.07	37.70	98.25	90.42	55.33	61.13
Ph.vi.	Phocidae	43.99	35.84	29.66	35.51	32.82	24.54	15.42	30.65	15.46	28.89	28.18	4.46	21.90	91.08	121.34	54.22	53.91
Ma.in.	Protocetidae	40.25	46.99	37.11	47.30	40.81	21.40	20.71	91.60	31.29	42.57	44.46	9.22	26.35	102.01	69.53	66.45	54.32
Prot.	Protocetidae	47.01	52.16	37.81	55.94	43.19	22.54	14.49	89.40	34.29	41.70	34.12	8.11	32.34	98.40	63.79	52.51	54.32
Qa.ar.	Protocetidae	56.35	63.12	55.20	67.69	55.90	30.00	16.50	115.00	44.00	54.00	57.02	8.50	37.02	117.87	69.38	61.18	52.53
Re.do.	Remingtonocetidae	46.87	55.97	32.25	60.89	34.46	27.54	19.26	52.64	36.17	54.00	55.00	8.28	34.19	108.00	85.28	89.30	84.18

Table 4.4. Seventeen L3 measurements of 25 non-cetaceans and seven cetaceans. Species abbreviations follow Table 4.1. Measurement abbreviations follow Figure 4.1. Linear measurements are in mm; angular measurements are in degrees. Asterisks (*) indicate estimates.

Species	Family	CL	CWa	CHa	CWp	CHp	NCW	NCH	NSH	NSL	PreW	PosW	PedW	PedL	MaxW	APAngNS	CCAngTP	DVAngTP
An.am.	Antilocapridae	31.65	20.93	16.06	22.97	15.38	12.31	9.94	35.46	27.97	20.35	20.85	4.15	25.00	112.06	88.52	64.18	68.71
Ca.hi.	Bovidae	30.42	18.25	14.05	20.11	12.09	12.10	8.75	20.61	27.75	18.03	18.35	5.20	21.30	82.61	90.68	76.22	84.66
Ce.ze.	Bovidae	24.42	16.95	10.51	20.11	9.45	10.91	7.90	21.62	30.54	16.78	17.04	3.61	20.10	81.02	82.00	74.12	75.07
Ga.gr.	Bovidae	36.12	23.95	20.63	26.74	19.77	14.48	11.28	43.69	45.16	21.24	22.18	5.75	27.65	152.40	92.39	73.44	70.85
Hi.ni.	Bovidae	47.23	33.21	27.81	36.81	26.76	19.33	15.80	43.89	40.11	30.05	30.45	5.26	35.03	167.00	90.69	76.39	85.06
Ma.ki.	Bovidae	18.14	10.40	6.11	11.60	6.31	7.93	5.59	14.45	18.20	10.26	10.59	1.95	13.16	47.00	90.73	55.80	52.38
Ov.ca.	Bovidae	40.91	32.00	21.97	33.05	20.92	13.74	10.36	40.68	34.20	24.27	25.97	8.88	32.28	*127.50	88.67	71.23	74.09
Ca.lu.g	Canidae	29.40	24.09	18.08	24.36	16.55	11.93	9.15	35.46	16.38	14.21	15.89	1.87	25.03	66.85	65.27	48.68	63.85
Ca.lu.s	Canidae	30.83	24.25	16.73	26.99	16.11	13.69	9.02	34.83	19.91	19.82	18.44	3.30	25.30	72.57	75.04	52.96	72.34
Od.vi.	Cervidae	34.19	22.66	17.62	24.82	15.75	14.91	9.76	32.98	31.15	21.90	24.90	5.17	24.89	102.89	88.47	63.80	61.16
Eq.bu.	Equidae	46.99	38.31	30.56	43.09	30.74	19.61	18.03	62.23	39.36	28.35	31.92	8.19	35.33	235.00	77.50	85.76	89.26
Ac.ju.	Felidae	42.00	26.74	22.08	30.35	21.40	12.72	10.55	34.38	19.00	20.51	22.97	4.10	31.49	71.01	72.08	35.82	35.39
Ly.ru.	Felidae	30.64	16.68	10.31	18.00	11.20	10.84	8.55	18.21	8.87	14.53	14.93	1.48	22.80	40.14	45.62	31.78	44.84
Le.ca.	Leporidae	18.37	8.69	5.52	11.00	6.04	5.72	4.07	10.00	4.40	6.92	9.34	1.15	15.53	35.64	59.41	33.97	40.46
Ao.ci.	Mustelidae	14.32	10.03	5.98	10.47	6.40	8.78	5.47	9.28	6.98	10.59	10.89	1.09	10.93	27.21	60.73	53.28	59.28
En.lu.	Mustelidae	29.18	22.42	15.93	22.81	16.51	14.26	9.78	41.34	14.92	20.09	22.68	4.35	21.00	57.06	79.54	57.72	65.62
Gu.gu.	Mustelidae	24.03	19.67	11.86	20.81	11.73	12.50	8.36	18.67	9.50	12.82	10.08	2.21	16.87	35.88	62.06	35.26	57.95
Lo.ca.	Mustelidae	21.40	14.11	8.74	15.48	8.91	11.51	7.26	15.42	9.48	16.76	15.24	1.75	16.51	37.01	73.12	51.76	63.03
Lo.fe.	Mustelidae	15.30	11.31	6.90	12.53	6.81	9.02	5.68	10.23	5.46	13.02	12.97	1.88	11.54	25.74	68.50	46.96	44.24
Ma.pe.	Mustelidae	20.99	12.55	6.24	13.09	6.64	8.82	6.35	13.97	10.22	11.26	11.41	1.43	17.60	26.40	50.39	43.37	40.15
Pt.br.	Mustelidae	27.06	25.29	15.23	26.03	16.12	15.26	7.18	20.26	17.98	23.44	23.16	4.55	18.64	52.46	78.00	53.15	80.25
Ha.gr.	Phocidae	55.45	44.16	40.50	43.93	44.27	21.41	14.82	42.00	22.63	43.95	48.81	10.09	35.92	125.16	118.24	46.24	54.90
Hy.le.	Phocidae	85.87	60.59	50.28	58.25	54.31	44.93	24.85	34.68	34.96	61.92	61.36	10.00	49.42	153.51	90.37	77.30	60.72
Mo.sc.	Phocidae	67.26	44.14	35.07	42.60	37.99	31.29	22.90	32.21	27.28	43.82	37.84	8.46	39.05	110.44	93.12	53.80	52.57
Ph.vi.	Phocidae	45.02	37.13	29.72	36.71	34.68	24.30	14.55	31.38	12.88	31.71	34.31	4.93	24.60	90.65	119.83	44.83	56.50
Ba.ac.	Balaenopteridae	151.00	154.00	122.80	156.00	121.69	47.74	64.28	365.00	127.83	40.62	13.63	12.50	92.09	640.00	119.35	82.80	89.46
Ba.is.	Basilosauridae	314.50	173.30	157.20	178.80	159.40	92.80	40.00	130.00	93.00	100.20	56.10	20.70	80.20	285.00	87.43	58.52	45.97
Do.at.	Basilosauridae	71.09	94.00	80.38	94.42	84.72	42.30	36.26	97.34	48.63	57.45	26.45	11.08	38.16	193.00	88.39	63.42	48.13
De.de.	Delphinidae	26.92	35.66	33.04	36.65	33.27	18.13	25.41	84.95	17.25	5.44	3.67	2.99	14.66	21.40	108.15	103.92	88.15
Ma.in.	Protocetidae	44.46	43.30	40.08	52.30	41.57	18.90	22.61	96.49	32.59	44.92	55.54	13.47	27.01	111.38	72.47	72.90	59.74
Qa.ar.	Protocetidae	57.62	64.60	55.08	69.72	54.74	29.54	17.32	116.36	40.74	55.20	57.11	10.50	36.58	139.78	72.35	57.94	50.51
Re.do.	Remingtonocetidae	48.29	58.23	33.85	60.49	35.75	29.47	19.45	52.75	34.13	56.00	58.71	8.80	36.25	128.00	83.13	91.97	78.53

Table 4.5. Seventeen LX measurements of 25 non-cetaceans and four cetaceans. Species abbreviations follow Table 4.1. Measurement abbreviations follow Figure 4.1. Linear measurements are in mm; angular measurements are in degrees. Asterisks (*) indicate estimates.

Species	Family	CL	CWa	CHa	CWp	CHp	NCW	NCH	NSH	NSL	PreW	PosW	PedW	PedL	MaxW	APAngNS	CCAngTP	DVAngTP
An.am.	Antilocapridae	31.80	21.75	16.66	24.75	15.25	12.48	10.28	33.58	25.50	21.73	22.15	4.88	26.41	*114.00	89.37	63.76	65.38
Ca.hi.	Bovidae	31.28	18.27	12.86	20.66	11.41	12.52	9.30	19.86	27.23	19.41	21.15	5.87	22.87	84.48	90.26	75.96	83.97
Ce.ze.	Bovidae	23.90	17.86	9.79	20.67	9.42	11.86	8.15	20.87	29.48	17.97	19.11	3.10	19.44	86.37	81.24	73.48	72.97
Ga.gr.	Bovidae	37.91	24.63	19.84	28.39	20.51	15.52	11.13	39.78	41.96	23.10	23.34	5.01	28.60	157.00	94.44	74.12	69.84
Hi.ni.	Bovidae	47.17	34.69	27.94	38.62	26.10	21.26	17.20	43.20	42.23	32.48	33.08	5.35	33.88	175.00	90.35	82.55	84.03
Ma.ki.	Bovidae	18.62	10.64	6.30	12.65	5.89	8.50	5.80	13.31	18.69	11.05	12.11	2.24	13.74	50.03	91.72	56.78	54.82
Ov.ca.	Bovidae	42.15	32.48	22.01	32.27	20.96	14.04	12.24	41.41	38.46	27.24	27.93	9.36	33.68	131.20	88.42	68.94	73.72
Ca.lu.g	Canidae	32.68	24.88	17.27	27.05	16.71	13.88	10.36	36.99	13.00	14.01	12.96	1.66	29.25	76.54	59.47	43.43	48.32
Ca.lu.s	Canidae	32.29	25.01	16.53	28.29	16.58	16.04	8.22	35.09	13.16	18.48	16.07	3.16	27.90	76.62	79.93	33.51	69.25
Od.vi.	Cervidae	35.19	23.64	17.41	25.84	15.41	16.68	10.82	31.57	30.59	25.73	28.92	5.28	25.43	106.33	88.28	70.41	62.02
Eq.bu.	Equidae	45.79	39.35	29.49	49.95	28.03	21.84	19.32	64.02	39.88	30.74	36.13	6.74	34.57	238.00	84.84	82.25	89.68
Ac.ju.	Felidae	48.19	27.97	20.64	32.03	20.53	15.35	12.79	34.49	11.27	23.02	23.78	3.29	35.14	74.87	72.88	22.74	44.38
Ly.ru.	Felidae	33.95	18.36	10.54	18.88	11.25	12.55	10.13	18.87	5.37	16.39	15.51	1.48	24.70	43.81	59.34	31.59	44.89
Le.ca.	Leporidae	18.56	10.15	5.43	12.38	6.85	6.51	4.81	11.74	4.58	10.72	11.46	1.70	14.84	38.40	39.20	34.30	47.79
Ao.ci.	Mustelidae	14.61	9.68	6.18	11.60	6.71	7.97	4.66	10.61	6.82	11.06	10.83	1.75	10.86	28.90	63.54	51.96	64.33
En.lu.	Mustelidae	29.60	22.25	16.75	24.59	16.29	11.05	8.74	45.40	13.93	22.94	22.48	5.22	22.14	56.54	81.22	45.56	53.55
Gu.gu.	Mustelidae	24.03	19.67	11.86	20.81	11.73	12.50	8.36	18.67	9.50	12.82	10.08	2.21	16.87	35.88	62.06	35.26	57.95
Lo.ca.	Mustelidae	21.83	14.15	8.98	15.89	8.97	11.16	7.08	15.78	9.12	16.28	13.83	2.28	16.96	39.52	72.47	46.95	63.21
Lo.fe.	Mustelidae	15.30	11.31	6.90	12.53	6.81	9.02	5.68	10.23	5.46	13.02	12.97	1.88	11.54	25.74	68.50	46.96	44.24
Ma.pe.	Mustelidae	20.97	12.64	6.97	13.38	6.95	9.18	6.30	14.70	7.20	11.14	10.41	1.67	16.75	29.20	52.37	44.20	46.76
Pt.br.	Mustelidae	27.06	25.29	15.23	26.03	16.12	15.26	7.18	20.26	17.98	23.44	23.16	4.55	18.64	52.46	78.00	53.15	80.25
Ha.gr.	Phocidae	55.45	44.16	40.50	43.93	44.27	21.41	14.82	42.00	22.63	43.95	48.81	10.09	35.92	125.16	118.24	46.24	54.90
Hy.le.	Phocidae	79.12	59.05	52.54	60.76	53.78	39.13	21.90	31.97	35.00	68.14	60.95	12.31	52.52	166.00	89.36	68.10	57.93
Mo.sc.	Phocidae	67.26	44.14	35.07	42.60	37.99	31.29	22.90	32.21	27.28	43.82	37.84	8.46	39.05	110.44	93.12	53.80	52.57
Ph.vi.	Phocidae	45.02	37.13	29.72	36.71	34.68	24.30	14.55	31.38	12.88	31.71	34.31	4.93	24.60	90.65	119.83	44.83	56.50
Ma.in.	Protocetidae	46.21	44.48	37.67	57.08	35.98	22.09	21.75	96.94	33.97	53.27	56.22	12.41	26.02	111.84	69.71	73.15	47.20
Qa.ar.	Protocetidae	66.05	66.73	53.82	74.34	52.58	34.73	15.70	122.25	37.66	52.72	56.00	9.24	38.91	116.01	70.90	51.84	41.90
Ro.ka.	Protocetidae	54.82	57.36	44.81	66.40	47.39	29.95	14.15	84.62	30.96	53.59	52.87	12.94	26.07	116.98	69.85	62.30	69.53
Re.do.	Remingtonocetidae	50.98	56.84	34.40	61.96	37.40	30.69	19.50	53.00	36.50	61.60	63.08	11.30	39.19	130.00	83.80	83.97	69.30

Table 4.6. Seventeen LY measurements of 25 non-cetaceans and three cetaceans. Species abbreviations follow Table 4.1. Measurement abbreviations follow Figure 4.1. Linear measurements are in mm; angular measurements are in degrees. Asterisks (*) indicate estimates.

Species	Family	CL	CWa	CHa	CWp	CHp	NCW	NCH	NSH	NSL	PreW	PosW	PedW	PedL	MaxW	APAngNS	CCAngTP	DVAngTP
An.am.	Antilocapridae	31.88	22.72	16.05	28.04	14.81	14.54	11.19	31.43	29.35	23.36	26.46	4.07	24.82	*117.00	86.41	63.79	65.04
Ca.hi.	Bovidae	30.47	19.24	11.50	22.91	11.35	14.39	10.25	19.33	27.94	22.56	25.04	5.69	22.25	88.71	91.18	69.82	78.77
Ce.ze.	Bovidae	22.92	21.17	9.11	22.45	9.13	13.19	9.48	18.60	25.30	19.87	21.21	3.99	20.59	88.13	79.48	73.63	72.94
Ga.gr.	Bovidae	38.30	25.40	20.11	32.41	18.75	16.26	11.93	36.94	39.41	24.48	28.95	4.26	28.56	*162.00	91.46	70.27	68.68
Hi.ni.	Bovidae	48.09	35.58	28.50	43.27	25.27	22.67	16.83	41.40	38.41	34.75	39.08	4.48	33.40	184.00	87.69	73.24	86.40
Ma.ki.	Bovidae	18.92	11.68	5.98	14.10	5.78	9.38	6.55	13.36	17.78	12.49	13.96	1.82	14.97	51.66	85.69	57.15	56.87
Ov.ca.	Bovidae	42.09	33.94	21.41	37.40	20.25	17.20	12.16	38.78	32.78	28.51	32.04	9.80	31.64	133.59	82.57	66.13	73.50
Ca.lu.g	Canidae	32.33	25.73	16.59	28.40	17.15	13.49	9.04	31.61	12.27	14.02	14.92	3.60	25.66	81.36	56.56	30.44	44.37
Ca.lu.s	Canidae	30.81	26.55	16.38	29.61	15.88	15.11	7.18	30.04	8.75	17.00	21.35	3.97	25.24	80.77	83.78	30.97	64.71
Od.vi.	Cervidae	33.72	24.51	16.08	28.60	14.18	18.74	13.21	29.32	24.17	29.05	32.16	4.37	26.48	101.67	88.81	70.79	66.68
Eq.bu.	Equidae	45.49	48.14	26.53	48.31	23.90	24.32	20.90	61.90	21.64	33.40	34.42	7.60	35.18	212.00	77.80	69.43	91.81
Ac.ju.	Felidae	45.84	30.97	20.44	33.27	21.27	15.07	11.38	33.68	8.79	23.69	29.83	4.44	32.54	80.05	76.86	24.46	47.24
Ly.ru.	Felidae	32.02	19.03	10.86	19.64	11.97	11.97	8.99	16.67	5.27	16.28	17.93	1.62	24.71	50.26	56.50	39.74	51.37
Le.ca.	Leporidae	17.90	10.60	5.20	13.48	6.49	7.24	5.30	13.20	4.81	11.02	11.63	1.56	13.70	39.21	51.71	33.24	50.29
Ao.ci.	Mustelidae	15.21	10.66	6.54	12.33	6.82	7.57	4.08	11.35	7.16	11.24	11.46	2.11	12.05	30.21	65.84	60.98	69.16
En.lu.	Mustelidae	29.78	22.92	16.64	25.53	15.66	11.59	10.85	46.29	12.07	22.02	26.06	7.09	21.39	56.64	78.52	40.52	49.22
Gu.gu.	Mustelidae	24.68	20.15	11.55	21.97	11.28	12.69	7.90	20.00	7.12	10.57	12.43	2.46	16.52	37.43	62.41	44.59	65.43
Lo.ca.	Mustelidae	22.10	15.20	8.77	17.37	9.29	11.29	5.76	16.07	9.06	14.67	12.61	2.37	16.91	40.79	65.05	54.50	60.03
Lo.fe.	Mustelidae	15.28	11.64	6.95	13.08	7.35	9.41	6.16	10.01	6.23	13.68	12.59	2.14	11.56	30.17	64.90	53.06	51.97
Ma.pe.	Mustelidae	21.74	12.93	7.04	14.32	7.62	8.97	5.40	12.45	5.47	10.85	11.20	2.22	17.79	28.52	43.96	42.64	55.19
Pt.br.	Mustelidae	28.34	25.33	16.46	28.16	16.88	15.45	6.13	21.42	16.12	24.55	21.11	4.65	18.91	54.77	81.45	55.67	67.74
Ha.gr.	Phocidae	52.08	44.42	41.10	45.25	46.17	24.36	16.27	38.76	25.59	52.70	50.10	12.06	34.63	115.18	110.40	32.52	51.00
Hy.le.	Phocidae	84.05	60.52	51.87	60.47	53.54	40.60	24.86	32.50	37.23	64.60	62.11	12.32	50.99	156.00	93.29	72.07	55.54
Mo.sc.	Phocidae	63.70	44.43	36.55	44.14	38.63	28.55	20.37	29.92	22.77	44.21	37.46	10.52	37.70	111.23	90.72	61.29	52.18
Ph.vi.	Phocidae	43.86	37.25	30.79	37.01	37.49	25.29	15.98	27.81	14.60	37.28	32.43	4.26	23.89	89.89	114.87	44.77	51.92
Ma.in.	Protocetidae	46.02	48.83	36.27	64.85	36.83	24.83	21.11	99.37	32.96	53.78	48.85	10.49	25.25	114.93	70.17	52.55	47.68
Qa.ar.	Protocetidae	69.42	70.56	53.53	78.59	51.17	39.00	13.74	128.50	47.07	54.34	51.27	9.71	44.55	136.00	70.50	60.88	51.91
Re.do.	Remingtonocetidae	51.72	57.55	37.83	64.65	38.39	31.45	20.35	54.12	36.32	62.84	63.11	11.89	34.85	133.00	75.46	74.20	63.07

Table 4.7. Seventeen LZ measurements of 25 non-cetaceans and three cetaceans. Species abbreviations follow Table 4.1. Measurement abbreviations follow Figure 4.1. Linear measurements are in mm; angular measurements are in degrees. Asterisks (*) indicate estimates.

Species	Family	CL	CWa	CHa	CWp	CHp	NCW	NCH	NSH	NSL	PreW	PosW	PedW	PedL	MaxW	APAngNS	CCAngTP	DVAngTP
An.am.	Antilocapridae	29.56	24.46	16.44	31.64	13.72	17.55	12.11	29.72	27.71	27.56	35.05	4.68	19.78	109.69	89.36	59.51	65.93
Ca.hi.	Bovidae	25.91	21.43	11.11	26.09	11.11	16.73	11.64	19.72	19.60	26.31	28.52	6.13	19.30	78.11	88.04	75.89	79.49
Ce.ze.	Bovidae	21.12	20.59	9.47	23.75	9.05	14.50	12.00	16.51	12.09	21.65	26.35	3.53	16.07	77.50	60.26	67.66	71.40
Ga.gr.	Bovidae	34.19	30.94	19.37	42.01	17.09	19.19	13.04	34.10	23.56	29.74	41.28	6.65	24.46	123.28	84.68	64.21	67.43
Hi.ni.	Bovidae	46.28	36.06	26.83	52.44	23.63	28.24	17.17	40.43	29.12	40.99	49.70	6.78	31.00	*154.00	80.08	64.23	86.18
Ma.ki.	Bovidae	16.99	13.11	5.94	16.12	5.90	10.77	6.32	12.29	13.44	14.20	17.55	2.38	12.80	50.26	79.29	52.17	55.66
Ov.ca.	Bovidae	38.04	36.10	20.64	39.90	20.10	18.33	14.28	38.80	28.18	33.15	39.82	12.96	25.27	115.75	79.45	66.69	74.33
Ca.lu.g	Canidae	25.90	27.46	17.08	29.04	16.20	14.59	8.46	29.57	7.89	16.34	33.03	6.77	17.57	76.15	82.31	28.48	58.80
Ca.lu.s	Canidae	25.68	27.81	15.79	29.81	15.92	12.52	7.32	26.00	8.38	22.35	37.73	8.72	17.42	70.89	94.37	29.91	64.81
Od.vi.	Cervidae	28.64	28.01	14.04	29.56	12.74	21.26	14.11	27.65	16.60	33.02	35.47	6.99	21.31	76.99	75.41	59.12	64.07
Eq.bu.	Equidae	42.28	46.24	22.33	40.75	20.07	26.85	21.44	58.69	21.83	32.96	36.77	9.90	27.39	195.00	71.25	64.64	89.70
Ac.ju.	Felidae	35.87	31.82	20.29	32.65	20.56	15.62	9.32	32.43	14.47	29.87	39.85	6.41	26.40	86.18	84.36	50.42	66.07
Ly.ru.	Felidae	24.62	19.56	11.10	18.80	11.59	12.11	6.77	15.70	5.27	18.58	23.49	2.65	17.71	49.47	58.91	38.72	57.25
Le.ca.	Leporidae	13.76	12.35	5.08	13.73	6.10	6.57	4.84	14.85	6.93	11.33	12.50	2.26	9.53	39.96	75.10	47.91	63.52
Ao.ci.	Mustelidae	13.32	11.19	6.58	12.27	6.95	7.71	3.38	10.59	7.33	11.97	10.69	3.17	8.92	30.43	72.49	54.03	71.17
En.lu.	Mustelidae	27.11	23.62	15.05	25.96	15.18	13.53	10.94	42.02	14.07	27.03	34.04	8.24	18.82	53.31	89.50	47.05	59.38
Gu.gu.	Mustelidae	22.81	21.99	11.20	22.51	11.65	12.68	7.07	18.78	6.35	13.09	22.90	3.59	15.97	45.60	67.21	48.28	69.96
Lo.ca.	Mustelidae	19.16	16.01	9.21	17.80	9.65	10.39	5.08	15.32	9.00	13.45	17.05	3.00	14.45	38.70	73.90	67.12	83.70
Lo.fe.	Mustelidae	14.02	12.28	7.54	14.13	7.66	9.21	5.17	9.14	5.65	13.60	15.66	2.82	10.38	29.63	77.34	64.26	65.03
Ma.pe.	Mustelidae	16.76	12.98	7.44	14.26	7.75	7.88	3.92	12.89	6.65	11.04	14.24	4.22	12.33	32.56	54.38	62.41	75.47
Pt.br.	Mustelidae	27.66	26.20	16.77	29.28	16.10	15.78	5.42	22.74	10.19	22.12	26.77	4.22	19.12	59.52	85.93	60.17	69.42
Ha.gr.	Phocidae	45.25	44.17	43.52	46.91	45.44	29.30	18.97	34.02	22.13	53.98	52.83	13.74	34.27	114.57	101.31	41.32	43.12
Hy.le.	Phocidae	66.84	61.90	52.41	66.54	52.01	38.60	22.99	29.42	31.24	64.41	68.25	13.30	44.41	147.12	90.21	63.09	53.85
Mo.sc.	Phocidae	57.63	43.90	36.85	42.28	37.58	30.43	20.51	24.52	22.49	46.18	52.08	12.50	36.40	107.18	91.76	59.12	53.21
Ph.vi.	Phocidae	39.49	37.98	31.77	35.31	33.98	25.59	15.65	28.24	14.39	35.44	34.75	6.88	21.15	90.63	120.67	51.70	55.56
Ma.in.	Protocetidae	50.27	61.06	38.45	64.31	35.93	27.40	20.60	103.62	39.21	53.19	55.88	10.68	26.65	132.57	63.39	53.88	57.50
Qa.ar.	Protocetidae	70.69	72.16	49.94	76.35	52.12	34.88	18.76	133.08	51.30	53.00	58.32	11.18	44.96	129.00	73.02	71.04	57.69
Re.do.	Remingtonocetidae	52.85	59.81	36.93	57.92	38.52	29.34	17.37	56.00	34.00	63.15	53.89	12.00	32.55	128.13	68.29	73.71	63.25

Table 4.8. Eigenvalues and eigenvector coefficients (loadings) for PCs I and II of each PCA.

Analysis	PC	Eigenvalue	Percent of Variance	Eigenvector Coefficients (Loadings)															
				CL	CWa	CHa	CWp	CHp	NCW	NCH	NSH	NSL	PreW	PosW	PedW	PedL	MaxW	APAngNS	CCAngTP	DVAngTP
L1	I	13.234	77.8%	0.267	0.269	0.272	0.269	0.270	0.257	0.261	0.245	0.231	0.262	0.263	0.260	0.259	0.256	0.190	0.121	0.034
	II	1.820	10.7%	-0.142	-0.060	-0.056	-0.076	-0.091	-0.108	-0.083	0.077	0.205	-0.059	-0.050	0.027	-0.127	0.096	0.151	0.623	0.671
L2	I	13.356	78.6%	0.261	0.264	0.268	0.266	0.264	0.252	0.257	0.243	0.231	0.260	0.261	0.258	0.252	0.253	0.188	0.172	0.114
	II	1.890	11.1%	-0.174	-0.139	-0.109	-0.133	-0.155	-0.157	-0.143	0.139	0.236	-0.102	-0.122	0.055	-0.135	0.168	0.285	0.539	0.575
L3	I	13.280	78.1%	0.261	0.266	0.268	0.267	0.264	0.251	0.260	0.242	0.225	0.261	0.262	0.259	0.254	0.251	0.194	0.152	0.129
	II	1.870	11.0%	-0.185	-0.140	-0.119	-0.115	-0.172	-0.154	-0.130	0.073	0.322	-0.103	-0.098	0.083	-0.133	0.187	0.190	0.558	0.559
LX	I	12.959	76.2%	0.263	0.269	0.271	0.271	0.265	0.257	0.262	0.238	0.224	0.265	0.263	0.251	0.255	0.254	0.205	0.118	0.110
	II	2.120	12.5%	-0.190	-0.137	-0.123	-0.104	-0.167	-0.126	-0.125	-0.023	0.360	-0.059	-0.003	0.133	-0.165	0.158	0.199	0.567	0.543
LY	I	12.797	75.3%	0.266	0.270	0.269	0.274	0.261	0.268	0.264	0.239	0.220	0.266	0.271	0.251	0.261	0.254	0.210	0.073	0.059
	II	2.095	12.3%	-0.147	-0.109	-0.139	-0.068	-0.197	-0.024	-0.019	-0.056	0.348	0.000	0.007	-0.009	-0.105	0.155	0.158	0.611	0.587
LZ	I	12.781	75.2%	0.274	0.274	0.269	0.275	0.262	0.270	0.262	0.235	0.235	0.271	0.271	0.250	0.271	0.257	0.167	0.018	-0.069
	II	1.860	10.9%	0.011	-0.025	-0.107	0.041	-0.154	0.055	0.095	0.065	0.257	0.015	-0.049	-0.056	0.034	0.159	-0.299	0.625	0.607

Table 4.9. PC scores by species for PCs I and II of each PCA.

		L1 PCA		L2 PCA		L3 PCA		LX PCA		LY PCA		LZ PCA	
Species	**Family**	**PC-I**	**PC-II**	**PC-I**	**PC-II**	**PC-I**	**PC-II**	**PC-I**	**PC-II**	**PC-I**	**PC-II**	**PC-I**	**PC-II**
An.am.	Antilocapridae	0.846	1.293	0.866	1.386	0.828	1.143	0.846	1.031	0.939	1.110	1.156	0.633
Ca.hi.	Bovidae	-0.233	1.815	0.113	1.964	0.115	2.155	0.093	2.317	0.154	2.125	-0.049	1.721
Ce.ze.	Bovidae	-1.056	2.126	-0.774	2.261	-0.761	2.099	-0.954	2.087	-0.816	2.080	-1.617	1.554
Ga.gr.	Bovidae	1.925	1.034	2.107	1.381	2.188	1.516	2.101	1.449	2.096	1.427	2.240	0.905
Hi.ni.	Bovidae	3.543	1.123	3.649	0.730	3.877	1.116	3.978	1.387	3.891	1.741	3.855	2.050
Ma.ki.	Bovidae	-4.348	0.089	-4.040	1.402	-4.131	1.423	-4.030	1.576	-3.917	1.260	-3.857	-0.519
Ov.ca.	Bovidae	2.491	0.799	2.854	1.134	2.693	1.095	2.838	1.186	2.848	1.103	2.843	1.431
Ca.lu.g	Canidae	-0.494	0.503	-0.549	-0.133	-0.552	-0.234	-0.729	-1.510	-0.771	-2.340	-0.105	-2.381
Ca.lu.s	Canidae	0.191	0.181	0.159	0.048	0.351	0.343	0.027	-0.642	-0.184	-1.015	0.085	-2.208
Od.vi.	Cervidae	0.984	0.490	1.119	0.750	1.223	0.708	1.443	0.954	1.455	1.207	1.016	0.512
Eq.bu.	Equidae	4.497	1.344	4.736	1.380	4.630	1.342	4.707	1.423	4.334	1.378	3.567	2.449
Ac.ju.	Felidae	1.043	-2.497	0.570	-2.937	0.650	-2.531	0.798	-3.150	1.091	-2.896	1.565	-0.253
Ly.ru.	Felidae	-3.037	-2.313	-3.317	-2.566	-2.985	-2.276	-2.484	-2.388	-2.438	-1.514	-2.652	-1.309
Le.ca.	Leporidae	-6.680	-1.878	-6.839	-0.789	-6.560	-1.039	-6.013	-1.034	-5.772	-1.104	-5.515	-0.597
Ao.ci.	Mustelidae	-5.398	1.185	-5.605	0.400	-5.660	0.672	-5.605	1.141	-5.492	1.345	-5.868	-0.072
En.lu.	Mustelidae	0.408	0.132	0.536	0.408	0.266	0.258	-0.014	-0.453	0.128	-1.268	0.531	-0.948
Gu.gu.	Mustelidae	-2.091	0.343	-2.309	-0.297	-2.699	-1.046	-2.786	-0.871	-2.819	-0.274	-2.418	-0.200
Lo.ca.	Mustelidae	-2.940	-0.073	-2.853	-0.098	-2.912	0.277	-3.045	0.344	-3.390	0.303	-3.583	1.230
Lo.fe.	Mustelidae	-4.892	0.059	-4.905	-0.587	-5.074	-0.457	-5.254	-0.293	-5.091	0.069	-5.043	-0.172
Ma.pe.	Mustelidae	-4.681	-1.181	-4.734	-0.971	-4.759	-1.019	-4.798	-0.696	-5.055	-0.811	-5.106	0.961
Pt.br.	Mustelidae	-0.216	1.136	-0.242	0.699	-0.033	0.557	-0.164	0.963	-0.309	0.545	-0.485	0.069
Ha.gr.	Phocidae	4.876	-1.016	4.938	-1.180	4.707	-1.528	4.687	-1.135	4.813	-1.906	5.148	-2.513
Hy.le.	Phocidae	7.152	-0.871	6.982	-1.802	6.941	-1.325	6.773	-1.131	6.887	-0.528	6.605	-0.205
Mo.sc.	Phocidae	5.014	-2.386	4.662	-1.617	4.754	-1.766	4.711	-1.417	4.563	-0.864	4.701	-0.632
Ph.vi.	Phocidae	3.096	-1.438	2.877	-0.964	2.903	-1.483	2.874	-1.138	2.853	-1.173	2.987	-1.505
Ba.ac.	Balaenopteridae	-	-	-	-	11.658	0.070	-	-	-	-	-	-
Ba.is.	Basilosauridae	-	-	-	-	12.162	-3.839	-	-	-	-	-	-
Do.at.	Basilosauridae	-	-	-	-	7.718	-2.058	-	-	-	-	-	-
De.de.	Delphinidae	-	-	-	-	0.721	2.025	-	-	-	-	-	-
Ma.in.	Protocetidae	4.902	0.062	4.771	-1.022	5.150	-0.482	5.035	-0.904	4.949	-1.371	5.493	0.557
Prot.	Protocetidae	4.848	-0.610	4.575	-1.634	-	-	-	-	-	-	-	-
Qa.ar.	Protocetidae	6.708	-0.265	6.306	-1.776	6.289	-1.793	6.139	-2.492	6.646	-1.251	7.043	1.094
Ro.ka.	Protocetidae	-	-	-	-	-	-	5.545	-0.466	-	-	-	-
Re.do.	Remingtonocetidae	5.183	1.067	5.788	0.375	5.821	0.287	5.952	0.161	5.796	0.126	5.352	1.383

REFERENCES

Alexander, R. M., N. J. Dimery, and R. F. Ker. 1985. Elastic structures in the back and their role in galloping in some mammals. Journal of Zoology (London) 207: 467-482.

Alexander, R. M., V. A. Langman, and A. S. Jayes. 1977. Fast locomotion of some African ungulates. Journal of Zoology (London) 183: 291-300.

Bajpai, S., and J. G. M. Thewissen. 2000. A new, diminutive Eocene whale from Kachchh (Gujarat, India) and its implications for locomotor evolution of cetaceans. Current Science 79: 1478-1482.

Bebej, R. M. 2009. Swimming mode inferred from skeletal proportions in the fossil pinnipeds *Enaliarctos* and *Allodesmus* (Mammalia, Carnivora). Journal of Mammalian Evolution 16: 77-97.

Boszczyk, B. M., A. A. Boszczyk, and R. Putz. 2001. Comparative and functional anatomy of the mammalian lumbar spine. The Anatomical Record 264: 157-168.

Buchholtz, E. A. 1998. Implications of vertebral morphology for locomotor evolution in early Cetacea. Pp. 325-351 in J. G. M. Thewissen (ed.), The Emergence of Whales: Evolutionary Patterns in the Origin of Cetacea. Plenum Press, New York.

Buchholtz, E. A. 2001. Vertebral osteology and swimming style in living and fossil whales (Order: Cetacea). Journal of Zoology (London) 253: 175-190.

Buchholtz, E. A. 2007. Modular evolution of the cetacean vertebral column. Evolution & Development 9: 278-289.

Buchholtz, E. A., and S. A. Schur. 2004. Vertebral osteology in Delphinidae (Cetacea). Zoological Journal of the Linnean Society 104: 383-401.

Buchholtz, E. A., E. M. Wolkovich, and R. J. Cleary. 2005. Vertebral osteology and complexity in *Lagenorhynchus acutus* (Delphinidae) with comparison to other delphinoid genera. Marine Mammal Science 21: 411-428.

Coughlin, B. L., and F. E. Fish. 2009. Hippopotamus underwater locomotion: reduced-gravity movements for a massive mammal. Journal of Mammalogy 90: 675-679.

Fish, F. E. 1993. Power output and propulsive efficiency of swimming bottlenose dolphins (*Tursiops truncatus*). Journal of Experimental Biology 185: 179-193.

Fish, F. E. 1994. Association of propulsive swimming mode with behavior in river otters (*Lutra canadensis*). Journal of Mammalogy 75: 989-997.

Fish, F. E. 2002. Balancing requirements for stability and maneuverability in cetaceans. Integrative and Comparative Biology 42: 85-93.

Fish, F. E., and C. A. Hui. 1991. Dolphin swimming - A review. Mammal Review 21: 181-195.

Fish, F. E., S. Innes, and K. Ronald. 1988. Kinematics and estimated thrust production of swimming harp and ringed seals. Journal of Experimental Biology 137: 157-173.

Fish, F. E., J. E. Peacock, and J. J. Rohr. 2003. Stabilization mechanism in swimming odontocete cetaceans by phased movements. Marine Mammal Science 19: 515-528.

Gál, J. M. 1993. Mammalian spinal biomechanics: I. Static and dynamic mechanical properties of intact intervertebral joints. Journal of Experimental Biology 174: 247-280.

Gingerich, P. D. 1998. Paleobiological perspectives on Mesonychia, Archaeoceti, and the origin of whales. Pp. 423-449 in J. G. M. Thewissen (ed.), The Emergence of Whales: Evolutionary Patterns in the Origin of Cetacea. Plenum Press, New York.

Gingerich, P. D. 2003. Land-to-sea transition in early whales: evolution of Eocene Archaeoceti (Cetacea) in relation to skeletal proportions and locomotion of living semiaquatic mammals. Paleobiology 29: 429-454.

Gingerich, P. D. 2005. Aquatic adaptation and swimming mode inferred from skeletal proportions in the Miocene desmostylian *Desmostylus*. Journal of Mammalian Evolution 12: 183-194.

Gingerich, P. D., M. Arif, M. A. Bhatti, M. Anwar, and W. J. Sanders. 1997. *Basilosaurus drazindai* and *Basiloterus hussaini*, new Archaeoceti (Mammalia, Cetacea) from the middle Eocene Drazinda Formation, with a revised interpretation of ages of whale-bearing strata in the Kirthar Group of the Sulaiman Range, Punjab (Pakistan). Contributions from the Museum of Paleontology, University of Michigan 30: 55-81.

Gingerich, P. D., S. M. Raza, M. Arif, M. Anwar, and X. Zhou. 1994. New whale from the Eocene of Pakistan and the origin of cetacean swimming. Nature 368: 844-847.

Gingerich, P. D., B. H. Smith, and E. L. Simons. 1990. Hind limbs of Eocene *Basilosaurus*: evidence of feet in whales. Science 249: 154-157.

Gingerich, P. D., M. ul-Haq, I. H. Khan, and I. S. Zalmout. 2001a. Eocene stratigraphy and archaeocete whales (Mammalia, Cetacea) of Drug Lahar in the eastern Sulaiman Range, Balochistan (Pakistan). Contributions from the Museum of Paleontology, University of Michigan 30: 269-319.

Gingerich, P. D., M. ul-Haq, W. von Koenigswald, W. J. Sanders, B. H. Smith, and I. S. Zalmout. 2009. New protocetid whale from the middle Eocene of Pakistan: birth on land, precocial development, and sexual dimorphism. PLoS ONE 4: e4366.

Gingerich, P. D., M. ul-Haq, I. S. Zalmout, I. H. Khan, and M. S. Malkani. 2001b. Origin of whales from early artiodactyls: hands and feet of Eocene Protocetidae from Pakistan. Science 293: 2239-2242.

Grand, T. I. 1997. How muscle mass is part of the fabric of behavioral ecology in East African bovids (*Madoqua*, *Gazella*, *Damaliscus*, *Hippotragus*). Anatomy and Embryology 195: 375-386.

Grauer, J. N., J. S. Erulkar, T. C. Patel, and M. M. Panjabi. 2000. Biomechanical evaluation of the New Zealand white rabbit lumbar spine: a physiologic characterization. European Spine Journal 9: 250-255.

Hildebrand, M. 1959. Motions of the running cheetah and horse. Journal of Mammalogy 40: 481-495.

Howell, A. B. 1944. Speed in Animals: Their Specializations for Running and Leaping. University of Chicago Press, Chicago, 270 pp.

Hulbert, R. C., Jr. 1998. Postcranial osteology of the North American middle Eocene protocetid *Georgiacetus*. Pp. 235-267 in J. G. M. Thewissen (ed.), The Emergence of Whales: Evolutionary Patterns in the Origin of Cetacea. Plenum Press, New York.

Hulbert, R. C., Jr., R. M. Petkewich, G. A. Bishop, D. Bukry, and D. P. Aleshire. 1998. A new middle Eocene protocetid whale (Mammalia: Cetacea: Archaeoceti) and associated biota from Georgia. Journal of Paleontology 72: 907-927.

Jackson, D. A. 1993. Stopping rules in principal components analysis: a comparison of heuristical and statistical approaches. Ecology 74: 2204-2214.

Long, J. H., Jr., D. A. Pabst, W. R. Shepherd, and W. A. McLellan. 1997. Locomotor design of dolphin vertebral columns: bending mechanics and morphology of *Delphinus delphis*. Journal of Experimental Biology 200: 65-81.

Madar, S. I. 2007. The postcranial skeleton of early Eocene pakicetid cetaceans. Journal of Paleontology 81: 176-200.

Madar, S. I., J. G. M. Thewissen, and S. T. Hussain. 2002. Additional holotype remains of *Ambulocetus natans* (Cetacea, Ambulocetidae), and their implications for locomotion in early whales. Journal of Vertebrate Paleontology 22: 405-422.

Pabst, D. A. 1993. Intramuscular morphology and tendon geometry of the epaxial swimming muscles of dolphins. Journal of Zoology (London) 230: 159-176.

Pabst, D. A. 2000. To bend a dolphin: convergence of force transmission designs in cetaceans and scombrid fishes. American Zoologist 40: 146-155.

Rose, K. D., and W. von Koenigswald. 2005. An exceptionally complete skeleton of *Palaeosinopa* (Mammalia, Cimolesta, Pantolestidae) from the Green River Formation, and other postcranial elements of the Pantolestidae from the Eocene of Wyoming (USA). Palaeontographica Abteilung A 273: 55-96.

Schilling, N., and D. R. Carrier. 2010. Function of the epaxial muscles in walking, trotting and galloping dogs: implications for the evolution of epaxial muscle function in tetrapods. Journal of Experimental Biology 213: 1490-1502.

Slijper, E. J. 1946. Comparative biologic-anatomical investigations on the vertebral column and spinal musculature of mammals. Verhandelingen der Koninklijke Nederlandsche Akademie van Wetenschappen, Afdeling Natuurkunde, Tweede Sectie 42: 1-128.

Slijper, E. J. 1947. Observations on the vertebral column of the domestic animals. The Veterinary Journal 103: 376-387.

Smith, F. A., S. K. Lyons, S. K. Morgan Ernest, K. E. Jones, D. M. Kaufman, T. Dayan, P. A. Marquet, J. H. Brown, and J. P. Haskell. 2003. Body mass of late Quaternary mammals. Ecology 84: 3403.

Tarasoff, F. J., A. Bisaillon, J. Piérard, and A. P. Whitt. 1972. Locomotory patterns and external morphology of the river otter, sea otter, and harp seal (Mammalia). Canadian Journal of Zoology 50: 915-929.

Thewissen, J. G. M., and F. E. Fish. 1997. Locomotor evolution in the earliest cetaceans: functional model, modern analogues, and paleontological evidence. Paleobiology 23: 482-490.

Thewissen, J. G. M., S. T. Hussain, and M. Arif. 1994. Fossil evidence for the origin of aquatic locomotion in archaeocete whales. Science 263: 210-212.

Thewissen, J. G. M., S. I. Madar, and S. T. Hussain. 1996. *Ambulocetus natans*, an Eocene cetacean (Mammalia) from Pakistan. Courier Forschungsinstitut Senckenberg 190: 1-86.

Thewissen, J. G. M., E. M. Williams, L. J. Roe, and S. T. Hussain. 2001. Skeletons of terrestrial cetaceans and the relationship of whales to artiodactyls. Nature 413: 277-281.

Uhen, M. D. 1998. Middle to late Eocene basilosaurines and dorudontines. Pp. 29-61 in J. G. M. Thewissen (ed.), The Emergence of Whales: Evolutionary Patterns in the Origin of Cetacea. Plenum Press, New York.

Uhen, M. D. 2004. Form, function, and anatomy of *Dorudon atrox* (Mammalia, Cetacea): an archaeocete from the middle to late Eocene of Egypt. University of Michigan Papers on Paleontology 34: 1-222.

Uhen, M. D. 2008. New protocetid whales from Alabama and Mississippi, and a new cetacean clade, Pelagiceti. Journal of Vertebrate Paleontology 28: 589-593.

Williams, T. M. 1989. Swimming by sea otters: adaptations for low energetic cost locomotion. Journal of Comparative Physiology A 164: 815-824.

Zhou, X., W. J. Sanders, and P. D. Gingerich. 1992. Functional and behavioral implications of vertebral structure in *Pachyaena ossifraga* (Mammalia, Mesonychia). Contributions from the Museum of Paleontology, University of Michigan 28: 289-319.

Chapter 5

Three-Dimensional Rigid Body Modeling of the L4-L5 Joints in the Archaeocetes *Remingtonocetus domandaensis* and *Maiacetus inuus* (Mammalia, Cetacea)

INTRODUCTION

Virtual 3D modeling is utilized in a range of approaches developed for engineering and manufacturing to investigate complex structures and dynamic systems. In recent years, the technology has been introduced into zoology and paleontology, offering great promise for evolutionary investigation of form and function (O'Higgins et al., 2011). Paleontologists have used this technology in three different ways. Some have used it to articulate entire skeletons in order to test different stances and postures related to locomotion (e.g., Chapman et al., 1999; Walters et al., 2000; Wood et al., 2011). Others have performed finite element analyses to study the stresses and strains on fossil skeletons due to externally applied forces, though this technique has rarely been used to study postcranial material (e.g., Rayfield, 2007, and references therein). Most recently, multibody dynamic analyses have been used to study the actual biomechanics of both living and fossil animals.

Multibody dynamic analyses assess the motion and behavior of systems composed of multiple interconnected objects (O'Higgins et al., 2011). Most studies performed to date have focused on the biomechanics of crania, jaws, and teeth in extant reptiles (Moazen et al., 2008; Curtis et al., 2009, 2010a, 2010b) and mammals (Langenbach et al., 2002, 2006; Curtis et al., 2008), including humans (Koolstra and van Eijden, 2005, 2006). Fossil studies utilizing these methods have included investigation of cranial kinesis in hadrosaurs (Rybczynski et al., 2008), theropod trackways (Gatesy et al., 1999), and the gait and stance of *Tyrannosaurus rex* (Hutchinson et al., 2003, 2005). Multibody studies of vertebral column function are less common. While there are exceptions (e.g., Aziz et al., 2008), most of these studies have focused solely on the human spine (e.g., Sharma et al., 1995; Kumaresan et al., 1999; Lee and Terzopoulos, 2006; Natarajan et al., 2006; Rohlmann et al., 2006; Little and Adam, 2009). Multibody analyses of vertebral function in fossil taxa are nearly absent from the literature.

Stevens and Parrish (1999, 2005) utilized a 3D modeling approach to study the posture of the cervical region in sauropod dinosaurs. Their objective was to determine the neutral positions and relative flexibility of the necks in various taxa, thereby testing hypotheses of their feeding habits. Models were constructed using DinoMorph, a program that builds parametric representations of vertebrae using 24 adjustable parameters (Stevens, 2002). Neutral position and degree of flexibility between adjacent vertebrae were mainly constrained by the position, size, and shape of articulating zygapophyses. Synovial capsules prevent zygapophyseal disarticulation by becoming taut at the extremes of intervertebral movement. Stevens and Parrish (1999) described

how manipulations of muscle and ligament preparations of avian necks demonstrate that the synovial capsules become taut when overlap of articulating zygapophyses is reduced to 50%. They used this criterion for determining the maximum range of motion in the cervical regions of the sauropods under study.

Stevens and Parrish (1999, 2005) recognized that muscles, ligaments, and fascia may have further constrained vertebral movement, describing their results as a "best case" scenario. While some studies of cervical biomechanics have also used this criterion (e.g., Snively and Russell, 2007), others have criticized it (Sander et al., 2009), suggesting that zygapophyseal overlap is a poor criterion for delimiting the extremes of intervertebral motion in modern animals with long necks (Dzemski and Christian, 2007). Stevens and Parrish (1999) certainly attempted to take into account the effects of soft tissue in defining the constraints of their models, but by not explicitly including them in the models, the validity of their results has been called into question.

Soft tissues are critical for understanding the biomechanics of vertebrates (Witmer, 1995; Long et al., 1997; Buchholtz, 2001). The body axis owes its flexibility and elasticity to soft tissues including intervertebral discs, ligaments, and epaxial muscles (Slijper, 1946; Gál, 1993a, 1993b), and only a small fraction of bending stiffness is predicted by skeletal features alone (Long et al., 1997). Recent studies of cranium and jaw biomechanics utilized simulated jaw musculature to predict bite forces and mechanics (Langenbach et al., 2002, 2006; Moazen et al., 2008; Curtis et al., 2010a, 2010b) and temporomandibular joint load (Koolstra and van Eijden, 2005, 2006; Moazen et al., 2008; Curtis et al., 2010a). Multibody dynamic studies of the vertebral column

have focused on the role of epaxial muscles in moving the spine (Lee and Terzopoulos, 2006; Rohlmann et al., 2006) and the role of ligaments and intervertebral discs in maintaining the stability of the spine and passively resisting movement (Sharma et al., 1995; Kumaresan et al., 1999; Natarajan et al., 2006; Aziz et al., 2008; Little and Adam, 2009). However, such studies of the vertebral column rarely extend beyond medical research on humans.

Multibody dynamic modeling offers an additional means to test functional hypotheses in fossil taxa. In this chapter, I describe a study using 3D rigid body modeling to compare the passive resistance to flexion and extension in the L4-L5 joints of *Remingtonocetus domandaensis* and *Maiacetus inuus*. These models include reconstructed intervertebral discs and simulated ligaments to further constrain intervertebral motion above and beyond any osteologically-defined limits. Ranges of motion in flexion and extension are estimated in response to applied moments for a variety of conditions in order to understand the effects of individual ligaments and their properties. Range of motion comparisons between *R. domandaensis* and *M. inuus* in these trials provide insight into the functional differences in the lumbar spines of these taxa, which is relevant for understanding their locomotor behaviors.

MATERIALS AND METHODS

Specimens

GSP-UM 3551 and 3552 are the most complete specimens of *Maiacetus inuus* and *Remingtonocetus domandaensis*, respectively. L4 and L5 vertebrae in both were

preserved in articulation and are nearly complete. The distal neural spines and transverse processes are missing on L4 and L5 of GSP-UM 3551, as is the distal neural spine on L4 in GSP-UM 3552. However, the articulating pre- and postzygapophyses in both specimens are intact. Thus, because the L4-L5 joint was well-preserved in both specimens, it was selected as the exemplar joint for this study.

Methods

Constructing the Vertebral Models — Vertebrae were scanned using a NextEngine Desktop 3D Laser Scanner (Model 2020i). Meshes were aligned, fused, patched, smoothed, and decimated (to reduce the time needed to run simulations) using NextEngine ScanStudio Core software (Version 1.7.3) and exported as stereolithography (STL) files. These files were imported into Autodesk 3ds Max 2010 (formerly known as 3D Studio Max) and converted into editable meshes. *Bend* modifiers were applied to models as necessary to correct bent processes, such as neural spines. *Stretch* modifiers were applied to models to reconstruct incomplete neural spines when necessary. *Symmetry* modifiers were then used to make each model bilaterally symmetrical, reflecting the left side in both cases. After all necessary modifications, the edited models were exported as STLs to be used in the rigid-body dynamics simulations.

Assembling the Multibody Dynamic Models — For each species, symmetrical STLs of L4 and L5 vertebrae were imported into Visual-Safe MAD 6.0 (by ESI Group) for pre-processing. Vertebrae were aligned in the reference space with the x-axis

representing the anteroposterior axis, the y-axis representing the dorsoventral axis, and the z-axis representing the bilateral axis. Vertebrae were placed such that the postzygapophyses of L4 were centered over the prezygapophyses of L5 and the centra were spaced to the same degree as the articulated specimens were preserved (approximately 10 mm in both cases; Fig. 5.1). Vertebral surfaces were converted into finite element models and assigned a null material. A node-to-surface-intersect contact was defined between the vertebrae, essentially making them rigid bodies and preventing intersection of their surfaces.

An intervertebral disc (IVD) was created for each joint because it plays a prominent role in resisting most intervertebral movements (Gál, 1993b). Previous studies have modeled IVDs in many different ways. Some studies have modeled an IVD using a single homogeneous material (Aziz et al., 2008), while others built very complex models, in which all elements of an IVD (annulus fibrosus, nucleus pulposus, and collagen fibers) were created separately (Rohlmann et al., 2006; Little and Adam, 2009). Nothing is known about the structure of IVDs in early cetaceans, so they are conservatively constructed here using a single homogeneous material (following Aziz et al., 2008).

The discs themselves were created de novo using the Mesh context of Visual-Safe MAD. The shape of each disc was derived from the shapes of the corresponding vertebral epiphyses on either end of the disc (following Little and Adam, 2009). The anterior epiphyseal surface of L5 was copied, aligned to a curve marking the boundary of the disc, and remeshed to convert the surface features from triads to quadrilaterals.

This new mesh was then copied, thus providing two meshes with matching quadrilateral features to serve as the anterior and posterior faces of the IVD. The nodes of these meshes were then projected onto the appropriate epiphyseal surfaces, allowing the faces of the IVD to match the contours of the centrum faces and ensuring that there was no overlap between the vertebrae and IVD. Three layers of bricks were then created, connecting the anterior and posterior faces of the IVD, to complete construction of the disc mesh (Fig. 5.1).

There is also a wide array of intervertebral ligaments that help to resist flexion and extension in modern mammals. The supraspinous (SSL) and interspinous (ISL) ligaments run between adjacent neural spines and are stretched during flexion. These ligaments are typically highly extensible, thus contributing relatively little to resisting flexion (Adams et al., 1980; Hukins et al., 1990). The ligamenta flava (LF) run between the laminae of the neural arches, just dorsal to the neural canal. These ligaments often serve as some of the primary resistance to vertebral flexion in modern mammals (Dumas et al., 1987; Adams et al., 1988; Hukins et al., 1990; Gál, 1993b; Gillespie and Dickey, 2004). The synovial capsules or capsular ligaments (CL) of the zygapophyses prevent dislocation of articulated pre- and postzygapophyses. In many cases, they serve as some of the principal resistance to both flexion and extension (Adams et al., 1980; Dumas et al., 1987; Gál, 1993b; Sharma et al., 1995). Anterior (ALL) and posterior (PLL) longitudinal ligaments run between ventral and dorsal aspects of adjacent centra. When studied, the ALL and PLL, which resist extension and flexion respectively (Panjabi

et al., 1975), typically rank as some of the stiffest intervertebral ligaments (Hukins et al., 1990; Sharma et al., 1995).

Some multibody dynamic analyses reconstructed intervertebral ligaments as finite element models (e.g., Kumaresan et al., 1999), but most have modeled them as tension-only connector elements or springs (e.g., Rohlmann et al., 2006; Aziz et al., 2008; Little and Adam, 2009). Ligaments were modeled in Visual-Safe MAD using Kelvin restraint elements, which consist of a spring and a damper in parallel. The dampers were inactivated in these models, making the Kelvin restraints tension-only springs.

Simulated ligaments are illustrated in Figure 5.2. The SSL restraints connected the apices of the neural spines. The ISL restraints connected the blades of the neural spines, about halfway along their heights. Parallel right and left LF restraints ran from the ligamentous pits present in the anterior laminae of L5 to the posterior neural arch of L4, just dorsal to the neural canal. Right and left CL restraints were idealized as a single connection between the centers of overlapping zygapophyseal faces (following Little and Adam, 2009). PLL and ALL restraints ran along the midline, connecting the dorsal and ventral aspects of the centra respectively.

Material Properties — Ideally, the material properties of the soft tissues modeled here would come from studies of the vertebral column in modern cetaceans or artiodactyls. Unfortunately, there are very few data available for non-humans in the literature (Aziz et al., 2008; Busscher et al., 2010). A number of studies have shown that quadrupeds can serve as suitable models for human spines in certain situations (Wilke et al., 1997a, 1997b; Smit, 2002; Schmidt et al., 2005; Busscher et al., 2010), but it is

rarely asked whether the converse is true. The loading regimes of human and quadruped spines are essentially the same (Smit, 2002), and comparative studies have shown that the basic mechanisms of passive resistance in the vertebral column transcend differences in taxonomy, posture, and locomotion (Gál, 1993b). Thus, given these basic similarities and the paucity of non-human data in the literature, it is here deemed reasonable to use data from studies of the human spine to serve as a starting point for the properties of the soft tissues modeled in this study.

The material used here to construct the IVDs required definition of an elastic modulus and density. Values ranging from 2.56 MPa (Natarajan et al., 2006) to 4.20 MPa (Goel et al., 1995; Sharma et al., 1995) have been utilized for the elastic modulus of the IVD annulus fibrosus in previous studies. A median value of 3.15 MPa (Rohlmann et al., 2006) is used here as a baseline. Density estimates of IVDs are unavailable in the literature. Since the IVD is about 75% water (Martini et al., 2000; Natarajan et al., 2006), the density of water (1000 kg/m^3) was used here as an estimate of IVD density.

The load-elongation relationships of ligaments are not linear (Chazal et al., 1985). Thus, each ligament was assigned a unique force-displacement curve to define its properties. Rohlmann et al. (2006) provided ligament stiffnesses for three different strain ranges for all of the ligaments included here. This data provides the baseline properties for the ligaments in this analysis (Table 5.1).

Effects of Soft Tissue Parameters — Variation in the material properties of soft tissues can significantly alter the degree of angular motion at an intervertebral joint (Kumaresan et al., 1999). In order to determine how sensitive the results of these

simulations are to the assigned properties of the soft tissues, a series of trials (Table 5.2) was performed, varying the stiffnesses for the IVD and all the ligaments (following Little and Adam, 2009). For the trials in which the stiffness of the IVD was changed, the elastic modulus was decreased or increased by the percentage indicated. For the trials in which the stiffnesses of the ligaments were altered, the stiffnesses for each of the strain ranges were decreased or increased by 25% (Table 5.1).

In addition, a series of trials (Table 5.2) was performed, excluding each ligament in turn (following Aziz et al., 2008). These trials allow the relative contribution of each ligament to resisting flexion and extension to be quantified. The baseline properties of the IVD and ligaments were maintained in these trials.

Simulations — For each set of conditions, a pure moment of 12 Nm was applied to the L4 vertebra, with the L5 vertebra locked in place, to produce either extension (dorsal bending) or flexion (ventral bending). An output body was created to measure the angular displacement of L4 during the simulation. Completed models, which included vertebrae, IVDs, ligaments, applied moments, and output bodies, were exported from Visual-Safe MAD as extensible markup language (XML) files. These files were then processed using MADYMO (by TNO Automotive Safety Solutions, or TASS), a mathematical dynamic modeling solver that can process multibody, finite element, and computation fluid dynamic models. The output files produced by the MADYMO simulation were then imported back into Visual-Safe MAD for visualization and analysis.

RESULTS

The results of all trials are summarized in Table 5.3 and Figures 5.3-5.4. For the base condition, the L4-L5 joint of *Remingtonocetus domandaensis* exhibits a total sagittal range of motion (ROM) of 7.92°, with slightly greater flexibility in extension (4.07°) compared to flexion (3.84°). The L4-L5 joint of *Maiacetus inuus* exhibits a total ROM (8.79°) 11.0% greater than that of *R. domandaensis*, with much greater flexibility in extension (5.18°) compared to flexion (3.61°).

In most cases, variations in soft tissue properties affect *Remingtonocetus domandaensis* and *Maiacetus inuus* similarly, so these results are discussed together. Differences in the stiffness of IVDs do relatively little to affect total ROM in most cases (Fig. 5.5). IVDs with elastic moduli between 10% and 75% of the base value increase total ROM by 1.6%-7.9%. A 25% increase in the elastic moduli of IVDs decreases the total ROM by just 1.6%-1.8%. The one change in IVD stiffness that alters total ROM significantly is increasing the elastic modulus by an order of magnitude (1000%). This greatly reduces the total ROM by 41.4%-44.7%.

Differences in ligament stiffness have a greater impact on total ROM than differences in IVD stiffness (Fig. 5.5). A 25% reduction in ligament stiffness increases total ROM by 13.2%-14.3%. A 25% increase in ligament stiffness decreases total ROM by 9.5-9.8%. While the absolute angles of rotation differ for each set of soft tissue properties, the differences in ROM between *Remingtonocetus domandaensis* and *Maiacetus inuus* are similar, regardless of condition. In each trial, *M. inuus* possesses a total ROM 9.5%-17.7% greater than that of *R. domandaensis* (Fig. 5.3).

Removal of individual ligaments increased the ROM relative to the base condition in every case, though the differences for some ligaments were negligible (Figs. 5.4-5.5). Joints lacking the ISL (0.7%-0.8%) and PLL (0.7%-1.4%) exhibit only very slight increases in ROM. Joints lacking the LF (2.4%-3.3%) and SSL (3.0%-3.7%) exhibit slightly greater increases in ROM, though these increases pale in comparison to the increases brought on by removal of the ALL and CLs, which increase ROM by 54.1%-62.6% and 57.9%-81.4% respectively.

In most cases, removal of a given ligament does relatively little to affect the ROM difference between *Remingtonocetus domandaensis* and *Maiacetus inuus*, with *M. inuus* exhibiting a greater ROM than *R. domandaensis* in all but one trial. Configurations lacking the ISL, LF, PLL, and SSL result in differences (11.1%-12.0%) that are very close to that of the base condition (11.0%). Removal of the ALL results in a much larger difference (17.2%). The lone exception occurs in joints lacking CLs. This represents the only set of conditions in which *R. domandaensis* exhibits a greater total ROM (14.36°) than *M. inuus* (13.88°), though the difference is just 3.4%.

DISCUSSION

Range of Motion

For the base set of conditions, the L4-L5 joint of *Remingtonocetus domandaensis* exhibited a ROM of 7.92°, while that of *Maiacetus inuus* exhibited a ROM of 8.79°. These values fall within the ROMs documented or estimated for the lumbar joints of several other mammals. Human lumbar joints exhibit ROMs from about 7°-10° (Hukins

et al., 1990; Sharma et al., 1995). This range is not significantly different from those of pigs (6.5° for the L4-L5 joint; Aziz et al., 2008), sheep (7.13°-11.01°; Wilke et al., 1997a), or bovine calves (5.3°-10.4°; Wilke et al., 1997b). However, all of these values are significantly less than those documented for *Oryctolagus cuniculus* (domestic rabbit), which exhibited lumbar ROMs ranging from 17.96°-21.30° (Grauer et al., 2000).

Yet it is difficult to compare the results obtained here with those of prior studies due to the use of different methods. Some of the aforementioned results were obtained from measurements of ligamentous preparations of vertebral columns (e.g., Hukins et al., 1990; Wilke et al., 1997a, 1997b; Grauer et al., 2000), while others were obtained from studies utilizing finite element models and multibody dynamic modeling (e.g., Sharma et al., 1995; Aziz et al., 2008). Even when similar methods are used, however, results can differ significantly from study to study. ROM data for human spines, in particular, have been shown to vary widely from one analysis to another (Wilke et al., 1997a, 1997b). This underscores the importance of carrying out comparative studies that utilize identical parameters for the subjects under study, as this is essential for any reliable conclusions to be drawn.

In the case of this study, the most relevant comparison is not between the archaeocetes studied here and any modern taxa, but between the archaeocetes themselves. Because conditions were held constant, any differences in the ROM between *Remingtonocetus domandaensis* and *Maiacetus inuus* are attributable to the vertebral morphology itself and how that affects the architecture of the reconstructed soft tissues. The ROM of *M. inuus* for the base condition is 0.87° (or 11.0%) greater than

that of *R. domandaensis*. But this, of course, raises the question: how significant is that difference?

Few studies have quantified the ROMs of multiple taxa using precisely the same setup and conditions. Schmidt et al. (2005) measured the ROMs of vertebral segments in human and porcine cervical spines. They found that the total dorsoventral ROMs of the C2-T1 segments were about 22.4° in pigs and 20.4° in humans, resulting in a difference of just 2.0° (or approximately 0.3° per joint). Their findings were based on studies of six human and six porcine spines, so they were also able to determine that the ranges of values exhibited by each taxon were nearly identical. Based on this data, they argued that the porcine cervical spine was a good model for the human cervical spine in flexion and extension due to their biomechanical similarities.

It would be ideal if multiple vertebral positions from several individuals of *Remingtonocetus domandaensis* and *Maiacetus inuus* could be compared to determine, with some statistical confidence, how different the ROMs in these taxa are. However, this is not currently possible. First of all, the specimens studied here are the only known specimens of these taxa complete enough to enable this type of study. And, secondly, the L4-L5 joint was chosen in particular because it is one of the few joints with all zygapophyses intact in both specimens. One alternative way to shed light on whether or not the ROM difference between these taxa is significant is to study the same joint in other archaeocetes, including both more primitive and more derived taxa. This would provide a more comprehensive assessment of the range of flexibilities present in early

cetaceans and give some context to the difference observed between *R. domandaensis* and *M. inuus*.

Effects of Soft Tissue Properties

Changes in soft tissue properties affect the absolute ROM in every trial, with changes in ligament stiffness generally having larger effects on ROM than IVD stiffness (except when increasing the stiffness of the IVD by an order of magnitude). These results differ from those of Little and Adam (2009), who found that differences in IVD stiffness had a greater effect on ROM, even with smaller changes in parameters. This difference can likely be attributed to the fact that Little and Adam (2009) constructed a much more complex IVD, simulating the annulus fibrosus, nucleus pulposus, and collagen ligaments separately. It is likely that the behavior of these more complex IVDs represent a closer approximation to the behavior of actual IVDs, suggesting that the effects found by Little and Adam (2009) may be more accurate. However, while this may affect the *absolute* results of the simulations performed here, it should not affect the *comparative* results because the IVDs of *Remingtonocetus domandaensis* and *Maiacetus inuus* were modeled the same way.

The absolute ROMs exhibited by these models can change significantly depending on the soft tissue parameters used, a finding which is certainly no surprise. Yet the relative difference in ROM between the taxa studied here changes little with different soft tissue properties. *Maiacetus inuus* maintains a ROM 9.5%-17.7% greater than that of *Remingtonocetus domandaensis* in all of the trials testing the sensitivity of

the models to soft tissue parameters. These results demonstrate that this disparity is due to differences in morphology and the subsequent architecture of the modeled soft tissues, not simply the properties assigned to the IVD and individual ligaments. While it is desirable for multibody dynamic simulations to approximate the actual biomechanics of a system as closely as possible, the validity of comparative analyses need not rest on the achievement of this ideal situation, since the conditions should be the same in all individuals being compared.

Effects of Individual Ligaments

Trials involving systematic removal of individual ligaments shed light on which elements of the model contribute the most to resisting intervertebral motion. This study finds that the ALL and CLs contribute much more to motion resistance than any of the other ligaments, with the SSL, LF, PLL, and ISL all contributing relatively little. This is generally consistent with previous studies. The ALL is generally found to be the stiffest (thus, most restrictive) of the intervertebral ligaments (Panjabi et al., 1975; Dumas et al., 1987; Myklebust et al., 1988; Hukins et al., 1990; Richter et al., 2000; Rohlmann et al., 2006), and zygapophyseal joints are known to play a critical role in restricting motion, especially in extension (Adams et al., 1980; Sharma et al., 1995; Aziz et al., 2008). However, the relatively low resistance contributed by the LF in the simulations here is surprising based on prior analyzes of vertebral function.

Studies of intact vertebral columns have shown the LF to be significant contributors to the resistance of flexion (Chazal et al., 1985; Gillespie and Dickey, 2004).

The multibody dynamic model of Aziz et al. (2008) also demonstrated that intervertebral motion increased substantially in the absence of LF. However, they modeled the LF differently, using a bundle of springs (the exact number was not specified) to simulate the LF. In the models performed here, LF were simulated by two restraints, one on either side of the midline. Had additional restraints been added, akin to the model of Aziz et al. (2008), it undoubtedly would have increased the relative contribution of the LF to resisting flexion. But, again, while this may affect the absolute values of the resultant ROMs, it should not significantly affect the comparative difference between *Remingtonocetus domandaensis* and *Maiacetus inuus* since the LF of both taxa were modeled the same way.

Systematic removal of individual ligaments also helps to elucidate what exactly contributes to the differences observed between the taxa under study. For nearly all of the trials in which ligaments were removed, *Maiacetus inuus* maintains a ROM 11.1%-17.2% greater than that of *Remingtonocetus domandaensis*. The lone exception occurs in the trials lacking CLs. Removal of right and left CLs causes the ROM exhibited by *R. domandaensis* to increase by 81.4% to 14.36°. *M. inuus* displays a more modest, though still significant, increase of 57.9% to 13.88°. This is the only case in which the ROM of *R. domandaensis* is greater than that of *M. inuus* (though by just 3.4%). This is likely due to differences in the orientation of their zygapophyses and the implications that has for the architecture of the CLs.

Several studies have shown that the primary resistance at zygapophyseal joints is not due to bony contact, but almost entirely due to the CLs (Adams et al., 1988; Sharma

et al., 1995), at least in taxa with non-revolute zygapophyses (Gál, 1993b). The fibers of CLs are arranged at right angles to the zygapophyseal surfaces (Panjabi et al., 1975); thus, a difference in the orientation of the zygapophyses results in a difference in the orientation of the ligaments. The strain incurred by any ligament is sensitive to its orientation with respect to the plane in which motion occurs (Sharma et al., 1995), so even if the force-displacement properties of two ligaments are the same (as they are here), they could behave very differently depending on their orientation.

The zygapophyses of L4 and L5 in *Remingtonocetus domandaensis* and *Maiacetus inuus* are slightly different from one another. The prezygapophyses of L5 in *R. domandaensis* face dorsomedially, resulting in CLs that are angled more medially to attach to the postzygapophyses of L4. The prezygapophyses of L5 in *M. inuus* also face dorsomedially, but have a much stronger dorsal component. This results in the CLs having less of a medial, and more of a dorsal orientation. Given that the motion is occurring in the sagittal plane, this should stretch the CLs of *M. inuus* less than those of *R. domandaensis* for a given angle of rotation. For the base conditions, the CLs of *R. domandaensis* are stretched to about 166% of their original lengths during maximum flexion and extension, while those of *M. inuus* are stretched to about 153% of their original lengths. Because these ligaments were assigned the same force-displacement properties, the CLs of *R. domandaensis* were being strained more than those of *M. inuus*, thus contributing greater resistance to flexion and extension.

Given the similarity in ROMs between *Remingtonocetus domandaensis* and *Maiacetus inuus* when CLs are removed, it appears that differences in ROMs in all other

trials are largely due to differences in CL strain caused by zygapophyseal morphology. The more dorsally-oriented prezygapophyses of L5 in *M. inuus* allowed the CLs to experience less strain in flexion and extension than the more medially-oriented prezygapophyses of L5 in *R. domandaensis*, resulting in an intervertebral joint that was less restrictive to dorsoventral motion. These results validate the attention paid to zygapophyseal joint morphology in discerning the relative mobility of the spine in extinct taxa. However, except in cases in which taxa possess revolute zygapophyses (Gál, 1993b), it is likely not bony contact between the joint surfaces themselves that restricts motion, but rather the strain experienced by the CLs due to the zygapophyseal morphology.

Conclusions

The multibody dynamic modeling simulations performed here allow the relative mobility of the L4-L5 joints in *Remingtonocetus domandaensis* and *Maiacetus inuus* to be compared quantitatively, while taking into account the biomechanical effects of soft tissue. For nearly all sets of conditions, the L4-L5 joint of *M. inuus* exhibits a greater ROM than the same joint of *R. domandaensis*. These results support the conclusions of the multivariate analyses in Chapter 4, which suggested that *M. inuus* had a more mobile lumbar spine than *R. domandaensis*.

Trials systematically removing individual ligaments demonstrate that the disparity between taxa is due primarily to the CLs, which are oriented differently in the two species due to differences in zygapophyseal morphology. The 0.87° (or 11.0%)

difference in ROM between *Remingtonocetus domandaensis* and *Maiacetus inuus* (using base conditions) appears rather modest, but if a similar difference is exhibited across all lumbar joints (T13-L1 through L6-S1), it would result in the lumbar region of *M. inuus* having a ROM 6.09° greater than that of *R. domandaensis*. This disparity could have important functional implications for locomotor mode. Determination of the significance of this difference will require study of lumbar joints from additional archaeocete taxa to provide a broader context for comparison.

This study also underscores the importance of a comparative framework for these types of analyses, echoing recent reviews of the potential for this type of technology (Rayfield, 2007; O'Higgins et al., 2011). Given current knowledge, it is difficult, if not impossible, to ascertain how close the ROM estimates generated here approximate the actual mobility these fossil animals were capable of in life. But despite this uncertainty, the results of comparative analyses offer valuable information about the relative capabilities of extinct creatures (Rayfield, 2007). Three-dimensional virtual analyses provide a highly controlled and quantitative means of quantitatively testing functional hypotheses. As long as they are utilized in a comparative framework, they offer much potential for studying the evolutionary biomechanics of extinct forms.

Figure 5.1. Rigid body models of the L4-L5 joints of *Remingtonocetus domandaensis* and *Maiacetus inuus* in right lateral (A) and dorsal (B) views. Anterior is to the right. Axes in 3D coordinate space are indicated at left. Methods for generating the vertebral surfaces and intervertebral discs are described in the text.

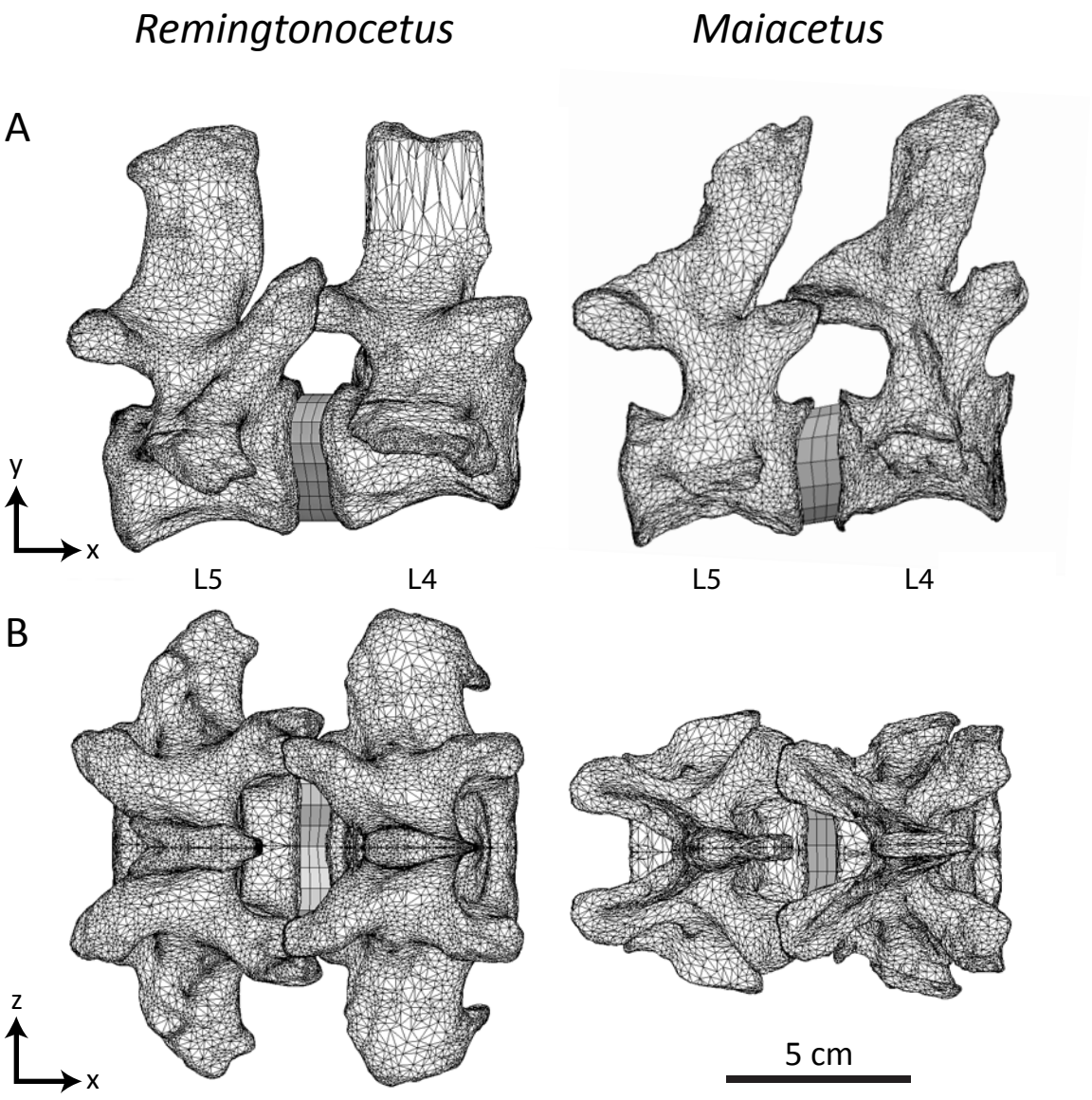

Figure 5.2. Ligaments simulated in multibody dynamic models, illustrated for *Remingtonocetus domandaensis*. Axes in 3D coordinate space are indicated at the left of each figure. A. Midline ligaments pictured in right lateral view (anterior to the right), including the supraspinous ligament (SSL), interspinous ligament (ISL), posterior longitudinal ligament (PLL), and anterior longitudinal ligament (ALL). B. Right and left ligamenta flava (LF) pictured in dorsal view (anterior to the right). C. Right capsular ligament (CL) pictured in posterior view between right postzygapophysis (PosZ) of L4 and right prezygapophysis (PreZ) of L5. The left CL is not pictured.

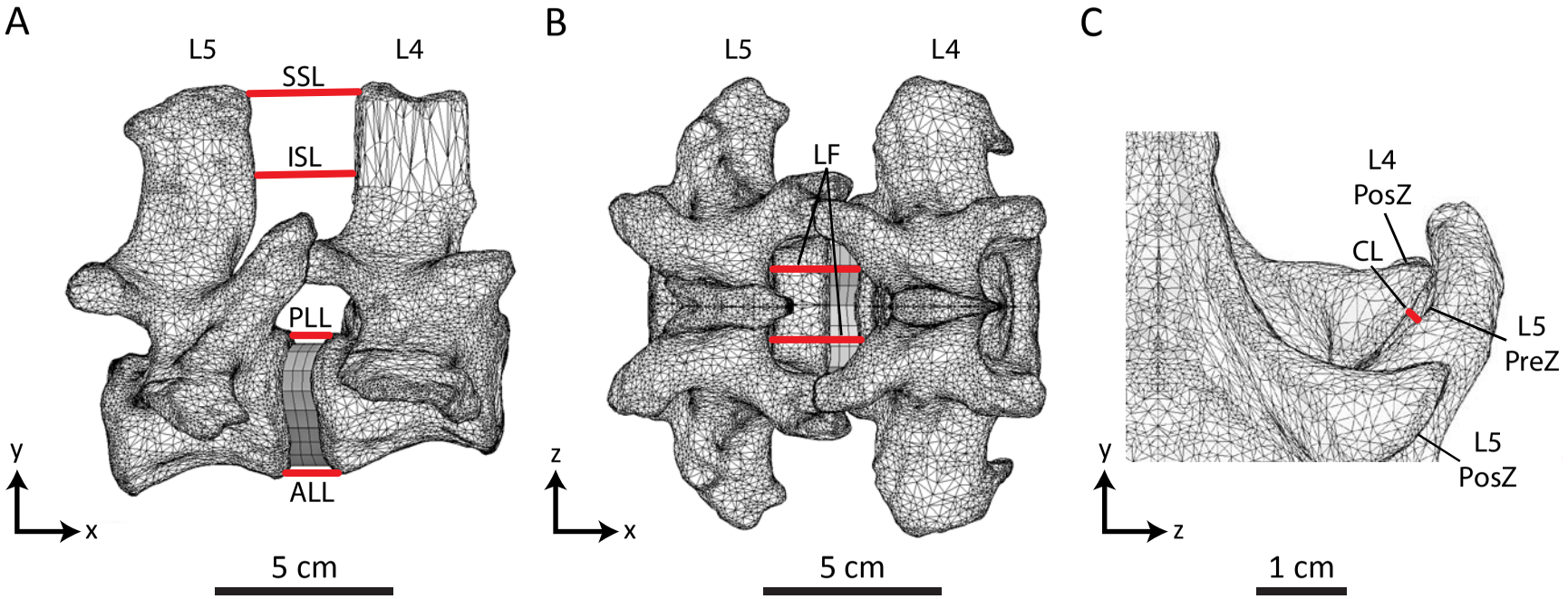

Figure 5.3. Total range of motion (extension + flexion) for L4-L5 joints of *Remingtonocetus domandaensis* and *Maiacetus inuus* with varying soft tissue parameters. Trial conditions are described in Table 5.2. Note the relative uniformity of the difference between *R. domandaensis* and *M. inuus* regardless of the trial.

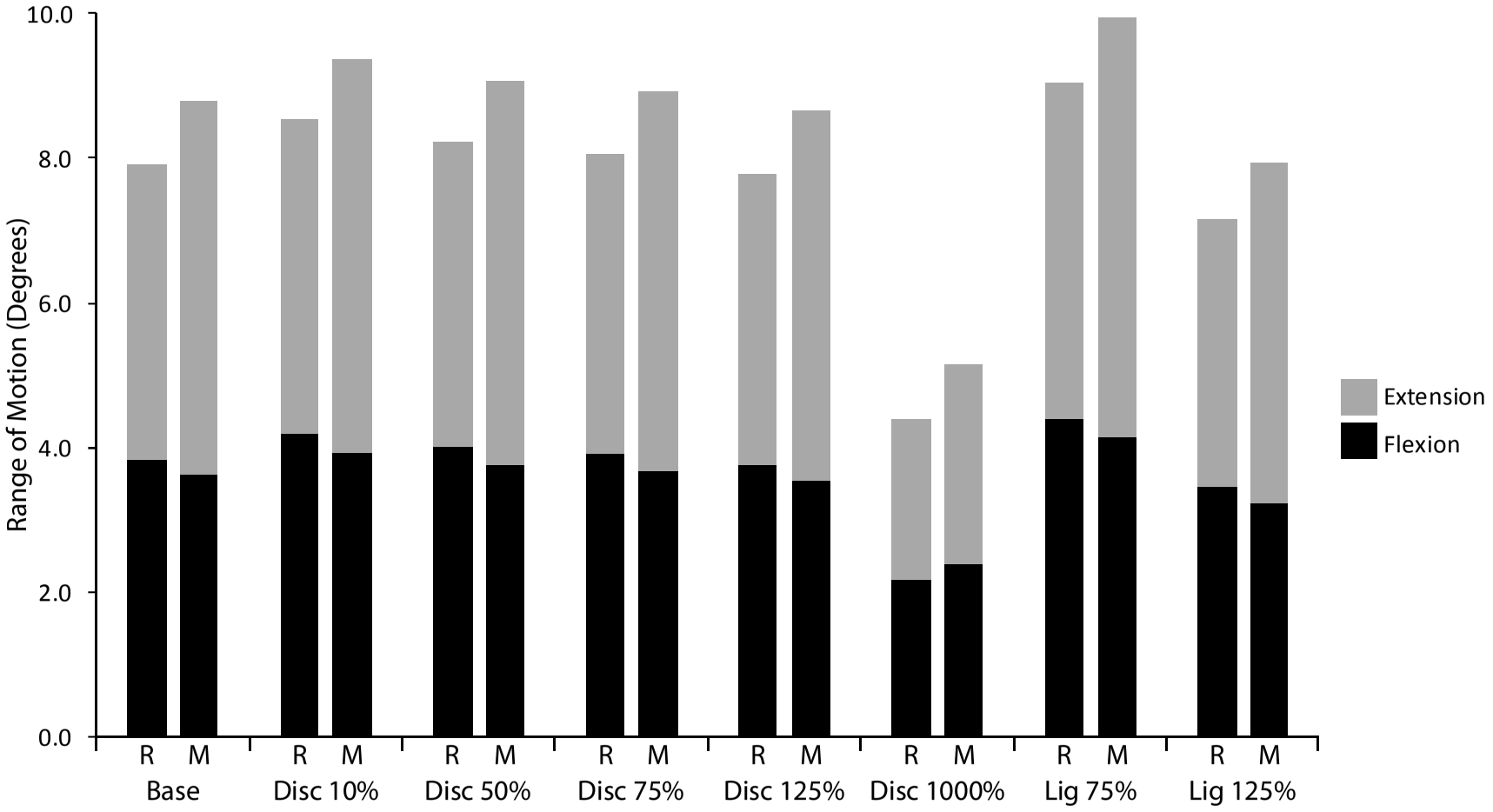

Figure 5.4. Total range of motion (extension + flexion) for L4-L5 joints of *Remingtonocetus domandaensis* and *Maiacetus inuus* with various ligaments removed from the models. Trial conditions are described in Table 5.2. Note the relative uniformity of the difference between *R. domandaensis* and *M. inuus* in all trials, except for the trials in which the capsular ligaments were removed (No CL).

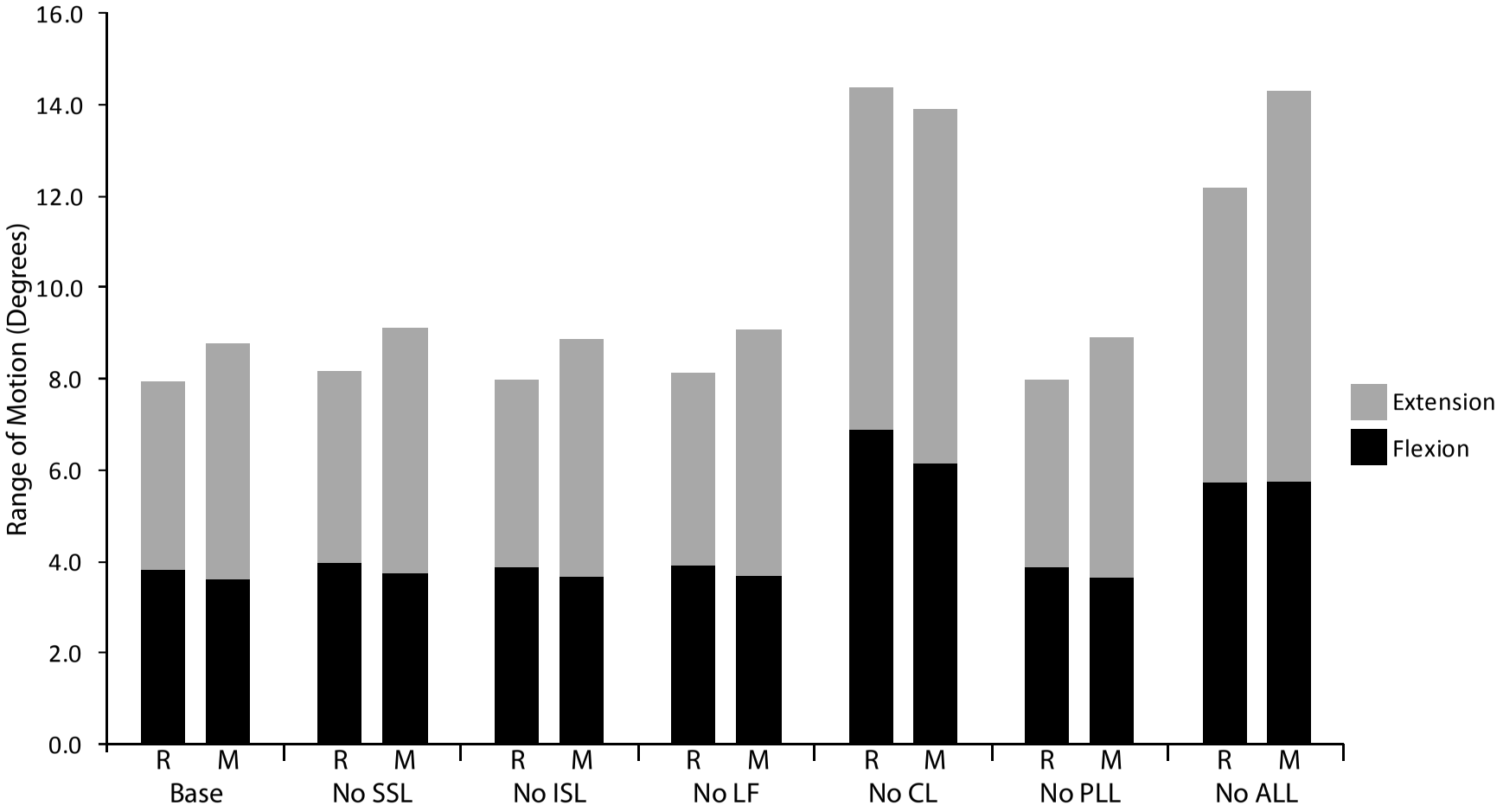

Figure 5.5. Differences in total range of motion (ROM) between base conditions and trial conditions for the L4-L5 joints of *Remingtonocetus domandaensis* (A) and *Maiacetus inuus* (B). Trial conditions are described in Table 5.2. Positive differences indicate increased ROM compared to base conditions, while negative differences indicate decreased ROM compared to base conditions. Note the similar patterns between the two taxa, except for the trials in which capsular ligaments were removed (No CL).

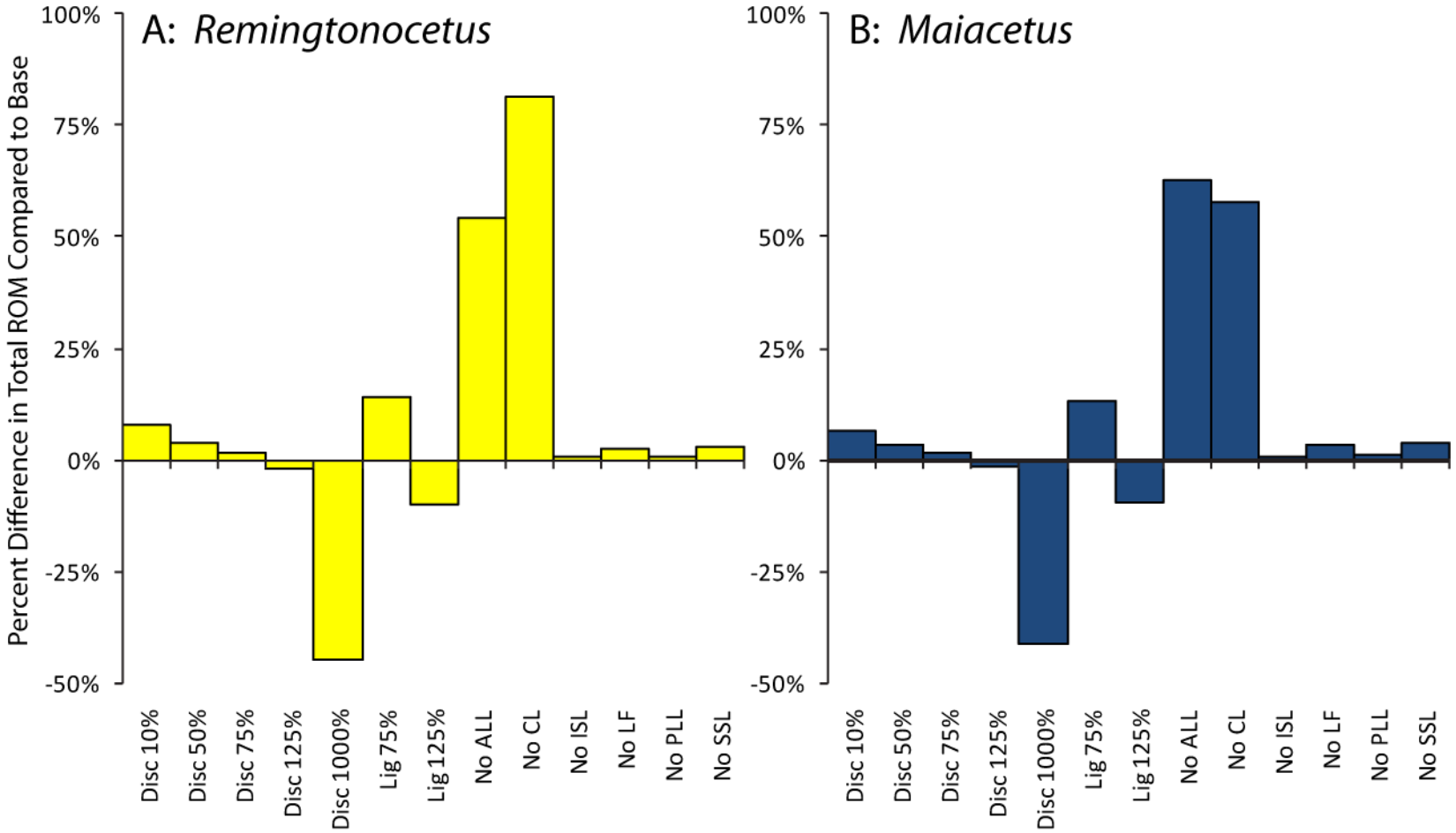

Table 5.1. Force-displacement properties of modeled ligaments for three strain ranges. Data are from Rohlmann et al. (2006). Strain percentages are for increases over original length. Stiffness is measured in N/mm. Trials varying ligament stiffness are described in Table 5.2. Abbreviations: anterior longitudinal ligament (ALL), capsular ligaments (CL), interspinous ligaments (ISL), ligamenta flava (LF), posterior longitudinal ligaments (PLL), and supraspinous ligament (SSL).

	Ligament	Strains	Stiffness	Strains	Stiffness	Strains	Stiffness
Base	ALL	0.0% - 12.2%	347.0	12.2% - 20.3%	787.0	> 20.3%	1864.0
	CL	0.0% - 25.0%	36.0	25.0% - 30.0%	159.0	> 30.0%	384.0
	ISL	0.0% - 13.9%	1.4	13.9% - 20.0%	1.5	> 20.0%	14.7
	LF	0.0% - 5.9%	7.7	5.9% - 49.0%	9.6	> 49.0%	58.2
	PLL	0.0% - 11.1%	29.5	11.1% - 23.0%	61.7	> 23.0%	236.0
	SSL	0.0% - 20.0%	2.5	20.0% - 25.0%	5.3	> 25.0%	34.0
Lig 75%	ALL	0.0% - 12.2%	260.3	12.2% - 20.3%	590.3	> 20.3%	1398.0
	CL	0.0% - 25.0%	27.0	25.0% - 30.0%	119.3	> 30.0%	288.0
	ISL	0.0% - 13.9%	1.1	13.9% - 20.0%	1.1	> 20.0%	11.0
	LF	0.0% - 5.9%	5.8	5.9% - 49.0%	7.2	> 49.0%	43.7
	PLL	0.0% - 11.1%	22.1	11.1% - 23.0%	46.3	> 23.0%	177.0
	SSL	0.0% - 20.0%	1.9	20.0% - 25.0%	4.0	> 25.0%	25.5
Lig 125%	ALL	0.0% - 12.2%	433.8	12.2% - 20.3%	983.8	> 20.3%	2330.0
	CL	0.0% - 25.0%	45.0	25.0% - 30.0%	198.8	> 30.0%	480.0
	ISL	0.0% - 13.9%	1.8	13.9% - 20.0%	1.9	> 20.0%	18.4
	LF	0.0% - 5.9%	9.6	5.9% - 49.0%	12.0	> 49.0%	72.8
	PLL	0.0% - 11.1%	36.9	11.1% - 23.0%	77.1	> 23.0%	295.0
	SSL	0.0% - 20.0%	3.1	20.0% - 25.0%	6.6	> 25.0%	42.5

Table 5.2. Simulation trials with varying soft tissue properties and conditions.

Condition	Description
Base	All ligaments present; IVD and ligament stiffness at 100% of base
Disc 10%	All ligaments present; IVD stiffness reduced to 10% of base
Disc 50%	All ligaments present; IVD stiffness reduced to 50% of base
Disc 75%	All ligaments present; IVD stiffness reduced to 75% of base
Disc 125%	All ligaments present; IVD stiffness increased to 125% of base
Disc 1000%	All ligaments present; IVD stiffness increased to 1000% of base
Lig 75%	All ligaments present; ligament stiffness reduced to 75% of base
Lig 125%	All ligaments present; ligament stiffness increased to 125% of base
No ALL	ALL removed; IVD and ligament stiffness at 100% of base
No CL	CL removed; IVD and ligament stiffness at 100% of base
No ISL	ISL removed; IVD and ligament stiffness at 100% of base
No LF	LF removed; IVD and ligament stiffness at 100% of base
No PLL	PLL removed; IVD and ligament stiffness at 100% of base
No SSL	SSL removed; IVD and ligament stiffness at 100% of base

Table 5.3. Range of motion results (measured in degrees) compared for *Remingtonocetus domandaensis* and *Maiacetus inuus* for all trial conditions. Positive differences indicate a greater ROM for *M. inuus* for a given set of conditions, while negative differences indicate a greater ROM for *R. domandaensis* for a given set of conditions. These results are also summarized in Figures 5.3-5.4.

Condition	*Remingtonocetus*			*Maiacetus*			Extension Difference		Flexion Difference		ROM Difference	
	Extension	Flexion	ROM	Extension	Flexion	ROM	Absolute	Percent	Absolute	Percent	Absolute	Percent
Base	4.07	3.84	7.92	5.18	3.61	8.79	1.11	27.1%	-0.23	-6.1%	0.87	11.0%
Disc 10%	4.35	4.19	8.54	5.43	3.92	9.36	1.08	24.7%	-0.26	-6.3%	0.81	9.5%
Disc 50%	4.22	4.00	8.23	5.32	3.75	9.07	1.10	26.1%	-0.26	-6.4%	0.84	10.2%
Disc 75%	4.14	3.92	8.06	5.25	3.67	8.93	1.11	26.8%	-0.25	-6.3%	0.87	10.7%
Disc 125%	4.00	3.77	7.78	5.11	3.55	8.65	1.10	27.5%	-0.22	-5.9%	0.88	11.3%
Disc 1000%	2.22	2.16	4.38	2.76	2.39	5.15	0.54	24.5%	0.23	10.6%	0.77	17.7%
Lig 75%	4.65	4.40	9.05	5.80	4.15	9.95	1.16	24.9%	-0.25	-5.7%	0.91	10.0%
Lig 125%	3.67	3.47	7.14	4.71	3.24	7.95	1.04	28.2%	-0.22	-6.4%	0.81	11.4%
No ALL	6.43	5.76	12.20	8.55	5.74	14.30	2.12	32.9%	-0.02	-0.4%	2.10	17.2%
No CL	7.48	6.88	14.36	7.73	6.14	13.88	0.25	3.4%	-0.74	-10.7%	-0.49	-3.4%
No ISL	4.10	3.87	7.97	5.23	3.63	8.86	1.12	27.4%	-0.23	-6.1%	0.89	11.1%
No LF	4.18	3.93	8.11	5.38	3.70	9.08	1.20	28.8%	-0.23	-5.8%	0.97	12.0%
No PLL	4.10	3.87	7.98	5.27	3.64	8.91	1.16	28.4%	-0.23	-5.9%	0.93	11.7%
No SSL	4.20	3.95	8.15	5.39	3.72	9.11	1.19	28.2%	-0.23	-5.8%	0.96	11.7%

REFERENCES

Adams, M. A., P. Dolan, and W. C. Hutton. 1988. The lumbar spine in backward bending. Spine 13: 1019-1026.

Adams, M. A., W. C. Hutton, and J. R. R. Stott. 1980. The resistance to flexion of the lumbar intervertebral joint. Spine 5: 245-253.

Aziz, H. N., F. Galbusera, C. M. Bellini, G. V. Mineo, A. Addis, R. Pietrabissa, and M. Brayda-Bruno. 2008. Porcine models in spinal research: calibration and comparative finite element analysis of various configurations during flexion-extension. Comparative Medicine 58: 174-179.

Buchholtz, E. A. 2001. Vertebral osteology and swimming style in living and fossil whales (Order: Cetacea). Journal of Zoology (London) 253: 175-190.

Busscher, I., A. J. van der Veen, J. H. van Dieën, I. Kingma, G. J. Verkerke, and A. G. Veldhuizen. 2010. *In vitro* biomechanical characteristics of the spine: a comparison between human and porcine spinal segments. Spine 35: E35-E42.

Chapman, R. E., A. F. Andersen, and S. J. Jabo. 1999. Construction of the virtual *Triceratops*: procedures, results, and potentials. Journal of Vertebrate Paleontology 19: 37A.

Chazal, J., A. Tanguy, M. Bourges, G. Gaurel, G. Escande, M. Guillot, and G. Vanneuville. 1985. Biomechanical properties of spinal ligaments and a histological study of the supraspinal ligament in traction. Journal of Biomechanics 18: 167-176.

Curtis, N., M. E. H. Jones, S. E. Evans, P. O'Higgins, and M. J. Fagan. 2009. Visualising muscle anatomy using three-dimensional computer models - an example using the head and neck muscles of *Sphenodon*. Palaeontologia Electronica 12: 1-18.

Curtis, N., M. E. H. Jones, S. E. Evans, P. O'Higgins, and M. J. Fagan. 2010a. Feedback control from the jaw joints during biting: an investigation of the reptile *Sphenodon* using multibody modeling. Journal of Biomechanics 43: 3132-3137.

Curtis, N., M. E. H. Jones, S. E. Evans, J. Shi, P. O'Higgins, and M. J. Fagan. 2010b. Predicting muscle activation patterns from motion and anatomy: modelling the skull of *Sphenodon* (Diapsida: Rhynchocephalia). Journal of the Royal Society Interface 7: 153-160.

Curtis, N., K. Kupczik, P. O'Higgins, M. Moazen, and M. J. Fagan. 2008. Predicting skull loading: applying multibody dynamics analysis to a macaque skull. The Anatomical Record 291: 491-501.

Dumas, G. A., L. Beaudoin, and G. Drouin. 1987. *In situ* mechanical behavior of posterior spinal ligaments in the lumbar region. An *in vitro* study. Journal of Biomechanics 20: 301-310.

Dzemski, G., and A. Christian. 2007. Flexibility along the neck of the ostrich (*Struthio camelus*) and consequences for the reconstruction of dinosaurs with extreme neck length. Journal of Morphology 268: 701-714.

Gál, J. M. 1993a. Mammalian spinal biomechanics: I. Static and dynamic mechanical properties of intact intervertebral joints. Journal of Experimental Biology 174: 247-280.

Gál, J. M. 1993b. Mammalian spinal biomechanics: II. Intervertebral lesion experiments and mechanisms of bending resistance. Journal of Experimental Biology 174: 281-297.

Gatesy, S. M., K. M. Middleton, F. A. Jenkins, Jr., and N. H. Shubin. 1999. Three-dimensional preservation of foot movements in Triassic theropod dinosaurs. Nature 399: 141-144.

Gillespie, K. A., and J. P. Dickey. 2004. Biomechanical role of lumbar spine ligaments in flexion and extension: determination using a parallel linkage robot and a porcine model. Spine 29: 1208-1216.

Goel, V. K., B. T. Monroe, L. G. Gilbertson, and P. Brinckmann. 1995. Interlaminar shear stresses and laminae separation in a disc: finite element analysis of the L3-L4 motion segment subjected to axial compressive loads. Spine 20: 689-698.

Grauer, J. N., J. S. Erulkar, T. C. Patel, and M. M. Panjabi. 2000. Biomechanical evaluation of the New Zealand white rabbit lumbar spine: a physiologic characterization. European Spine Journal 9: 250-255.

Hukins, D. W. L., M. C. Kirby, T. A. Sikoryn, R. M. Aspden, and A. J. Cox. 1990. Comparison of structure, mechanical properties, and functions of lumbar spinal ligaments. Spine 15: 787-795.

Hutchinson, J. R., F. C. Anderson, S. S. Blemker, and S. L. Delp. 2005. Analysis of hindlimb muscle moment arms in *Tyrannosaurus rex* using a three-dimensional musculoskeletal computer model: implications for stance, gait, and speed. Paleobiology 31: 676-701.

Hutchinson, J. R., F. C. Anderson, and S. L. Delp. 2003. A 3-D dynamic analysis of musculoskeletal contributions to body support during bipedal locomotion. Journal of Vertebrate Paleontology 23: 64A.

Koolstra, J. H., and T. M. G. J. van Eijden. 2005. Combined finite-element and rigid-body analysis of human jaw joint mechanics. Journal of Biomechanics 38: 2431-2439.

Koolstra, J. H., and T. M. G. J. van Eijden. 2006. Prediction of volumetric strain in the human temporomandibular joint cartilage during jaw movement. Journal of Anatomy 209: 369-380.

Kumaresan, S., N. Yoganandan, and F. A. Pintar. 1999. Finite element analysis of the cervical spine: a material property sensitivity study. Clinical Biomechanics 14: 41-53.

Langenbach, G. E. J., F. Zhang, S. W. Herring, and A. G. Hannam. 2002. Modelling the masticatory biomechanics of a pig. Journal of Anatomy 201: 383-393.

Langenbach, G. E. J., F. Zhang, S. W. Herring, T. M. G. J. van Eijden, and A. G. Hannam. 2006. Dynamic mechanics in the pig mandibular symphysis. Journal of Anatomy 209: 69-78.

Lee, S.-H., and D. Terzopoulos. 2006. Heads up! Biomechanical modeling and neuromuscular control of the neck. ACM Transactions on Graphics 25: 1188-1198.

Little, J. P., and C. J. Adam. 2009. The effect of soft tissue properties on spinal flexibility in scoliosis. Spine 34: E76-E82.

Long, J. H., Jr., D. A. Pabst, W. R. Shepherd, and W. A. McLellan. 1997. Locomotor design of dolphin vertebral columns: bending mechanics and morphology of *Delphinus delphis*. Journal of Experimental Biology 200: 65-81.

Martini, F. H., M. J. Timmons, and M. P. McKinley. 2000. Human Anatomy. 3rd Edition. Prentice Hall, Upper Saddle River, NJ, 806 pp.

Moazen, M., N. Curtis, S. E. Evans, P. O'Higgins, and M. J. Fagan. 2008. Rigid-body analysis of a lizard skull: modelling the skull of *Uromastyx hardwickii*. Journal of Biomechanics 41: 1274-1280.

Myklebust, J. B., F. A. Pintar, N. Yoganandan, J. F. Cusick, D. Maiman, T. J. Myers, and A. Sances, Jr. 1988. Tensile strength of spinal ligaments. Spine 13: 526-531.

Natarajan, R. N., J. R. Williams, and G. B. J. Andersson. 2006. Modeling changes in intervertebral disc mechanics with degeneration. Journal of Bone and Joint Surgery 88: 36-40.

O'Higgins, P., S. N. Cobb, L. C. Fitton, F. Gröning, R. Phillips, J. Liu, and M. J. Fagan. 2011. Combining geometric morphometrics and functional simulation: an emerging toolkit for virtual functional analyses. Journal of Anatomy 218: 3-15.

Panjabi, M. M., A. A. White, III, and R. M. Johnson. 1975. Cervical spine mechanics as a function of transection of components. Journal of Biomechanics 8: 327-336.

Rayfield, E. J. 2007. Finite element analysis and understanding the biomechanics and evolution of living and fossil organisms. Annual Review of Earth and Planetary Sciences 35: 541-576.

Richter, M., H.-J. Wilke, P. Kluger, L. Claes, and W. Puhl. 2000. Load-displacement properties of the normal and injured lower cervical spine in vitro. European Spine Journal 9: 104-108.

Rohlmann, A., L. Bauer, T. Zander, G. Bergmann, and H.-J. Wilke. 2006. Determination of trunk muscle forces for flexion and extension by using a validated finite element model of the lumbar spine and measured in vivo data. Journal of Biomechanics 39: 981-989.

Rybczynski, N., A. Tirabasso, P. Bloskie, R. Cuthbertson, and C. M. Holliday. 2008. A three-dimensional animation model of *Edmontosaurus* (Hadrosauridae) for testing chewing hypotheses. Palaeontologia Electronica 11: 1-14.

Sander, P. M., A. Christian, and C. T. Gee. 2009. Sauropods kept their heads down: response. Science 323: 1671-1672.

Schmidt, R., M. Richter, L. Claes, W. Puhl, and H.-J. Wilke. 2005. Limitations of the cervical porcine spine in evaluating spinal implants in comparison with human cervical spinal segments. Spine 30: 1275-1282.

Sharma, M., N. A. Langrana, and J. Rodriguez. 1995. Role of ligaments and facets in lumbar joint stability. Spine 20: 887-900.

Slijper, E. J. 1946. Comparative biologic-anatomical investigations on the vertebral column and spinal musculature of mammals. Verhandelingen der Koninklijke Nederlandsche Akademie van Wetenschappen, Afdeling Natuurkunde, Tweede Sectie 42: 1-128.

Smit, T. H. 2002. The use of a quadruped as an in vivo model for the study of the spine – biomechanical considerations. European Spine Journal 11: 137-144.

Snively, E., and A. P. Russell. 2007. Craniocervical feeding dynamics of *Tyrannosaurus rex*. Paleobiology 33: 610-638.

Stevens, K. A. 2002. DinoMorph: parametric modeling of skeletal structures. Senckenbergiana Lethaea 82: 23-34.

Stevens, K. A., and J. M. Parrish. 1999. Neck posture and feeding habits of two Jurassic sauropod dinosaurs. Science 284: 798-800.

Stevens, K. A., and J. M. Parrish. 2005. Digital reconstructions of sauropod dinosaurs and implications for feeding. Pp. 178-200 in K. A. Curry Rogers and J. A. Wilson (eds.), The Sauropods: Evolution and Paleobiology. University of California Press, Berkeley.

Walters, R. F., R. E. Chapman, R. A. Snyder, and B. J. Mohn. 2000. Using virtual skeletons as a basis for reconstructing fossil vertebrates. Journal of Vertebrate Paleontology 20: 76A.

Wilke, H.-J., A. Kettler, and L. E. Claes. 1997a. Are sheep spines a valid biomechanical model for human spines? Spine 22: 2365-2374.

Wilke, H.-J., S. T. Krischak, K. H. Wenger, and L. E. Claes. 1997b. Load-displacement properties of the thoracolumbar calf spine: experimental results and comparison to known human data. European Spine Journal 6: 129-137.

Witmer, L. M. 1995. The Extant Phylogenetic Bracket and the importance of reconstructing soft tissues in fossils. Pp. 19-33 in J. J. Thomason (ed.), Functional Morphology in Vertebrate Paleontology. Cambridge University Press, Cambridge.

Wood, A. R., R. M. Bebej, C. L. Manz, D. L. Begun, and P. D. Gingerich. 2011. Postcranial functional morphology of *Hyracotherium* (Equidae, Perissodactyla) and locomotion in the earliest horses. Journal of Mammalian Evolution 18: 1-32.

Chapter 6

Summary and Conclusions

SUMMARY

Rigorous assessment of locomotor morphology in fossil cetaceans of different ages is important for understanding the evolutionary origin of whales from terrestrial ancestors. The changes undergone by the vertebral column are especially important for understanding this transition because the swimming abilities of cetaceans hinge on the functional constraints of their spines. However, little is known about vertebral function in some of the earliest cetaceans, and locomotor interpretations of some taxa based on gross morphology are equivocal. In order for a more complete and accurate picture of cetacean evolution to be constructed, the locomotor capabilities of early forms must be elucidated, and quantitative methods must be developed to test functional interpretations based on qualitative assessments of morphology.

This dissertation set out to provide insight into the locomotor capabilities of a little-studied early cetacean and to develop quantitative methods to assess spinal biomechanics across multiple taxa. One objective was to document and study the vertebral morphology and function of the archaeocete *Remingtonocetus domandaensis*, based on a previously undescribed specimen that preserved a mostly complete

precaudal vertebral column. The other objective was to devise methods for interpreting vertebral function in mammals so that the functional capabilities of early cetaceans could be meaningfully compared. This dissertation contributes the following to our understanding of early cetacean evolution.

Chapter 2 systematically reviewed the members of the archaeocete family Remingtonocetidae, clarifying its checkered taxonomic history and compiling specimen lists for all six recognized species (*Attockicetus praecursor*, *Andrewsiphius sloani*, *Dalanistes ahmedi*, *Kutchicetus minimus*, *Remingtonocetus domandaensis*, and *Remingtonocetus harudiensis*). This chapter also tested the hypothesis that *D. ahmedi* and *R. domandaensis*, which co-occur in the middle Domanda Formation of Pakistan, might be males and females of a single sexually-dimorphic species (as initially suggested by Gingerich et al., 2001). Comparisons of postcranial proportions, dental measurements, and stratigraphic ranges suggest that these taxa are not sexually-dimorphic members of a single species. They should continue to be regarded as separate (though closely related) species, differing primarily on the basis of overall body size, the proportions of premolars and molars, and the relative length of lumbar vertebrae.

Chapter 3 described the morphology and function of the vertebral column in *Remingtonocetus domandaensis*, based on the newly described specimen GSP-UM 3552. The cervical vertebrae, with their long centra and imbricating transverse processes, appear uniquely adapted for stabilizing the head and neck during swimming, while retaining some dorsoventral mobility and providing ample area for attachment of

muscles that control and move the unusually long skull. The lumbar vertebrae possess features indicating that this region was not especially mobile, suggesting that undulation of the lumbus was not utilized to generate propulsion during swimming. Instead, the lumbus appears built to stabilize the lower back in response to forces exerted on it by powerful retraction of the hind limbs. When combined with knowledge of sacral and femoral morphology, it appears that *R. domandaensis* was a highly specialized foot-powered swimmer that utilized movements of its lumbar column very little during swimming.

The principal components analyses of lumbar proportions performed in Chapter 4 yielded useful information about lumbar function in both living mammals and fossil cetaceans. First, the analyses showed, for living mammals, that the anteroposterior lengths of the centrum and neural spine and the craniocaudal and dorsoventral angles of the transverse processes are indicative of the functional capabilities of the mammalian lumbar region. Lumbar vertebrae of dorsostable mammals are marked by relatively short centra, anteroposteriorly-expanded neural spines, and transverse processes with little to no cranial or ventral inclination. Lumbar vertebrae of dorsomobile mammals, on the other hand, possess relatively long centra, anteroposteriorly shorter neural spines, and cranioventrally-oriented transverse processes. These differences provide sound justification for functional interpretations of vertebral morphology in fossil taxa.

Secondly, Chapter 4 provided a quantitative context for comparing the lumbar vertebrae of archaeocetes with those of modern mammals, allowing relative mobility to

be assessed. *Remingtonocetus domandaensis* possesses lumbar vertebrae more similar to those of mammals with less mobile lumbar spines, while the lumbar regions of protocetid and basilosaurid archaeocetes (including *Maiacetus inuus*, *Qaisracetus arifi*, *Dorudon atrox*, and *Basilosaurus isis*) appear to be increasingly mobile. Basilosaurids possess the most mobile lumbar regions of all. The anterior lumbar vertebrae of representative modern cetaceans, especially the short-beaked saddleback dolphin (*Delphinus delphis*), signal a more stable lumbar region, which is consistent with how their spine is utilized during caudal oscillation (Buchholtz and Schur, 2004; Buchholtz et al., 2005). These results suggest that the evolution of the lumbar region in cetaceans was marked by an increase in mobility within Protocetidae and Basilosauridae, followed by a decrease in mobility as aquatic locomotion became increasingly refined within the Neoceti.

The multibody dynamic modeling analyses performed in Chapter 5 illustrate a novel way for comparing the biomechanics of the spine in fossil taxa while taking into account the effects of soft tissues (intervertebral discs and ligaments) in limiting movement. The L4-L5 joint of *Maiacetus inuus* displayed a dorsoventral range of motion 11.0% greater (on average) than that of *Remingtonocetus domandaensis*, regardless of the soft tissue parameters utilized. Systematic removal of individual ligaments demonstrates that the difference observed between the taxa is due primarily to disparities in the capsular ligaments. The difference in the angles of the zygapophyseal facets between these species results in less strain being exerted on the capsular ligaments of *M. inuus* for a given angle of motion. This allows greater rotation

for a given moment strength relative to the joint of *R. domandaensis*. These results are consistent with interpretations based on morphology and multivariate analyses of lumbar proportions that suggested that *R. domandaensis* had a less mobile lumbar spine than *M. inuus*.

In sum, this dissertation demonstrates that *Remingtonocetus domandaensis* possessed a vertebral column most consistent with an animal that utilized powerful movements of its hind limbs to generate underwater propulsion rather than undulatory movements of its spine. Its lumbar region does not appear especially mobile, and its robust sacrum would have prevented any continuity of function between lumbar, sacral, and caudal vertebrae. This interpretation calls into question assertions that earlier archaeocetes, with a similar or more restrictive vertebral morphology, swam by vertebral undulation (Thewissen et al., 1994, 1996; Thewissen and Fish, 1997; Bajpai and Thewissen, 2000; Madar et al., 2002; Madar, 2007). There is currently no sound evidence to suggest that any archaeocetes more primitive than *R. domandaensis* used dorsoventral undulation during swimming.

Contemporary and later protocetid archaeocetes, on the other hand, appear to have possessed a more mobile lumbar spine. Based on limb proportions, it is clear that some protocetids utilized limbs to generate propulsion during swimming to some degree (Gingerich, 2003; Gingerich et al., 2009). It is possible that increased flexibility of the lumbus first evolved to increase the length of the power stroke during pelvic paddling, akin to the strategy used by river otters (Fish, 1994), and it may even be true that *Remingtonocetus domandaensis* was capable of doing this to a small extent. But it

is clear that protocetids could have flexed and extended their lumbar regions to a greater degree than any previous cetaceans. Protocetids with a reduced sacrum achieved continuity of form and function between the lumbus and tail, allowing dorsoventral movements in the lumbar vertebrae to potentially initiate an undulatory wave that propagated posteriorly down the spine during swimming. This mode of swimming was almost certainly the dominant locomotor mode used by the first obligately aquatic archaeocete cetaceans.

The aim of this dissertation was not to elucidate all of the details of locomotor evolution in early cetaceans, but to offer two robust starting points for future study: one comparative and one methodological. First, this study effectively demonstrates the functional capabilities of the spine in *Remingtonocetus domandaensis*, indicating that its lumbar spine was less mobile than those of contemporary and later protocetids. The results yielded from gross morphology, multivariate analyses, and virtual biomechanics are consistent and mutually reinforcing, thus providing a reliable point of comparison for assessing the functional capabilities of later archaeocetes on the main line of cetacean evolution.

Secondly, this dissertation offers a set of quantitative methods for assessing functional hypotheses that are based solely on gross morphology. Multivariate analyses of skeletal measurements in modern taxa, whose lifestyles and ecologies are known, provide a rigorous means for extracting the functional implications of morphology in fossil forms, and they can be applied to virtually any measurable aspect of morphology. The multibody dynamic analyses provide an additional means of quantitatively

comparing the biomechanics of extinct species. While it may prove extremely difficult to determine how close the ranges of motion estimated by these virtual models approach the actual values exhibited by these animals in life, their utility in a comparative context, in which all parameters can be controlled, cannot be overstated. This new technology can be extended to other taxa and adapted to other areas of anatomy to aid in understanding the biomechanics of fossil forms. The methods demonstrated here show how the functional capabilities of extinct species can be understood and compared in rigorous and meaningful ways.

CONCLUDING REMARKS

There are still many things that have yet to be discovered about how cetaceans evolved from terrestrial mammals into some of the most highly derived and specialized aquatic animals on earth today. But in just the past few decades, their origin has gone from being one of evolution's biggest mysteries to one of its most spectacular examples. Further study of how this transition occurred will continue to provide insight into how evolutionary and ecological processes operate on long time scales.

At the same time, studies of whale evolution can also provide material for major public outreach. By uncovering and documenting all of the intricate details of how this transition progressed, we can have an excellent example of macroevolution to demonstrate to a sometimes incredulous public, helping them both to see *that* evolution happened and to understand *how* evolution occurred. In so doing, this work

can hopefully inspire non-scientists to take delight in living in a complex, evolving world with a long and rich history.

REFERENCES

Bajpai, S., and J. G. M. Thewissen. 2000. A new, diminutive Eocene whale from Kachchh (Gujarat, India) and its implications for locomotor evolution of cetaceans. Current Science 79: 1478-1482.

Buchholtz, E. A., and S. A. Schur. 2004. Vertebral osteology in Delphinidae (Cetacea). Zoological Journal of the Linnean Society 104: 383-401.

Buchholtz, E. A., E. M. Wolkovich, and R. J. Cleary. 2005. Vertebral osteology and complexity in *Lagenorhynchus acutus* (Delphinidae) with comparison to other delphinoid genera. Marine Mammal Science 21: 411-428.

Fish, F. E. 1994. Association of propulsive swimming mode with behavior in river otters (*Lutra canadensis*). Journal of Mammalogy 75: 989-997.

Gingerich, P. D. 2003. Land-to-sea transition in early whales: evolution of Eocene Archaeoceti (Cetacea) in relation to skeletal proportions and locomotion of living semiaquatic mammals. Paleobiology 29: 429-454.

Gingerich, P. D., M. ul-Haq, I. H. Khan, and I. S. Zalmout. 2001. Eocene stratigraphy and archaeocete whales (Mammalia, Cetacea) of Drug Lahar in the eastern Sulaiman Range, Balochistan (Pakistan). Contributions from the Museum of Paleontology, University of Michigan 30: 269-319.

Gingerich, P. D., M. ul-Haq, W. von Koenigswald, W. J. Sanders, B. H. Smith, and I. S. Zalmout. 2009. New protocetid whale from the middle Eocene of Pakistan: birth on land, precocial development, and sexual dimorphism. PLoS ONE 4: e4366.

Madar, S. I. 2007. The postcranial skeleton of early Eocene pakicetid cetaceans. Journal of Paleontology 81: 176-200.

Madar, S. I., J. G. M. Thewissen, and S. T. Hussain. 2002. Additional holotype remains of *Ambulocetus natans* (Cetacea, Ambulocetidae), and their implications for locomotion in early whales. Journal of Vertebrate Paleontology 22: 405-422.

Thewissen, J. G. M., and F. E. Fish. 1997. Locomotor evolution in the earliest cetaceans: functional model, modern analogues, and paleontological evidence. Paleobiology 23: 482-490.

Thewissen, J. G. M., S. T. Hussain, and M. Arif. 1994. Fossil evidence for the origin of aquatic locomotion in archaeocete whales. Science 263: 210-212.

Thewissen, J. G. M., S. I. Madar, and S. T. Hussain. 1996. *Ambulocetus natans*, an Eocene cetacean (Mammalia) from Pakistan. Courier Forschungsinstitut Senckenberg 190: 1-86.